Voor Noor* en Hannes*

Universiteit Gent
Faculty of Medicine and Health Sciences
Department of Basic Medical Sciences

Study of the etiology of neurolathyrism, a human neurodegenerative disease with nutritional causes

Marijke Van Moorhem

Promotor: Prof. Dr. Luc Leybaert
Co-promotor: Hon. Prof. Dr. Fernand Lambein

2011

Thesis submitted in fulfilment of the requirements for the degree of “Doctor in Biomedical Sciences”
November 29, 2011

Promotor:	Prof. Dr. Luc Leybaert Ghent University, Belgium
Co-promotor:	Hon. Prof. Dr. Fernand Lambein Ghent University, Belgium
Chairman:	Prof. Dr. Claude Cuvelier Ghent University, Belgium
Reading committee:	Prof. Dr. Koen Paemeleire Ghent University, Belgium
	Prof. Dr. Peter Nunn University of Portsmouth, United Kingdom
	Prof. Dr. Hubert Thierens Ghent University
	Dr. Joëlle Nsimire Chabwine Geneva University Hospital, Switzerland

Other members of the examination committee:

Prof. Dr. Jan Phillippé
Ghent University, Belgium

Prof. Dr. Geert Callewaert
University of Leuven, campus Kortrijk, Belgium

Cover illustration:
Grass pea flower (Ethiopia)

Table of contents

List of abbreviations

ACI: 2-(3-amino-3-carboxypropyl)isoxazolin-5-one
AEQ: aequorin
AIDA: (RS)-1-aminoindan-1,5-dicarboxylic acid
ALS: amyotrophic lateral sclerosis
ALS/PD: ALS combined with features of Parkinsonism and Alzheimer-type dementia
AMPA: α-amino-3-hydroxy-5-methyl-4-isoxazole propionic acid
Aβ: amyloid β
ANOVA: analysis of variance
Asc: L-ascorbic acid
ATA: aurintricarboxylic acid
ATP: adenosine triphosphate
BAIB: β-aminoisobutyric acid
BAPN: β-aminoproprionitrile
BAPTA: 1,2-bis(o-aminophenoxy)ethane-N,N,N',N'-tetraacetic acid
BBB: blood-brain barrier
BCEC: brain capillary endothelial cells
BCIP/NBT: 5-bromo-4-chloro-3-indolyl/nitro blue tetrazolium
bFGF: basic fibroblast growth factor
BIA: β-(isoxazolin-5-on-2yl)-alanine
BK: bradykinin
BSA: bovine serum albumin
CAG codon: cytosine-adenine-guanine codon
Cat: catalase
CEI: 2-cyanoethyl-isoxazolin-5-one
CGG codon: cytosine-guanine-guanine codon
cGMP: cyclic guanosine monophosphate
CICR: Ca^{2+}-induced Ca^{2+}-release
CNQX: 6-cyano-7-nitroquinoxaline-2,3-dione
CNS: central nervous system
CPP: 3-(2-carboxypiperazin-4-yl)propyl-1-phosphonic acid
CSF: cerebrospinal fluid
Cys: L-cysteine
DAG: diacylglycerol
DABA: 2,4-diaminobutanoic acid
DAPA: 2,3-diaminopropionic acid
DAPI: 4',6-diamidine-2-phenylindole-dihydrochloride
D-AP5: DL-2-Amino-5-phosphonopentanoic acid
DMEM: Dulbecco's Modified Eagle Medium
DNA: deoxyribonucleic acid
D-Ser: D-serine
EAAC: excitatory amino acid carrier
EAAT: excitatory amino acid transporter
EB: β-estradiol 3-benzoate
EGTA: ethylene glycol tetraacetic acid
ER: endoplasmic reticulum
FBS: fetal bovine serum
FCCP: p-trifluoromethoxy carbonyl cyanide phenyl hydrazone
FCS: fetal calf serum
FITC: fluorescein isothiocyanate

GDP: guanosine-5’-diphosphate
GFAP: glial fibrillary acidic protein
GLAST: glutamate/aspartate transporter
GLT-1: glutamate transporter-1
GluR2: glutamate-receptor subunit 2
GPCR: G-protein-coupled receptor
GPX: glutathione peroxidase
GRX: glutaredoxin
GS: glutamine synthetase
GSH: γ-glutamylcysteinyl glycine
GTP: guanosine-5’-triphosphate
H_2DCFDA: 2'-7' dichlorodihydrofluorescein diacetate
HAM: Human T cell leukemia virus type 1 (HTLV-1)-associated myelopathy
Har: homoarginine
HBSS: Hanks’ balanced salt solution
Hepes: 4-(2-hydroxyethyl)piperazine-1-ethanesulfonic acid
HPLC: high performance liquid chromatography
HTLV-1: Human T cell leukemia virus type 1
Ig: immunoglobulin
IL: interleukin
iNOS: inducible nitric oxide synthase
IP_3: inositol 1,4,5-trisphosphate
KA: kainate
KRB-Hepes: Krebs-Ringer buffer
LBD: ligand-binding domain
L-BMAA: L-β-methylamino-alanine
L-β-ODAP: β-N-oxalyl-L-α,β-diaminopropionic acid
L-BOAA: β-oxalylamino-L-alanine
L-Glu: L-glutamate
L-OAP: L-3-oxalylamino-2-aminopropionic acid
L. sativus: *Lathyrus sativus L.*
LY: Lucifer yellow
Ψ_m: mitochondrial membrane potential
MCPG: (S)-α-methyl-4-carboxyphenylglycine
MEM: Modified Eagle Medium
Met: L-methionine
mGluR: metabotropic glutamate-receptor
MiCa: mitochondrial Ca^{2+} channel
MK-801: (+)-5-methyl-10,11-dihydro-S*H*-dibenzo[a,d]cyclohepten-5,10-imine maleate
mRNA: messenger ribonucleic acid
MSCC: mechano-sensitive Ca^{2+} channels
MTS: 3-(4,5-dimethylthiazol-2-yl)-5-(3-carboxymethoxyphenyl)-2-(4-sulfophenyl)-2H-tetrazolium salt
M.W.: Molecular weight
NADH: reduced nicotinamide adenine dinucleotide
NAS: 1-naphthyl acetyl-spermine
NBQX: 2,3-dioxo-6-nitro-1,2,3,4-tetrahydrobenzo[f]quinoxaline-7-sulfonamide
NCX: Na^+/Ca^{2+} exchanger
NF-κB: nuclear factor κB
NMDA: N-methyl-D-aspartate
NO(S): nitric oxide (synthase)
NP-40: Nonidet P-40

OCN^-: cyanate
$PBSD^+$: phosphate-buffered salt solution with divalent cations
PD: Parkinson's disease
PDA: phorbol 12,13-diacetate
PDC: L-trans-pyrrolidine-2,4-dicarboxylic acid
Pe: permeability coefficient
PI: propidium iodide
PI_3: phosphatidylinositol 3
PIP_2: phosphatidylinositol 4,5 bisphosphate
PITC: phenyl isothiocyanate
PKB: protein kinase B
PLC: phospholipase C
PMCA: plasma membrane Ca^{2+} ATPase
PrSSG: protein-glutathione mixed disulfides
PS: phosphatidylserine
PSM: portosystemic myelopathy
PTP: permeability transition pore
RBE4: rat brain endothelial cells
Rh-123: Rhodamine 123
RIPA: radio-immunoprecipitation assay buffer
RNS: reactive nitrogen species
RO(C)C: receptor-operated (Ca^{2+}) channel
ROS: reactive oxygen species
r.p.m.: revolutions per minute
SCN^-: thiocyanate
S.E.M.: standard error of the mean
SERCA: sarco-/endoplasmic reticulum Ca^{2+}-ATPase
SIB1893: (*E*)-2-methyl-6-(2-phenylethenyl)pyridine
SNARE: soluble *N*-ethylmaleimide-sensitive factor attachment protein receptor
SPCA: secretory-pathway Ca^{2+} ATPases
SOCE: store operated Ca^{2+} entry
SO(C)C: store-operated (Ca^{2+}) channel
SOD: superoxide dismutase
TBS: tris-buffered saline
Tg: thapsigargin
TNF: tumor necrosis factor
Trans-ACPD: (±)-1-Aminocyclopentane-*trans*-1,3-dicarboxylic acid
TRPM7: transient receptor potential melastatin 7
TSP: tropical spastic paraparesis
TUNEL: Terminal deoxynucleotidyl transferase dUTP nick end labeling
UP: uniporter
VDAC: voltage-dependent anion channel
VEGF: vascular endothelial growth factor
VFT: Venus Flytrap
VO(C)C: voltage-operated (Ca^{2+}) channel
V. sativa: *Vicia sativa*
x_c^-: glutamate-cystine antiporter

Summary

Prolonged exclusive consumption of grass pea (*Lathyrus sativus* L.) seeds under certain conditions initiates the development of neurolathyrism, a disease characterized by neurodegeneration, which results in a spastic paraparesis. The neuro-excitatory amino acid β-N-oxalyl-L-α,β-diaminopropionic acid (L-β-ODAP) present in grass pea was proposed as the cause of the disease. Although the mechanism of its action has not been conclusively elucidated, excitotoxicity and oxidative stress-related dysfunctions have been proposed to explain at least part of its neurotoxicity. The deficiency of grass pea in the sulphur-containing amino acids methionine (Met) and cysteine (Cys) may contribute to the L-β-ODAP-induced increase in oxidative stress.

In this research project, the effect of L-β-ODAP was studied as compared to L-glutamate on the permeability of the blood-brain barrier (BBB), on the survival and functioning of neuronal and glial cells, and free amino acids were analyzed in urine of neurolathyrism patients.

An *in vitro* model for the BBB, consisting of brain capillary endothelial cells (BCEC) co-cultured with glial cells, was exposed to L-β-ODAP or the excitatory amino acid L-glutamate. Acute exposure to either L-β-ODAP or L-glutamate had no effect on the BBB permeability, whereas chronic exposure to L-β-ODAP (but not to L-glutamate) increased its permeability. Since no information is available about L-β-ODAP transport across the BBB, this increased permeability may indicate a possible entry point of L-β-ODAP into the central nervous system (CNS).

Once L-β-ODAP entered the CNS, neurotoxicity can be initiated. Although neurolathyrism research has largely focused on the direct neurotoxic effects of L-β-ODAP, non-neuronal cells such as glial cells may also be involved in this process. Therefore, gliotoxicity of L-β-ODAP was studied in C6 glioma cells and primary glial cells. Cell death was evaluated by propidium iodide (PI) staining, whereas cell survival was quantified by the 3-(4,5-dimethylthiazol-2-yl)-5-(3-carboxymethoxyphenyl)-2-(4-sulfophenyl)-2H-tetrazolium salt (MTS) absorbance. Apoptosis was studied by measuring caspase activity or the presence of phosphatidylserine (PS) on the outside of the plasma membrane (with Annexin V). Treatment of C6 glioma cells with L-β-ODAP or L-glutamate for 24 h induced cell death, which could be prevented by adding Cys or ascorbic acid (Asc) (but not Met) in the treatment medium. In primary glial cells, L-β-ODAP induced cell death at similar concentrations as in C6 glioma cells, whereas L-glutamate had no effect on the viability of these cells. In contrast with C6 glioma cells, inclusion of antioxidants (Cys, Asc, and Met) had no protective effect. However, when sub-types of glial cells were identified using fluorescent markers for astrocytes (glial fibrillary acidic protein;

GFAP), microglia (ED-1) or oligodendrocytes (O4), microglia appeared to be the most susceptible subtype for L-β-ODAP-induced toxicity, while mitochondria of astrocytes appeared to be swollen upon exposure to L-β-ODAP, as was verified by transmission electron microscopic analysis. The latter may correspond to an early stage in mitochondrial dysfunction.

L-β-ODAP can also exert direct neurotoxic actions. In previous studies, L-β-ODAP was generally described as an α-amino-3-hydroxy-5-methyl-4-isoxazole propionic acid (AMPA)- receptor agonist, an inhibitor of L-glutamate transport and a stimulus for L-glutamate release, thereby contributing to or mimicking L-glutamate excitotoxicity. As a key factor in excitotoxic damage is intracellular Ca^{2+} overload, the effect of chronic exposure of neuronal cells to L-β-ODAP or L-glutamate on the cytoplasmic, mitochondrial and endoplasmic Ca^{2+} handling was studied in N2a neuroblastoma cells, using the luminescent protein aequorin (AEQ), specifically targeted towards one of these cellular compartments. A 24 h treatment of N2a neuroblastoma cells with sub-toxic concentrations of L-β-ODAP (but not L-glutamate) appeared to increase acute mitochondrial, endoplasmic and cytoplasmic Ca^{2+} responses to bradykinin (BK). Moreover, the mitochondrial membrane potential – visualized with Rhodamine-123 - was hyperpolarized in cells treated with L-β-ODAP.
In primary motor neurons, grown on a glial cell feeder layer, the effect of acute exposure to L-β-ODAP or L-glutamate was studied while intracellular Ca^{2+} responses ($[Ca^{2+}]_i$) were registered using the fluorescent Ca^{2+} indicator Fluo-3. L-β-ODAP appeared to induce a $[Ca^{2+}]_i$ increase by activating AMPA-receptors, including Ca^{2+}-permeable AMPA-receptors. When motor neuron survival was studied after a 24 h exposure to L-β-ODAP or L-glutamate, these AMPA-receptors appeared to be involved in cell death induced by these excitatory amino acids, since inclusion of the AMPA-receptor blocker 2,3-dioxo-6-nitro-1,2,3,4-tetrahydrobenzo[f]quinoxaline-7-sulfonamide (NBQX) or the Ca^{2+}-permeable AMPA-receptor antagonist 1-naphthyl acetyl-spermine (NAS) prevented L-β-ODAP or L-glutamate-induced cell death. Similarly, inclusion of the antioxidants Met or Cys in the treatment medium protected the neurons from L-β-ODAP- or L-glutamate-induced toxicity, suggesting the involvement of oxidative stress.

In addition to these cellular experiments, a field study was performed in Ethiopia to investigate the amino acid metabolism of neurolathyrism patients compared to healthy subjects (see appendix). Therefore, urine and plasma samples were collected from 50 participants (21 neurolathyrism patients and 29 controls), living in the same area where grass pea is a common food. A sample was taken at the start of the study, when most people used to consume grass pea frequently, after which a grass pea free diet was offered during two weeks. A second and third urine and plasma sample were taken after one and two weeks, to investigate the change in the amino acid profile. Urine

samples were analyzed by high performance liquid chromatography (HPLC), while patient data were collected using a questionnaire. Although our results are of preliminary nature, elevated levels of homoarginine were found in urine of neurolathyrism patients, which may refer to malnutrition. The increased homoarginine excretion normalized to control levels after two weeks of a grass pea free diet.

Samenvatting

Overconsumptie van zaailathyruszaden (*Lathyrus sativus* L.) kan leiden tot de ontwikkeling van neurolathyrisme, een ziekte gekenmerkt door neurodegeneratie met een spastische verlamming van de onderste ledematen tot gevolg. Het in zaailathyrus aanwezige neuro-exciterende aminozuur β-N-oxalyl-L-α,β-diaminopropionzuur (L-β-ODAP) wordt algemeen beschouwd als het oorzakelijk agens. Het exacte werkingsmechanisme werd nog niet conclusief opgehelderd, maar men veronderstelt dat zowel excitotoxiciteit als oxidatieve stress-gerelateerde storingen deels de neurotoxiciteit verklaren, waarbij de deficiëntie van zaailathyrus voor de zwavelhoudende aminozuren methionine (Met) en cysteïne (Cys) kan bijdragen tot de L-β-ODAP-geïnduceerde toename van oxidatieve stress.

In dit onderzoeksproject bestudeerden we zowel het effect van L-β-ODAP in vergelijking met L-glutamaat op de permeabiliteit van de bloed-hersenbarrière (BHB) als op de overleving en werking van neuronale en gliale cellen. Daarnaast analyseerden we de vrije aminozuren in de urine van neurolathyrismepatiënten.

Een *in vitro* model van de BHB, bestaande uit capillaire endotheelcellen van de hersenen in co-cultuur met gliale cellen, werd blootgesteld aan L-β-ODAP of het excitatorische aminozuur L-glutamaat. Acute blootstelling aan L-β-ODAP of L-glutamaat had geen effect op de BHB permeabiliteit, terwijl chronische blootstelling aan L-β-ODAP (maar niet aan L-glutamaat) deze permeabiliteit verhoogde. Aangezien er geen specifiek transportmechanisme van L-β-ODAP over de BHB gekend is, suggereert deze verhoogde permeabiliteit een mogelijke toegangsweg voor L-β-ODAP tot in het centraal zenuwstelsel.

Eenmaal in het centraal zenuwstelsel, kan L-β-ODAP neurotoxiciteit uitlokken. Hoewel neurolathyrisme-onderzoek meestal gericht is op directe neurotoxische effecten van L-β-ODAP, kunnen ook niet-neuronale cellen zoals gliale cellen betrokken zijn bij dit proces. Daarom werd gliotoxiciteit bestudeerd in C6 gliomacellen en primaire gliale cellen. Celdood werd bepaald d.m.v. propidium iodide (PI) kleuring, terwijl celoverleving gekwantificeerd werd door de absorbantie van 3-(4,5-dimethylthiazol-2-yl)-5-(3-carboxymethoxyphenyl)-2-(4-sulfophenyl)-2H-tetrazoliumzout (MTS). Apoptose werd bestudeerd door de caspase-activiteit te meten of de aanwezigheid van fosfatidylserine (PS) op de buitenzijde van het plasmamembraan (d.m.v. Annexine V). Behandeling van C6 gliomacellen met L-β-ODAP of L-glutamaat gedurende 24 u induceerde celdood, die kon vermeden worden door toevoeging van Cys of ascorbinezuur (Asc) (maar niet door Met) aan het behandelingsmedium. In primaire gliale cellen induceerde L-β-ODAP celdood bij vergelijkbare

concentraties als in C6 gliomacellen, terwijl L-glutamaat geen effect had op de celoverleving. In tegenstelling tot C6 gliomacellen, had toevoeging van antioxidanten (Cys, Asc en Met) geen beschermend effect. Wanneer echter de subtypes van gliale cellen geïdentificeerd werden door fluorescente merkers voor astrocyten ('glial fibrillary acidic protein'; GFAP), microglia (ED-1) of oligodendrocyten (O4), bleken microglia het meest vatbare subtype te zijn voor L-β-ODAP-geïnduceerde toxiciteit. De mitochondria van astrocyten waren gezwollen na blootstelling aan L-β-ODAP, hetgeen bevestigd werd door analyse met de transmissie-elektronenmicroscoop en wat kan wijzen op een vroeg stadium van mitochondriale dysfunctie.

L-β-ODAP kan ook rechtstreeks neurotoxisch zijn. In vorige studies werd L-β-ODAP algemeen beschreven als een α-amino-3-hydroxy-5-methyl-4-isoxazole propionic acid (AMPA)- receptor agonist, een inhibitor van L-glutamaattransport en een stimulus voor L-glutamaatvrijstelling, waarbij het de excitotoxiciteit van L-glutamaat zou verhogen of zou nabootsen. Aangezien intracellulaire Ca^{2+}-overbelasting een cruciale factor is in excitotoxische schade, werd het effect van chronische blootstelling van neuronale cellen aan L-β-ODAP of L-glutamaat op cytoplasmatische, mitochondriale en endoplasmatische Ca^{2+}-reacties bestudeerd in N2a neuroblastomacellen, d.m.v. de luminescente proteïne aequorine (AEQ) dat specifiek gericht was naar een van deze cellulaire compartimenten. We vonden dat een behandeling van N2a neuroblastomacellen gedurende 24 u met sub-toxische L-β-ODAP-concentraties (maar niet met L-glutamaat) acute mitochondriale, endoplasmatische en cytoplasmatische Ca^{2+}-reacties op bradykinine (BK) verhoogde. Bovendien was de mitochondriale membraanpotentiaal – zichtbaar d.m.v. Rhodamine-123 - gehyperpolariseerd in cellen die behandeld waren met L-β-ODAP.

In primaire motorneuronen die groeiden op een gliale voedingsbodem, werd het effect van acute blootstelling aan L-β-ODAP of L-glutamaat bestudeerd terwijl intracellulaire Ca^{2+}-reacties ($[Ca^{2+}]_i$) geregistreerd werden door de fluorescente Ca^{2+}-indicator Fluo-3. We stelden vast dat L-β-ODAP een stijging in $[Ca^{2+}]_i$ veroorzaakte door de activering van AMPA-receptoren, waaronder ook Ca^{2+}-permeabele AMPA-receptoren. Wanneer de overleving van motorneuronen bestudeerd werd na een blootsteling van 24 u aan L-β-ODAP of L-glutamaat, bleken deze AMPA-receptoren betrokken te zijn in de celdood die door deze exciterende aminozuren geïnduceerd werd. Dit bleek uit het beschermend effect dat inclusie van de AMPA-receptor antagonist 2,3-dioxo-6-nitro-1,2,3,4-tetrahydrobenzo[f]quinoxaline-7-sulfonamide (NBQX) of de Ca^{2+}-permeabele AMPA-receptor antagonist 1-naphthyl acetyl-spermine (NAS) had tegen celdood die veroorzaakt werd door L-β-ODAP of L-glutamaat. Ook toevoeging van de antioxidanten Met of Cys aan het behandelingsmedium bleek protectief te zijn tegen L-β-ODAP- of L-glutamaat-geïnduceerde toxiciteit, wat mogelijk kan wijzen op een rol van oxidatieve stress.

Naast deze cellulaire experimenten, werd ook een veldstudie uitgevoerd in Ethiopië (zie Appendix). Het aminozuurmetabolisme van neurolathyrismepatiënten werd vergeleken met dat van gezonde deelnemers. Hiervoor werden urine- en plasmastalen verzameld van 50 deelnemers (21 neurolathyrismepatiënten en 29 controles), afkomstig van eenzelfde regio waar zaailathyrus basisvoedsel is. Er werd een staal afgenomen bij het begin van de studie, op het moment dat zaailathyrus een belangrijk onderdeel van de voeding uitmaakte. Vervolgens werd gedurende twee weken een dieet aangeboden zonder zaailathyrus. Een tweede en derde urine- en plasmastaal werden afgenomen na één en twee weken, om een eventuele wijziging van het aminozuurprofiel te bestuderen. Urinestalen werden geanalyseerd met behulp van 'high performance liquid chromatography' (HPLC). Patiëntendata werden verzameld aan de hand van een vragenlijst. Hoewel onze resultaten van preliminaire aard zijn, vonden we verhoogde waarden van homoarginine in urine van neurolathyrismepatiënten, wat kan wijzn op ondervoeding. We stelden vast dat de verhoogde homoarginine-excretie normaliseerde tot controlewaarden na een zaailathyrus-vrij dieet van twee weken.

CHAPTER 1

Introduction

CHAPTER 1: INTRODUCTION

1.1. Neurolathyrism

1.1.1. History and epidemiology

Lathyrus sativus L. (L. sativus) has been an important crop both for human consumption and for animal feed or fodder since ancient times, with the origin of its cultivation around 6000 B.C. Seeds have been found as offerings in tombs of Egyptian Pharaohs (Kuo et al. 2000) whereas in Spain the earliest data about the presence of *L. sativus* come from Neolithic sites (Alicante and Malaga) (Pena-Chocarro and Pena 1999). In old writings, the disease state associated with consumption of *L. sativus* is characterized by "trembling of legs and loosening of joints". Ancient Hindu writings of around 400 BC, Hippocrates (460-377 BC), Pliny the Elder (23-79 AD), Pedanius Dioskurides (50 AD) and Galen (130-210 AD) already reported these symptoms. Centuries later, in 1671, the Duke George of Württenberg banned the use of more than 50 % *L. sativus* in bread because of its ability to 'paralyze' legs. In 1690, the Italian physician Bernardino Ramazzini described an outbreak of neurolathyrism in Mondena. In 1705 and 1714 two edicts under Duke Leopold of Württenberg enforced further the banning of its use. The name 'lathyrismus' was coined by Cantani of Naples (1873) to describe the disease. During the 18^{th}, 19^{th} and 20^{th} centuries, outbreaks of neurolathyrism occurred throughout Europe, Northern Africa, the Middle East, Afghanistan, Russia, and India (Spencer 1995; Getahun et al. 2002b). More specifically, in Bangladesh an epidemic of neurolathyrism occurred between 1829 and 1831, and many people were affected in the provinces of Catalonia and Castilla during or just after the Spanish Civil War (1936-1939) when food shortages forced peasants to rely heavily on 'Las gachas', a *L. sativus* gruel consumed since ancient times as part of their regular diet (Hugon et al. 1993; Getahun et al. 2002b).

The highest incidence of neurolathyrism on record developed between December 1942 and the end of February 1943 among German prisoners of a war camp in Vapniarca, a town in Ukraine occupied by Germany during the Second World War. Dr. A. Kessler, one of the prisoners, noted many details on the diet and neurological symptoms of the prisoners and the neurolathyrism victims. In summary, 60 % of the inmates had developed various levels of neurolathyrism, the highest incidence ever reported in the literature. This episode has allowed Lambein et al. to deduce the β-N-oxalyl-L-α,β-diaminopropionic acid (L-β-ODAP) threshold level under the conditions of this forced labor camp. It was concluded that more than 500 mg of L-β-ODAP per adult person per day is sufficient to induce neurolathyrism (Lambein et al. 2001). In Ethiopia neurolathyrism is known as 'Yeguaya beshita' in Amharic, the official language spoken in Ethiopia, which is defined as a disease caused by the

consumption of *L. sativus* seeds 'guaya'. In 1947 an epidemic was reported from the neighboring Serae region of Eritrea following a famine in 1946 (Ferro-Luzzi 1947).

In Europe, a drastic reduction in the cultivation of *L. sativus* occurred in Spain after the 1960's, due to agricultural mechanization and abandonment of small scale farming. Before that time, it used to be a relatively common crop in almost every province and nowadays it is still cultivated on a small scale, using traditional methods in the provinces of Castilla, Navarra and La Mancha. For human consumption, *L. sativus* is usually used uncooked as a green snack, dried, cooked in a stew, milled into flour and cooked as a gruel (*gachas*) or puree, or as roasted seeds (Pena-Chocarro and Pena 1999).

These days, *L. sativus* is generally used for soil amelioration because of its high efficiency of nitrogen fixation and it is still cultivated for human consumption in Asia (Haque et al. 1996), Africa (Getahun et al. 1999), Europe (De Falco and Pardo 2000; Milczak et al. 2001; Mikic et al. 2010) and Latin America (Mera et al. 2000). More specifically in Bangladesh it is the most important pulse crop, occupying 30 % of the total pulse-growing area. In India, *L. sativus* ranks third after chickpea and pigeon pea and in Ethiopia fourth after faba bean, field pea and chickpea in both area and production of the food legumes cultivated (Kuo et al. 2000). A recent issue of the European Grain Legumes Magazine (issue 54, 2009) was entirely devoted to *Lathyrus*.

Recent epidemics of neurolathyrism have been reported in the Indian subcontinent between 1970 and 1974 (Bangladesh, India, Nepal, Pakistan) (Ludolph et al. 1987), in Afghanistan in 2001, in Gansu Province, China, in Ethiopia in 1976/7 and in 1997 (Haimanot et al. 1990; Haque et al. 1996; Getahun et al. 2002b) and in parts of Europe (Greece, Spain)(Haque et al. 1994; Spencer 1995; Getahun et al. 2005; Tekle Haimanot et al. 2005). The prevalence of the epidemic in the northwest region of Ethiopia in the mid seventies varied between 60 and 300/10,000, whereas in Bangladesh in 1976, a prevalence between 2.9 and 18.8/10,000 was reported. The annual incidence in Ethiopia is estimated at 1.7 per 10,000, but peak occurrences were observed during the 1984/85 major famine and in 1994. Between 1997 and 1998 an epidemic was reported affecting 2000 people in only one district in less than a year (Getahun et al. 1999; Getahun et al. 2002b).

In a survey in Bangladesh by Haque et al. (1996) the prevalence varied between 3/10,000 and 36/10,000, being higher near riverbeds. This prevalence rate is lower than that observed in affected regions in Ethiopia and in India (290/10,000 and 192/10,000, respectively). The male: female ratio described in several studies varied between 7:1 (Haque et al. 1996), 10:1 (Ludolph et al. 1987), 2.5:1 (Haimanot et al. 1990), 2:1 (Cohn and Streifler 1981) and 2.8:1 (Haque et al. 1996). Not only female hormones, but also cultural habits are proposed to explain this sex ratio. For example in Bangladesh and India males traditionally eat first, so during famine, little or no food (including grass pea) is left

for the remaining female members (Haque et al. 1996). Although the disease is supposed to be epidemic in nature, the disease can also occur sporadically (Haque et al. 1994). Affected families usually have a single case of neurolathyrism although the whole family is sharing the same food (Hugon et al. 1988; Haimanot et al. 1990).

Risk and protective factors

All major famines and chronic food shortages in Ethiopia from the mid-1970s until now have been accompanied by reports on neurolathyrism epidemics (Getahun et al. 2003). However, people from the same family with a similar diet do not all develop neurolathyrism, suggesting a certain susceptibility of patients. Several factors are proposed to explain this susceptibility for neurolathyrism including young age and male sex (Haimanot et al. 1990; Haque et al. 1996). Females were younger at onset of paralysis than males, but the age at onset was not associated with the type of grass pea preparation consumed, the duration of the consumption, or the degree of disability (Getahun et al. 2002a). Other suggested factors are heavy physical labor (Haimanot et al. 1990), diarrheal episode, febrile illness and Zn^{2+} deficiency (Haimanot et al. 1990; Lambein et al. 1994), blood group O (Getahun et al. 2002a), illiteracy, large family size and exclusive use of clay utensils (Getahun et al. 2005), low socio-economic status, dependence on agriculture, and harsh environmental conditions (Spencer 1999). Generally, the manner of grass pea food preparation has been linked to the risk to develop neurolathyrism. For instance, the consumption of grass pea in roasted, boiled and raw unripe seeds has been associated with a 10 times or more increased risk for neurolathyrism, whereas no raised risk has been noted for the fermented pancake, unleavened bread or gravy preparations. A possible explanation for these observations is that roasted and green unripe *L. sativus* seeds are traditionally consumed on their own. It has been suggested that the use of cereals in a *L. sativus* flour mixture reduced the risk for paralysis if they contain more than a third of cereals in the mixture. Mixing the food with gravy that contains condiments with antioxidant activity reduced it by a factor 4. Boiled seeds, fermented pancake and unleavened bread are such preparations in which cereals are sometimes used. The hypothesis raised that cereals that are rich in vitamins and minerals may improve the micronutrient balance. Additionally, *L. sativus* is, as are other leguminous seeds, deficient in methionine and cysteine. Cereals such as wheat, teff and maize are rich in these sulphur-containing amino acids, so they may compensate for this deficiency when consumed together (Getahun et al. 1999; Getahun et al. 2002a; Getahun et al. 2003; Getahun et al. 2005).

One of the observations for which no explanation was provided so far, is that soaking grass pea in water before cooking, roughly halves the risk of neurolathyrism, whereas cooking in clay utensils more than quadruples it (Getahun et al. 2005).

There are some beliefs that steam or vapor from boiling, smoke from roasting or the dust from harvesting *L. sativus* seeds as well as walking or lying on the straw and the stalks of grass pea would trigger the onset of the disease. Additionally, the pancake and raw forms are considered to be the most 'poisonous' when consumed with protein rich foods such as milk (Haimanot et al. 1990; Getahun et al. 2002b).

Some suggestions for the safe consumption of *L. sativus* were made, anticipating on these observations. Studies with ascorbic acid (Asc) proposed that L-β-ODAP can be removed from seeds when they are treated with lime water overnight and then cooked for 25 minutes. This method was proposed to serve as a simple procedure to detoxify the *L. sativus* seeds in real households (Jahan and Ahmad 1993). In India, attempts to ban the cultivation of *L. sativus* could not succeed, but the intervention of market forces had some effect. The price of *L. sativus* became higher than that of wheat, making this crop well beyond the reach of the poor (Gopalan 1999).

L. sativus and L-β-ODAP

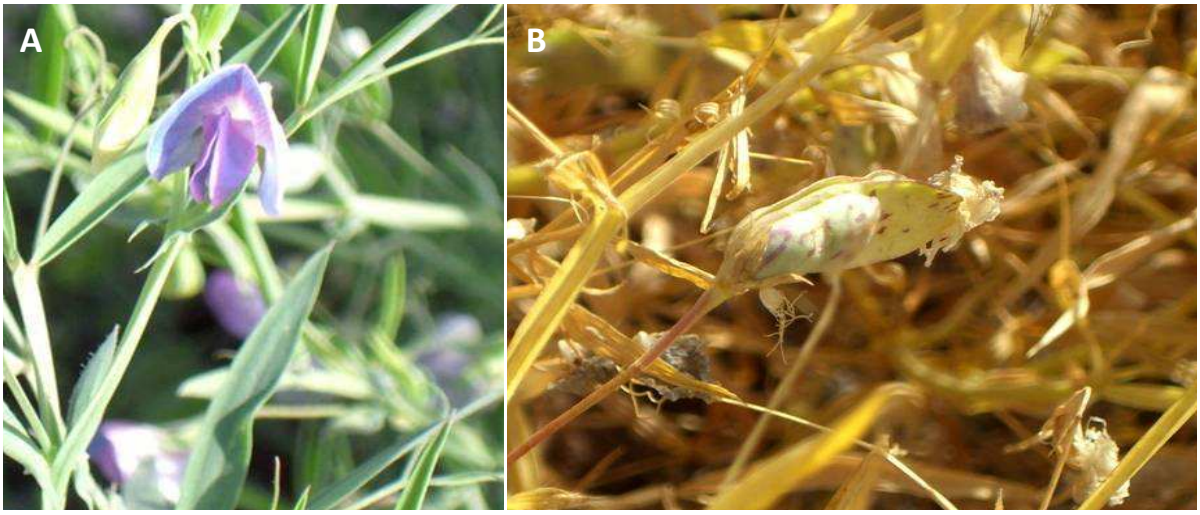

Fig. 1: *Lathyrus sativus* L. *L. sativus*, commonly known as grass pea, is a drought tolerant legume belonging to the family Fabaceae (Leguminosae) and the genus *Lathyrus*, which comprises about 187 species and subspecies, some of which can be used as food or feed, or as ornamental. Grass pea is also known as chickling pea, blue vetchling, Indian vetch, chickling vetch (UK and North America), khesari (India and Bangladesh), san lee dow (China), guaya (Ethiopia), pois carré (France), khesari dal, theora, batura (India), gharas (Pakistan), zaailathyrus (the Netherlands), pisello bretonne (Italy) and almorta, guija, tito (Spain). Grass pea flowers can be purple, pink, blue or white, whereas seeds may be white, yellow, green-yellow, brown, grey or black. **A.** Purple grass pea flower (Ethiopia). **B.** Ripe grass pea seeds (Ethiopia).

L. sativus or grass pea (Fig. 1) is a traditional popular crop because of its easy cultivation, its relative resistance to abiotic and biotic stress (drought, flood and insect attack), and its good yield with relatively little labor expenditures of protein-rich and tasty seeds (Khan et al. 1994; Lambein et al. 1994; Getahun et al. 2002b). It does not require any fertilizers and hence its cost of production is very low as compared to other crops. As a nitrogen fixing legume, it also improves the fertility of the soil and is often used in crop rotation (Haimanot et al. 1990; Haque et al. 1994; Getahun et al. 2002b).

The seeds of *L. sativus* are highly nutritious with a high content of protein, vitamins and minerals (Table 1). Like other cool season food legumes, grass pea is deficient in methionine, tryptophan and cysteine. The pulse has long been used for homeopathic treatment. The substance prepared from the ripe seeds was recommended in spastic spinal paralysis, multiple sclerosis, myelitis, weakness and paralysis of the lower extremities and rheumatic paralysis (Getahun et al. 2002b).

Vitamins	**Essential amino acids (g/100g protein)**	**Other compounds (% of dry weight of the seeds)**	**L-β-ODAP (g/kg seeds)**
Carotene	Arginine (7.85)	Globulin (13.3%)	22 (India)
Thiamine	Lysine (6.94)	Pentosans (6.8 %)	5-8 (Bangladesh)
Riboflavin	Isoleucine (6.59)	Albumin (6.69%)	≤ 5 (Ethiopia)
Nicotinic acid	Leucine (6.57)	Glutelin (3.8%)	0.3-8.7 (China)
Biotin	Valine (4.68)	Phytin (3.6%)	1.5 – 4.9 (Pakistan)
Pantothenis acid	Phenylalanine (4.14)	Sucrose (1.5%)	1.5 – 5.8 (Afghanistan)
Folic acid	Histidine (2.51)	Lignin (1.5%)	
Pyridoxine	Threonine (2.34)	Prolamine (1.5%)	
Ascorbic acid	Tryptophan (0.40)		
Dehydroascorbic acid	Methionine (0.38)		

Table 1: Content of *L. sativus*. *L. sativus* is rich in protein, vitamins and minerals, however, it is deficient in methionine and cysteine. The L-β-ODAP content varies between different regions of cultivation.

Despite the beneficial properties, prolonged consumption of grass pea carries a risk to develop the neurodegenerative disease neurolathyrism. Before the discovery of L-β-ODAP, it was pointed out that the seeds of *L. sativus* itself were harmless, but that the danger of the disease neurolathyrism laid probably in the contamination of the latter with other peas, such as *Vicia sativa* (*V. sativa*), containing β-cyano-L-alanine which was proposed to be the causative agent of neurolathyrism at that time (Ressler 1962).

After its discovery in 1964, the non-protein amino acid L-β-ODAP (M.W. 179,13 g) (Fig. 2), present in *L. sativus* seeds, was suggested to be the causal agent of human neurolathyrism (Murti et al. 1964; Rao et al. 1964; Spencer et al. 1986; Lambein et al. 2007). It is generally accepted that *L. sativus*

contains 1-2 % L-β-ODAP (Warren et al. 2004), although the L-β-ODAP content varies greatly between seeds cultivated in different regions (see table 1). The estimated daily intake is 15-150 mg/kg/d of L-β-ODAP (Kessler 1947; Spencer 1995). Botanical and biochemical research has discovered several physiological functions of L-β-ODAP in the plant, such as being a carrier for Zn^{2+}-ions (Lambein et al. 1994) and a scavenger for hydroxyl ions (Gongke et al. 2001).

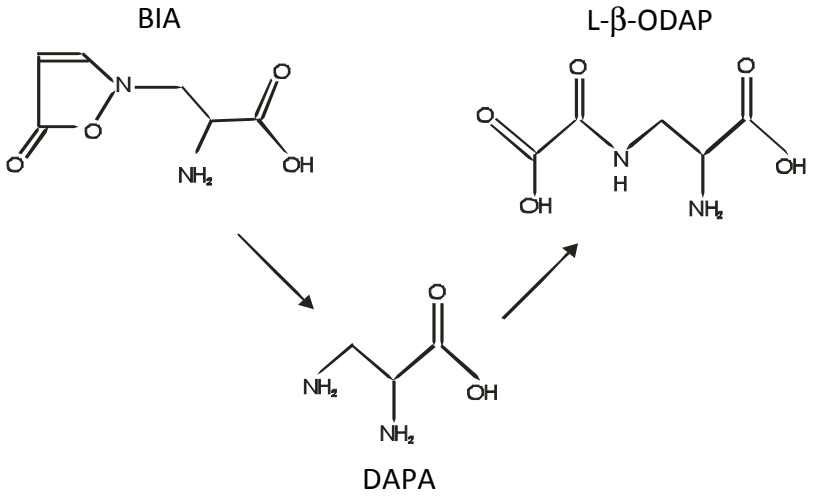

Fig. 2: The biosynthesis of L-β-ODAP. BIA (β-(isoxazolin-5-on-2yl)-alanine), a non-protein amino acid present at high concentration in the seedlings of grass pea and the common garden pea (*Pisum sativum*), is the biosynthetic precursor of L-β-ODAP. DAPA (2,3-diaminopropionic acid) is the short-lived intermediate, being oxalylated with oxalyl-coenzyme A to become L-β-ODAP (Lambein et al. 1994; Lambein et al. 2007).

Attempts to remove L-β-ODAP from the otherwise nutritive and environment-resistant crop have been made worldwide by many different methods (Kuo et al. 2000). A strong relationship between environmental factors and the concentration of L-β-ODAP in grass pea seeds was found. Drought, Zn^{2+} deficiency, iron oversupply and the presence of heavy metals in the soil can considerably increase the level of L-β-ODAP in the seeds grown in farmer's fields as compared to more optimal experimental fields (Gongke et al. 2001). The deficiency of Zn^{2+} in Bangladesh and the high concentration of iron in Ethiopian soils both have an increasing effect on the L-β-ODAP level in the seeds. The presence of cadmium in the soil can increase the L-β-ODAP level up to six-fold.

One study indicated that bacterial fermentation improves the nutritive value of a grass pea seed meal. Tannin, phytic acid and L-β-ODAP could be significantly reduced in grass pea fermented with *Bacillus* sp. isolated from common carp intestine (Ramachandran et al. 2005). A double solid state fermentation with *Aspergillus orizae* and *Rhizopus oligosporus* could reduce the L-β-ODAP level with over 90 % and improve the amino acid composition (Kuo et al. 1995).

Additionally, the rate of L-β-ODAP synthesis and accumulation varies during plant development, being increased in young seedlings and in developing fruits (Addis and Narayan 1994). The content of total amino acids and of total non-essential, essential, and sulphur-containing amino acids increases with increasing maturity of *L. sativus* seeds. Methionine is, however, an amino acid limiting the biological value, irrespective of the degree of maturity (Korus et al. 2003).

The chemistry of L-β-ODAP is remarkable as in aqueous solution it can isomerize spontaneously and form the less toxic α-isomer by a zero order reaction affected by pH and temperature and involving a cyclic intermediate. For example, at 100°C after 1.5 h, an equilibrium is reached with a ratio of 60 % β-isomer and 40 % α-isomer (Padmajaprasad et al. 1997)

Clinical aspects

Neurolathyrism is initially characterized by a reversible onset of leg weakness that develops after an average latency period of 2-3 months of continuous daily intake of 400 g *L. sativus* seeds, although some patients report consumption of less than a month before contracting the disease (Haimanot et al. 1990). Three modes of presentation of spastic paraparesis have been described. Most common is a sudden onset in which the affected individual complains of heavy, weakened legs after falling down, awakening from sleep or after heavy daytime work. Some subjects report a subacute onset of walking disability, whereas others experience a progression of leg weakness, spanning a period of up to three months. Some patients report a significant improvement of symptoms early in the course of the disease when discontinuing grass pea intake. After these initial changes disappear, the irreversible spastic paraparesis develops gradually (Ludolph et al. 1987; Spencer 1995; Ludolph and Spencer 1996; Spencer 1999). The prominent feature of the spastic paraparesis is a greatly increased extensor muscle tone in the lower limbs involving quadriceps and gastrocnemius muscles, resulting in toe-walking, scissoring, and an unsteady gait. This clinical picture, diagnostically recognized as symmetrical and a pyramidal distribution of leg weakness (‘heavy legs’), with exaggerated thigh adductor, patellar, and ankle reflexes is consistent with the neuropathological evidence of degeneration of Betz cells and of anterior and dorsolateral corticospinal tracts in thoracic, lumbar and sacral regions of the spinal cord (Fig. 3) (Ludolph et al. 1987; Haque et al. 1994). Some of the patients with long-lasting neurolathyrism have been reported to develop a clinical course resembling that of amyotrophic lateral sclerosis (ALS), with progressive worsening of the manifestations and involvement of lower (spinal) motor neurons (La Bella and Piccoli 2000). The cognitive state, sensory system, cerebellar function, cranial nerve function and life expectancy of neurolathyrism patients does not show a decline (Spencer 1995; Paleacu et al. 1999), though some people report cognitive deficits, mood disturbances and vivid dreams (Kunig et al. 1994).

In India, the degree of neurological impairment has been classified according to the extent of walking difficulty and the need for physical support (Hugon et al. 1993). The majority is mildly affected having difficulty with running, but they can walk without aid ("no-stick stage"). Muscle spasm restricts movement of ankle and knee joints, causing the victim to walk on the balls of the feet, tilting the pelvis. The more severely affected persons, with pronounced adductor spasticity, walk with a characteristic scissoring gait and require the support of one ("1-stick stage") or two crutches ("2-tick stage"). The most serious cases develop tonic paraplegia in flexion and are forced to crawl or use a wheelchair ("crawler stage") (Hugon et al. 1988). Most neurolathyrism patients reside in one of the first two stages (Haimanot et al. 1990). With the exception of severely affected individuals, the arms are clinically uninvolved, and speech, swallowing, eye movements, mentation, sensation, and proprioception appear normal in all cases (Hugon et al. 1988; Hugon et al. 1993).

Treatment

Most health workers and neurolathyrism patients know that neurolathyrism is incurable but preventable. Some Ethiopian patients seek for whatever alternative healing is available, ranging from consulting a health institution, seeking advice from a traditional healer, using holy water, applying massage with different oils and lubricants, or attending an Islamic service (Haimanot et al. 1990; Getahun et al. 2002b). A study in Bangladesh showed that 43 % of the patients visited a medical doctor, whereas 21 % never consulted a physician nor a traditional healer (Haque et al. 1996).

At present there is no adequate treatment available for neurolathyrism. However, studies have been performed with the centrally acting muscle relaxant tolperisone HCl. Its exact mechanism of action is still unknown, but it is known to inhibit voltage-gated Na^{+}- and Ca^{2+}-channels, which probably contributes to a depression of excitability and synaptic transmission (Kocsis et al. 2005). When administered to neurolathyrism patients for a period of 3 months (150 mg/day (Haque et al. 1994) or 150 mg twice daily (Melka et al. 1997)), tolperisone HCl had a beneficial effect. A general subjective improvement was reported by 75 % of the neurolathyrism patients, and 60 % of the treated patients had a normal tone after 3 months, the spontaneous clonus before treatment disappeared or reduced drastically, and the time to walk 100 meters decreased. Additionally, all treated patients reported increased power and improved physical abilities. The best results were obtained in patients residing in stage I and II (Haque et al. 1994; Melka et al. 1997). However, continued treatment with chemical muscle spasmolytics such as tolperisone HCl in remote rural settings is impractical.

In addition to tolperisone treatment, dorsal rhizotomy or incomplete surgical transsection of the thigh adductor muscles has been evaluated, with some limited success (Spencer 1995).

1.1.2. Experimental model for neurolathyrism

Producing a satisfactory experimental model for neurolathyrism has been difficult. In experimental settings, the disease has been reported in ducks, geese, hens, peacocks, pigs, oxen, sheep, cows, bullocks and horses fed *L. sativus* peas. The horse seemed to be the most susceptible species. Though the disease has been reported in so many species, only limited symptoms, including spastic paraparesis, could be induced in rabbit, guinea pig, dog, hen, and macaque (Spencer 1995). Acute neurotoxic properties of L-β-ODAP depended on the maturity of the species, probably affected by the maturity of the blood-brain barrier (BBB) (see 'entry of L-β-ODAP in the central nervous system'). Adult animals are often refractory to the effects of L-β-ODAP but can be made susceptible by inducing an acidotic state (Rao et al. 1967; Cheema et al. 1969).

One of the first studies to evaluate the relation between L-β-ODAP and neurolathyrism was performed by Rao et al., 1967. Intrathecal injection of the neurotoxin in adult monkeys induced paralysis affecting both lower limbs, without affecting the upper limbs. However, in most cases the paralysis was transient (Rao et al. 1967). Hugon et al. investigated a model of primate lathyrism in well-nourished macaques and defined the clinical and electrophysiological features of the beginning phase of the disorder (Hugon et al. 1988). Abnormal neurological signs were observed 3 - 10 months after starting the grass pea diet, including spastic paraparesis, and neurophysiological evidence was found for corticospinal deficit. Neuropathological examination revealed minor chromatolytic changes and pigmentation of cortical motor neurons (Betz cells), with sparse loss of nerve fibers in the corticospinal tracts. Taken together, these findings were consistent with the early, reversible stage of human neurolathyrism. When pure L-β-ODAP was administered, latency to onset of neurological deficit was shortened and signs of motor neuron dysfunction were more pronounced (Spencer 1999). In another study, young adult monkeys were fed cooked *L. sativus*, and they became paralyzed in 3 – 7 weeks. However, when their diet was supplemented with ascorbic acid, no paralysis was observed. Similarly, when the monkeys were kept on an ascorbic acid free diet without *L. sativus*, L-β-ODAP administration produced neurolathyrism manifestations in these animals within 2 hours. Again, ascorbic acid protected these animals from the neurotoxic effect of L-β-ODAP (Jahan and Ahmad 1993).

Guinea pigs depend on dietary ascorbic acid, so they can be a good model for the effect of ascorbic acid on L-β-ODAP toxicity. Guinea pigs that were fed with grass pea seeds without supplementation of ascorbic acid displayed neurolathyrism symptoms, whereas ascorbic acid supplementation to the diet protected them from becoming paralyzed. Similarly, when fed with an ascorbic acid deficient diet, without *L. sativus* seeds, administration of L-β-ODAP induced the development of

neurolathyrism. Again, ascorbic acid protected the animals from this paralysis (Jahan and Ahmad 1993; Amba et al. 2002; Kusama-Eguchi et al. 2005).

There are remarkable species differences in susceptibility to L-β-ODAP: whereas chicks are readily susceptible to transient intoxication by L-β-ODAP, adult rats or mice do not develop neurodegenerative changes (Rao 1978), though behavioral changes reminiscent of an excitable status can be reproducibly detected (La Bella and Piccoli 2000).

In one-day old chicks, injection of *L. sativus* extracts resulted in retraction of the head and twisting and stiffening of the neck and paralysis resulting in inability of the bird to stand and move about. These symptoms were transient at low dosages but permanent at successive low dosages or at high doses (Roy et al. 1963).

When injected intraperitoneally to immature mice, L-β-ODAP induced lesions in the retina, hypothalamus and lower medulla. This pattern of damage is similar to that demonstrated in animals after oral or subcutaneous administration of glutamate (Olney et al. 1976).

When administered *in vivo* to rats at non-convulsant doses, L-β-ODAP increases cerebellar cyclic guanosine monophosphate (cGMP) and induces down-regulation of glutamate receptors in the frontal cortex (La Bella et al. 1996). Rat neonates within 20 hr after birth showed severe convulsions of the limbs a few minutes after subcutaneous injection with L-β-ODAP. In some cases they showed hyperactivity with vocalization (Kusama-Eguchi et al. 2005). When Wistar rats within 8 h after birth were treated with L-β-ODAP under their dorsal skin, and separated from the second day from their mother for 6 h, more paraparesis occurred (Kusama-Eguchi et al. 2009).

1.2. Neurolathyrism, a motor neuron disease

"Motor neuron disease" is the term used for all disorders involving selective loss of function of the upper and/or lower motor neurons innervating the voluntary limb muscles and muscles depending on motor cranial nerves (Fig. 3). Spasticity usually predominates over weakness in cases of upper motor neurons disorders. Therefore, based on the clinical symptoms of spasticity, increased muscle tone of the lower extremities, ankle and patellar clonus, Babinski's sign and a spastic gait, neurolathyrism has been classified as a motor neuron disease (Spencer 1995; Donaghy 1999; Paleacu et al. 1999). Accordingly, upper motor neurons (in some studies specified as Betz cells) and anterior and dorsolateral corticospinal tracts in thoracic, lumbar and sacral regions of the spinal cord have been found to show degenerative changes (Striefler et al. 1977; Ludolph et al. 1987; Ludolph and Spencer 1996). It has been hypothesized that neurolathyrism may be a central axonopathy with

distal manifestations dominated by degeneration of the longest corticospinal tract, or that cortical motor neuron loss is the primary event (Spencer 1995).

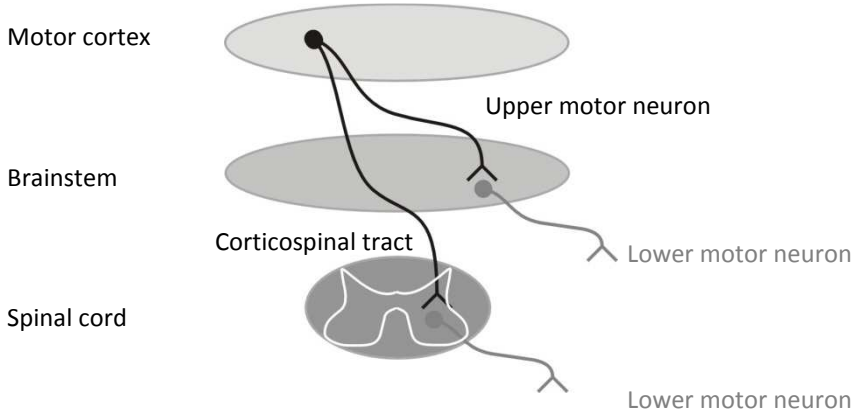

Fig. 3: Upper and lower motor neurons. The final output from the central nervous system to skeletal muscle is from the motor neurons in the ventral horn of the spinal cord or in the brainstem. Neurons from the corticospinal tract are some of the longest in the body, because they run from the cerebral cortex in the top of the skull all the way down into the cord. Area 4 (M1) is differentiated from all other areas of the cortex by having a number of particularly big cells in layer V, the giant Betz cells. Their size suggests that they might be the origin of the corticospinal tract. The Betz cells are the largest 'upper motor neurons', whereas the spinal motor neurons are referred to as 'lower motor neurons' (Carpenter 2003).

Searching for a representative animal model for neurolathyrism, it has been shown that administration of ^{14}C-L-β-ODAP to rats resulted in maximal accumulation of the radiolabel in the spinal cord (Rao 1978; Sriram et al. 1998). And when [^{3}H]-L-β-ODAP was injected in monkeys, the concentration was markedly higher in the lower third of the spinal cord compared to other regions of the central nervous system (CNS), that is likely to be involved in the paralysis affecting the lower extremities (Rao 1978). Recently, newborn rat pups showed characteristic paraparesis of the hind legs after injection of L-β-ODAP subcutaneously, and after the induction of stress (separation from the mother for 5-6 h). This paraparesis was correlated with a decreased number of motor neurons in the lumbar and sacral cord segments (Kusama-Eguchi et al. 2009).

Only in the most severe cases the upper limbs are affected (Ludolph and Spencer 1996). It is not clear why the legs are affected earlier and to a greater degree than the arms, but some hypotheses were raised such as a greater reserve of cortical motor neurons regulating the function of the upper extremities compared to that for lower limbs, the larger surface area of perikarya and dendritic arbors of cortical neurons supplying the lumbar cord and the greater energy demands in neurons with longer axons (Spencer 1995).

In almost all cases the spinal nerve roots were normal. However, involvement of the lower motor neurons (α-motor neurons in the lumbar spinal cord) has been described in long-standing neurolathyrism patients (Drory et al. 1992).

Some clinical reports of early neurolathyrism describe a stumbling gait and incoordination, consistent with cerebellar dysfunction. To that perspective, the accumulation of radioactive L-β-ODAP in the cerebellum tissue of squirrel monkey was an interesting observation (Mehta et al. 1980). Some evidence was also found of cognitive dysfunctions among neurolathyrism patients (Paleacu et al. 1999; Shinomol and Muralidhara 2007).

The question remains why specifically motor neurons are affected. Studies on another motor neuron disease, ALS, refer to an intrinsic selective vulnerability of motor neurons to AMPA-receptor-mediated toxicity, although the mechanisms are only partially understood. Both a disturbance in Ca^{2+} homeostasis and increased oxidative stress are described as possible mechanisms, not necessarily occurring separately (Kruman et al. 1999; Marambaud et al. 2009; Shi et al. 2010). First, the AMPA-receptor complexes of spinal motor neurons appear to be relatively deficient for glutamate-receptor subunit 2 (GluR2). Presence of these GluR2 subunits renders AMPA-receptors impermeable to Ca^{2+} due to the presence of a positively charged arginine in the receptor's ion channel. Consequently, neurons expressing AMPA-receptors that lack a GluR2 subunit will be more permeable to Ca^{2+} compared to other neurons (Van Den Bosch and Robberecht 2000; Van Damme et al. 2002a; Corona and Tapia 2007). In addition to their typical lack of the Ca^{2+}-binding proteins parvalbumin and calbindin D-28k (Ince et al. 1993; Elliott and Snider 1995; Reiner et al. 1995; Van Den Bosch et al. 2002a), spinal motor neurons are specifically vulnerable to intracellular Ca^{2+} overload. Secondly, the lack of Ca^{2+}-binding proteins not only exposes neurons to AMPA-/kainate(KA)-mediated excitotoxicity (Reiner et al. 1995; Palecek et al. 1999; Van den Bosch et al. 2002b), but also makes them more vulnerable to oxidative stress (Hugon et al. 1996). The higher vulnerability of motor neurons to oxidative stress may also come from their stronger dependency on the glutathione precursor methionine content in the cells, as they have shown to be the most methionine-immunoreactive cell bodies in gluteraldehyde-fixed rat brain sections (Amara et al. 1995). Finally, the mitochondrial density in motor neurons appeared to be lower compared to non-motor neurons, which may result in a decreased Ca^{2+} buffering capacity in response to AMPA-receptor-induced Ca^{2+} transients (Grosskreutz et al. 2007), and probably also a more limited protection against oxidative stress.

In summary, following the ALS model, the selective degeneration of motor neurons in case of neurolathyrism may be explained both by their higher Ca^{2+} influx upon excitation and the restricted Ca^{2+} buffering capacity, together with their higher vulnerability to oxidative stress due to a stronger methionine dependency and a lower mitochondrial density.

1.2.1. Entry of L-β-ODAP in the central nervous system

The non-protein amino acid L-β-ODAP (also known as β-oxalylamino-L-alanine (L-BOAA) or L-3-oxalylamino-2-aminopropionic acid (L-OAP)) was discovered in grass pea and related species by two groups in 1964 and was suggested as the causative agent of neurolathyrism (Murti et al. 1964; Rao et al. 1964; Lambein et al. 2007). Since then, neurolathyrism research has been focused mainly on this excitatory amino acid, especially in the CNS. Assuming that L-β-ODAP is directly responsible for the degeneration of motor neurons, it is essential to know whether this toxin can cross the BBB. The BBB isolates neurons from the circulating blood. In concert with pericytes, astrocytes and microglia, this endothelial structure maintains the chemical composition of the neuronal environment required for adequate functioning of neuronal circuits in the adult brain (Fig. 4). The term BBB is used for the barrier between blood and brain as well as between blood and spinal cord (sometimes called blood-spinal cord barrier), as these barriers are generally considered as similar. However, the spinal cord barrier has been reported to show greater permeability to interferons and tumor necrosis factor α (TNF-α) than the brain barrier (Pan et al. 1997; Choi and Kim 2008).

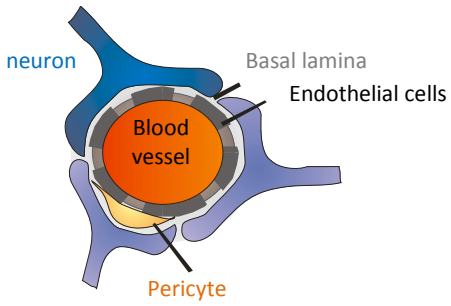

Fig. 4: The blood-brain barrier (BBB). The BBB is a highly selective lipophilic barrier between the systemic blood circulation and the CNS, formed by endothelial cells. Brain endothelial cells have an extremely low permeability due to tight junctions. Endothelial cells are in close contact with endfeet of astrocytes, which are separated from the former by the basal lamina, in which pericytes are situated (Abbott et al. 2010).

L-β-ODAP was found in blood a few (2 – 6) hours after consumption of grass pea, attaining a maximal concentration of 177 µM 4 h after consumption of 100 g *L. sativus*, indicating that L-β-ODAP is absorbed along the gastro-intestinal tract. Urinary and fecal L-β-ODAP excretion is almost negligible, suggesting that a major portion of the dietary consumed L-β-ODAP is metabolized in humans, with oxalate proposed as the main metabolite of L-β-ODAP (Pratap Rudra et al. 2004). Unfortunately, blood samples were only taken from one volunteer and next to urinary and fecal excretion, biliary excretion of L-β-ODAP has never been studied.

Reported results of the presence of L-β-ODAP in the CNS are controversial. Intraperitoneal administration of L-β-ODAP to 12-day old rats caused typical convulsions and a significant concentration of the neurotoxin was detected in the brain (Cheema et al. 1969). Similarly, L-β-ODAP was found in the lower part of the CNS (part of the thoracic region together with the lumbar and sacral region of the spinal cord) of rat neonates, after subcutaneous injection (Kusama-Eguchi et al. 2005), it even induced severe hemorrhage at the caudal half of the spinal cord, suggesting a disturbed BBB (Kusama-Eguchi et al. 2009). In adult animals however, intraperitoneal administration did not cause any convulsions and no L-β-ODAP could be detected in the brain, suggesting that L-β-ODAP can only enter the CNS in animals with an immature BBB. On the contrary, Rao (1978) described that [^{3}H]ODAP was detectable in the CNS of species both nonsusceptible for neurolathyrism like the adult rat or mice and susceptible species like the day old chick (Rao 1978) indicating that in some species L-β-ODAP can also cross a mature BBB. Most studies on the entry of L-β-ODAP in the CNS were performed in primates. Rao (1978) described that [^{3}H]ODAP enters the CNS of the adult rhesus monkey, attaining the highest CNS concentration 75 min after intraperitoneal injection (0.17 % radioactivity of the injected dose (200 mg)), with a markedly higher radioactivity in the lower third of the spinal cord compared to other parts of the CNS. In addition, the cerebrospinal fluid (CSF) collected by lumbar puncture from two monkeys had a radioactivity corresponding to 5.8 µg L-β-ODAP per mL, which corresponds to 32.38 µM L-β-ODAP (Rao 1978). Similarly, intraperitoneal administration of L-β-ODAP was toxic for young male squirrel monkeys with a mature BBB and unchanged L-β-ODAP was recovered from the brain of intoxicated animals (Parker et al. 1979). When the distribution of radioactive L-β-ODAP was measured in tissue of the squirrel monkey 1, 24 and 72 h after an injected dose, the half-life for disappearance was longer for the brain and spinal cord than for any tissue except bone. More specifically, it was suggested that the cerebellum may sequester L-β-ODAP to reach neurotoxic concentrations (Mehta et al. 1980). Unfortunately, it is not known whether L-β-ODAP can enter the BBB of humans after consumption of grass pea. When amino acid levels of CSF were studied in 50 patients with neurolathyrism and 12 healthy volunteers, the levels of excitatory amino acids glutamate appeared to be increased (281%), as well as the concentration of the inhibitory amino acids glycine and taurine (277% and 198%, resp.), with a significant correlation between the level of glycine and the duration of the disease. Threonine, serine and alanine levels were also increased. In contrast to reports on other motor neuron diseases where an increase of isoleucine was observed, a significant decrease of isoleucine was found in neurolathyrism patients. These results suggest a disturbance of amino acid metabolism due to excitotoxic damages caused by L-β-ODAP (Khan et al. 1995). Additionally, the methionine excretion has been found to drop in neurolathyrism patients (Rudra and Chaudhury 1952).

Taken together, these results suggest that L-β-ODAP can enter the CNS in most species. However, no human data are available, so our conclusion relies on experimental models - with the restriction that so far no satisfying animal model has been identified for neurolathyrism. It was suggested that its entry into the CNS is more a time dependent than a concentration dependent phenomenon (Rao 1978) and that the onset of the symptoms may be related to a disturbance of some physiological balance brought about by L-β-ODAP rather than to the presence and levels of the neurotoxin *per se* (Rao 1978).

Malnutrition is also suggested to increase the amount of L-β-ODAP entering the brain, although no studies have been performed yet to address this question (Bridges et al. 1991). How L-β-ODAP enters the brain is unknown, but it has been hypothesized to be transported by the carrier for other anionic amino acids such as L-glutamate and L-aspartate (Oldendorf and Szabo 1976; Khan et al. 1993; Smith 2000). Since reactive oxygen and nitrogen species (ROS and NOS) can contribute to increased BBB permeability, directly by decreasing the synthesis of proteins involved in tight junctions between cells, or indirectly by activation of metalloproteinases, oxidative stress could induce increased BBB permeability in neurolathyrism patients. This 'opening-up' of the BBB may allow neurotoxins or inflammatory cells to enter the brain (Halliwell 2006).

1.3. Mechanisms of L-β-ODAP neurotoxicity

The critical cellular actions of L-β-ODAP that culminate in neuronal degeneration are yet to be established. The most frequently described mechanisms are excitotoxicity and oxidative stress.

1.3.1. Excitotoxicity

What is excitotoxicity?

Excitotoxicity is the term to describe neuronal injury induced by excessive stimulation of glutamate receptors, by mechanisms which include the disturbance of intracellular Ca^{2+} homeostasis and excessive free radical production (Shaw 2005). It was described for the first time in newborn mice, as subcutaneous injection of monosodium glutamate induced acute necrosis in several regions of the developing brain (Olney 1969). Glutamate is the major excitatory transmitter in the human CNS. Under normal physiological conditions, glutamatergic neurotransmission is finely tuned. The intracellular glutamate concentration has been estimated to be rather high compared to the extracellular concentration, as the concentration of free glutamate in homogenized rat brain was

found to be approximately 10 mM, whereas the extracellular glutamate concentration is generally below 1 µM. The highest glutamate concentration is found within presynaptic vesicles (100 mM), which results in concentrations between 2 and 1000 µM in the synaptic cleft. Excitotoxic damage is expected to occur when the extracellular concentration exceeds 2 mM (Meldrum 2000; Emerit et al. 2004). Normally, presynaptically released glutamate binds to surface receptors on postsynaptic neurons (Fig. 5). This binding activates postsynaptic neurons by inducing depolarization and an intracellular (cytoplasmic) Ca^{2+} increase. Glutamate is subsequently removed from the synaptic cleft by glutamate transporters (excitatory amino acid transporters; EAAT), located in the plasma membrane of both neurons and astrocytes. In astrocytes glutamate is converted into glutamine by glutamine synthetase. Glutamine is released into the extracellular space, taken up by presynaptic neurons and converted into glutamate by glutaminase. Glutamate is then stored into presynaptic vesicles, ready for the next glutamate-glutamine cycle (Doble 1999; Hertz 2006).

In many neurodegenerative diseases, a role for excitotoxicity has been proposed in its etiology and its progression. The ability of neurons to prevent excitotoxic damage is related to their Ca^{2+} buffering capacity, accomplished by Ca^{2+} binding proteins and Ca^{2+} sequestration in mitochondria and the ER. It is generally accepted that during intracellular Ca^{2+} overload, these organelles take up Ca^{2+}, which may infer stress and dysfunction of the organelles (see 'Ca^{2+} homeostasis'). The elevated cytoplasmic Ca^{2+} concentrations will further amplify the process of glutamate exocytosis. Additional to this Ca^{2+} induced vesicular release, intracellular cytosolic glutamate may be released by cell lysis and slowing or reversal of glutamate transporters subsequent to depolarization, contributing to elevated glutamate concentrations in the synaptic cleft. Elevated extracellular glutamate concentrations will further depolarize postsynaptic neurons, which will in turn increase $[Ca^{2+}]_i$ and induce glutamate exocytosis. This process that has been called the 'glutamatergic loop' includes the spreading of excitotoxicity to neighboring cells (Doble 1999).

Glutamate-receptors

Glutamate receptors are primarily expressed on the dendrites of post-synaptic neurons but they are also present on both astrocytes and oligodendrocytes. Two types of glutamate receptors have been defined according to the mechanism by which their activation gives rise to a postsynaptic current. i) Ionotropic glutamate receptors form the ion channel pore that is activated when glutamate binds to the receptor. ii) Metabotropic glutamate receptors (mGluRs) indirectly activate ion channels on the plasma membrane through a signaling cascade that involves G proteins and second messengers.

Ionotropic glutamate receptors

Ionotropic glutamate receptors are membrane proteins composed of four large subunits that form a central ion channel pore. Generally, these receptor subunits consist of four domains: an amino-terminal domain, an extracellular ligand-binding domain, a transmembrane domain and an intracellular carboxy-terminal domain. The initial step to activate ionotropic glutamate receptors is binding of the agonist such as L-glutamate to the ligand-binding domain. The structure of ionotropic glutamate receptors, more specifically N-methyl-D-aspartate (NMDA)-receptors, is illustrated in figure 5. Ionotropic receptors include NMDA- and non-NMDA receptors. The latter are also termed AMPA/KA-receptors.

Glutamate, released at an axon terminal, binds to the ligand-binding domain (LBD) of ionotropic glutamate receptor subunits on the plasma membrane of the apposing neuron and opens receptor-coupled channels that permit passage of K^+ out of the target cell and Na^+ and sometimes Ca^{2+} into the target cell. Inward passage of Na^+ ions effects membrane depolarization and may trigger an action potential in the post-synaptic neuron if enough glutamate receptors are activated. The flux of Ca^{2+} ions induces long-term changes in the efficacy of synaptic connections. Failure to control the influx and intracellular concentration of Na^+ and Ca^{2+} within narrow physiological limits may trigger reversible or irreversible pathophysiological changes in the nerve cell (Spencer 1999).

NMDA-receptors

The NMDA-receptor is a hetero-oligomeric protein. Three subunits have been identified: GluN1, GluN2A-D and GluN3A-B. For activation of the NMDA-receptor, two GluN1 subunits need to assemble with two GluN2 subunits or with one GluN2 and one GluN3 subunit.

NMDA-receptors are ligand-gated ion channels that permit the entry of Na^+ and Ca^{2+} and the efflux of K^+. At resting potential, Mg^{2+} creates a voltage-dependent block. Depolarization of the neuron will remove the Mg^{2+}-block by driving Mg^{2+} out of the channel pore, whereas increasing Mg^{2+} concentrations will reduce the probability of channel opening. In addition to the transmembrane Mg^{2+}-binding site, NMDA- receptors also carry L-glutamate binding sites and glycine binding sites on the extracellular ligand binding domain of the GluN2 or GluN1/GluN3 subunit, respectively (see Fig. 5). For activation of the receptor, simultaneous binding of L-glutamate and glycine is needed. In addition to glycine, D-serine (and to a lesser extent L-serine) is an agonist of the GluN1 and GluN3 subunit, having its binding site also on the ligand binding domain. D-serine is synthesized from L-

serine by serine racemase in both astrocytes and neurons (Doble 1999; Traynelis et al. 2010). A number of selective agonists and antagonists for NMDA-receptors have been identified (Table 2).

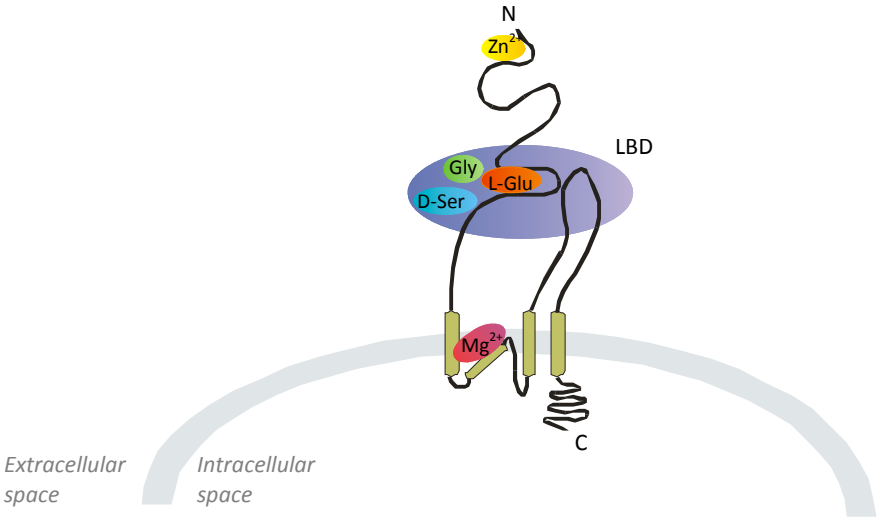

Fig. 5: Schematic presentation of a subunit of the NMDA-receptor. Each NMDA-receptor subunit has a similar structure. The extracellular domain contains the N-terminal domain and a ligand-binding domain (LBD). At the LBD, GluN1 and GluN3 subunits bind the co-agonist glycine (Gly) and D-serine (D-Ser) whereas GluN2 subunits bind L-glutamate (L-Glu). The membrane domain consists of three trans-membrane segments and a re-entrant loop and is responsible for the receptor's Na^+- and Ca^{2+}-permeability and the Mg^{2+} block. The C-terminal domain resides in the cytoplasm.

Receptor	Ionic selectivity	Agonists	Antagonists
NMDA-receptor	Na^+, K^+, Ca^{2+}	NMDA, quinolinic acid, ibotenic acid	D-AP5, selfotel, MK-801, CPP
AMPA-receptor	Na^+, K^+	Quisqualate, AMPA, KA	CNQX, NBQX
Ca^{2+}-permeable AMPA-receptor	Na^+, K^+, Ca^{2+}	Quisqualate, AMPA, KA	NAS
Metabotropic glutamate receptor		Trans-ACPD, quisqualate, ibotenic acid	phenylglycines

Table 2: Well known Glu-R (ant)agonists. D-AP5: DL-2-Amino-5-phosphonopentanoic acid; CNQX: 6-cyano-7-nitroquinoxaline-2,3-dione; CPP: 3-(2-carboxypiperazin-4-yl)propyl-1-phosphonic acid; MK-801: (+)-5-methyl-10,11-dihydro-S*H*-dibenzo[a,d]cyclohepten-5,10-imine maleate; NAS: 1-naphthyl acetyl-spermine; NBQX: 2,3-dioxo-6-nitro-1,2,3,4-tetrahydrobenzo[f]quinoxaline-7-sulfonamide; NMDA: N-methyl-D-aspartate; trans-ACPD: (±)-1-Aminocyclopentane-*trans*-1,3-dicarboxylic acid.

Non-NMDA-receptors

Non-NMDA-receptors are AMPA- and KA-receptors, which are referred to collectively as AMPA/KA-receptors as it is difficult to differentiate between these two subtypes. Nine basic subunits have been identified, termed GluR1-7 and KA1-2. These subunits exist in different isoforms, generated by

alternative splicing. AMPA-receptors are composed of homo- or hetero-oligomers formed from GluR1-4 subunits. The synthesis of the GluR2 subunit protein is subject to an unusual RNA editing process where a CAG codon in the messenger ribonucleic acid (mRNA) is converted into a CGG codon, thus imposing an arginine residue instead of a glutamine residue in the protein. This change converts the Ca^{2+}-permeability of the ion channel into a Ca^{2+}-impermeable channel. So generally, GluR2 plays a dominant role in heteromeric assemblages, making most AMPA-receptors Ca^{2+}-impermeable (Doble 1999; Traynelis et al. 2010). However, Ca^{2+}-permeable AMPA-receptors have been characterized in motor neurons (Carriedo et al. 1996).

AMPA/KA-receptors are ligand-gated cation channels allowing entry of Na^{+} and sometimes Ca^{2+}, and the exit of K^{+} upon activation by glutamate, AMPA or KA (Table 2). Selective agonists for AMPA/KA-receptors are AMPA, KA, domoic acid, and quisqualate. Competitive antagonists include 6-cyano-7-nitroquinoxaline-2,3-dione (CNQX) and 2,3-dioxo-6-nitro-1,2,3,4-tetrahydrobenzo[f]quinoxaline-7-sulfonamide (NBQX). Certain spider and wasp venom toxins, as well as 1-naphthyl acetyl-spermine (NAS), also antagonize responses mediated by AMPA/KA-receptors, more specifically AMPA-receptors which do not contain the GluR2 subunit (Doble 1999).

Metabotropic glutamate receptors

Metabotropic glutamate receptors are G-protein-coupled receptors. Three groups, with a total of eight sub-types have been characterized. Metabotropic glutamate receptors are composed of an extracellular region, a transmembrane region, and an intracellular region. The extracellular region is composed of a Venus Flytrap (or VFT) module that binds glutamate, and a cysteine-rich domain that is thought to play a role in transmitting the conformational change induced by ligand binding from in the VFT module to the transmembrane region. The transmembrane region consists of seven transmembrane domains. Glutamate binding to the extracellular region of a metabotropic glutamate receptor causes activation of G proteins bound to the intracellular region, which are composed of α, β, and γ subunits. In their inactive state, G proteins are bound to guanosine 5'-diphosphate (GDP), but activation of the G protein causes the exchange of guanosine 5'-triphosphate (GTP) for GDP within the α subunit. Activated G protein subunits then modulate the function of multiple biochemical pathways and ion channels in the cell. Activation of receptors belonging to group I leads to stimulation of phospholipase C (PLC), whilst activation of those belonging to groups II and III leads to inhibition of adenylate cyclase activity (Meldrum 2000; Niswender and Conn 2010).

L-β-ODAP as a glutamate-receptor agonist

AMPA-receptors

Two years after its discovery in grass pea, L-β-ODAP was identified for the first time as a powerful excitatory substance in spinal interneurons and Betz cells of cats (Watkins et al. 1966). Later, electrophysiological studies of frog spinal cord characterized L-β-ODAP as a potent glutamate receptor agonist, resembling actions of KA more than those of NMDA (Pearson and Nunn 1981). MacDonald and Morris (1984) further ascribed the site of action of L-β-ODAP to non-NMDA-receptors, as the L-β-ODAP-induced depolarization of cultured mouse spinal neurons was not blocked by NMDA antagonist D-2-amino-5-phosphono-valerate (D-AP5) (MacDonald and Morris 1984; Bridges et al. 1989). Compared to other known neuro-excitatory amino acids, L-β-ODAP was found to be more potent than L-glutamate (Watkins et al. 1966; Mehta et al. 1980). This effect of L-β-ODAP on AMPA-receptors is the most thoroughly investigated effect of L-β-ODAP, therefore, we overview the main results of the *in vitro* experiments (Table 3) – in cell cultures and organotypic slices – and *in vivo* experiments in different species.

In vitro, cell membrane depolarization and an increase in input conductance upon L-β-ODAP application was observed in cultured mouse spinal cord neurons (MacDonald and Morris 1984), in Retzius neurons from the leech (Cemerikic et al. 2001) and in rat hippocampal slices. In these slices, the depolarization resulted from non-NMDA-receptor activation, since it was D-AP5-insensitive and CNQX-sensitive (Bridges et al. 1989). Comparative binding experiments in rodent synaptosomes revealed that L-β-ODAP was approximately 10-fold less potent than AMPA, but two-fold more potent than the endogenous transmitter glutamate (Ross et al. 1989; Spencer 1999). Additionally, radioligand binding assays revealed that only 1 μM L-β-ODAP was sufficient to inhibit half of the ^{3}H-AMPA binding to quisqualate sites in a stereospecific way (Bridges et al. 1988; Bridges et al. 1989). When cloned glutamate receptors were expressed in *Xenopus* oocytes, L-β-ODAP behaved as a potent agonist at AMPA-receptors that were constructed by α1 (which corresponds to GluR1 (Kawamoto et al. 1997)) homomeric (Ca^{2+} permeable) or α1/α2 (GluR1/GluR2) heteromeric (not Ca^{2+} permeable) receptor clones with potency comparable to L-glutamate (Kusama-Eguchi et al. 1996).

Neurotoxicity, resulting from L-β-ODAP-induced AMPA-receptor activation, was confirmed by the effective antagonism of neuronal loss in cultured mouse cortical neurons by the broad spectrum antagonist kynurenate and phorbol 12,13-diacetate (PDA), while not by the selective NMDA-receptor antagonist D-AP5 (Ross and Spencer 1987; Weiss et al. 1989). Kynurenate also blocked L-β-ODAP-induced cell death of rat cerebellar granule cells (Staton and Bristow 1997).

Species	[L-β-ODAP]	Cell type	Reference
Xenopus	0.3 mM, EC_{50} 34 µM (α_1), 9 µM (α_1/α_2)	*Xenopus* oocytes expressing rat NMDA receptor	(Kusama-Eguchi et al. 1996)
Mouse	0.01 – 200 µM	Brain synaptic membranes	(Ross et al. 1989)
Rat	IC_{50}: 47 µM (CPP) or 700 µM (glycine)	Cerebral cortex synaptic membrane	(Kusama-Eguchi et al. 1996)
Rat	IC_{50}: 47 µM	Cerebral cortex synaptic membrane	(Ikegami et al. 1995)
Rat		Synaptic membranes	(Bridges et al. 1989)
Rat	0.1 – 100 µM	Synaptic membranes	(Bridges et al. 1988)
Rat		Hippocampal slices	(Bridges et al. 1989)
Leech	1 – 100 µM	Retzius neurons (ventral nerve cord)	(Cemerikic et al. 2001)
Guinea pig	200 µM	Hippocampal mossy fiber synaptosomes	(Gannon and Terrian 1989)
Rat	10-300 µM, 24-48 h	Primary cortical neuron/glia culture	(Kusama-Eguchi et al. 2004)
Mouse	24 h 20 - 100 µM	Mixed cortical cell culture (neuronal and glial elements)	(Weiss et al. 1989)
Mouse		Explants of spinal cord and frontal cortex	(Spencer et al. 1987)

Table 3: L-β-ODAP as a glutamate receptor agonist. Overview of *in vitro* experiments in different species confirming the agonistic effects of L-β-ODAP on glutamate receptors, indicating the L-β-ODAP concentrations used, the species and cell type.

In vivo, NBQX greatly reduced the cellular damage 24 h after co-injection with L-β-ODAP in the rat hippocampus (Willis et al. 1993). In newborn mice, intracerebroventricular administration of PDA together with L-β-ODAP blocked the symptoms induced when only L-β-ODAP was administered (arm and leg rigidity, seizures, resting arm and hand tremor and postsynaptic neuronal edema) (Ross and Spencer 1987; Spencer et al. 1987). In human hippocampus (obtained from autopsy material of 4 neurolathyrism patients), L-β-ODAP displaced [^{3}H]AMPA binding completely with a potency similar to glutamate (Kunig et al. 1994).

In summary, *in vitro* cell culture experiments have proven L-β-ODAP to be an AMPA-receptor agonist in mouse spinal and cortical neurons and cerebellar granule cells, in rodent synaptosomes, and in leech Retzius neurons. This was also confirmed in rat hippocampal slices and *in vivo* in rat and human hippocampus and in newborn mice.

NMDA-R

At relatively high concentrations, L-β-ODAP exhibits a weak inhibitory activity against the glycine site of cloned mouse NMDA-receptors in *Xenopus* oocytes (see Table 3) (Kusama-Eguchi et al. 1996). In addition, in radioligand assay experiments, L-β-ODAP exhibited a dose-dependent inhibition of [^{3}H]-3-(2-carboxypiperazin-4-yl)propyl-1-phosphonic acid ([^{3}H]CPP) (a competitive antagonist of NMDA-receptors) binding (Ikegami et al. 1995). Another interference of L-β-ODAP with NMDA-receptors was proposed by its carrier function for Zn^{2+} in grass pea (Lambein et al. 1994). Extracellular Zn^{2+} is known

to inhibit NMDA-receptors, by binding on its binding site on the amino-terminal domain of NMDA-receptor subunits. So Zn^{2+} depletion (for instance due to chelation by L-β-ODAP) may indirectly lead to NMDA-receptor activation by reducing the Zn^{2+}-mediated inhibition. Other consequences of chelation of Zn^{2+} (or Cu^{2+}) by L-β-ODAP are discussed later, in the 'oxidative stress' section. When administered to rats, non-convulsive doses of L-β-ODAP increases *in vivo* cerebellar cGMP, a second messenger modulated by NMDA and non-NMDA excitatory amino acid receptors (La Bella et al. 1993). A chronic stimulation of the NO/cGMP pathway has recently been shown to increase the intrinsic excitability of motor neurons (Gonzalez-Forero et al. 2007).

Metabotropic glutamate receptors

Recently, the involvement of metabotropic glutamate receptors on excitotoxicity has been attracting increasing interest. Although antagonists acting on the AMPA-receptor prevented most of the neurotoxicity of rat primary cortical neuron/glia cultures, antagonists acting on group I metabotropic glutamate receptors, including (RS)-1-aminoindan-1,5-dicarboxylic acid (AIDA), (S)-α-methyl-4-carboxyphenylglycine (MCPG) and (*E*)-2-methyl-6-(2-phenylethenyl)pyridine (SIB1893) partially and significantly prevented neuronal death due to L-β-ODAP. Since these antagonists did not have any inhibitory effects on the currents through group I mGluRs expressed in *Xenopus* oocytes, the neurotoxicity induced by L-β-ODAP may be partially mediated by the activation of group I metabotropic glutamate receptors by an indirect mechanism (Kusama-Eguchi et al. 2004).

L-β-ODAP excitotoxicity

L-β-ODAP has been shown to contribute to the glutamatergic loop in several ways. Na^{+}-dependent high-affinity glutamate transport systems by which glutamate is removed from synaptic regions have shown to be inhibited by L-β-ODAP in rat brain and spinal cord (Ross et al. 1985), increasing extracellular glutamate levels. Additionally, L-β-ODAP may facilitate spontaneous and stimulus-evoked presynaptic glutamate release, as was seen in guinea pig synaptosomes (Gannon and Terrian 1989). Also, the evidence that L-β-ODAP is transported by the x_c^- antiporter (Warren et al. 2004), suggests that extracellular glutamate levels may be elevated by transport of glutamate out of the cell. K_i values for L-β-ODAP-induced inhibition of the x_c^- antiporter were comparable to those for glutamate and cystine, indicating the high degree to which L-β-ODAP can mimic the conformations of these dicarboxylic acids and effectively bind to the substrate site of the system x_c^- transport protein (Fig. 6) (Warren et al. 2004). In line with this hypothesis, increased glutamate concentrations have been found in CSF of neurolathyrism patients (Khan et al. 1995).

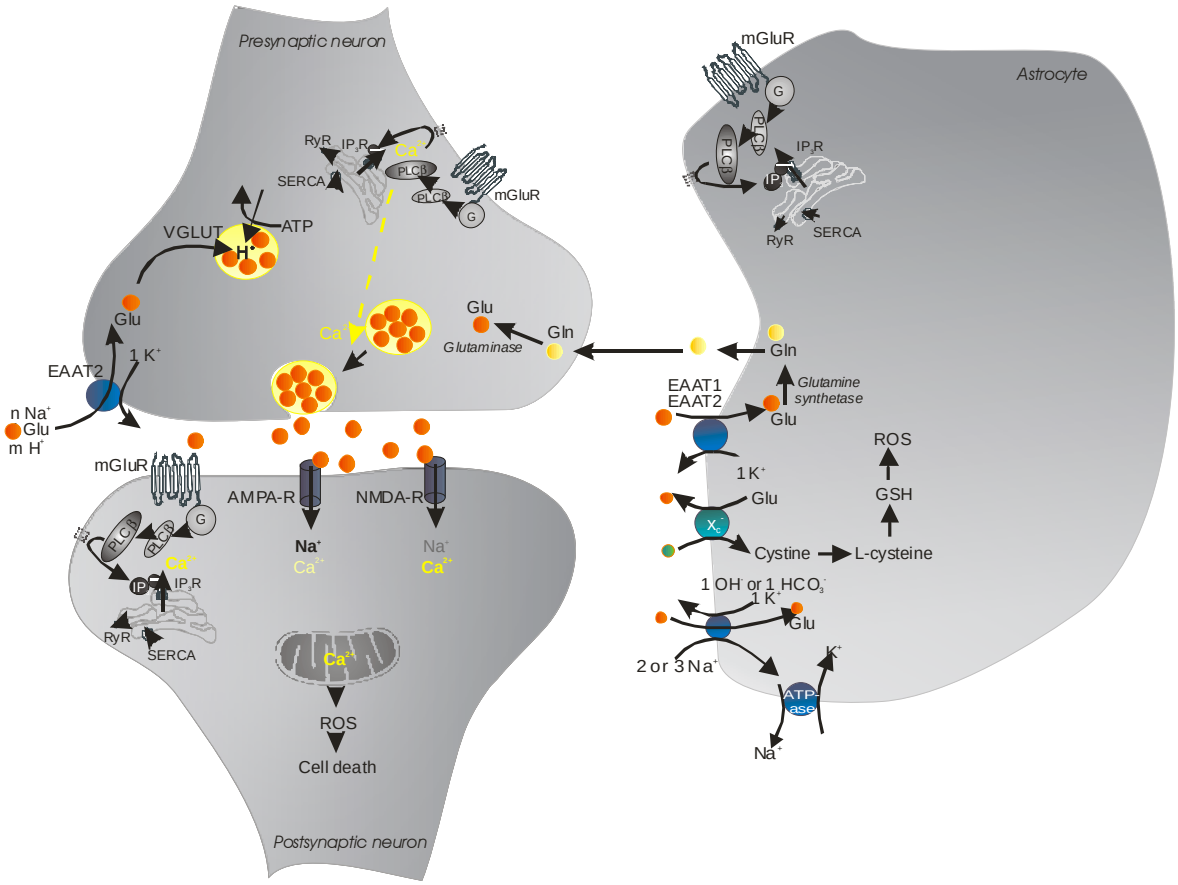

Fig. 6: Excitotoxicity. Glutamate is released presynaptically and binds to ionotropic (AMPA-receptors, NMDA-receptors) and mGluR on postsynaptic neurons. In case of excitotoxicity, overstimulation of these receptors by elevated glutamate levels can result in excessive Ca^{2+} increase, which may contribute to the 'glutamatergic loop' or lead to mitochondrial Ca^{2+} overload, reactive oxygen species (ROS) overproduction and ultimately cell death. Glutamate is removed from the synaptic cleft by glutamate transporters, located both on neurons and astrocytes. In astrocytes glutamate is converted into glutamine by glutamine synthetase (GS). Glutamine is released into the extracellular space, taken up by neurons and converted into glutamate by glutaminase. Increased extracellular glutamate levels will also inhibit the x_c^- antiporter, limiting the uptake of cystine, which results in increased oxidative stress by reduced γ-glutamylcysteinyl glycine (GSH) synthesis.

The majority of the excitotoxic effects of L-β-ODAP occur long after the initial toxin exposure, suggesting that the initial excitatory action of the neurotoxin is not sufficient to produce the observed neurotoxicity. A study from Chase *et al.* (2007) supports a mechanism by which the compound is initially sequestered into a cellular compartment and subsequently released, leading to persistent activation of postsynaptic receptors. This model suggests that following intake, L-β-ODAP crosses the BBB and is sequestered within the brain and spinal cord, probably by system x_c^- (this is discussed more in detail in the section about gliotoxicity). Circulating cystine in the CSF may then trigger the subsequent release of L-β-ODAP, leading to persistent activation of non-NMDA-receptors (Chase et al. 2007).

1.3.2. Glutamate transporters

The removal of glutamate from the extracellular space (especially the synaptic cleft) is crucial for the adequate functioning of the CNS. Therefore, brain cells express different proteins in the plasma membrane to transport glutamate, distinctly localized either in neurons or in astrocytes (Table 4).

Glutamate transporter		**Generally expressed in**	**Exceptions**
EAAT1	GLAST	Astroglial cells in mature and normal CNS	Some ependymal cells Some neurons in retina
EAAT2	GLT	Astroglial cells in mature and normal CNS	Some ependymal cells Some neurons in retina
EAAT3	EAAC	Glutamatergic, GABAergic, cholinergic and aminergic neurons	
EAAT4		Purkinje cells	
EAAT5		Retina (Müller cells and neurons)	

Table 4: Localization of glutamate transporters. GLAST (EAAT1) and GLT (EAAT2) are almost exclusively expressed in astroglial cells, whereas EAAC (EAAT3) is generally expressed in neurons (Danbolt 2001).

Moreover, astrocytes have been reported to respond to neuronal activity: a period of modified neuronal activity (sensory stimulation as whisker activation of mice) and subsequent synaptic release of glutamate induces an increased expression of the glutamate transporters GLT-1 and the glutamate/aspartate transporters (GLAST) (Genoud et al. 2006).

Alterations in glutamate transporter activity or expression are involved in the etiology of neurodegenerative diseases. In ALS, impairment of GLT has been observed as a result of mutant SOD1 mediated oxidation (Shaw 2005; Ilieva et al. 2009). The exact mechanism is not known, but mutant SOD1 has been linked to activation of caspase 3 and cleavage of the carboxyl terminal of GLT-1 (Jackson et al. 1999; Boston-Howes et al. 2006). A 30-90 % loss of GLT protein in motor cortex and spinal cord has been found to be responsible for elevated glutamate levels in CSF of patients with sporadic ALS. This glutamate transporter dysfunction is considered not to be the primary factor leading to development of ALS, but important in the propagation of motor neuron loss. In Alzheimer's disease a redistribution and altered expression of GLAST has been proposed to contribute to decreased glutamate transporter activity, associated with increased excitotoxicity and neurodegeneration (Maragakis and Rothstein 2004).

In neurolathyrism research, aspartate and glutamate transport was found to be reduced in synaptosomes exposed to L-β-ODAP (Table 5) (Ross et al. 1985).

Species	[L-β-ODAP]	Cell type	Reference
Xenopus	< 1 mM	GLAST expressing oocytes	(Kusama-Eguchi et al. 1997)
Xenopus	1 mM	Glutamate transporters expressing oocytes	(Kusama-Eguchi et al. 2004)
Rat	1 mM	Brain and spinal cord synaptosomal fractions	(Ross et al. 1985)

Table 5: Effect of L-β-ODAP on glutamate transporters. Overview of *in vitro* experiments in different species confirming the inhibitory effect of L-β-ODAP on glutamate transporters, indicating the L-β-ODAP concentrations used, the species and cell type.

Kusama-Eguchi *et al.* measured the effect of L-β-ODAP on [^{14}C]L-glutamate uptake by *Xenopus* oocytes having expressed human GLAST, GLL-1 (a liver subtype of GLT) and excitatory amino acid carrier (EAAC). L-β-ODAP inhibited [^{14}C]L-glutamate uptake by the expressed EAAC and GLAST, but did not inhibit that of GLL-1 (Kusama-Eguchi et al. 2004). Previously it was described that L-β-ODAP could also serve as a weak substrate of GLAST (Kusama-Eguchi et al. 1997).

1.3.3. Ca^{2+} homeostasis

Ca^{2+} is a universal and physiologically important signaling ion, involved in many processes such as muscle contraction, neurotransmitter release, fertilization, cell death and blood clotting. While extracellular Ca^{2+} is present at a free concentration of 1-1.5 mM, only a tiny fraction of the intracellular Ca^{2+} is present as free Ca^{2+} ions in solution, being ~100 nM under basal conditions, but rising up to 1-10 µM upon cell activation. The tight spatial and temporal regulation of these elevations in cytosolic free Ca^{2+} concentration ($[Ca^{2+}]_i$) generates an enormous versatility in Ca^{2+} signals which control a wide range of cellular processes, including gene expression, cell-cycle progression, learning and memory, cell death, muscular contraction, secretion and synaptic plasticity (Berridge et al. 2000). To exert control over cytosolic Ca^{2+}, cells must chelate, compartmentalize, or extrude it (Clapham 2007), for which the cells express a range of proteins.

Ca^{2+} ON mechanisms

$[Ca^{2+}]_i$ can increase via entry of external Ca^{2+} or the release from internal stores. External Ca^{2+} can enter the cell via voltage-operated Ca^{2+} channels (VOCCs), receptor-operated Ca^{2+} channels (ROCCs) or store-operated Ca^{2+} channels (SOCCs) (Berridge et al. 2000). A universal mechanism for Ca^{2+} signaling is its release from intracellular compartments of which the most prominent actively sequestering Ca^{2+} compartments – and Ca^{2+} distribution systems - are the endoplasmic reticulum (ER) and mitochondria, spreading like a three-dimensional web within cells.

G-protein-coupled receptors activating PLCβ and tyrosine kinase activating PLCγ cleave phosphatidylinositol-4,5-bisphosphate (PIP_2) into 1,4,5-inositol trisphosphate (IP_3) and diacylglycerol (DAG). IP_3 binding to the IP_3-receptor ER channel allows diffusion of Ca^{2+} from the ER to increase $[Ca^{2+}]_i$. In addition to IP_3-receptors, ryanodine receptors are also expressed on the membrane of the ER, mediating the release of Ca^{2+} into the cytosol in response to ryanodine (< 1 μM concentrations). Moreover, a positive feedback mechanism exists where a small amount of cytosolic Ca^{2+} near the receptor will cause it to release even more Ca^{2+}, which is called Ca^{2+}-induced Ca^{2+}-release (CICR).

Ca^{2+} OFF mechanisms

Generally, basal cytoplasmic $[Ca^{2+}]$ is maintained at low levels by Ca^{2+}-binding proteins such as calbindin or parvalbumin and by ATPase pumps removing Ca^{2+} from the cytosol into the ER (via sarco-/endoplasmic reticulum Ca^{2+} ATPases; SERCA pumps) or out of the cell (via plasma membrane Ca^{2+} ATPases; PMCA pumps) (Fig. 7). These ATPases exchange protons for two (SERCA) or one (PMCA) Ca^{2+} per ATP hydrolyzed. Ca^{2+} can also be extruded to the outside of the cell by the Na^+/Ca^{2+} exchanger (NCX), exchanging one Ca^{2+} ion for three Na^+ ions (Berridge et al. 2000; Clapham 2007). In the brain, three different genotypes have been identified (NCX 1-3) of which the NCX3 isoform contributes to the maintenance of $[Ca^{2+}]_i$ homeostasis, thereby preventing mitochondrial membrane collapse and cell death (see section 'Mitochondrial Ca^{2+} homeostasis' and 'Intracellular Ca^{2+} overload and cell death'). This isoform is crucial in extruding Ca^{2+} upon glutamate stimulation and the early cleavage of NCX3 contributes to Ca^{2+} overload (Szydlowska and Tymianski). Another mechanism of Ca^{2+} uptake is the mitochondrial uniporter (see section 'Mitochondrial Ca^{2+} homeostasis').

Mitochondrial Ca^{2+} homeostasis

The distribution of various Ca^{2+} compartments ensures that Ca^{2+} is only briefly present in the cytoplasm before undergoing sequestration (SERCA) and extrusion (PMCA, NCX). For example, mitochondria are often closely associated with the ER providing the conditions for a local communication between the two organelles (Csordas et al. 2006). Ca^{2+} released from the ER creates a microdomain of high $[Ca^{2+}]$ which is preferentially taken up by mitochondria, this way acting as temporary sinks. Mitochondria sequester large amounts of Ca^{2+} rapidly during the development of a Ca^{2+} signal. They have an enormous capacity to accumulate Ca^{2+} and the mitochondrial matrix contains buffers that prevent the free concentration from rising too high. During the recovery phase Ca^{2+} is released back slowly (Berridge et al. 2000). In neurons, mitochondria are often found clustered at sites of high channel activity. Mitochondrial Ca^{2+} uptake is driven by the mitochondrial

membrane potential (negative inside) through the low-affinity uniporter (half-maximal activation around 15 µM). Whereas Ca^{2+} readily diffuses through large pores in the mitochondrial outer membrane, it crosses the inner mitochondrial membrane via ion channels and transporters, utilizing the electrochemical potential. One Ca^{2+} uptake mechanism across the inner mitochondrial membrane has been identified as a Ca^{2+}-selective ion conductance channel, named MiCa (mitochondrial Ca^{2+} channel) (Clapham 2007). Recently it has been suggested that the affinity for Ca^{2+} of the uniporter can be modulated by certain protein kinases, although this modulation still requires further clarification. Another interesting, yet largely neglected mechanism for mitochondrial Ca^{2+} influx is the Ca^{2+}-induced activation of Ca^{2+} uptake. It produces a substantial acceleration of the Ca^{2+}-uptake rate if non-energized mitochondria are first exposed to micromolar Ca^{2+} concentrations. The molecular mechanisms of this effect are not yet elucidated (Giacomello et al. 2007). Once the cytosolic Ca^{2+} has returned to its resting level, Ca^{2+} is extruded from mitochondria by several efflux mechanisms. These mechanisms appear to be regulated by the Ca^{2+}, Na^{+} or H^{+} concentrations outside and/or inside the mitochondria. The Na^{+}/Ca^{2+} antiporters are electrogenic and accordingly a negative membrane potential inside favors Ca^{2+} extrusion. A large load of Ca^{2+} can be transported back into the cytoplasm, from which it is either returned to the ER or exported from the cell.

Intracellular Ca^{2+} overload and cell death

In many neurodegenerative disorders uncontrolled Ca^{2+} influx into the cell leads to Ca^{2+} neurotoxicity and it is known that the route by which Ca^{2+} ions gain access to the intracellular space is a crucial determinant for cell death induction. During intracellular Ca^{2+} overload, ER and mitochondria take up Ca^{2+}, which may result in ER / mitochondrial stress. Mitochondrial stress or mitochondrial dysfunction, which will be discussed later, includes the imbalance of mitochondrial dynamics, mutations in the mitochondrial genome, excessive ROS production and misfolded protein associations or interactions with the mitochondria. ER stress, which is a cellular stress condition involving ER dysfunction induced by unfolded proteins, viral infection or Ca^{2+} overload, compromises the ability to produce properly folded proteins, and misfolded or unfolded proteins will accumulate. At this point, two pathways may be activated: (1) Activation of the 'unfolded protein response' normally counteracts the effects of the original stress by maintaining the protein-folding capacity of the ER. Initially, protein synthesis is inhibited to temporarily stop production of new proteins. Subsequently, chaperone genes that promote protein folding and translocation of misfolded proteins from the ER for proteasome-dependent degradation are induced. (2) In the 'ER overload response' pathway the ER sends a signal to activate the nuclear factor κB (NF-κB). The mechanism of NF-κB activation is not entirely clear, but it has been suggested that reactive oxygen intermediates act as

second messengers since antioxidants have shown to inhibit NF-κB activation. NF-κB translocates to the nucleus where it activates transcription of immune response and pro-inflammatory genes, such as interferon and cytokine genes. Both pathways prevent accumulation of non-functional and potentially toxic protein products, but may also contribute to their elimination when abnormalities become too extensive, leading to cell death (Herr and Debatin 2001; Orrenius et al. 2003; Lindholm et al. 2006; Lai et al. 2007; Brown 2010). Prolonged ER stress may also activate pro-caspase-12, which acts on effector caspases to induce apoptosis (Nakagawa et al. 2000).

Ca^{2+} can also accumulate in mitochondria (Fig. 7) when $[Ca^{2+}]_i$ rises. Elevated mitochondrial Ca^{2+} stimulates mitochondrial dehydrogenases, which are key enzymes for reduced nicotinamide adenine dinucleotide (NADH) synthesis and mitochondrial energy production (Denton et al. 1988). A $[Ca^{2+}]_i$ increase can furthermore induce the translocation of Bax, an apoptosis-inducing protein, to mitochondria (Smaili et al. 2009), resulting in pore formation and interaction with the permeability transition pore (PTP) components by binding to the voltage-dependent anion channel (VDAC) (Shimizu et al. 1999). PTP opening can also be induced by high concentrations of Ca^{2+} in the mitochondrial matrix, nitrosative and oxidative stress, thiol oxidation and low mitochondrial membrane potential ($\Delta\Psi_m$), which allows the passage of large molecules into the matrix space. As a consequence, swelling of mitochondria and rupture of the outer mitochondrial membrane leads to loss of mitochondrial function, production of reactive oxygen species (ROS) and reactive nitrogen species (RNS), causing oxidation and nitrosylation of membranes, proteins and nucleic acids. These processes promote the release of pro-apoptotic factors such as cytochrome c, triggering the activation of caspases, ultimately inducing apoptotic cell death (Orrenius et al. 2003). Mitochondrial Ca^{2+} increase may hyperpolarize the $\Delta\Psi_m$ by stimulating the mitochondrial ATP production due to Ca^{2+}-sensitive dehydrogenases (pyruvate dehydrogenase, oxoglutarate dehydrogenase and NAD^+-isocytrate dehydrogenase) in the matrix and inner mitochondrial membrane that contribute to ATP synthesis (Denton et al. 1988). Hyperpolarization of the $\Delta\Psi_m$ will attract more Ca^{2+} to the mitochondria. At a certain level of mitochondrial Ca^{2+} loading, mitochondrial functions will be disturbed, leading to a collapse of the $\Delta\Psi_m$. This will ultimately lead to necrosis in case of ATP depletion or apoptosis after opening of the PTP, cytochrome c release and caspase activation (Csordas and Hajnoczky 2009). On the other hand, oxidative stress may also damage plasma membrane Ca^{2+} exporters or Ca^{2+} pumps in the ER. Neurons have a high degree of Ca^{2+} trafficking across their membranes, indicating that interference with Ca^{2+} sequestration and/or disruption of ATP supply produces especially rapid rises in $[Ca^{2+}]_i$. As mentioned before, increased $[Ca^{2+}]_i$ interferes with mitochondrial function, increasing production of ROS (Halliwell 2006). The lack of the Ca^{2+}-binding proteins parvalbumin and calbindin D-28k exposes spinal motor neurons to AMPA-mediated

excitotoxicity (Ince et al. 1993; Elliott and Snider 1995; Reiner et al. 1995; Hugon et al. 1996; Palecek et al. 1999; Van den Bosch et al. 2002b), making these cells specifically vulnerable to cell death induced by oxidative stress or by AMPA-excitotoxicity.

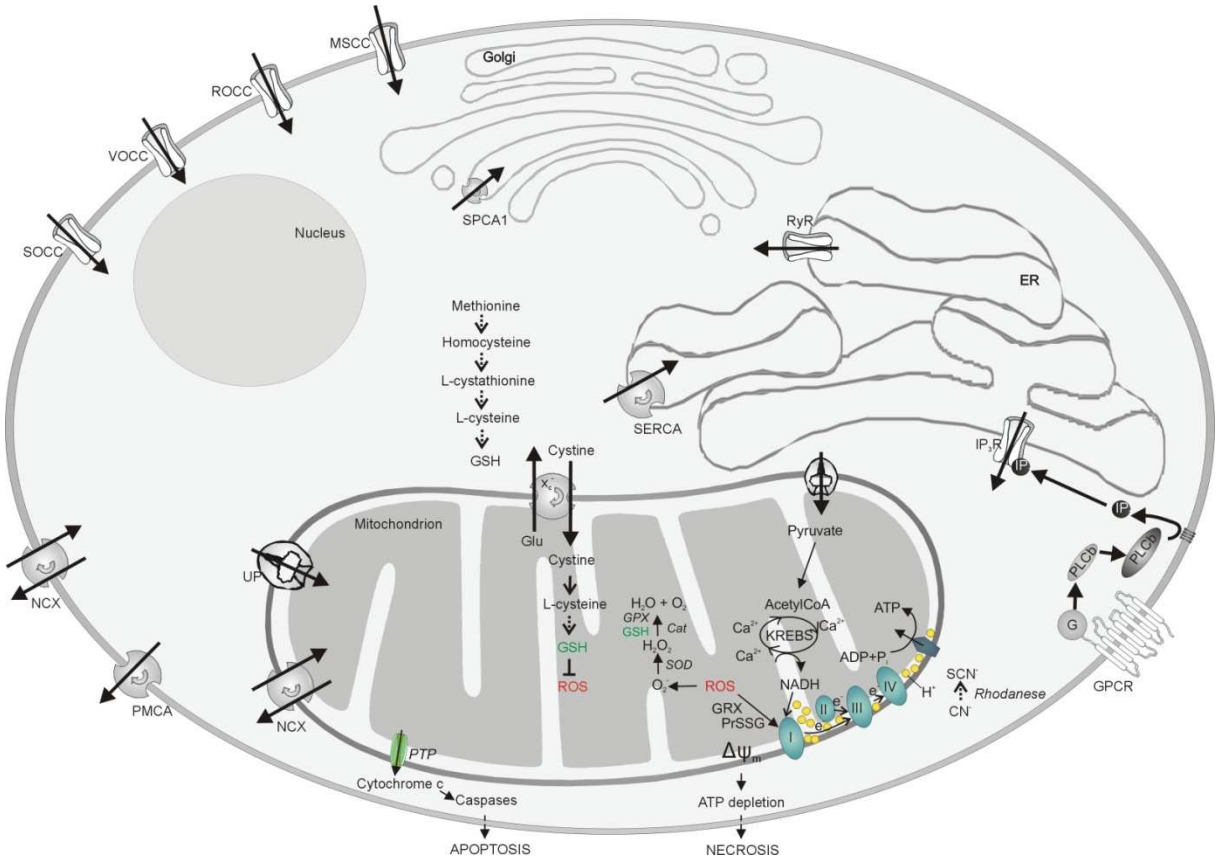

Fig. 7: Ca^{2+} homeostasis and oxidative stress. Ca^{2+} homeostasis: Ca^{2+} enters the cytosol from the extracellular space through store- (SOCC), voltage- (VOCC), receptor- (ROCC) operated Ca^{2+} channels, mechano-sensitive Ca^{2+} channels (MSCC) or G-protein-coupled receptors (GPCR). Cytosolic Ca^{2+} may also rise after release from intracellular stores via IP_3Rs and RYRs. Ca^{2+} is removed from the cytosol by plasma-membrane Ca^{2+} ATPases (PMCA) and Na^+/Ca^{2+} exchangers, while sarco-/endoplasmic Ca^{2+} ATPases (SERCA), secretory-pathway Ca^{2+} ATPases (SPCA) and the low-affinity mitochondrial uniporter (UP) collect Ca^{2+} in the intracellular stores. **Oxidative stress:** Abundantly charged redox carriers in the mitochondrial electron transport chain (high $\Delta\Psi_m$) are likely to produce free radicals. In that case, electrons (e^-) can be transferred to oxygen, generating superoxide (O_2^-) and other ROS. In intact mitochondria, O_2^- is neutralized by superoxide dismutase (SOD), catalase (Cat) and glutathione peroxidase (GPX). L-β-ODAP has been demonstrated to inhibit mitochondrial complex I, by the formation of protein-glutathione mixed disulfides (PrSSG), which is normally reduced by glutaredoxin (GRX) using GSH. Met and Cys are the precursors of GSH, with cystathionine-γ-lyase as the rate limiting enzyme. Mitochondrial Ca^{2+} may stimulate ATP production by Ca^{2+}-sensitive dehydrogenase enzymes. However, mitochondrial Ca^{2+} overload can induce cell death via necrosis (in case of $\Delta\Psi_m$ collapse and ATP depletion) or apoptosis (when cytochrome c is released upon opening of the permeability transition pore (PTP) and caspases are activated). Cyanide (CN^-), which is proposed as a key player in konzo, is converted by rhodanese into thiocyanate (SCN^-). (NCX: Na^+/Ca^{2+} exchanger).

1.3.4. Oxidative stress

Oxidative stress (Fig. 7) is a disturbance of the redox homeostasis caused by a disbalance between the production of free radicals - such as ROS and RNS - and the ability of the cell to efficiently neutralize and remove these potentially toxic substances. Free radicals are most frequently generated in mitochondria, especially when the redox carriers in the mitochondrial electron transport chain are abundantly charged with electrons. In that case, the potential energy for H^+ transfer from the mitochondrial matrix into the intermembrane space is high, which is reflected by a strongly negative $\Delta\Psi_m$. As a consequence, electrons can be transferred to oxygen, generating superoxide (O_2^-) and other members of the ROS family. In structurally and functionally intact mitochondria, ROS are neutralized by enzymes such as superoxide dismutase (SOD), catalase, glutathione peroxidase (GPX) and the endogenous thiol antioxidant GSH to maintain the redox homeostasis. Most GSH is localized in the cytosol, but there is a small pool within mitochondria. Mitochondrial damage with a decreased antioxidant defense capacity (i.e. GSH depletion) is a prerequisite for net ROS production. Once this occurs, a vicious cycle starts whereby ROS further damages mitochondria, resulting in increased free radical generation and more pronounced loss of antioxidant capacity. Previous studies indicated that the mitochondrial GSH pool plays an important role in maintaining cell viability upon exposure to deleterious conditions (Muyderman et al. 2009).

Increases in $[Ca^{2+}]_i$ may result in nitric oxide (NO) production. This gaseous free radical can induce and inhibit neuronal cell death, sometimes at the same time. It is synthesized from L-arginine (or to a lesser extent from homoarginine that is present in *L. sativus*), catalyzed by nitric oxide synthase (NOS). In the brain, two types of NOS (nNOS; type I; mainly in neurons and eNOS; type III; mainly in endothelium) are produced in a rapid, Ca^{2+}-dependent manner, while an inducible and Ca^{2+}-independent form (Type II; iNOS) can be induced by pathophysiological processes such as inflammation and ischemia being produced by glial cells. Generally, high NO levels (20 – 200 nM) have been associated with cell death, whereas low levels of NO (0.2 – 2 nM) are generally considered to be protective. In neurons, NO induces neuronal depolarization which stimulates L-glutamate release. Consequent NMDA-receptor activation induces a Ca^{2+}-influx which activates nNOS to produce NO. NO reacts rapidly with O_2^- to form peroxynitrite ($ONOO^-$), the most reactive RNS (Emerit et al. 2004), which activates poly-ADP-ribose polymerase. Poly-ADP-ribose polymerase is a DNA-repair enzyme, but overactivation of this enzyme depletes NAD^+ (a substrate of the enzyme), which will cause ATP depletion because ATP is used to remake NAD^+. ATP depletion in turn induces necrotic cell death. Another consequence of NO production is the induction of mitochondrial permeability transition. Sustained mitochondrial permeability transition generally leads to the induction of necrosis, whereas transient mitochondrial permeability transition can lead to apoptosis due to

mitochondrial membrane disruption, cytochrome c release and caspase activation. In addition to the deleterious effects of high levels of NO, low levels of NO may be protective. More specifically, low levels of NO from nNOS in neurons and astrocytes may inhibit the inflammatory activation of astrocytes and microglia (Brown 2010).

All aerobic cells can suffer oxidative damage, but the brain is often considered to be especially sensitive (Halliwell 2006) due to its high O_2 consumption (Emerit et al. 2004) and a specific handling of GSH precursors. Cytosolic GSH is the main buffer for the maintenance of the redox homeostasis and is synthesized from L-cysteine, L-glutamate and glycine. Elevated extracellular glutamate, caused by pathological conditions combined with the excitotoxic loop, may limit the ability of the x_c^- antiporter to take up cystine (McBean 2002), possibly resulting in increased oxidative stress. The higher vulnerability to oxidative stress may also result from a different cellular content of L-Met, a precursor of L-cysteine. Using specific methionine antibodies, it was shown that motor neurons are the most Met-immunoreactive cell bodies in glutaraldehyde-fixed rat brain sections (Amara et al. 1995), indicating a stronger dependency on this GSH precursor compared to other cells.

Oxidative stress in neurodegenerative diseases

Oxidative stress, including mitochondrial dysfunction and GSH depletion, has been implicated in a variety of neurodegenerative diseases (for a review see Halliwell, 2006). For instance, glutamine synthetase can be easily damaged by oxidative stress, leading to intracellular accumulation of glutamate by inhibiting its conversion to glutamine (Emerit et al. 2004). In Parkinson's disease, complex-I dysfunction and oxidative stress have been identified as a consequence of accumulation of α-synuclein in mitochondria of human dopaminergic neurons (Devi et al. 2008) and in the substantia nigra GSH levels are reduced (Halliwell 2006). In this context, rotenone – a specific inhibitor of complex I – has for example been applied as an experimental model for Parkinson's disease (Samantaray et al. 2007). In Alzheimer's disease the involvement of mitochondrial damage with the consequent activation of caspases and induction of apoptosis has been clearly documented (Emerit et al. 2004) and cytochrome c oxidase deficiency has been observed in dystrophic neurites of senile plaques in the frontal cortex (Perez-Gracia et al. 2008). Cytochrome c oxidase (complex IV of the electron transfer chain in mitochondria) normally transfers an electron from cytochrome c to ultimately establish an electrochemical potential used by ATP synthase to synthesize ATP, so a deficiency for this enzyme generally results in dysfunction of mitochondrial respiration. In ALS, mitochondrial complex I and IV were reported to display decreased activities (Mattiazzi et al. 2002) and in familial ALS patients, SOD-1 mutations have been well-documented (Rosen et al. 1993).

Oxidative stress may also be related to the impaired ability of the mutant enzyme to bind Zn^{2+} (Emerit et al. 2004) and in mutant SOD expressing cells mitochondrial GSH levels are lower compared to controls (Muyderman et al. 2009). In konzo patients, a deficiency in sulphur-containing amino acids might contribute to the pathophysiological picture, since these amino acids are needed for the activity of the mitochondrial enzyme rhodanese. Rhodanese performs the conversion of cyanides to thiocyanate in a normal nutritional state (Fig. 7). Cyanide may also be converted to cyanate, a neurotoxic species that is known to induce neuronal and axonal damage. Plasma cyanate has been found to increase drastically in rats treated with cyanide when they were maintained on a diet lacking sulphur amino acids (Tor-Agbidye et al. 1999a).

Oxidative stress in neurolathyrism

Increased ROS generation and altered mitochondrial respiration are also considered to be involved in the etiology of neurolathyrism. *In vivo* studies in rats indicated the involvement of ROS, as L-β-ODAP induced neurotoxicity following focal hippocampal injection could be prevented by free radical scavengers such as dimethyl sulphoxide, dimethylthiourea, dimethylformamide or mannitol (Willis et al. 1994; La Bella and Piccoli 2000). In mice, consumption of *L. sativus* significantly increased the cortical and cerebellar levels of ROS and malondialdehyde, while decreasing the activity of the anti-oxidizing enzymes catalase, GPX and glutathione-S-transferase. This L-β-ODAP-induced oxidative stress in turn was found to inhibit cystathionine-γ-lyase, the rate-limiting enzyme responsible for the synthesis of cysteine from methionine. Consequently, GSH synthesis decreases even more, thereby amplifying the oxidative stress load (Diwakar and Ravindranath 2007; Shinomol and Muralidhara 2007).

Recently, L-homoarginine, present at about 1 % of the dry weight in the seeds of *L. sativus*, was suggested to slow down NO synthesis and to act as a substrate for eNOS and nNOS. Another amino acid, β-cyanoalanine, is mentioned because seeds of *L. sativus* are sometimes contaminated with seeds of *V. sativa*, containing β-cyanoalanine, which can lead to hyperactivity, tremors, convulsions and rigidity. It inhibits cystathionase, resulting in impaired defense against oxidative stress. The same is true for methionine sulfoximine, inhibiting γ-glutamylcysteine synthetase, hence inhibiting GSH synthesis (Nunn et al. 2010)

In vitro, L-β-ODAP has been shown to interact with mitochondrial respiration, inhibiting mitochondrial complex I (NADH dehydrogenase) (Pai and Ravindranath 1993; Sriram et al. 1998; Warren et al. 2004), although one group was not able to reproduce and confirm these findings (Table 6) (Sabri et al. 1995). This effect of L-β-ODAP was observed *in vitro* in mouse brain slices and *in vivo* in selected regions of mouse CNS (lumbosacral cord and motor cortex), after exposure to very low L-β-

ODAP concentrations (0.1 pM – 1 nM; 5 – 60 min) and this was also accompanied by a loss of GSH. At higher L-β-ODAP concentrations and longer exposure times (1 nM; 1 h), complex II (succinate dehydrogenase) and complex II-III (succinate-cytochrome c oxidase) were also inhibited.

Species	[L-β-ODAP]	Cell type	Reference
Rat	1-10 mM, 4 d	Ventral spinal cord hybrid motor neuron cell line	(La Bella et al. 1996)
Mouse	0.01 pM – 1 µM, 1 h	Sagittal brain slices	(Sriram et al. 1998)
Mouse	1 nM, 1 h	Saggital brain slices	(Diwakar et al. 2006)
Mouse	0.1 pM	Brain slices	(Pai and Ravindranath 1993; Sabri et al. 1995)
Rat	0.1 pM	Brain slices	(Pai and Ravindranath 1993; Sabri et al. 1995)
SH-SY5Y and N2a cells	1 mM, 24 h	MMP	(Saeed et al. 2008)
LRM55 glioma cells SNB19 glioma cells	100 – 500 µM		(Warren et al. 2004)
Rat	0.1 pM - 1 nM, 5 – 60 min	Sagittal brain slices	(Sriram et al. 1998)
Mouse	5 pM – 1 mM, 1 h	Brain homogenate, mitochondria, slices	(Sabri et al. 1995)

Table 6: L-β-ODAP induced oxidative stress. Overview of *in vitro* experiments in tissues of different species confirming L-β-ODAP-induced oxidative stress.

After the initial inhibition, mitochondrial complex I activity rebounded after incubation with the thiol-reducing agent dithiothreitol (Sriram et al. 1998), which was associated with upregulation of glutaredoxin (thioltransferase), an enzyme that reduces protein-glutathione mixed disulfides (PrSSG) (Fig. 7). During oxidative stress, mitochondrial complex I is especially vulnerable for oxidative modification, because of its cysteine residues – the target of PrSSG formation - in its active sites (Kenchappa et al. 2002). Consequently, the upregulation of glutaredoxin after L-β-ODAP treatment might be a defense mechanism triggered by L-β-ODAP induced oxidative damage. In line with this idea, pre-treatment with antioxidant thiols such as glutathione isopropyl ester and α-lipoic acid neutralized the inhibition of complex I by L-β-ODAP (Sriram et al. 1998). The effects of L-β-ODAP on mitochondrial targets can possibly be explained by its transport into the cell by the x_c^- antiporter. Additionally, increased extracellular glutamate depletes cells of cystine by blocking the gradient-driven glutamate/cystine antiporter system x_c^- (Himi et al. 2003; Lewerenz et al. 2006). As an inhibitor of the antiporter x_c^-, L-β-ODAP can limit the amount of L-cystine that is transported into cells and, consequently, decrease the capacity of the cells to synthesize and maintain appropriate intracellular GSH levels. In turn, the decreased GSH levels render the cells more vulnerable to oxidative damage, which was significant enough to produce the observed cytotoxicity (Murphy et al. 1990; La Bella et al. 1996; Warren et al. 2004). Similarly, L-β-methylamino-alanine (L-BMAA), an analogue of L-β-ODAP in cycad plants, was found to inhibit x_c^- mediated cystine uptake leading to

decreased GSH production (Liu et al. 2009). Elevated extracellular cystine concentrations, or removal of extracellular glutamate have been found to prevent glutamate-induced neurotoxicity (Schubert and Piasecki 2001).

Interestingly, loss of mitochondrial complex I activity in the motor cortex and lumbar cord after chronic treatment of mice with L-β-ODAP (with vacuolation and dendritic swelling of neurons), was only found in male, not in female mice (Sriram et al. 1998). This gender-specific neuroprotection may be attributed to estrogen-mediated upregulation of glutaredoxin, which inhibited L-β-ODAP-induced mitochondrial membrane depolarization in human (SH-SY5Y) neuroblastoma cells. These observations can serve as an explanation for the lower incidence of neurolathyrism in women compared to men (Kenchappa and Ravindranath 2003; Kenchappa et al. 2004; Diwakar et al. 2006). Similar gender-related differences have been described for Parkinson's disease (Saeed et al. 2008). For ALS, there is a complex interaction between gender and clinical phenotypes, but there is evidence that it is more common in men than in women (McCombe and Henderson 2010).

Neuronal vulnerability to oxidative stress may increase due to a disturbed regulation of the intracellular free Cu^{2+} or Zn^{2+} concentration. Zn^{2+} and Cu^{2+} are two ions which are generally bound to proteins. Their intracellular free concentration needs to be tightly regulated in neurons, since either too much or too little free Cu^{2+} or Zn^{2+} in brain cells can lead to increased vulnerability to oxidative stress. Excess free Cu^{2+} may catalyze the formation of reactive hydroxyl radicals, whereas a deficiency of Cu^{2+} will compromise the control of oxidative reactions as it is part of the enzyme SOD1 (Mathie et al. 2006). More specifically, SOD1 requires binding of both Zn^{2+} and Cu^{2+} and the formation of a disulfide bond to be active. In the absence of the metal cofactors or upon reduction of the disulfide, SOD1 is inactive. Likewise, Zn^{2+} deficiency induces oxidative stress and apoptotic death (Mackenzie et al. 2007), probably caused by Zn^{2+} deficient SOD1 (Shaw 2005). Aberrant interactions of amyloid β (Aβ) with Cu^{2+} and Zn^{2+} in Alzheimer's disease have been shown to promote the toxicity and aggregation of Aβ, which renders the Aβ peptide toxic to neurons and probably also reduces the free concentrations of the two metals, impairing the function of SOD1. In epilepsy, elevated Zn^{2+} concentrations have been detected prior to seizure activity, whereas the Zn^{2+} concentration in the brain was lower after seizure activity compared to control mice (Mathie et al. 2006). In ALS, the loss of Zn^{2+} from either wild-type or ALS SOD-mutants was sufficient to induce apoptosis in cultured motor neurons, depending on Cu^{2+} binding to SOD and endogenous NO production (Estevez et al. 1999). In neurolathyrism, L-β-ODAP is capable of forming a complex with Cu^{2+} and Zn^{2+} (Davis et al. 1990; Malisza et al. 1997). Therefore, one aspect of its neurotoxicity is possibly related to the induction of Zn^{2+}-deficiency, which has been shown to diminish superoxide scavenging and increase

tyrosine nitration by SOD and generate superoxide at the expense of antioxidants. Moreover, it has been shown that wild-type SOD could become toxic if a Zn^{2+} chelator accumulates in neurons (Estevez et al. 1999).

1.4. Other effects of L-β-ODAP

1.4.1. Inhibition of inositol phosphate hydrolysis

L-β-ODAP inhibits noradrenalin-stimulated hydrolysis of phosphoinositide in rat cerebral cortical slices (Table 7), at high Na^+ concentrations (120 mM). The effect probably originates from a decreased tyrosine hydroxylase activity, as a loss of tyrosine hydroxylase immunoreactivity was found in the intranigral injection sites following L-β-ODAP intranigral injection. This enzyme converts L-tyrosine to L-DOPA, dopamine and ultimately noradrenalin and adrenaline (Jope et al. 1990; Lindstrom et al. 1990; Ormandy and Jope 1990; Sabri et al. 1995).

Species	[L-β-ODAP]	Cell type	Reference
Chick	0.007-10 µM	Synaptic plasma membrane	(Jain et al. 1998)
Mouse	0.007-10 µM	Synaptic plasma membrane	(Jain et al. 1998)
Rat	0.007-10 µM	Synaptic plasma membrane	(Jain et al. 1998)
Rat	10 µM	Cortical synaptosomes	(Lindstrom et al. 1990)
Rat	IC_{50}: 300 µM	Cerebral cortical slices	(Ormandy and Jope 1990)

Table 7: Other effects of L-β-ODAP. In vitro experiments on the effects of L-β-ODAP on inositol phosphate hydrolysis, VEGFR-2 and tyrosine aminotransferase.

1.4.2. Decreased VEGFR-2 expression

Recently, increasing interest has been attributed to the role of vascular endothelial growth factor (VEGF) in neurodegenerative disorders, having - besides angiogenic effects - neuroprotective effects on many neuronal cell types in the CNS, i.e. protective against excitotoxic stimuli. In the standard model of ALS, i.e. in mice overexpressing the G93A mutant SOD1 protein, and in dopaminergic neurons, which undergo neurodegeneration in Parkinson's disease, VEGF has been shown to exert neuroprotective effects. These neuroprotective effects have been confirmed *in vitro*, but also *in vivo* in acute or chronic models of neurodegeneration. In Alzheimer's disease, VEGF levels are increased in the CNS and plasma and is co-localized with Aβ-plaques (for a review see Ruiz de Almodovar et al., 2009). Neuroprotective effects of VEGF are predominantly mediated by VEGFR-2. A downregulation of VEGFR-2 has previously been described as a result of chronic stress conditions (Ruiz de Almodovar

et al. 2009), more specifically in Wistar rats exposed to (cold) immobilization, forced (cold) swimming, crowding, isolation or vibration twice daily for 21 days (Heine et al. 2005). Similarly, in an animal model of newborn rats, exposed to stress before daily injection with L-β-ODAP a decreased VEGFR-2 expression was reported – while VEGF itself did not show a significant change (Kusama-Eguchi et al. 2010a).

1.4.3. Inhibition of tyrosine aminotransferase

Transport of L-β-ODAP into cells not only removes it from the external environment, but also provides a mechanism to accumulate L-β-ODAP in the cells. This was observed for L-BMAA in ALS/ Parkinson's disease (PD). Incorporation of L-BMAA into proteins has been suggested to play a role in the protein misfolding associated with neurodegenerative diseases (Liu et al. 2009). Accumulation of L-β-ODAP inside cells also provides access to additional intracellular proteins as potential targets in its pathological pathways, such as tyrosine amino transferase and NADH dehydrogenase (Table 7) (Warren et al. 2004). Kalivendi et al. (1997) found that C57BL6J black mice are susceptible to L-β-ODAP neurotoxicity while BALB/c white mice are resistant but become susceptible if pretreated with tyrosine. They established that L-β-ODAP produces a stereospecific inhibition of tyrosine aminotransferase that results in increased synthesis of L-DOPA and dopamine in the brain. While these studies raise the possibility that tyrosine metabolism is involved in the acute behavioral toxicity of L-β-ODAP in mice, it is unclear whether they are relevant to the pathogenesis of human neurolathyrism (Shasi Vardhan et al. 1997; Jain et al. 1998).

1.5. Mechanisms of L-β-ODAP gliotoxicity

In the adult brain about 10^{11}-10^{12} neurons are supported and protected by at least twice as many neuroglial cells, including astrocytes, oligodendrocytes and microglial cells (Emerit et al. 2004). Although considerable attention has focused on the direct action of L-β-ODAP at glutamate receptors, each step in excitatory transmission represents a potential point where an imbalance could contribute to excitotoxicity. Disruption of the processes of release, uptake or metabolism of glutamate might lead to the accumulation of pathological levels of extracellular glutamate or L-β-ODAP. Moreover, glial cells have been suggested to assist neurons by supplying the GSH precursor cysteinyl-glycine, which neurons further cleave to release cysteine for uptake and use in GSH synthesis (Halliwell 2006). This concept of the 'nonautonomous nature' of neurons was also suggested in ALS pathology, where mitochondrial activity in astrocytes seemed to greatly influence

the ability to regulate motor neuron survival (Cassina et al. 2008). Therefore, L-β-ODAP may also exert its effects at any one or any combination of steps, which are not all neuron-specific. This raises the possibility that such CNS toxins may act on glial cells to indirectly induce neurodegeneration.

Species	[L-β-ODAP]	Cell type	Reference
Rat	2.1 ± 0.2 mM, 48h	Primary and secondary cortical astrocyte culture	(Bridges et al. 1991)
Rat	100 µM, 24 h	Cultured cortical astrocytes	(Miller et al. 1993)

Table 8: L-β-ODAP gliotoxicity. Details of *in vitro* experiments of L-β-ODAP gliotoxicity.

Gliotoxic effects of L-β-ODAP are indeed observed in a concentration and duration dependent and stereospecific manner (Table 8). When added to cultures of neonatal rat astrocytes for 48 h, 2.1 mM L-β-ODAP induced lysis of 50 % of the glial cells. If the L-β-ODAP was removed prior to the lysis of the astrocytes, many of the early morphological changes such as vacuole formation and cellular swelling, appeared to be reversible. Lower concentrations of L-β-ODAP (0.75 mM) were found to be more toxic if the duration of the exposure was increased (5 d). Relative to the concentrations of L-β-ODAP necessary to produce a neurotoxic effect *in vitro*, much higher levels of L-β-ODAP were required to bring about a substantial rate of death of the astrocytes. These findings suggest that neurons are much more vulnerable to L-β-ODAP and would most probably be affected long before the induction of gliotoxicity (Bridges et al. 1991). Some studies suggest that the overall impact of L-β-ODAP on the CNS represents a cumulative action at a number of distinct targets on both neurons and astrocytes (see also section 'neuron-astrocyte interactions'). Unlike L-β-ODAP, AMPA and KA did not induce gliotoxicity, opening up the possibility that L-β-ODAP has, in addition to its direct neurotoxicity, also glial cell-related toxic effects (Bridges et al. 1991). L-β-ODAP has been found to alter glial functions at lower concentrations (100 µM; 24 h), such as increasing glutamine synthetase activity. Overall, this effect might be interpreted as a compensatory protective measure of the cells against injury by an increased conversion of glutamate to glutamine. This effect was most likely evoked by the synthesis of new protein, since it was blocked by cycloheximide (Miller et al. 1993). Increased glutamine synthetase activity has also been associated with glutamate-induced $[Ca^{2+}]_i$ elevation in astrocytes. Increased $[Ca^{2+}]_i$ is known to stimulate the release of Mn^{2+} from mitochondria to the cytosol, though the mechanism is not completely understood. This way, glutamine synthetase, which is Mn^{2+}-sensitive and resides in the cytosol, is potentiated by the released Mn^{2+} (Wedler et al. 1994; Simpson and Russell 1998).

1.6. L-β-ODAP and cell death: apoptosis or necrosis?

Cell death can be defined as an irreversible loss of plasma membrane integrity. Based on morphological criteria, three types of cell death have been distinguished in mammalian cells. i) Apoptosis, which is considered as a highly regulated and energy-dependent process, is characterized by nuclear morphological changes (chromatin condensation and fragmentation), nuclear shrinkage, cell shrinkage, blebbing of the plasma membrane and formation of 'apoptotic bodies' that contain nuclear or cytoplasmic material. A family of common death effector molecules in various forms of apoptosis is the caspases, synthesized as inactive proenzymes which cleave substrates upon activation. ii) A second type of cell death is autophagy, which is characterized by accumulation of autophagic vacuoles in the cytoplasm. iii) Necrosis is the more accidental mode of cell death, though increasing evidence points to its regulation by signaling pathways as well. Morphologically, necrotic cell death is characterized by a gain in cell volume, swelling of organelles followed by plasma membrane rupture, which results in the loss of intracellular contents (Fulda et al. 2010).

Generally, glutamate probably induces neuronal cell death by an apoptotic cell death cascade, since caspase inhibitors were found to be effective in preventing glutamate-induced neurotoxicity (Schubert and Piasecki 2001). In ALS, motor neurons probably die by apoptosis, as was deduced from the structural morphology of degenerating motor neurons. This morphology was specified as attrition of the cell body and dendrites and a condensed cytoplasm and nucleus, as well as DNA fragmentation, which is compatible with apoptotic cell death. Increased expression and activities of pro-apoptotic proteins were found in the spinal cord, including caspase 1 and 3 (Martin 1999; Shaw 2005). In Parkinson's disease, neurotoxicity is probably also initiated by an apoptotic cascade, which was confirmed by post-mortem studies as well as *in vivo* and *in vitro* studies. In these studies morphological characteristics of apoptosis were observed, including condensed chromatin in the nucleus with intact cytoplasmic membranes and the presence of apoptotic bodies (Ochu et al. 1998; Hirsch et al. 1999). In PC12 cells increased caspase activity was observed upon exposure to 6-hydroxydopamine, which is a free radical-generating compound that has been used *in vivo* to generate animal models of Parkinson's disease (Ochu et al. 1998). Rotenone – also used to induce experimental Parkinson's disease – has also been found to increase caspase activity, ultimately leading to apoptosis (Samantaray et al. 2007).

L-β-ODAP mediated neuronal and glial death is a repeatedly investigated topic, but the type of cell death - apoptotic or necrotic - has not often been specified.

In a hybrid motor neuron cell line (VSC 4.1 cells), L-β-ODAP treatment resulted in apoptosis (Table 9), characterized by early fragmentation of nuclear DNA and morphological changes that characterize apoptosis such as shrinkage of cell bodies with condensation of cytoplasm, and blebbing of the membrane followed by detachment from the substrate. Cell size progressively decreased until dead cells became fragmented into small bodies. Cells showing advanced morphological criteria for apoptosis were also positive for propidium iodide (PI) staining, indicating cell membrane disruption and thus secondary necrosis. The induction of apoptosis seemed not to be dependent on protein synthesis, since the protein synthesis inhibitor cycloheximide had no protective effect. Endonucleases, however, seemed to play a role, because aurintricarboxylic acid (ATA; a multifunctional molecule also acting as inhibitor of endonucleases) showed a significant though incomplete protection (La Bella et al. 1996).

In cultured rat cerebellar granule cells L-β-ODAP (3 mM; 12 h) caused both apoptotic and necrotic cell death, probably being first apoptotic, resulting in secondary necrosis. Morphologically, apoptotic-like cell shrinkage, membrane blebbing and nuclear condensation was observed, as well as necrotic-like nuclear membrane disruption and swelling of organelles. After a longer exposure (24 - 48 h), the maximum necrotic-like cerebellar granule cell death above control was significantly higher than the apoptotic-like cell death. Biochemically, however, apoptotic-like DNA fragmentation could not be confirmed with agarose gel electrophoresis, but again the endonuclease inhibitor ATA decreased L-β-ODAP-induced apoptosis-like cell death (Staton and Bristow 1997).

Consumption of *L. sativus* seeds at different dosages results in an increased $[Ca^{2+}]_i$ and membrane fluidity, suggesting an overall membrane damage (Amba et al. 2002). It is known that changes in membrane permeability result in increased Ca^{2+} influx, impaired mitochondrial function, and the subsequent generation of ROS. Low levels of ROS act as second messengers and produce neurodegeneration by apoptosis, whereas high levels of ROS produce irreversible damage to cellular components and cause cell death by necrosis (Farooqui et al. 2004).

Species	[L-β-ODAP]	Cell type	Reference
Rat	0.5-10 mM, 24-48 h	Hybrid ventral spinal cord 4.1 cells	(La Bella et al. 1996)
Rat	300 µM – 3 mM, 30 min (+24 h), 24 h or 48 h.	Primary cerebellar granule cell culture	(Staton and Bristow 1997)

Table 9: Apoptosis or necrosis. Specifications of *in vitro* experiments with L-β-ODAP determining the type of cell death. The hybrid ventral spinal cord 4.1 cell line is a fusion product of the neuroblastoma N18TG2 cells with dissociated embryonic rat ventral spinal cord, which has certain similarities with mammalian motor neurons such as active VOCC's and expression of Ca^{2+}-binding proteins (La Bella et al. 1996)

These results suggest that L-β-ODAP toxicity in neurons is mainly an apoptotic process, sometimes resulting in secondary necrosis. Recently, a new animal model was proposed confirming apoptotic cell death. Newborn rats were injected daily with L-β-ODAP after stress induction (separation from their mother for 5 – 7 h). Paraparesis of the hind legs was accompanied with a significant loss of motor neurons in the lumbar and sacral segments of the spinal cord. The remaining motor neurons were smaller in size, some of them having vacuoles in the cytoplasm, less neurites, and replaced by numerous glial cells. Terminal deoxynucleotidyl transferase dUTP nick end labeling (TUNEL), a test specific for apoptosis, revealed positive cells at both ventral and dorsal parts of the lower thoracic, lumbar and sacral cord (Kusama-Eguchi et al. 2009).

1.7. Related diseases

1.7.1. Guam-ALS

ALS is a progressive degenerative disease of upper and lower motor neurons, resulting in the clinical features of muscular atrophy, weakness and spasticity, paralysis and ultimately death. Most ALS occurs sporadically, due to an unknown cause. One hypothesis is that the loss of motor neurons is mediated by chronic excitotoxicity. A rare subtype of ALS occurs in Guam and other Mariana islands in the Western Pacific, often combined with features of Parkinsonism and Alzheimer-type dementia (Guam ALS/PD). Similar to neurolathyrism, the prevalence of Guam ALS/PD is higher for males than for females, and advancing age has also been strongly correlated with this disease (Lynch et al. 2008). Risk factors proposed for this disease are both genetic and environmental, such as chronic nutritional deficiencies of environmental Ca^{2+} and Mg^{2+}, leading to a form of secondary hyperparathyroidism, as well as varying accumulation and distribution of metals such as aluminum, iron and Zn^{2+} in brain tissue (Lynch et al. 2008). The most frequently discussed environmental factor is chronic feeding of L-BMAA, an unusual excitatory amino acid found in the seed of the cycad *Cycas micronesica* (Weiss et al. 1989; Steele and McGeer 2008). Flour made of these seeds is known to be toxic and is therefore soaked in water for prolonged periods before consumption. Another source of L-BMAA on Guam has been suggested to be fruit bats, a culinary delicacy on the island, which apparently accumulate this compound (Nunn et al. 2010). Similar to L-β-ODAP, L-BMAA (also called MeDAP) is found to be a neuro-excitant at AMPA-/KA-receptors (and NMDA-receptors at high doses); however, it does not induce injury on astrocytes (Rao et al. 2006). For its glutamatergic effects, the presence of bicarbonate is needed to form a carbamate adduct on the side chain amino group, as L-BMAA lacks

the side chain carboxylic acid group of glutamate agonists and does not itself activate glutamate receptors (Fig. 8) (Vyas and Weiss 2009).

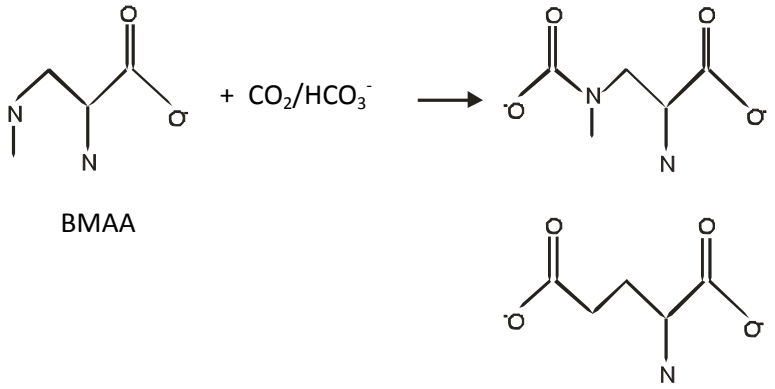

Fig. 8: L-BMAA as a glutamate receptor agonist. L-BMAA has no second carboxylic acid side chain. In the presence of bicarbonate, a carbamate adduct is formed, mimicking the dicarboxlylic acid structure of glutamate. In this conformation, L-BMAA can activate glutamate receptors (Vyas and Weiss 2009).

Motor neurons are selectively injured at relatively low L-BMAA concentrations compared to other spinal neurons. More specifically, a substantially higher L-BMAA-induced $[Ca^{2+}]_i$ increase and dose-dependent ROS generation was observed in motor neurons than in other spinal neurons (Rao et al. 2006). L-BMAA has also been found to drive system x_c^- to release glutamate in the extracellular space (Liu et al. 2009), probably contributing to the 'glutamatergic loop' (see 'excitotoxicity').

In addition to environmental factors, an increased presence of neurofibrillary tangles has been reported in brain and spinal cord tissues of Guam ALS patients, similar to those found in Alzheimer's disease. Additionally, a mutation in the transient receptor potential melastatin 7 (TRPM7) membrane channel - involved in homeostatic regulation of intracellular Ca^{2+} and Mg^{2+} - as well as TRPM2 was found in Guam ALS and Parkinson's disease (Lynch et al. 2008).

1.7.2. Osteolathyrism

The term 'lathyrism' is often used for both neurolathyrism and osteolathyrism, whereas the origin and the symptoms of these disorders are totally different. In osteolathyrism, both free β-aminoproprionitrile (BAPN) and *β-N-*(*γ*-L-glutamyl)aminopropionitrile (*γ*-glutamyl-BAPN), often referred to as osteolathyrogens are taken up from *L. odoratus*. In this disorder, the connective tissue is affected by inhibition of the formation of cross linkages between the polypeptide chains during the synthesis of collagen and elastin (Bell 2003; El Rouby et al. 2008; Ponseti and Brand 2008). In addition

to BAPN, 2-(3-amino-3-carboxypropyl)isoxazolin-5-one (ACI) is present in the seedlings of *L. odoratus*, with 2,4-diaminobutanoic acid (DABA) as its major metabolite (Nunn et al. 2010). A third compound is 2-cyanoethyl-isoxazolin-5-one (CEI), yielding BAPN. When given CEI, chicks show symptoms of osteolathyrism. Generally, osteolathyrism has been produced only in experimental animals fed *L. odoratus,* but in some neurolathyrism patients some skeletal changes have been observed (Weintroub et al. 1980; Haque et al. 1997). While BAPN and its *γ*-glutamyl derivative are not found in seeds of *L. sativus*, ACI, and CEI have been found in the seedlings. As it is the practice in certain areas of the world to eat the green parts of the plant when in season, osteolathyrism observed among some neurolathyrism patients may result from the ingestion of CEI (Bell 2003).

1.7.3. Konzo

Konzo is a non-progressive motor disorder reported in several remote areas of the Central African Republic, Mozambique, Tanzania, and the Democratic Republic of Congo. The disease mainly affects children and – in contradiction to neurolathyrism – women are more affected than men, especially women of childbearing age. Similar to neurolathyrism, konzo is generally characterized by a sudden onset of a spastic paraparesis. Some affected subjects may present with quadriparesis, blurred vision, nystagmus, and speech difficulties (Tshala-Katumbay et al. 2002). It was suggested that in konzo patients cortical motor neurons are primarily affected (Tshala-Katumbay et al. 2002). Epidemiological studies have shown that the disease is associated with cassava (*Manihot esculenta*) being the main source of food for populations prone to protein-calorie deficiency. The combination of the cyanogenic glucoside linamarin (α-hydroxylisobutyronitrile-β-D-glucopyranoside) in insufficiently processed roots and leaves of cassava and low protein intake has been implicated in outbreaks of konzo. Ingested linamarin is hydrolyzed to glucose and cyanohydrins, producing hydrogen cyanide by a catalytic reaction of bacterial β-glucosidase in the intestine (Sreeja et al. 2003). Free cyanide may inhibit cytochrome c oxidase, block mitochondrial electron transport and consequently induce energy failure. Therefore, cyanide must be sequestered by methemoglobin and metabolized, being converted to thiocyanate (SCN^-) by the liver enzyme rhodanese. This enzyme requires the rate-limiting co-factor sulfane sulphur, which is dependent on the availability of dietary sulphur-containing amino acids (Tor-Agbidye et al. 1999a). Decreased rhodanese activity, for instance due to lower intake of sulphur-containing amino acids, may induce accumulation of cyanate (OCN^-). Interestingly, OCN^- has been shown to increase the affinity of AMPA-receptors, possibly increasing synaptic responses in glutamatergic neurons (Shahi and Baudry 1992), suggesting the involvement of excitotoxicity in the etiology of konzo. The mechanisms by which OCN^- causes neuronal degeneration are not understood, but animal studies indicated that OCN^- induces hind limb weakness and

spasticity in rodents and monkeys, suggesting its involvement in konzo (Tor-Agbidye et al. 1999a; Tor-Agbidye et al. 1999b).

1.7.4. Tropical Spastic Paraparesis (TSP) or HTLV-1-associated myelopathy (HAM)

Tropical spastic paraparesis (TSP), also known as Human T cell leukemia virus type 1 (HTLV-1)-associated myelopathy (TSP/HAM), is a slowly progressive spastic paraparesis with an insidious onset in adulthood, with a neuropathology that reflects degeneration of the corticospinal tracts. It has been found all around the world (except in the Polar Regions), mainly in tropical and subtropical regions, affecting more women than men (almost 2:1) of low socioeconomic classes. HTLV-1 has been shown to disturb the astrocytes responsible for maintaining the BBB. HTLV-1 infected T-lymphocytes impair the catabolism and uptake of glutamate by astrocytes, which in turn may affect neuronal function and survival (Zaninovic 2004). Additionally, HTLV-1 protein p13 is targeted to the inner mitochondrial membrane and induces cell death by increasing mitochondrial ROS production, whereas p12 triggers Ca^{2+}-dependent apoptotic signals, including opening of the mitochondrial transition pore, by enhancing Ca^{2+} release from the ER (Saggioro et al. 2009; Silic-Benussi et al. 2010). In Bangladesh, no correlation was found between HTLV-1 infection and neurolathyrism (Haque et al. 1995).

1.7.5. Portosystemic myelopathy

Last but not least, symptoms very similar to neurolathyrism have been described for portosystemic myelopathy (PSM), a disorder observed in patients with cirrhosis and/or portosystemic shunting with a prevalence of 2 %. Though these two disorders probably differ too much to be 'related', it is noteworthy to mention some striking similarities. Similar to neurolathyrism, PSM is characterized by paresis of the extremities, Babinski signs and muscle spasticity in patients, usually only involving the lower extremities. Transcranial magnetic stimulation, which is a reliable method for testing the integrity of the motor pathways and for locating the sites of disruption, showed the absence of responses in the lower extremities and positive responses in the upper extremities, which indicate disruption of transmission in the corticospinal tracts between the cervical and thoracic segments of the spinal cord. Analysis of the CSF was normal. Of all reported cases (61 patients), 90 % were men, with the highest incidence between 40 and 50 years of age. PSM is associated with generalized astrocyte proliferation. Some hypotheses include nutritional deficiencies, vascular insufficiency, hematopoietic abnormalities of the liver, unknown metabolic imbalances, and toxins implicated in portosystemic encephalopathy such as ammonia, mercaptans, short-chain fatty acids and biogenic

amines. Prominent among these hypotheses is the presence of other unidentified injurious substances that are normally removed by the liver but escape removal by bypassing the liver via the portosystemic shunts and the lack of protective substances that are normally formed by the liver, but are decreased by virtue of the liver injury. There is no known beneficial treatment for PSM. However, improvement of PSM has been reported following protein restriction, broad spectrum antibiotic agents or lactulose therapy (Conn et al. 2006).

CHAPTER 2

Aims of the study

CHAPTER 2: Aims of the study

The aim of the present study was to better understand the mechanisms that are responsible for the degeneration of motor neurons in neurolathyrism patients. Therefore the effects of *L. sativus* on the survival and functioning of neuronal, glial and BBB endothelial cells were investigated. We focused on L-β-ODAP, which is believed to be a major causative neuro-excitatory amino acid in *L. sativus*, and also on L-methionine and L-cysteine, two sulphur-containing amino acids deficient in *L. sativus*.

2.1. Effect of L-β-ODAP on the BBB

L-β-ODAP is frequently described to be the causative agent for neurolathyrism, as it has been demonstrated to interact with neuro-excitation in various ways. Therefore, it is necessary to know whether L-β-ODAP can enter the CNS, i.e. if the BBB is permeable for L-β-ODAP. Previous studies did not lead to a conclusive result, since the presence of L-β-ODAP in the CNS was investigated in different species with a varying maturity of the BBB.
Our aim was to study the effects of L-β-ODAP, in comparison with L-glutamate, on an *in vitro* BBB model. More specifically, if the BBB permeability was affected after exposure to L-β-ODAP.

2.2. L-β-ODAP gliotoxicity

Neurons are functioning in close interaction with surrounding glial cells, comprising astrocytes, oligodendrocytes and microglial cells. Therefore, any effect of L-β-ODAP on glial cells may have implications for neuronal functioning. This brought us to investigate the effects of L-β-ODAP on glial cells and to explore the involvement of oxidative stress.

2.3. L-β-ODAP neurotoxicity

Although the mechanism of the action of L-β-ODAP has not been conclusively elucidated, it has been shown that L-β-ODAP activates AMPA-receptors as a glutamate-analogue, inhibits Na^+-dependent high-affinity glutamate transport systems, facilitates spontaneous and stimulus-evoked presynaptic glutamate release and is transported by the x_c^- antiporter, which all support the hypothesis of L-β-ODAP being an excitotoxic agent. As Ca^{2+} is a key player in excitotoxicity, we first aimed to study the effect of L-β-ODAP on the Ca^{2+} homeostasis in neurons. Secondly, since Ca^{2+} overload may be closely linked to increased oxidative stress, and because grass pea is deficient for the sulphur-containing

amino acids L-methionine and L-cysteine (two precursors of the anti-oxidizing agent GSH), it was our aim to study the contribution of oxidative stress in L-β-ODAP-induced neurotoxicity.

The overall goal of this research project was to find strategies that could help in ameliorating the quality of life of the poorest of the poor in developing countries, with special attention towards a safe nutrition. As *L. sativus* is cultivated since the Neolithic times, no replacement is possible in the specific ecology in countries such as Ethiopia. If experimental evidence would indicate that the risk for developing neurolathyrism is significantly reduced by inclusion of antioxidants such as sulphur-containing amino acids in the diet, relatively simple preventive measures can be proposed.

CHAPTER 3

Results

CHAPTER 3: RESULTS

3.1. Effect of L-β-ODAP on the BBB

3.1.1. Abstract

Assuming that L-β-ODAP is responsible for the degeneration of motor neurons, its entry into the CNS must be verified. The CNS is separated from the blood by the BBB and the blood-spinal cord barrier. Passage of L-β-ODAP across the BBB has previously been studied, which has led to controversial results, but these studies generally point to the immaturity of the BBB as a determining factor. In this study, the possible toxic effects of L-β-ODAP on BBB endothelial cells were studied in an endothelial cell line (RBE4) and its effects on BBB permeability were investigated in an *in vitro* BBB model composed of brain capillary endothelial cells (BCEC) grown in a non-contact co-culture with glial cells. The results indicate that exposure of RBE4 cells to high concentrations of L-β-ODAP (5 mM) or L-glutamate (15 mM) for 24 h induced a significant reduction of cell survival. In primary BCEC cultures, acute exposure (2 h) to L-β-ODAP (100 µM – 5 mM) had no effect, whereas a chronic treatment (6 days) with relatively low L-β-ODAP concentrations (200 µM) resulted in an increased BBB permeability. In conclusion, the current results suggest that chronic exposure of brain endothelial cells to L-β-ODAP increases BBB permeability.

3.1.2. Introduction

The BBB and the blood-spinal cord barrier separate the circulating blood from neurons in the brain or spinal cord. These barriers are formed by endothelial cells adjoined by pericytes, astrocytes and microglia that all reside in close association with each other. Circulating blood may contain drugs and pathogens that are deleterious for neuronal cells and an effective separation is essential for normal activity. As already discussed in the general introduction (see section 'Entry of L-β-ODAP in the nervous system'), understanding of the passage of L-β-ODAP across the BBB is necessary in order to appreciate its contribution and role as a possible excitatory amino acid responsible for the degeneration of motor neurons. Studies to address this question have previously indicated that L-β-ODAP can enter the CNS in most species, but this was invariably linked to an immature BBB. An alternative explanation may be that L-β-ODAP has a toxic effect on the BBB, thereby disturbing its function and permeability. Additional observations corroborate this possibility such as the time dependency of the L-β-ODAP effect (Rao 1978) and malnutrition (Bridges et al. 1991) that all may act to influence the BBB permeability.

Here acute and chronic toxicity of L-β-ODAP was studied in an RBE4 cell line and its effects on the permeability (Pe) in primary BCECs co-cultured with glial cells forming an *in vitro* model of the BBB.

3.1.3. Methodology

For these experiments, L-β-ODAP was kindly provided by S. L. N. Rao (Lathyrus Technologies, Hyderabad, India) and L-glutamate was purchased from Sigma-Aldrich.

Cell cultures

RBE4 (rat brain endothelial) cells - kindly provided by Dr. F. Roux (Neurotech, Evry, France) - were grown on collagen-coated recipients (rat-tail collagen, Roche Diagnostics) and maintained in α-MEM/Ham's F10 (1:1) supplemented with 10 % fetal calf serum (FCS), 2 mM glutamine, 300 µg/ml G-418 antibiotic (Gibco, Invitrogen) and 1 ng/ml human recombinant basic fibroblast growth factor (bFGF - Roche Diagnostics) at 37 °C and 5 % CO_2 / 95 % O_2. In this medium, the approximate endogenous L-glutamate concentration is 400 µM (Ye and Sontheimer 1998).

Bovine BCECs were grown in a non-contact co-culture with rat glial cells as described previously (Cecchelli et al. 1999). In summary, glial cells were isolated from Sprague Dawley rat cerebral cortex and cultured for 3 weeks. At the end of this stabilization period, BCEC, seeded onto rat-tail collagen-coated polycarbonate filter inserts (Millicell-PC, 3 µm pore size, 30 mm diameter, Millipore Corporation) were placed into 6-well plates containing the glial cells. BCEC and glial cells were grown together for another 12 days after which BBB features fully developed. During this period, cells were kept in DMEM supplemented with 10 % newborn calf serum, 10 % horse serum, 2 mM L-glutamine, 50 µg/ml gentamicin and 1 ng/ml bFGF. This medium approximately contains 130 µM L-glutamate (Ye and Sontheimer 1998).

Determination of cell viability

RBE4 cells were treated with L-β-ODAP (0 - 5 mM) or L-glutamate (0 - 15 mM) for 24 h. Cell viability was assayed with the CellTiter 96® AQ_{ueous} One Solution Cell Proliferation Assay (Promega, Leiden, Netherlands). This assay measures 3-(4,5-dimethylthiazol-2-yl)-5-(3-carboxymethoxyphenyl)-2-(4-sulfophenyl)-2H-tetrazolium salt (MTS) which is reduced to a colored formazan product by metabolically active cells. The assay buffer was added to the cells as 1:10 (µL buffer / µL medium), and after a 2 h incubation (37 °C, dark) absorbance of the formazan formed was assessed at 490 nm

using a plate reader (Victor-3, type 1420, Perkin Elmer, Brussels, Belgium). Absorbance was evaluated as a percentage of control, corrected for a background signal (medium with assay buffer, without cells).

Transendothelial transport studies

Transendothelial permeability was measured as described previously (Cecchelli et al. 1999). Filter inserts containing confluent BCEC monolayers were separated from the glial cells, washed with 4-(2-hydroxyethyl)piperazine-1-ethanesulfonic acid (Hepes)-buffered Hank's Balanced Salt Solution (HBSS-Hepes: 0.81 mM $MgSO_4.7H_2O$, 0.95 mM $CaCl_2.2H_2O$, 137 mM NaCl, 0.18 mM $Na_2HPO_4.2H_2O$, 5.36 mM KCl, 0.44 mM KH_2PO_4, 5.55 mM D-Glucose, 25 mM Hepes, pH 7.4) and added to a six-well plate with each well containing 2.5 ml HBSS-Hepes (lower compartment). The filter insert (upper compartment) was filled with 1.5 ml HBSS-Hepes containing 50 µM Lucifer yellow (LY; 457 Da) as a transport marker. At different time points the filters were transferred to a new well and samples were then taken from each lower compartment. The temperature was kept at 37 °C. Aliquots were also taken from the upper compartment, at the beginning and the end of the experiment. The cleared volume was determined by dividing the fluorescence in the lower compartment at each time point by the concentration in the upper compartment and was plotted versus time. The slope of this curve, calculated by linear regression, corresponds to the permeability surface (PS) product and subtracting the PS product of an empty, coated filter gives the PS product of the endothelial monolayer. Subsequent division by the surface area of the filter membrane (4.2 cm^2) yields the permeability coefficient Pe.

3.1.4. Results

L-β-ODAP and L-glutamate induce RBE4 death after chronic exposure

To investigate the effect of L-β-ODAP on the BBB, the toxic concentration of L-β-ODAP was verified first, compared to L-glutamate, for a 24 h treatment of RBE4 cells. Fig. 9A depicts the percentage of survival of RBE4 cells after a 24 h treatment with L-β-ODAP or L-glutamate. For these experiments, cell survival was determined by the MTS assay, relative to the number of surviving cells in control cultures (exposed to vehicle). These results revealed that L-β-ODAP was not toxic unless very high concentrations were applied. At high concentrations, L-β-ODAP was more toxic than L-glutamate, as 5 mM L-β-ODAP and 15 mM L-glutamate brought about a similar toxicity level.

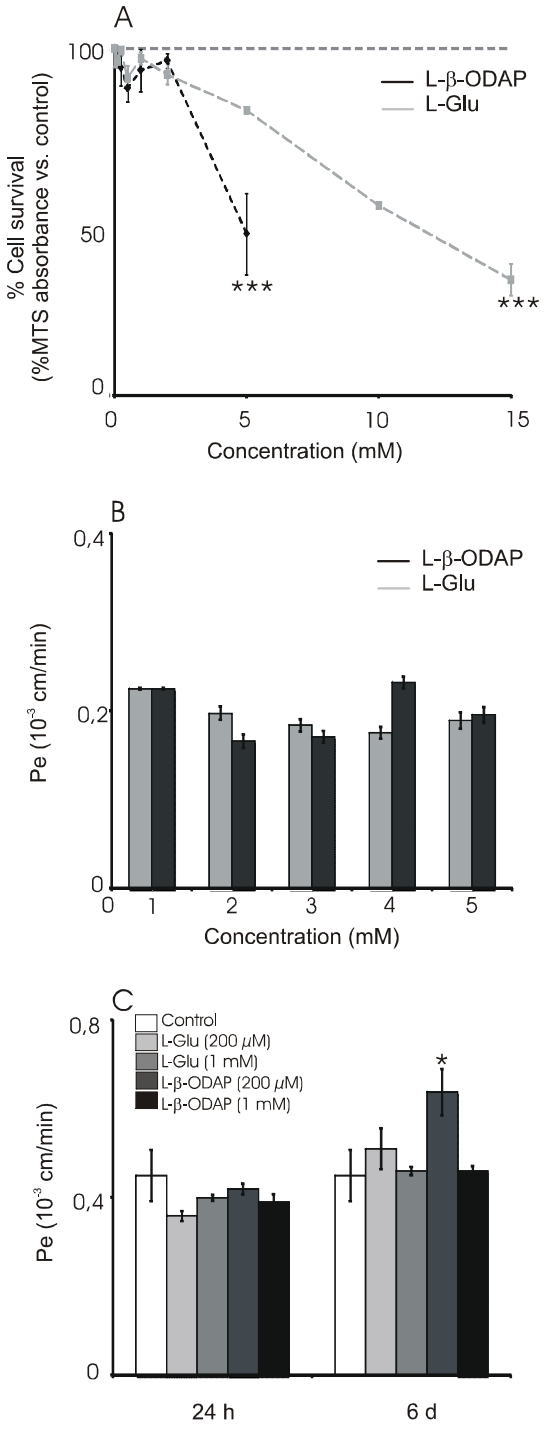

L-β-ODAP or L-glutamate does not increase BCEC permeability after acute exposure

To verify the results obtained in RBE4 cells, the effect of L-β-ODAP and L-glutamate was subsequently investigated in primary BCECs cultured on membranes with glial cells at the bottom of the well (non-contact co-cultures; these experiments were performed in collaboration with Dr. M. Culot and M. Sc. M. Kuntz). Concentrations of L-β-ODAP and L-glutamate up to 5 mM were tested with 2 h exposure times (Fig. 9B), but no effects were observed on the permeability for LY (Pe), demonstrating that neither L-β-ODAP nor L-glutamate alter BBB permeability after 2 h.

L-β-ODAP increases the permeability of BCEC after chronic exposure

Next to acute exposure, the effect of chronic exposure of BCEC to L-β-ODAP was investigated on the Pe (Fig. 9C). These results show that 24 h exposure of BCECs to 200 µM L-β-ODAP or L-glutamate did not alter the LY Pe. Similar Pe values were obtained after exposure to 1 mM of both compounds: 0.39 ± 0.02; $p > 0.05$ for L-β-ODAP, 0.40 ± 0.01; $p > 0.05$ for L-glutamate.

Fig. 9: L-β-ODAP and L-glutamate toxicity to the BBB. A. Percentage of cell survival of RBE4 cells after a 24 h exposure to L-β-ODAP (0 – 5 mM) or L-glutamate (0 – 15 mM) in culture medium. L-β-ODAP was more toxic than L-glutamate, as 5 mM L-β-ODAP and 15 mM L-glutamate brought about a similar significant toxicity level in the same time span. Data are presented as average ± S.E.M.; *** $p < 0.001$ vs. control; n = 4 (corresponding to the number of wells). **B.** Pe of BCEC after 2 h exposure to L-β-ODAP or L-glutamate (up to 5 mM; n = 3 for every condition). No significant effect was observed on the Pe. **C.** Pe of BCEC after exposure of 24 h or 6 days (6 d) to L-β-ODAP or L-glutamate (200 µM or 1 mM). The Pe was significantly increased when BCEC were exposed to 200 µM L-β-ODAP for 6 d. All data are presented as the average of 3 experiments ± S.E.M.; * $p < 0.05$ versus control.

However, when the cells were exposed during 6 days, 200 µM of L-β-ODAP increased the permeability significantly whereas the Pe values were not altered significantly after incubation with 200 µM L-glutamate or after incubation with 1 mM of these compounds (Fig. 9C).

3.1.5. Discussion

Our results in RBE4 cells indicate that exposure to L-β-ODAP and L-glutamate for 24 h is toxic at concentrations of 5 mM and 15 mM, respectively. Acute exposure (2 h) of BCECs to L-β-ODAP or L-glutamate (< 5 mM) did not affect the Pe, but upon longer exposure (6 days; 200 µM), L-β-ODAP significantly increased the Pe. L-glutamate did not have any effect on the BCEC integrity, indicating a specific effect of L-β-ODAP.

Surprisingly, these results were significant at only one concentration (200 µM) and seem to be time-dependent. This L-β-ODAP concentration (200 µM) corresponds to the maximum concentration of 177 µM detected in blood 4 h after consumption of 100 g *L. sativus* (Pratap Rudra et al. 2004), but is higher than the plasma concentration of 5.25 µM 5 h after intake of 200 g boiled grass pea reported by Nunn et al. (1994).

These results are in line with the experience that a single meal of grass pea or short term exposure to L-β-ODAP intake has no known deleterious effects in humans. Moreover, they bring up the interesting possibility that L-β-ODAP increases the BBB permeability after chronic exposure, thereby serving as a possible entry pathway of L-β-ODAP into the mature CNS after prolonged consumption of grass pea. Importantly, an elevation of BBB Pe is associated with additional consequences, including the generation of brain edema, due to the entry of serum proteins in the brain interstitium (Hatashita and Hoff 1990), and the disturbance of electrical excitability of neurons, due to entry of plasma potassium into the brain interstitium (David et al. 2009). Within this background of disturbed neural tissue functioning, L-β-ODAP may exert its toxic activities in the CNS ultimately leading to motor neuron degeneration, which will be discussed in the following sections.

3.1.6. Conclusion

Our results described in this section suggest that 6 days exposure of the BBB to L-β-ODAP increases the BBB permeability to molecules like LY (457 Da). This suggests that L-β-ODAP disturbs the BBB after prolonged intake of grass pea, in order to get access to the CNS, followed by possible toxic effects at the level of neurons and glial cells. These toxic effects may be more pronounced given the fact that a BBB Pe increase creates by itself a pathological condition.

3.2. L-β-ODAP gliotoxicity

3.2.1. Abstract

L-β-ODAP acts as an agonist of ionotropic α-amino-3-hydroxy-5-methyl-4-isoxazole propionic acid (AMPA)-/kainate (KA)-receptors and of metabotropic L-glutamate receptors. It inhibits Na^+-dependent glutamate uptake and glutamate-dependent cystine uptake, and furthermore inhibits complex-I of the mitochondrial electron transfer chain. These multifunctional effects take place in neurons as well as glial cells and result in the accumulation of L-glutamate in the extracellular space, the generation of free radicals and compromises the defense against free radicals. The latter probably plays a role in the pathogenesis of neurolathyrism as grass pea is deficient for L-methionine (Met) and L-cysteine (Cys), two precursors of glutathione (GSH) that confers antioxidant protection.

We here aimed to investigate the toxic effect of L-β-ODAP on glial cells and the possible role of oxidative stress in this process. Gliotoxicity was evaluated in C6 glioma cells and in primary glial cells after applying L-β-ODAP or L-glutamate for 24 h and quantifying cell survival or cell death. This study revealed that L-β-ODAP was toxic for both cell types when applied at millimolar concentrations, whereas L-glutamate was toxic for C6 glioma cells only. Inclusion of Cys or L-ascorbic acid (Asc) in the medium decreased the toxicity of L-β-ODAP and L-glutamate in C6 glioma cells (Met had no effect), suggesting an oxidative component in the gliotoxicity of these substances. However, in primary glial cells, Met, Cys and Asc did not confer any protection against L-β-ODAP toxicity. When sub-populations of glial cells were identified, microglia appeared to be the most vulnerable cell type for L-β-ODAP-induced toxicity. Ultrastructural analysis provided evidence that mitochondria of astrocytes were swollen after treatment with L-β-ODAP. These results indicate that glial cells are susceptible to L-β-ODAP toxicity but that supplementation with Cys or Met has no protective effect at the glial level. The observation that microglial cells are specifically targeted by L-β-ODAP is a novel finding with potentially important consequences as recent evidence suggests that these cells have neuroprotective properties in neurodegenerative diseases.

3.2.2. Introduction

As mentioned in the introduction of this thesis (see section 'Mechanisms of L-β-ODAP gliotoxicity'), an imbalance in each step of excitatory transmission represents a potential contributory factor to excitotoxicity, including the processes of release, uptake or metabolism of L-glutamate. Disturbances in these mechanisms may lead to the accumulation of extracellular L-glutamate. Increased extracellular L-glutamate concentrations, but also L-β-ODAP itself, may activate L-glutamate

receptors such as AMPA- or N-methyl-D-aspartate (NMDA)-receptors, ultimately leading to increased $[Ca^{2+}]_i$ and excitotoxicity. Clearance of L-glutamate from the synaptic cleft is mainly accomplished by Na^+-dependent glutamate transporters on astrocytes of which five structurally distinct subtypes have been identified and characterized: glutamate transporter 1 (GLT1), glutamate-aspartate transporter (GLAST), EAAC1, EAAT4 and EAAT5. In addition, glial cells have been suggested to assist neurons by supplying the GSH precursor cysteinyl-glycine, which neurons further cleave to release Cys for uptake and use in GSH synthesis (Halliwell 2006). In case of decreased cysteinyl-glycine supply of astrocytes to neurons, neuronal oxidative stress may thus be increased.

Previously, L-β-ODAP-induced gliotoxicity has been described in astrocytes (2.1 mM for 48 h induced 50 % toxicity) (Bridges et al. 1991). In addition, L-β-ODAP was found to be an inhibitor (Murphy et al. 1990) and a substrate (Warren et al. 2004) of the the L-glutamate-L-cystine antiporter (system x_c^-), providing a mechanism for decreased GSH production due to limited cystine uptake, and for intracellular accumulation of L-β-ODAP. Finally, increased glutamine synthetase activity has been described as a subgliotoxic effect of L-β-ODAP (Miller et al. 1993). Collectively, these data suggest that L-β-ODAP may indirectly contribute to neurodegeneration by acting on glial cells.

The aim of the present study was to elucidate the effect of L-β-ODAP, in comparison with L-glutamate, on the function and survival of glial cells and determine the involvement of an oxidative stress component. In C6 glioma cells, a glia-derived tumor cell line, the L-glutamate-L-cystine antiporter (system x_c^-), the L-glutamate transporters EAAC1, GLAST and GLT-1 and the metabotropic glutamate-receptors type I, II and III are expressed (Kato et al. 1992; Imura et al. 1999; Yao et al. 2005). This cell line therefore serves as an appropriate model to explore gliotoxic effects of L-β-ODAP and L-glutamate. However, there are notable differences between C6 glioma cells and astrocytes, such as the inability of C6 glioma cells to synthesize L-glutamine from L-glutamate (Brennan et al. 2006). Considering the importance of this step in maintaining low intrasynaptic L-glutamate concentrations, the C6 glioma cell studies were complemented with investigations on primary glial cell cultures.

Our results show that L-β-ODAP is toxic to C6 glioma and glial cells at millimolar concentrations. Cys and Asc, two anti-oxidative agents, were protective against L-β-ODAP and L-glutamate-induced cell death in C6 glioma cells, whereas Met had no effect. The effect of β-estradiol 3-benzoate (EB) inclusion in the treatment medium was also studied, as epidemiological data suggest that men are more susceptible to develop neurolathyrism compared to women, which may be related to a protective role for estrogens in L-β-ODAP-induced gliotoxicity. However, EB had no significant effects on L-β-ODAP toxicity in C6 glioma cells. In primary glial cells, inclusion of Met, Cys or Asc in the treatment medium had no protective effect on L-β-ODAP toxicity. It was however noticed in these cells that L-β-ODAP exposure resulted in mitochondrial swelling, which may correspond to an early

stage of mitochondrial dysfunction. Finally, immunostaining of the subpopulations of glial cells indicated that microglia were the most susceptible cell type to L-β-ODAP-induced toxicity.

3.2.3. Methodology

Cell culture

C6 cells were grown in Dulbecco's Modified Eagle Medium and Ham's F12 (DMEM:Ham's F12 (1:1); Invitrogen, Merelbeke, Belgium) with 10 % (v/v) fetal bovine serum (FBS) to which 100 U/mL penicillin, 100 µg/mL streptomycin, 0.25 µg/mL fungizone and 2 mM glutamine were added. Cells were incubated at 37 °C with 5 % CO_2 / 95 % O_2 in a fully humidified incubator. In this medium, the approximate endogenous L-glutamate concentration is 150 µM (Ye and Sontheimer 1998) and the Met concentration is estimated to be 117 µM (Martınez-Chantar et al. 2003). For Cys no estimation of the concentration in FBS could be found, but the endogenous cystine hydrochloride concentration in DMEM:Ham's F-12 medium is 114 µM. Cell cultures were utilized up to passage number 20.
Prior to experiments with EB (Sigma-Aldrich, Bornem, Belgium), cells were transferred from medium with 10 % FBS to 1 % FBS and cells were incubated in this serum-poor medium for 24 h.

For the cultured primary glial cells, the precursors of glial cells were extracted from neonatal rat cortex as previously described (Booher and Sensenbrenner 1972). The cerebral tissue was recovered and forced through a nylon sieve (80 µm porosity). The obtained cellular suspension was seeded in 6-well plates at 1.2 x 10^5 cells/mL medium. The glial cells were cultured in DMEM supplemented with 10 % fetal calf serum (FCS), 2 mM glutamine and 50 µg/mL gentamicin. The endogenous L-glutamate and Met concentrations in this medium are estimated to be 100 µM and 203 µM, respectively (Ye and Sontheimer 1998; Martınez-Chantar et al. 2003), whereas DMEM does not contain free Cys. The medium was refreshed every three days during three weeks, which was the time needed to obtain a stabilized culture.

Cell viability/cell death assays

C6 glioma cells were grown in 24-well or 96-well plates (Becton Dickinson, Erembodegem, Belgium) and treated with L-β-ODAP (kindly provided by S.L.N. Rao) or L-glutamate for 24 h (Sigma-Aldrich, Bornem, Belgium). For EB-experiments, the following 48 h the cells were treated in DMEM medium with 1% FBS. Cell viability was assayed with the CellTiter 96® AQ_{ueous} One Solution Cell Proliferation Assay (Promega, Leiden, Netherlands). This assay measures 3-(4,5-dimethylthiazol-2-yl)-5-(3-carboxymethoxyphenyl)-2-(4-sulfophenyl)-2H-tetrazolium salt (MTS) which is reduced to a colored

formazan product by metabolically active cells and is soluble in the medium. The assay buffer was added to the cells as 1:10 (µL buffer / µL medium), and after a 2 h incubation (37 °C, dark) absorbance was measured at 490 nm using a plate reader (Victor-3, type 1420, Perkin Elmer, Brussels, Belgium). Absorbance was evaluated as a percentage of control, corrected for a background signal (medium with assay buffer, without cells). Apoptotic cell death was determined with the Caspase-Glo® 3/7 assay (Promega, Leiden, Netherlands), estimating the activity of caspase-3 and -7. Caspase-Glo 3/7 reagent was diluted in the treatment medium after the exposure of the cells to L-β-ODAP or L-glutamate (1:3; v/v), incubated for 1 hour at room temperature and luminescence was measured with a plate reader (Victor-3, type 1420, Perkin Elmer, Brussels, Belgium). Necrotic cell death – characterized by a disrupted membrane - was studied using propidium iodide (PI; Invitrogen, Merelbeke, Belgium) together with 4',6-diamidine-2-phenylindole-dihydrochloride (DAPI) or Hoechst 33342 to determine the total number of cells – cell death was then expressed relative to the total number of cells present in the culture. Cells with a disrupted membrane, were detected after incubating the cells with 30 µM PI in 4-(2-hydroxyethyl)piperazine-1-ethanesulfonic acid (Hepes)-buffered Hank's Balanced Salt Solution (HBSS-Hepes: 0.81 mM $MgSO_4.7H_2O$, 0.95 mM $CaCl_2.2H_2O$, 137 mM NaCl, 0.18 mM $Na_2HPO_4.2H_2O$, 5.36 mM KCl, 0.44 mM KH_2PO_4, 5.55 mM D-Glucose, 25 mM Hepes, pH 7.4) for 20 min at 37 °C. After fixing the cells with 4 % paraformaldehyde (w/v; dissolved in phosphate-buffered salt solution (PBS) supplemented with Ca^{2+} and Mg^{2+} ($PBSD^+$)) for 20 min at room temperature, nuclei were visualized with DAPI (1 µg/ml; 5 min; in $PBSD^+$). Cells were mounted with Vectashield fluorescent mounting medium (VWR International, Leuven, Belgium), covered with a glass coverslip, and images were recorded with an inverted epifluorescence microscope (Nikon Eclipse TE 300, Analis, Gent). Staining with PI and Hoechst 33342 was performed without prior fixation. The cultures were incubated for 5 min in PBS containing Hoechst 33342 and PI (10 µg/mL) and fixated by 4 % paraformaldehyde. The percentage of dead cells was calculated from the number of PI positive nuclei versus the number of Hoechst 33342 marked nuclei.

Staining with annexin V-fluorescein isothiocyanate (FITC) and Hoechst 33342 was performed as follows: the cultures were rinsed twice with $PBSD^+$, stained with annexin V-FITC (1:50 dilution; Roche Diagnostics, Penzberg, Germany) and 2 µg/ml Hoechst 33342 in annexin V buffer (140 mM NaCl, 5 mM $CaCl_2$, 10 mM Hepes, pH 7.4) for 15 min at room temperature and rinsed another four times with $PBSD^+$.

Oxidative stress assay

To detect intracellular ROS generation, the probe 2'-7'-dichlorodihydrofluorescein diacetate (H_2DCFDA; Sigma-Aldrich) was used. H_2DCFDA has no fluorescence until it passively diffuses into cells,

where intracellular esterases cleave the acetates and the oxidation of H_2DCFDA by H_2O_2 produces a green fluorescent signal. C6 glioma cells were grown on 4-well plates (Novolab) to confluent cultures. The cells were loaded for 30 minutes with 50 µM H_2DCFDA in HBSS-Hepes, with 1 mM probenecid (Sigma-Aldrich). Subsequently, the cells were treated in culture medium with L-β-ODAP (5 mM), L-glutamate (15 mM) or H_2O_2 (200 µM) as a positive control, in a 5 % CO_2 / 95 % O_2 incubator at 37°C. Fluorescence intensity was registered after 15 min de-esterification and continued at different time points up to 24 h. For correction of background fluorescence the mean fluorescence of unloaded treated cells was subtracted from the measure fluorescence, which was further normalized for untreated cells (100 %).

Immunostaining of glial cells

Glial cells were characterized by immunostaining with ED-1, anti-O4 and glial fibrillary acidic protein (GFAP) (Molecular Probes, USA) in collaboration with Dr. M. Culot and M. Sc. M. Kuntz (Laboratoire de Physiopathologie de la Barrière Hémato-Encéphalique, Faculté Jean Perrin,Université Lille Nord de France, Lens, France). After fixation in 4 % paraformaldehyde (w/v; in $PBSD^+$) for 10 min at 4 °C, the cells were incubated in TNO (Tris 20 mM, NaCl 0.5 M, pH 7, 0.5 % ovalbumin), supplemented with horse serum (1:100). Microglia were visualized by ED-1, a monoclonal mouse immunoglobulin G (IgG) directed against rat CD68, a marker for activated microglia (30 min incubation). After rinsing with TNO, the cells were exposed to the secondary antibody (anti-mouse IgG; 1:100 in TNO), conjugated with a red (Alexa 568 nm) or green (Alexa 488 nm) fluorochrome, for 30 min at room temperature. Oligodendrocytes were marked with rat IgM anti-O4 (primary antibody diluted at 1:200 in TNO – incubation overnight at 4 °C) and visualized with a fluorescein (alexa 568 nm) conjugated with a mouse anti IgM antibody (1:100; 1 h). Astrocytes were characterized by the cytoskeletal marker GFAP. First the cells were premeabilized by saponin (0.1 %; w/v) for 10 min. A subsequent labeling with a rabbit anti-GFAP antibody (1:500 in TNO; 30 min; room temperature) and incubation with rabbit anti-globulin antibody, coupled with a green fluorochrome (Alexa® 488 nm; 30 min; room temperature) visualized the astrocytes.

In addition to this specific labeling, all nuclei of glial cells were marked with Hoechst 33342 (Sigma-Aldrich, St. Louis, USA) (2 min). The immunolabeling was visualized on a Leica DMRB fluorescence microscope (Leica, Microsystems, Wetzlar, Germany) and the images, registered by a CCD camera (Lheritier, Lhesa Electronique, Cergy, France), were processed by Adobe Photoshop (Adobe Systems, San Jose, CA).

Mitochondrial staining

Labeling with Rh-123 (5 µM; 30 min; 37 °C in HBSS-Hepes) was combined with Hoechst 33342 (2 µg/mL). Imaging was performed with the same equipment as described in the section "L-β-ODAP neurotoxicity – N2a neuroblastoma cells".

Transmission electron microscopy

Transmission electron microscopy was performed as described for N2a cells. Briefly, the cells were fixed (1 h; 2 % (v/v) with glutaraldehyde buffered with 0.1 M Na-cacodylate containing 1 mM $CaCl_2$; pH 7.4), rinsed in 0.1 M Na-cacodylate containing 7.5 % (w/v) sucrose, and post-fixed overnight in 4 % OsO_4 in 0.1 M Na-cacodylate. After dehydratation with ethanol the samples were infiltrated with a mixture of ethanol and LX-112 resin and polymerized for 48 h at 60 °C. The samples were stained with uranyl acetate and Reynold's lead citrate and the sections were examined by transmission electron microscopy.

Statistical analysis

Statistical significance was determined by one way ANOVA with post-hoc Bonferroni or its non-parametric analogues Mann-Whitney or Kruskal-Wallis, using GraphPad Instat software (GraphPad Software; San Diego, CA). Values represent mean ± S.E.M., *n* is the number of wells. Statistical significance is indicated in the graphs by one, two or three symbols for $p < 0.05$, $p < 0.01$ or $p < 0.001$ respectively.

3.2.4. Results

L-β-ODAP has toxic effects on C6 glioma cells and rat primary glial cells while L-glutamate is only toxic for C6 glioma cells

Toxic concentrations of L-β-ODAP and L-glutamate after 24 h treatment were determined by quantifying cell death using PI staining and cell survival quantified by the percentage of MTS absorbance compared to untreated cells (100 %). In C6 glioma cells, L-β-ODAP and L-glutamate were significantly and comparably toxic to the cells at 5 mM and 15 mM respectively (Fig. 10A). Cell survival measurements showed a similar toxicity pattern (Fig. 10B). Primary glial cells displayed a comparable concentration-dependent susceptibility to L-β-ODAP but the levels of cell death (or loss

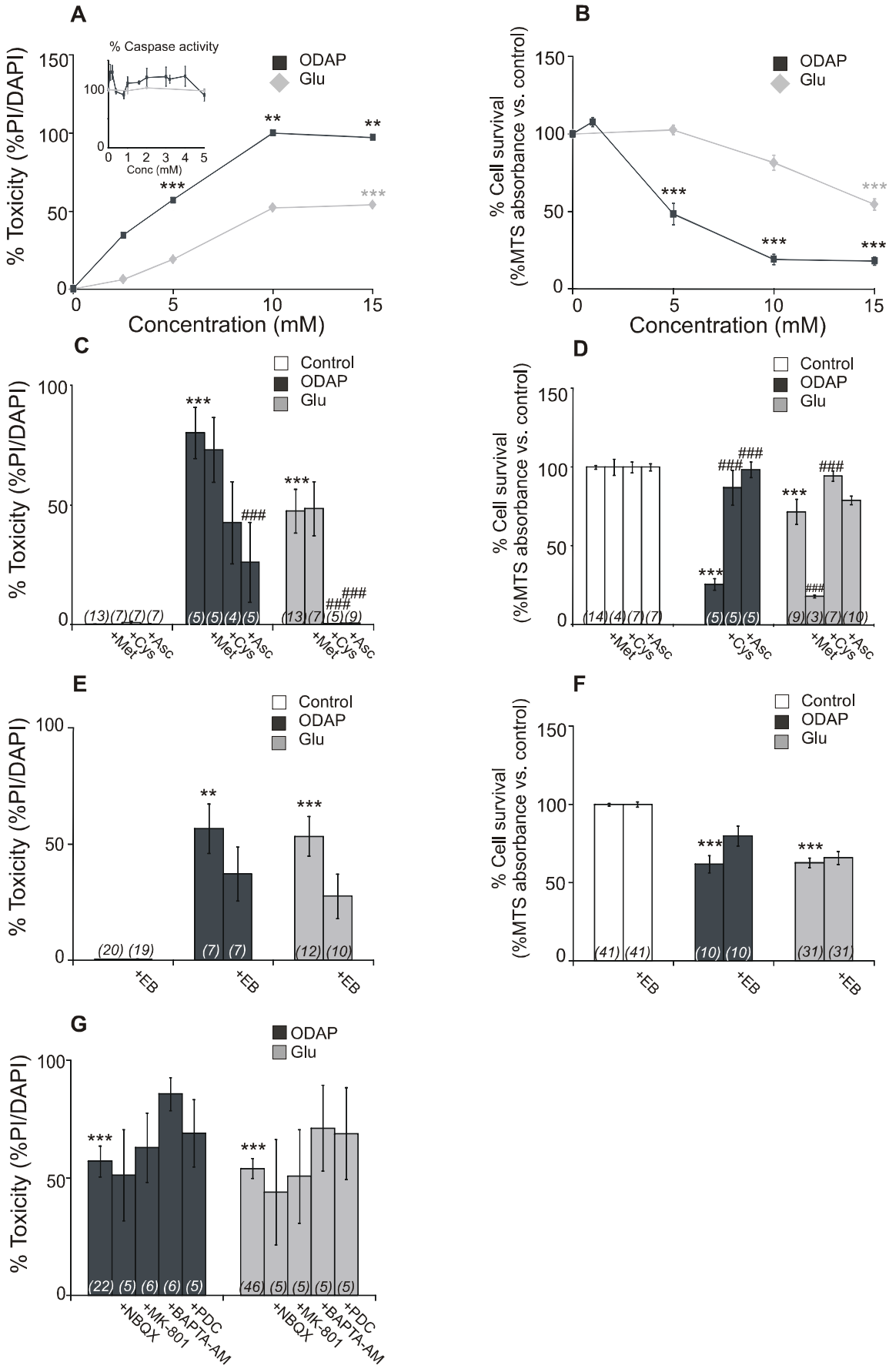
A
% Caspase activity
100
0
0 1 2 3 4 5
Conc (mM)
ODAP
Glu
% Toxicity (%PI/DAPI)
150
100
50
0
0 5 10 15
Concentration (mM)
B
ODAP
Glu
% Cell survival
(%MTS absorbance vs. control)
Concentration (mM)
C
Control
ODAP
Glu
% Toxicity (%PI/DAPI)
(13)(7)(7)(7)
(5)(5)(4)(5)
(13)(7)(5)(9)
+Met
+Cys
+Asc
D
Control
ODAP
Glu
% Cell survival
(%MTS absorbance vs. control)
(14)(4)(7)(7)
(5)(5)(5)
(9)(3)(7)(10)
E
Control
ODAP
Glu
% Toxicity (%PI/DAPI)
(20) (19)
(7) (7)
(12) (10)
+EB
F
Control
ODAP
Glu
% Cell survival
(%MTS absorbance vs. control)
(41) (41)
(10) (10)
(31) (31)
G
ODAP
Glu
% Toxicity (%PI/DAPI)
(22) (5) (6) (6) (5)
(46) (5) (5) (5) (5)
+NBQX
+MK-801
+BAPTA-AM
+PDC

Fig. 10: L-β-ODAP and L-glutamate toxicity in C6 glioma cells. A. Concentration-response curve of PI-positive cells (as a percentage of DAPI-stained nuclei) after 24 h treatment with L-β-ODAP or L-glutamate. Exposure of the cells to 5 mM of L-β-ODAP and 15 mM of L-glutamate resulted in a significant and comparable toxicity. Averages are represented ± S.E.M., statistical significance is represented by *** for $p < 0.001$ and ** for $p < 0.01$ as compared to control (n, being the number of wells, varies between 1 and 46). **Inset to A.** Concentration-response curve of caspase luminescence after 3 h exposure to L-β-ODAP or L-glutamate (0-5 mM; n = 2 - 16). No significant change in caspase luminescence was observed. **B.** Concentration-response curve of cell survival after 24 h treatment with L-β-ODAP or L-glutamate, measured by MTS absorbance, normalized to the absorbance in untreated cells (100 %). Exposure of the cells to 5 mM of L-β-ODAP and 15 mM of L-glutamate resulted in a significant and comparable toxic effect. Averages are represented ± S.E.M., statistical significance is represented by *** for $p < 0.001$ as compared to control, n varies between 4 and 44. **C.** Summary graph of cell death (% PI-positive nuclei) after treatment with L-β-ODAP (5 mM) or L-glutamate (15 mM) with inclusion of compounds with antioxidant capacity in the treatment medium. Cys (200 µM) and Asc (100 µM) protected the cells, whereas Met (200 µM) had no effect. Data are represented as described for A. ### is $p < 0.001$, being significantly different from L-β-ODAP of L-glutamate. **D.** Cell survival (% MTS absorbance) after exposure of the cells to L-β-ODAP (5 mM) or L-glutamate (15 mM) with inclusion of Met, Cys or Asc in the treatment medium. Cys (200 µM) and Asc (100 µM) protected the cells, whereas Met (200 µM) had no effect. Data are represented as described for A. **E-F.** Cell death (E) and cell survival (F) after exposure to L-β-ODAP (5 mM) or L-glutamate (15 mM) with inclusion of 17-β-estradiolbenzoate (EB; 10 µM) after 24 h pre-incubation with EB. No significant effect could be observed. **G.** Summary graph of PI-positive cells (% of DAPI-stained nuclei) after 24 h treatment with L-β-ODAP (5 mM) or L-glutamate (15 mM), together with NBQX (100 µM), MK-801 (10 µM), BAPTA-AM (1 µM) or PDC (2 mM). The cells were pre-incubated (30 min) with all agents except PDC. Average data are represented ± S.E.M. with *(n)* the number of wells; *** denotes $p < 0.001$ compared to control (untreated cells).

of viability) were less pronounced than in C6 glioma cells (Fig. 11C-D). In contrast to C6 glioma, L-glutamate had no toxic effects on primary glial cells (Fig. 11C-D). Measurements of caspase 3 and 7 activity demonstrated no significant activation of apoptotic signaling, neither in C6 glioma nor in primary glial cells exposed to L-β-ODAP or L-glutamate (insets to Fig. 10A and Fig. 11D). PS flip-flop towards the outer plasma membrane leaflet, measured with annexin V-FITC combined with Hoechst 33342 staining indicated a small increase in fluorescence signal in L-β-ODAP treated cells (5 mM, 24 h; Fig. 11E-F). Collectively, these data indicate that L-β-ODAP triggers necrotic and not apoptotic cell death, which is in line with the necrotic manifestations of vacuole formation, cell swelling and cell lysis reported by others (Bridges et al. 1991; Miller et al. 1993).

L-β-ODAP toxicity does not involve excitotoxicity in C6 glioma cells

Since L-β-ODAP is an AMPA-receptor agonist and Ca^{2+} seems to play a role in its toxicity to neurons, and since these ionotropic L-glutamate receptors were found to be present on glial cells as well (Albasanz et al. 1997), the involvement of L-glutamate-receptors and -transporters as well as Ca^{2+} was studied in L-β-ODAP and L-glutamate induced toxicity in C6 glioma cells. Therefore, the cells

were pre-incubated (30 min) with the AMPA-receptor antagonist 2,3-dioxo-6-nitro-1,2,3,4-tetrahydrobenzo[f]quinoxaline-7-sulfonamide (NBQX; 100 µM), the NMDA-receptor antagonist (+)-5-methyl-10,11-dihydro-S*H*-dibenzo[a,d]cyclohepten-5,10-imine maleate (MK-801; 10 µM), or the intracellular Ca^{2+} chelator 1,2-bis(o-aminophenoxy)ethane-N,N,N',N'-tetraacetic acid (BAPTA-AM; 1 µM), before co-treatment with L-β-ODAP (5 mM) or L-glutamate (15 mM) for 24 h. The effect of the competitive EAAT-inhibitor L-trans-pyrrolidine-2,4-dicarboxylic acid (PDC; 2 mM) was studied during 24 h co-treatment, without pre-incubation. However, none of these agents had any effect on L-β-ODAP or L-glutamate toxicity (Fig. 10G).

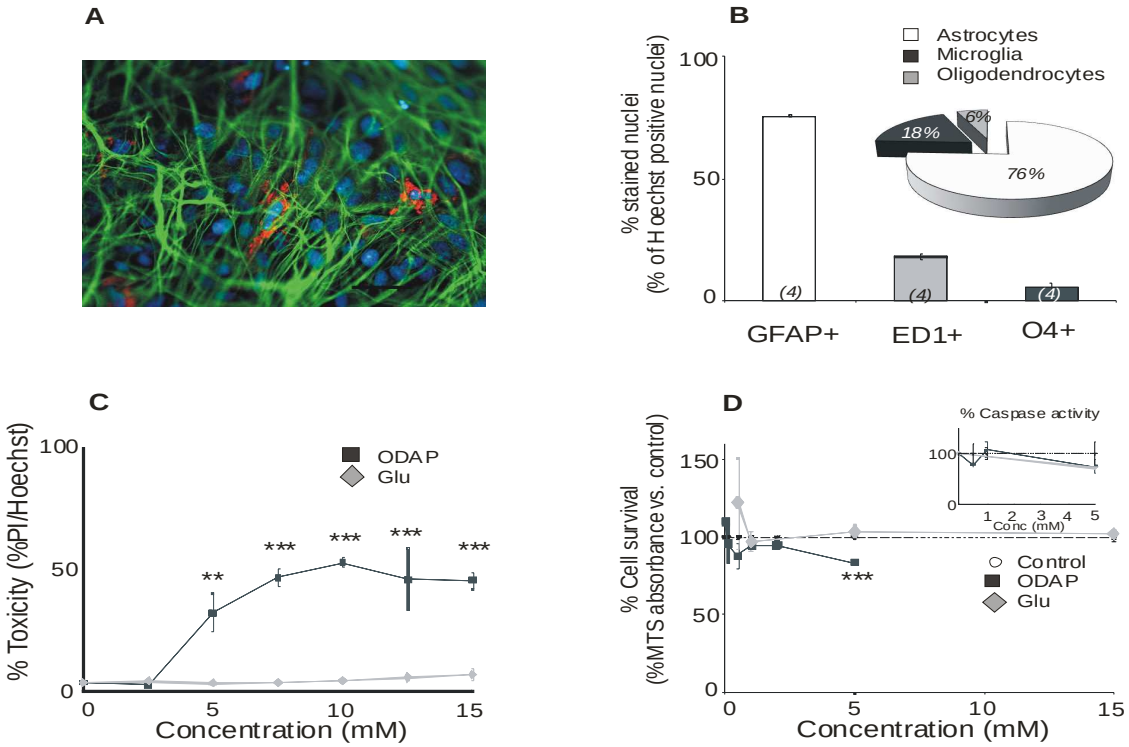

Fig. 11: Gliotoxicity of L-β-ODAP and L-glutamate in primary glial cells. A. Immunostaining of the primary glial cell cultures used in these experiments: astrocytes (green), microglia (red) and oligodendrocytes; nuclei were marked with Hoechst 33342 (blue). **B.** Percentage of subgroups of glial cells, corrected for the total number of Hoechst 33342-stained nuclei (100 %), counted from immunostained images (see Fig. A). The graph represents the average ± S.E.M. of four images. **C.** Concentration-response curve of the percentage of PI-positive cells (as % of Hoechst 33342-stained nuclei) after a 24 h exposure to 0 - 15 mM of L-β-ODAP or L-glutamate. Significant cell death was induced by L-β-ODAP (5 – 15 mM), but not by L-glutamate (0 – 15 mM). Data represent average ± S.E.M. of three independent experiments. Star signs indicate statistical significance vs. control: ** $p < 0.01$; *** $p < 0.001$. **D.** Concentration-response curve of cell viability after 24 h treatment of primary glial cells with L-β-ODAP or L-glutamate, measured by MTS absorbance. L-β-ODAP was significantly toxic at 5 mM, whereas L-glutamate was not toxic at any concentration used. Data are presented as average ± S.E.M. of at least 5 independent experiments (***$p < 0.001$ vs. control). **Inset to D.** Caspase activity in primary glial cells treated with L-β-ODAP (0 - 5 mM) or L-glutamate (0 - 100 mM) for 24 h, evaluated by the Caspase-Glo® 3/7 assay and normalized for untreated cells (100 %). Data are represented as in D.

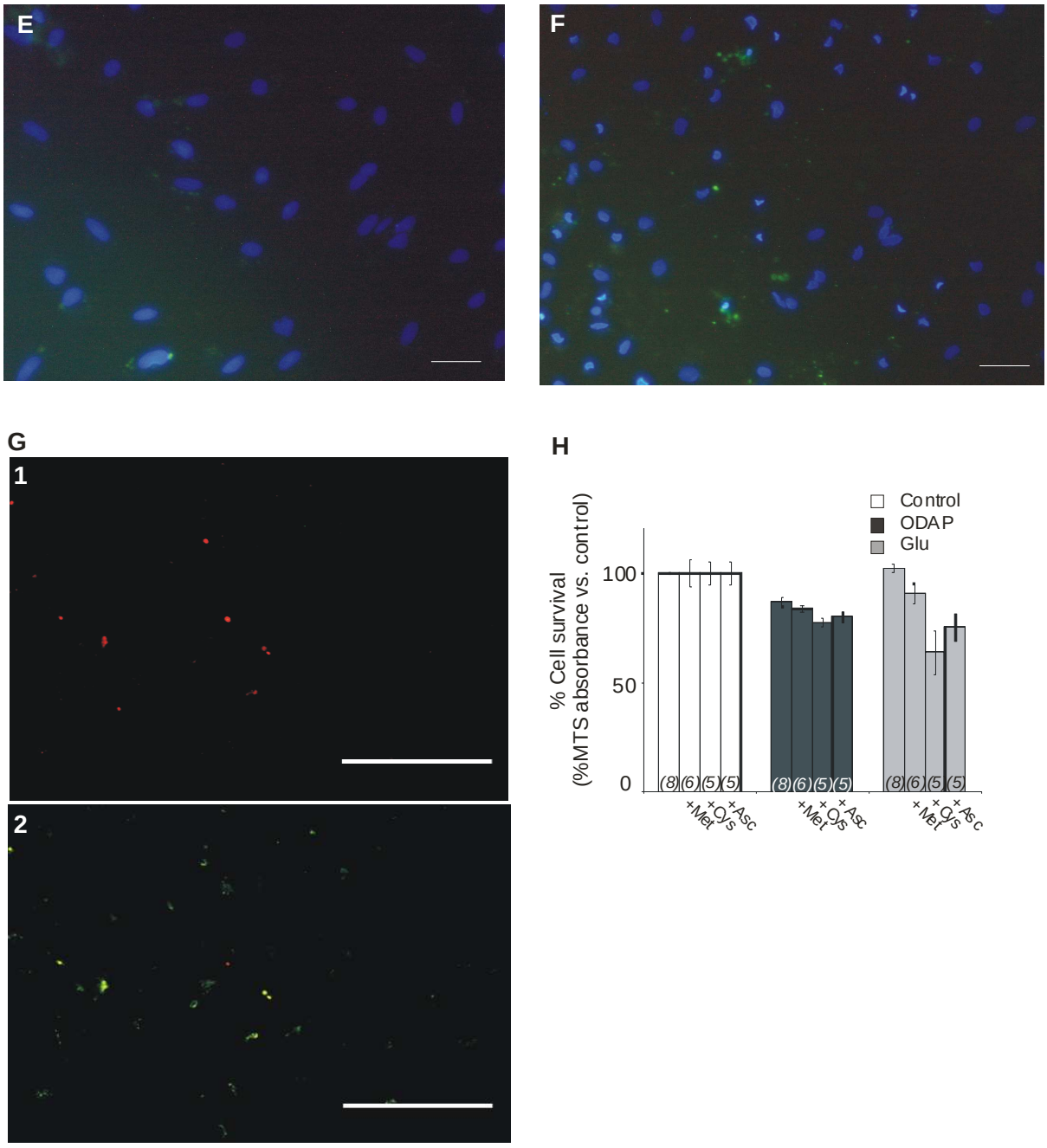

E. Annexin V-FITC combined with Hoechst 33342 staining of control (untreated) cells. The scalebar represents 50 µm. **F.** Annexin V-FITC combined with Hoechst 33342 staining of L-β-ODAP (5 mM; 24 h) treated cells. A small increase in green fluorescence can be observed compared to control (panel E). The scale bar represents 50 µm. **G.** Immunostaining of primary glial cell cultures with PI (G1) and the microglia-specific antibody ED-1 (G2) after treatment with L-β-ODAP (3 mM; 24 h) resulted in an almost identical staining pattern, indicating that microglial cells are most susceptible to L-β-ODAP-induced cell death. The scale bar represents 100 µm. **H.** Summary graph of cell survival, measured by MTS absorbance, after 24 h exposure to L-β-ODAP (5 mM) or L-glutamate (15 mM) with additional compounds with antioxidant capacity in the treatment medium: Met (200 µM), Cys (200 µM) or Asc (100 µM). No protective effect could be observed for any of the antioxidants. Data are presented as average ± S.E.M. with *(n)* being the number of wells.

L-β-ODAP and L-glutamate toxicity in C6 glioma cells is prevented by antioxidative acids

In addition to excitotoxicity and concomitant $[Ca^{2+}]_i$ increase, oxidative stress is proposed to be involved in L-β-ODAP-induced cell death. Therefore, cell death/viability was studied after treatment with L-β-ODAP (5 mM) or L-glutamate (15 mM), together with Met (200 µM), Cys (200 µM) or Asc (100 µM), for 24 h. The antioxidants did not induce any intrinsic toxicity when applied to cells that were not exposed to L-β-ODAP or L-glutamate (data not shown). In C6 glioma cells, the percentage of L-glutamate-induced cell death (15 mM) was almost completely neutralized by adding Cys (200 µM) or Asc (100 µM) in the treatment medium (Fig. 10C) and viability measurements showed a similar effect pattern (Fig. 10D). Addition of Met to the treatment medium did not protect the cells from L-glutamate-induced toxicity.

The influence of the antioxidant compounds on L-β-ODAP toxicity was similar to the effects of these substances on glutamate-triggered toxicity. Inclusion of Cys or Asc in the treatment medium increased the number of surviving cells significantly compared to cells exposed to L-β-ODAP only (Fig. 10D). Cell death was also significantly lower when Asc was included and was somehow decreased when Cys was added to the medium (Fig. 10C). Again, Met had no effect on L-β-ODAP-induced cell death or survival.

In contrast with our observations in C6 glioma cells, addition of Met (200 µM), Cys (200 µM) and Asc (100 µM) to the treatment medium did not confer any protection against L-β-ODAP-induced toxicity (5 mM) in primary glial cells (Fig. 11H).

As epidemiological data suggest a protective role of estrogen (the incidence of neurolathyrism is higher for men than for women), the effect of EB on L-β-ODAP and L-glutamate-induced toxicity was studied in C6 glioma cells. The cells were pre-incubated first with EB (10 µM) for 24 h, before a 24 h co-incubation with L-β-ODAP (5 mM) or L-glutamate (15 mM). There was no intrinsic effect of EB on cell survival in cells not exposed to L-β-ODAP (data not shown). As depicted in figures 10E-F, the small protective effect of EB against L-β-ODAP-induced toxicity was not significant.

The protective effect of Cys and Asc against L-β-ODAP and L-glutamate-induced toxicity in C6 glioma cells suggested the involvement of oxidative stress in the cell death mechanism. Therefore, oxidative stress was quantified using H_2DCFDA (for details see materials and methods), with H_2O_2 (200 µM) as a positive control. The fluorescence was measured at different time points up to 24 h, but no clear change in ROS production could be observed in cells exposed to L-β-ODAP or L-glutamate although exposure to H_2O_2 resulted in a significant increase compared to control (e.g. 359 % ± 64 % after 1 h; 194 % ± 8 % after 24 h, compared to a 100 % control signal).

L-β-ODAP specifically affects microglia

The primary glial cell cultures used in these experiments contained predominantly astrocytes (75.7 %), but also microglia (18.4 %) and oligodendrocytes (5.9 %) were present, as indicated by the specific staining of these subgroups with GFAP, ED-1 and O4, respectively (Fig. 11A-B). Exposure to 3 mM of L-β-ODAP for 24 h resulted in an almost identical staining pattern for PI and for ED-1 (Fig. 11G1-2), suggesting that mainly microglial cells were affected by the toxin.

L-β-ODAP induces changes in sub-cellular morphology of astrocytes

Images of primary glial cells exposed to L-β-ODAP (5 mM; 24 h) revealed morphological, sub-cellular changes that were readily observable under phase contrast microscopy (Fig. 12A-B). When the cytoskeletal marker GFAP was used these structures were visible as FITC-negative zones (Fig. 12C-D), suggesting that the altered appearance was specific for astrocytes. To identify the responsible subcellular structure, mitochondria were stained with Rh-123 (Fig. 12E-F). Such staining displayed a similar pattern as was observed by GFAP, suggesting mitochondria might be involved. Therefore, ultrastructural analysis was performed using transmission electron microscopy (these data were kindly provided by Prof. Dr. K. D'Herde). The results, shown in Fig. 12G-H, indicate that swollen mitochondria may be responsible for this ultrastructural change.

3.2.5. Discussion

These experiments revealed that 5 mM of L-β-ODAP induced cell death in C6 glioma cells and in primary glial cells after 24 h. This finding corresponds to the observations in primary rat astrocytes (Bridges et al. 1991), who reported that 2.1 mM L-β-ODAP applied 48 h caused cell death of 50 % of the cells. These values are much higher than the concentration of 177 µM 4 h following consumption of *L. sativus* as reported by Pratap Rudra et al. (2004) and the plasma concentration of 5.25 µM of healthy volunteers 5 h after intake of 200 g boiled grass pea reported by Nunn et al. (1994). However, it can not be excluded that chronic intake of grass pea over extended periods, for example 3 months (the average period of grass pea consumption before developing neurolathyrism), may lead to an accumulation of L-β-ODAP in the CNS. L-glutamate appeared to be toxic for C6 glioma cells after 24 h exposures, whereas toxic effects were absent in primary glial cells. The concentration needed to induce ± 50 % cell death in C6 glioma cells was three times less for L-β-ODAP (5 mM) compared to L-glutamate (15 mM). Probably L-β-ODAP exerts its toxicity by several mechanisms, being more complex and therefore more powerful compared to L-glutamate. The absence of L-

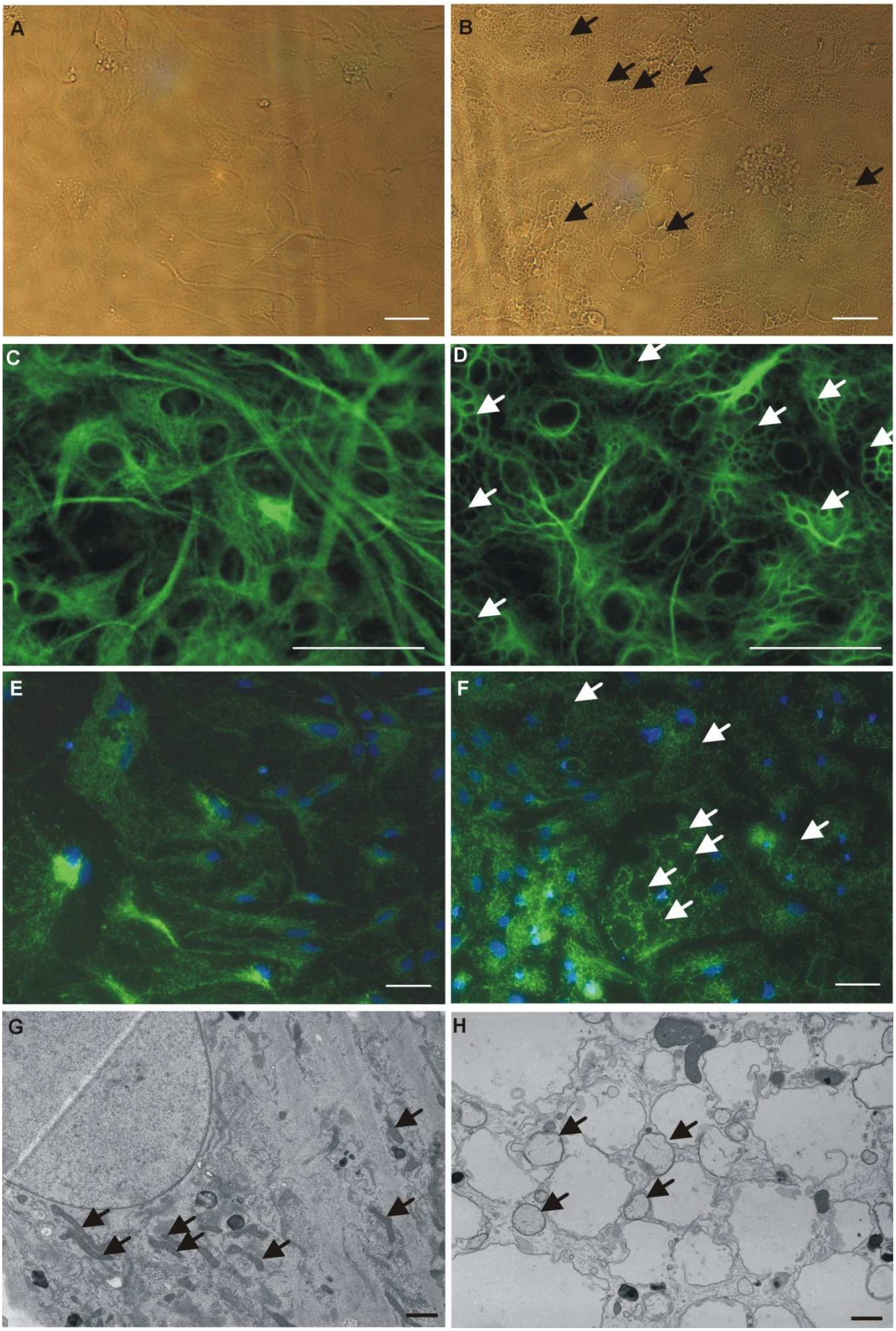
A
B
C
D
E
F
G
H

Fig. 12: Ultrastructural changes induced by L-β-ODAP. A-B. Phase-contrast image (10 x magnification) of control (untreated) cells (A) and cells treated with L-β-ODAP (5 mM; 24 h) (B). Glial cells exposed to L-β-ODAP revealed morphological, sub-cellular changes (arrows) that were not observed in untreated cells. Bar represents 50 µm. **C-D.** GFAP immunostaining of untreated glial cells (C) or cells exposed to L-β-ODAP (5 mM; 24 h) (D). In glial cells treated with L-β-ODAP, FITC-negative zones were observed (arrows) that may correspond to the changes depicted in panel B. Scale bar represents 25 µm. **E-F.** Rh-123 with Hoechst 33342 staining of untreated glial cells (E) or cells exposed to L-β-ODAP (5 mM; 24 h) (F). Cells treated with L-β-ODAP displayed a similar pattern of FITC-negative zones (arrows), distinct from nuclei, as was observed in panel D. Scale bar represents 50 µm. **G-H.** Ultrastructural analysis by transmission electron microscopy of untreated glial cells with normal mitochondria (arrows) (G) or cells exposed to L-β-ODAP (5 mM; 24 h) (H). Note that the mitochondria of L-β-ODAP-treated cells are clearly rounded and swollen, with some intermediate stages (arrows). Scale bar represents 1 µm.

glutamate toxicity in primary glial cells may be due to the conversion of L-glutamate to L-glutamine by glutamine synthetase. C6 glioma cells have been reported not to be able to synthesize L-glutamine from L-glutamate (Brennan et al. 2006), which may lead to accumulation of L-glutamate in these cells. Similarly, L-β-ODAP may be accumulated intracellularly after being transported into the cell by the x_c^- antiporter (Warren et al. 2004).

L-β-ODAP and L-glutamate toxicity in C6 glioma cells could not be inhibited by NMDA- or non-NMDA-receptor antagonists, probably due to the limited expression of ionotropic glutamate receptors (Albasanz et al. 1997). The EAAT-inhibitor PDC had also no effect on the gliotoxicity, though the presence of EAAT3 in C6 glioma cells has previously been reported (Yang and Kilberg 2002). Also Ca^{2+} seemed not to be involved in the L-β-ODAP- or L-glutamate-induced gliotoxicity, since the Ca^{2+} chelator BAPTA-AM had no effect. These data suggest that L-β-ODAP- and L-glutamate-induced gliotoxicity result from a mechanism that does not include binding to L-glutamate receptors or transporters, nor does it result from intracellular Ca^{2+} accumulation.

L-β-ODAP is described as a substrate (at 1 mM) (Murphy et al. 1990) and an inhibitor (at 250 µM) (Warren et al. 2004) of system x_c^-, the antiporter taking up cystine intracellularly while extruding L-glutamate. Elevated extracellular L-glutamate levels decrease the transport effected by this antiporter, as the driving force of this system is the natural concentration gradient of L-glutamate. This inhibiting effect of extracellular L-β-ODAP and L-glutamate may lead to a depletion of intracellular cystine, reducing the biosynthesis of glutathione and resulting in increased oxidative stress. No significant increase of ROS production was observed in this study, but a clear protective effect of the antioxidants Cys and Asc was found in C6 glioma cells. Increased oxidative stress has also been related to a disturbed function of mitochondrial complex I, which was previously described

as a mechanism of L-β-ODAP toxicity at concentrations in the order of 0.01 pM – 1 μM (Sriram et al. 1998; Ravindranath 2002). Met had no effect on L-β-ODAP or L-glutamate-induced cell death. At present, no satisfying explanation was found why Cys was protective while Met was not, nor why the antioxidants had no effect on L-β-ODAP-induced cell death in primary glial cells. So far, no differences in metabolism of antioxidants have been described for cell lines compared to primary glial cells.

The prevalence of neurolathyrism is higher for men than for women, which may indicate a role for estrogen. Neuroprotective effects of estrogen have been ascribed to the presence of a hydroxyl group (Behl et al. 1997) and its effect via specific estrogen-receptors (Manthey and Behl 2006). In C6 glioma cells, it has been described that estrogen may increase the activity of glutamine synthetase, reducing extra- and intracellular L-glutamate concentrations. The results point to some protective effect of estrogen against L-β-ODAP-induced gliotoxicity, although it did not attain statistical significance.

The identification of microglia as the most susceptible subtype of glial cells for L-β-ODAP-induced toxicity is definitely a novel and interesting observation. Microglial cells are known as the pathological sensors of the brain, causing activation of these cells and release of cytokines (Kreutzberg 1996). So far, microglial activation (but not toxicity) has been described in the brain and spinal cord of ALS patients (Henkel et al. 2004; Turner et al. 2004), but specific microglial cell death was only described recently in a study for Parkinson's disease (Schiess et al. 2010). The finding of L-β-ODAP-induced microglial cell death has important potential consequences: activation of microglial cells is generally considered as having a detrimental contribution to the pathological picture because of damaging effects on the neurons and other glial cells. However, recent work has suggested that microglia also have neuroprotective effects, for example in axonal injury models, in Parkinson's disease and in ALS (Appel et al. 2009). The fact that L-β-ODAP damages the microglial cells by preference leads us to conclude that an important neuroprotective cell player is removed from the brain and spinal cord of neurolathyrism patients. This is an important track for further, future research in this field.

In addition to the death of microglia, clear ultrastructural changes were observed in astrocytes, which were identified as swollen mitochondria. Similar histopathological changes were observed in motor neurons of ALS patients, specified as vacuolated and dilated mitochondria with disorganized cristae and membranes. This vacuole formation was due to the expansion of the mitochondrial intermembrane space and subsequent distention of the mitochondrial membranes. The mechanism of mitochondrial intermembrane space expansion is still unknown. For SOD1-mutants in ALS-related

research, mitochondrial permeability transition (expansion of matrix) and autophagy (in which lysosomes participate) has been ruled out, and these authors (Higgins et al. 2003) define this observation as a yet uncharacterized mechanism of mitochondrial degeneration.

3.2.6. Conclusion

Based on the results discussed in this section, it can be concluded that L-β-ODAP is gliotoxic, inducing necrosis in microglia and mitochondrial swelling in astrocytes. L-glutamate is only toxic in cells that do not metabolize L-glutamate, such as C6 glioma cells. Although the mechanism of L-β-ODAP-induced gliotoxicity has not been established, these results point to the involvement of microglia and mitochondrial dysfunction in astrocytes. These alterations in microglia and astrocytes may increase the susceptibility to pathological processes and lead to disturbed neuronal functioning, inducing neurodegeneration.

3.3. L-β-ODAP neurotoxicity – N2a neuroblastoma cells

This section is based on the following reference: Van Moorhem M, Decrock E, Coussee E, Faes L, De Vuyst E, Vranckx K, De Bock M, Wang N, D'Herde K, Lambein F, Callewaert G and Leybaert L. 2010. L-β-ODAP alters mitochondrial Ca^{2+} handling as an early event in excitotoxicity. Cell Calcium, 47(3): 287-296.

3.3.1. Abstract

The neurotoxin β-N-oxalyl-L-α,β-diaminopropionic acid (L-β-ODAP) is an L-glutamate analogue at α-amino-3-hydroxy-5-methyl-4-isoxazole propionic acid (AMPA)/kainate receptors in neurons and therefore acts as an excitotoxic substance. Chronic exposure to L-β-ODAP present in *Lathyrus sativus* L. (*L. sativus)* seeds is proposed as the cause of the neurodegenerative disease neurolathyrism, but the mechanism of its action has not been conclusively identified. A key factor in excitotoxic neuronal cell death is a disturbance of the intracellular Ca^{2+} homeostasis, including changes in the capacity of intracellular Ca^{2+} stores like the ER or mitochondria. In this study, aequorin and Ca^{2+} indicators were used in N2a neuroblastoma cells to investigate alterations of cellular Ca^{2+} handling after 24 h exposure to L-β-ODAP. These data demonstrate increased mitochondrial Ca^{2+} loading and hyperpolarization of the mitochondrial membrane potential (Ψ_m), which was specific for L-β-ODAP and not observed with L-glutamate. It can be concluded that L-β-ODAP disturbs the ER-mitochondrial Ca^{2+} signaling axis and thereby renders the cells more vulnerable to its excitotoxic effects that ultimately will lead to cell death.

3.3.2. Introduction

Chronic intake of the neuro-excitatory amino acid β-N-oxalyl-L-α,β-diaminopropionic acid (L-β-ODAP), present in *Lathyrus sativus L.(L. sativus*) seeds, is proposed to be responsible for the pathogenesis of the neurodegenerative disease neurolathyrism (Spencer et al. 1986). Much of the neuropathology caused by this neurotoxin appears to involve mitochondrial (Sriram et al. 1998) and enzymatic dysfunctions (Pai and Ravindranath 1993; Shasi Vardhan et al. 1997; Singh et al. 2004; Getahun et al. 2005). However, most of its effects can be attributed to structural similarities with L-glutamate and its ability to induce excitotoxicity by interacting with glutamate receptors (Ross et al. 1989), in particular AMPA-receptors for which L-β-ODAP is an agonist (Pearson and Nunn 1981; Bridges et al. 1989; Jain et al. 1998). L-glutamate exerts excitotoxic effects in several neurodegenerative diseases through a disturbed intracellular Ca^{2+} response. More specifically, a massive Ca^{2+} entry into the cells is caused by the activation of two types of ionotropic glutamate

receptors (in addition to other Ca^{2+} entry pathways such as voltage-gated Ca^{2+} channels): N-methyl-D-aspartate (NMDA)-receptors and Ca^{2+}-permeable α-amino-3-hydroxy-5-methyl-4-isoxazole propionic acid (AMPA)-receptors (Van Den Bosch and Robberecht 2000). A clear relationship has been described between excessive Ca^{2+} entry and L-glutamate-triggered neuronal injury which is thought to be mediated by inappropriate activation of Ca^{2+}-dependent proteases, lipases, phosphatases, endonucleases and the formation of oxidative free radicals all of which may lead to cell death (Arundine and Tymianski 2003).

Under normal conditions, neurons control intracellular Ca^{2+} levels through a complex interplay between Ca^{2+} entry, Ca^{2+} extrusion, Ca^{2+} buffering and internal Ca^{2+} storage. Internal Ca^{2+} stores, such as the endoplasmic reticulum (ER) and mitochondria, dynamically participate in the generation of cytoplasmic Ca^{2+} signals. The ER is involved in rapid signaling events associated with cell stimulation, supported by Ca^{2+} release channels (inositol 1,4,5-trisphosphate [IP_3] receptor and ryanodine receptor) and sarco-/endoplasmic reticulum Ca^{2+}-ATPase (SERCA) pumps residing in the endomembrane. The released Ca^{2+} is taken up by mitochondria that are in close apposition to the ER release sites (Rizzuto et al. 1998; Szabadkai et al. 2004; Csordas et al. 2006). Ca^{2+} uptake in mitochondria occurs via a uniporter and accumulated Ca^{2+} may leave the organelle via an antiporter in exchange for Na^+ or H^+. The ER-mitochondrial tandem is importantly involved in the pathways leading to cell death. Disruption of ER Ca^{2+} homeostasis triggers cellular stress responses that may lead to neurodegeneration by affecting post-translational protein processing (Verkhratsky 2004), whereas mitochondria avidly take up Ca^{2+} during Ca^{2+} overload conditions (Campanella et al. 2004), causing a reduction in the rate of ATP synthesis or the release of cytochrome c, resulting in necrosis or apoptosis, respectively.

The aim of the present work was to investigate the effect of chronic exposure of cells to sub-toxic L-β-ODAP concentrations on neuronal Ca^{2+} homeostasis. To resolve the early events and effects of this neurotoxin on Ca^{2+} handling, N2a neuroblastoma cells were used. These cells have a normal intracellular Ca^{2+} homeostasis and allow detailed Ca^{2+} studies in subcellular compartments. They do not express functional AMPA- or NMDA-receptors and are relatively resistant to L-β-ODAP- or L-glutamate-induced cell death. This approach made it possible to specifically investigate the intrinsic effects of the neurotoxin on cellular Ca^{2+} handling and to clearly separate these effects from the major disturbance of cellular Ca^{2+} homeostasis that occurs as a consequence of the cell death process. Since L-β-ODAP is often reported to be a glutamate-analogue in excitotoxic events (Watkins et al. 1966; Bridges et al. 1989; Ross et al. 1989; Jain et al. 1998), all experiments were performed with L-β-ODAP in parallel with L-glutamate, a prototypic excitotoxic amino acid (Doble 1999). The results show that chronic exposure to L-β-ODAP, but not to L-glutamate, modestly potentiates ER Ca^{2+} loading, while strongly increasing cytoplasmic Ca^{2+} changes, the negative mitochondrial potential

and the uptake of Ca^{2+} into the mitochondria. These changes indicate an early 'sensitizing' effect of L-β-ODAP that will attract more Ca^{2+} to the mitochondria that may ultimately lead to cell death. It can be concluded that L-β-ODAP alters cellular Ca^{2+} handling in a manner that prepares the way toward cell death that will be precipitated by its excitotoxic actions. These observations shed new light on the multiple faces of L-β-ODAP neurotoxicity.

3.3.3. Methodology

Cell culture

Parental N2a mouse neuroblastoma cells (N2a, ATTC number CCL131) and N2a cells stably transfected with mitochondrial aequorin (N2a-combiAEQ) were grown in Dulbecco's Modified Eagle Medium (D-MEM; Invitrogen) with 4500 mg/mL D-glucose, Glutamax™ I and 110 mg/L sodium pyruvate, supplemented with 5 % (v/v) fetal calf serum, 100 U/mL penicillin and 100 µg/mL streptomycin at 37 °C in a humidified incubator at 5 % CO_2/95 % air (v/v). Medium for N2a-combiAEQ cells was supplemented with 200 µg/mL hygromycin B. For some experiments cells were treated for 6 h in D-MEM without glucose containing 5 % (v/v) fetal calf serum, 100 U/mL penicillin, 100 µg/mL streptomycin and 2 mM L-glutamine.

Cell viability/cell death assays

N2a cells were grown in 24-well plates (Becton Dickinson, Erembodegem, Belgium) and treated with L-β-ODAP (kindly provided by S.L.N. Rao) or L-glutamate (2 mM, 6 or 24 h). In some experiments, the cells were additionally exposed to p-trifluoromethoxy carbonyl cyanide phenyl hydrazone (FCCP, 100 nM, 6 h) after 24 h pre-treatment with L-β-ODAP, L-glutamate or NMDA (2 mM, 24 h). Cell viability was assayed with the CellTiter 96® AQ_{ueous} One Solution Cell Proliferation Assay (Promega, Leiden, Netherlands). This assay measures 3-(4,5-dimethylthiazol-2-yl)-5-(3-carboxymethoxyphenyl)-2-(4-sulfophenyl)-2H-tetrazolium salt (MTS) which is reduced to a colored formazan product by metabolically active cells. The assay buffer was added to the cells as 1:10 (µL buffer / µL medium), and after a 2 h incubation (37 °C, dark) absorbance was assessed at 490 nm using a plate reader (Victor-3, type 1420, Perkin Elmer, Brussels, Belgium). Absorbance was evaluated as a percentage of control, corrected for a background signal (medium with assay buffer, without cells). Apoptotic cell death was determined with the Caspase-Glo® 3/7 assay (Promega, Leiden, Netherlands), estimating the activity of caspase-3 and -7. Caspase-Glo 3/7 reagent was diluted in the treatment medium after the exposure to L-β-ODAP or L-glutamate (1:3 or 1:6 (v/v)), incubated for 1 hour at room temperature and luminescence was measured with a plate reader (Victor-3, type 1420, Perkin Elmer,

Brussels, Belgium).

Cytoplasmic Ca^{2+} measurements

Cytoplasmic Ca^{2+} measurements were performed with the bioluminescent protein aequorin and with the fluorescent Ca^{2+} indicator Fura-2. Aequorin is a Ca^{2+}-sensitive photoprotein derived from the jellyfish *Aequoria victoria*. It is composed of an apoprotein and a hydrophobic prosthetic group, coelenterazine, and its polypeptide sequence includes three high affinity Ca^{2+}-binding sites. Ca^{2+} binding causes the rupture of the covalent link between the apoprotein and the prosthetic group, a reaction associated with the emission of one photon. The chimeric aequorin cDNA constructs were kindly provided by Dr. R. Rizzuto (University of Ferrara, Italy). N2a cells were transiently transfected with aequorin targeted to the cytoplasm (cyto-AEQ). To that purpose, cells cultured in 150 cm^2 flasks (TPP, Switzerland) were seeded on 18-mm gelatin-coated (2 %; w/v) coverslips in 12-well culture plates (TPP, Switzerland) at a density of 45000 – 70000 cells per cm^2. One day after seeding, the cells were transfected with the aequorin construct in medium (0.4 – 0.7 µg Cyto-AEQ per well) using Lipofectamine 2000 reagent (3 µL/µg plasmide; Invitrogen). One day after transfection, the cells received a 24 h treatment with L-β-ODAP or L-glutamate (2 mM). After this treatment, the cells were incubated for 90 min in medium supplemented with 5 µM wild-type (W) coelenterazine (Invitrogen) at 37 °C and 5 % CO_2/95 % air (v/v) washed with HEPES-buffered Krebs-Ringer buffer (KRB-Hepes; 121 mM NaCl, 5.4 mM KCl, 0.8 mM $MgCl_2.6H_2O$, 6 mM $NaHCO_3$, 5.5 mM glucose, 1.8 mM $CaCl_2.2H_2O$ and 25 mM Hepes, pH 7.3) and kept at 37 °C for another 30 min. Ca^{2+} uptake was measured at 37 °C while stimulating the cells with bradykinin (BK, 300 nM - 1 µM; Sigma) until complete recovery of the response to baseline level. Emitted light was measured using a low-noise photomultiplier with built-in amplifier-discriminator (Hamamatsu H7360-1) and collected using a photon-counting board (National Instruments PCI-6601).

The maximal luminescence level was determined by superfusion with digitonin (100 µM, Sigma) in a hypotonic solution composed of 10 mM $CaCl_2$ in H_2O, thus discharging the remaining aequorin pool (Fig. 13A). The emitted maximum signal can in principle be used for calibration purposes (Brini et al. 1995; Rizzuto et al. 1995), but this yielded unrealistic $[Ca^{2+}]_i$ values (aequorin-based measurements shown in Fig. 13B were therefore expressed in arbitrary units) and for this reason, these experiments were repeated with Fura-2. For Fura-2 experiments, N2a cells were grown on gelatin-coated (2 %; w/v) coverslips in 24-well plates, washed with HBSS-Hepes buffer (0.81 mM $MgSO_4.7H_2O$, 0.95 mM $CaCl_2.2H_2O$, 137 mM NaCl, 0.18 mM $Na_2HPO_4.2H_2O$, 5.36 mM KCl, 0.44 mM KH_2PO_4, 5.55 mM D-Glucose, 25 mM Hepes, pH 7.4) and loaded with 5 µM Fura-2-AM (Invitrogen, Molecular Probes) in HBSS-Hepes containing probenecid (1 mM; Sigma) and pluronic acid (0.01 %; w/v; Sigma). The cells

were incubated at 37 °C for 30 min, washed with HBSS-Hepes and de-esterified for 15 min at 37 °C. Imaging was performed on an inverted epifluorescence microscope (Nikon Eclipse TE 300, Analis, Ghent, Belgium) with a x 40 oil immersion objective lens (NA 1.4) and equipped with an electron multiplying CCD camera (Quantem 512SC, Photometrics, Tucson, AZ). Excitation, alternating between 340 nm and 387 nm (Fura2-B filterset from Semrock, AHF Analysentechnik, Tübingen, Germany), was done with a Lambda DG-4 filterswitch (Sutter Instrument Company, Novato, CA) at a rate of one image pair every 2 s. A 430 nm long-pass dichroic mirror was used in combination with emission bandpass-filtering at 510 nm (40 nm bandwidth). Ratio images were generated with software written in Microsoft Visual C^{++} 6.0, after background subtraction. Fura-2 *in situ* calibrations were carried out with Ca^{2+}-free (10 mM EGTA and 10 µM A23187) and Fura-2 saturating (20 µM digitonin and 10 mM $CaCl_2$) solutions; a Kd of 224 nM was used to convert ratios to $[Ca^{2+}]$.

ER Ca^{2+} measurements

N2a cells were transiently transfected with ER-AEQ using Lipofectamine, as described for cytoplasmic measurements. After 24 h treatment with L-β-ODAP or L-glutamate, the ER was depleted of Ca^{2+} by washing the cells with Ca^{2+}-free KRB-Hepes containing 0.6 mM EGTA and making them permeable to Ca^{2+} with 5 µM ionomycin (Sigma) during 1 min. Subsequently the cells were loaded with 5 µM low-sensitivity coelenterazine N (Molecular Probes) at 4 °C for 1 h. Ionomycin was removed by washing the cells with Ca^{2+}-free KRB-Hepes containing 2 % (w/v) bovine serum albumin (BSA) and 1 mM EGTA. Endoplasmic Ca^{2+} uptake was evaluated at 22 °C by supplying extracellular Ca^{2+} (1.8 mM) in KRB-Hepes solution. At the time of maximal ER loading, cells were stimulated with BK (300 nM). Maximal signal determination and calibration were done as pointed out in the cytoplasmic aequorin measurements – calibration yielded realistic $[Ca^{2+}]_{ER}$ values.

Some experiments were also performed on permeabilized cells. For these experiments again the low affinity coelenterazine N (5 µM, 37 °C, 90 min) was used for reconstitution of the targeted aequorin. Permeabilization of the cells was obtained by a 1 min superfusion of the coverslips with a digitonin (100 µM)-containing Ca^{2+}-free intracellular solution (composed of 120 mM KCl, 10 mM Hepes, 1 mM $MgCl_2.6H_2O$, 0.44 mM EGTA, 10 mM NaCl, 2 mM KH_2PO_4, 1 mM succinic acid, 2 mM Na-ATP and 1 mM pyruvic acid - pH 7.4). Thereafter, ER Ca^{2+} uptake was stimulated by switching to 200 nM free Ca^{2+} IC solution. Counts were calibrated as described for intact cells with digitonin and $CaCl_2$ in H_2O.

Mitochondrial Ca^{2+} measurements

N2a-combiAEQ cells were used to quantify Ca^{2+} changes in the mitochondria ($[Ca^{2+}]_m$). One day after seeding, the cells received L-β-ODAP or L-glutamate treatment and were thereafter treated as described for cytoplasmic aequorin measurements. Maximal signal determination and calibration were done as pointed out above.

Some mitochondrial Ca^{2+} measurements were also done with Rhod-FF, a mitochondrial Ca^{2+} indicator with a Kd of 19 µM. N2a cells were loaded with Rhod-FF-AM (5 µM; Invitrogen, Molecular Probes) at 37 °C for 30 min in HBSS-Hepes containing 1 mM probenecid and 0.01 % (w/v) pluronic acid, followed by 15 min de-esterification. Imaging was performed with the same equipment as described for the Fura-2 assay, but with excitation at 556 nm and long-pass filtering at 590 nm. Each experiment was concluded by exposure to digitonin (100 µM) and $CaCl_2$ (10 mM) in HBSS-Hepes to obtain a maximal signal, as in the aequorin experiments. The area under the curve of the BK response (at least 10 regions of interest per coverslip) was then expressed as a fraction of the maximal signal and the response was set to 100 % in control cells, with *n* corresponding to the number of coverslips.

Mitochondrial membrane potential

The fluorescence signal of the cationic dye Rhodamine 123 (Rh-123) was measured in cells loaded with the dye (5 µM) for 30 min at 37 °C in HBSS-Hepes. Nuclei were stained simultaneously with Hoechst 33342 (2 µg/mL). Imaging was performed with the same equipment as described for the Fura-2 assay. The average Rh-123 fluorescence intensity in recorded images was normalized to the number of Hoechst 33342-positive nuclei and the response in control cells was set to 100 %.

Intracellular ATP

The intracellular ATP concentration was determined using a bioluminescent luciferin/luciferase assay kit (Sigma). In this procedure, ATP assay mix was diluted in dilution buffer (1:25, v/v).

Cells were seeded in 6-well plates and treated with L-β-ODAP or L-glutamate. After treatment, the cells were rinsed with ice-cold phosphate-buffered salt solution supplemented with Ca^{2+} and Mg^{2+} ($PBSD^+$, composed of 137 mM NaCl, 2.68 mM KCl, 0.90 mM $CaCl_2$, 0.334 mM $MgCl_2.6H_2O$, 1.47 mM KH_2PO_4, 6.46 mM $Na_2HPO_4.2H_2O$, pH 7.4). Cells were then lysed in 200 µL lysis buffer (Somatic cell ATP releasing reagent; Sigma). Lysates were boiled for 5 min and subsequently centrifuged (5 min, 14 000 r.p.m.). Three aliquots of 10 µL supernatant were used to determine total cellular ATP concentration by mixing it with diluted ATP assays mix (final dilution 1:500, v/v). Luminescence was

measured with a plate reader. This signal was corrected for the protein concentration in the lysates using a BioRad DC protein assay kit (Nazareth, Belgium) and a plate reader with spectrophotometric measurement at 590 nm with a long-pass filter.

Western blot analysis

N2a cells were grown in 75 cm^2 flasks (Nunc brand products, Roskilde, Denmark), treated with L-β-ODAP (2mM) or L-glutamate (2 mM) for 24 h, and harvested. Cells were resuspended and homogenized in radio-immuno precipitation assay buffer (RIPA: 25 mM Tris (pH 8.2), 50 mM NaCl, 0.5 % NP-40, 0.5 % deoxycholate, 0.1 % SDS, 20 µL/mL mini EDTA-free protease inhibitor cocktail, 0.055 g/mL β-glycerophosphate, 1 mM DTT and 20 µL/mL phosphatase inhibitor cocktail). Protein concentration was determined using a BioRad DC protein assay kit (BioRad, Nazareth, Belgium). 100 µg protein lysates were separated on a 10 % SDS-polyacrylamide gel (in Tris-glycine buffer: 1g/L SDS, 3.3 g/L tris and 14.4 g/L glycine) and transferred to a nitrocellulose membrane (GE Healthcare, Buckinghamshire, UK). Membranes were blocked with 5 % (w/v) non-fat milk in Tris-buffered saline (TBS) containing 0.3 % (v/v) Tween-20 for 1 h. Subsequently, the membrane was probed with a polyclonal rabbit antibody specific to SERCA2b (1/1000 dilution; kindly provided by Prof. Dr. F. Wuytack and Dr. P. Vangheluwe, University of Leuven, Belgium (Wuytack et al. 1989)) in 1 % (w/v) non-fat milk in TBS with 0.3 % (v/v) Tween-20 followed by alkaline phosphatase-conjugated goat anti-rabbit (1/8000 dilution; Sigma). Detection was carried out using the 5-bromo-4-chloro-3-indolyl/nitro blue tetrazolium (BCIP/NBT) kit (Zymed, Invitrogen) according to manufacturer's instructions. As a loading control, the membranes were probed with a rabbit anti-rat β-tubulin antibody (1/1000 dilution; Abcam, Cambridge, UK) or total protein staining was carried out with SYPRO® Ruby protein blot dye (Invitrogen, Molecular Probes). Protein expression was quantified using Image J software.

Transmission electron microscopy

The N2a cells were fixed by immersion for 1 h in 2 % (v/v) glutaraldehyde buffered with 0.1 M Na-cacodylate containing 1 mM $CaCl_2$ (pH 7.4). After a rinse in 0.1 M Na-cacodylate containing 7.5 % (w/v) sucrose, the explants were post-fixed overnight in 4 % OsO_4 in 0.1 M Na-cacodylate. After dehydratation with ethanol (50 % for 15 min, 70 % for 20 min, 90 % for 30 min and 100 % for 90 min) (v/v), the samples were infiltrated with a mixture of ethanol and LX-112 resin (1:1 (v/v) for 30 min and 1:2 (v/v) for 30 min; Ladd Research Industries, USA). They were finally infiltrated with 100 % resin for 120 min, and then polymerized for 48 h at 60 °C. The samples were stained with uranyl

acetate and Reynold's lead citrate and the sections were examined by transmission electron microscopy.

Statistics

Statistical significance was determined by one way ANOVA with post-hoc Bonferroni or its non-parametric analogues Mann-Whitney or Kruskal-Wallis, using GraphPad Instat software (GraphPad Software; San Diego, CA). Values represent mean ± S.E.M., *n* is the number of coverslips, wells or lysates, normalized for day to day variability. Statistical significance is indicated in the graphs by one, two or three symbols for $p < 0.05$, $p < 0.01$ or $p < 0.001$ respectively.

3.3.4. Results

To investigate the effect of L-β-ODAP or L-glutamate on cellular Ca^{2+} homeostasis, Ca^{2+} was measured in three different cell compartments: cytoplasm, ER and mitochondria, both in control cells and cells treated with 2 mM L-β-ODAP or L-glutamate over a time period of 24 h. To that purpose, aequorin specifically targeted to the cytoplasm, ER or mitochondria was used. Twenty-four hour treatment of N2a neuroblastoma cells with 2 mM of L-β-ODAP or L-glutamate did not result in significant apoptotic or necrotic cell death (data not shown), based on caspase activity and MTS absorbance assays (see Methodology). In these cells, L-β-ODAP was significantly toxic starting from 10 mM, whereas even higher concentrations of L-glutamate were needed (data not shown). Additionally, exposure of these cells to L-glutamate in the micro- and millimolar range did not elicit intracellular Ca^{2+} responses (data not shown), indicating absence of functional AMPA- and NMDA-receptors (as well metabotropic L-glutamate receptors linking to PLC activation).

L-β-ODAP treatment potentiates bradykinin-triggered cytoplasmic Ca^{2+} changes in N2a cells

We used N2a mouse neuroblastoma cells transiently transfected with aequorin, to investigate intracellular cytoplasmic Ca^{2+} responses ($[Ca^{2+}]_i$) elicited by 300 nM BK. This substance mobilizes Ca^{2+} from the intracellular stores by binding to surface receptors thereby generating IP_3 (Yano et al. 1984). Binding of IP_3 to its receptors on the endoplasmic reticulum (ER) (Foskett et al. 2007) induces the release of Ca^{2+} from the ER. **T**he BK-triggered transient $[Ca^{2+}]_i$ changes appeared to be significantly potentiated in L-β-ODAP treated cells (~19 % larger as compared to control, $p < 0.05$, Fig. 13B-C). By contrast, L-glutamate treatment did not influence the magnitude of the BK-triggered $[Ca^{2+}]_i$ changes (Fig. 13). A stronger potentiating effect of L-β-ODAP occurred when $[Ca^{2+}]_i$ changes were measured

with Fura-2 (~83% potentiation, $p < 0.05$, Fig. 13D-E), presumably because Fura-2 is better suited for measurements in the 100-1000 nM $[Ca^{2+}]_i$ range. To investigate the contribution of Ca^{2+} entry, Fura-2 experiments were repeated in extracellular Ca^{2+}-free conditions (no added Ca^{2+} with 1 mM EGTA). Under those conditions, L-β-ODAP again potentiated the BK-triggered $[Ca^{2+}]_i$ elevation (~144% potentiation, $p < 0.05$, Fig. 13F), suggesting that increased Ca^{2+} entry is not involved in the potentiation of the cytoplasmic Ca^{2+} response. This effect was confirmed in another experiment where the stores were first emptied by thapsigargin (Tg - 2 µM, applied for 3 min) under zero extracellular Ca^{2+} conditions (no added Ca^{2+} with 1 mM EGTA) followed by re-introduction of extracellular Ca^{2+} (0.95 mM) (Fig. 13G-H). The $[Ca^{2+}]_i$ transient caused by reintroducing extracellular Ca^{2+} is related to store-operated Ca^{2+} entry (SOCE - (Thastrup et al. 1989; Targos et al. 2005) and neither L-β-ODAP nor L-glutamate did significantly affect it (L-β-ODAP slightly increased SOCE but this was not statistically significant – see Fig. 13H). L-β-ODAP stimulation of BK-triggered $[Ca^{2+}]_i$ transients was not the consequence of differences in the resting $[Ca^{2+}]_i$ level, which averaged 63 ± 14 nM over control and treated groups (Fura-2 measurements; n = 9).

L-β-ODAP treatment potentiates ER Ca^{2+} loading

We next investigated whether L-β-ODAP treatment stimulated ER Ca^{2+} loading, thereby delivering larger BK-triggered $[Ca^{2+}]_i$ responses. For these experiments, N2a cells were transiently transfected with aequorin specifically targeted to the ER. ER Ca^{2+} concentration ($[Ca^{2+}]_{ER}$) was first lowered by pre-incubation under Ca^{2+}-free conditions (no added Ca^{2+} with 0.6 mM EGTA and 5 µM ionomycin). After removal of ionomycin, $[Ca^{2+}]_{ER}$ changes were measured in response to a switch from Ca^{2+}-free conditions to a normal extracellular Ca^{2+} concentration of 1.8 mM, a protocol that results in reloading of the ER with Ca^{2+}. The data for loading after treatment with L-β-ODAP are not significantly different from control values (~15 % above the responses observed in control non-treated cells, $p > 0.05$, Fig. 14), though the rate of uptake was significantly higher than in control cells ($d[Ca^{2+}]/dt$ = 30 ± 4 µM/min versus 25 ± 3 µM/min in control; n = 11; $p < 0.05$). Interestingly, L-glutamate treatment had no influence on ER Ca^{2+} loading or its kinetics (Fig. 14A-B).

At the time of maximal ER loading, BK was applied to investigate the emptying of the ER Ca^{2+} store. The Ca^{2+} store content was reduced from 100 % to ~75 % after BK-triggered emptying in control as well as L-β-ODAP or L-glutamate treated cells (n = 11), indicating no significant direct effect of these treatments on store emptying. These results are in line with the results depicted in Fig. 13H showing that $[Ca^{2+}]_i$ transients triggered by Tg are not altered by L-β-ODAP treatment.

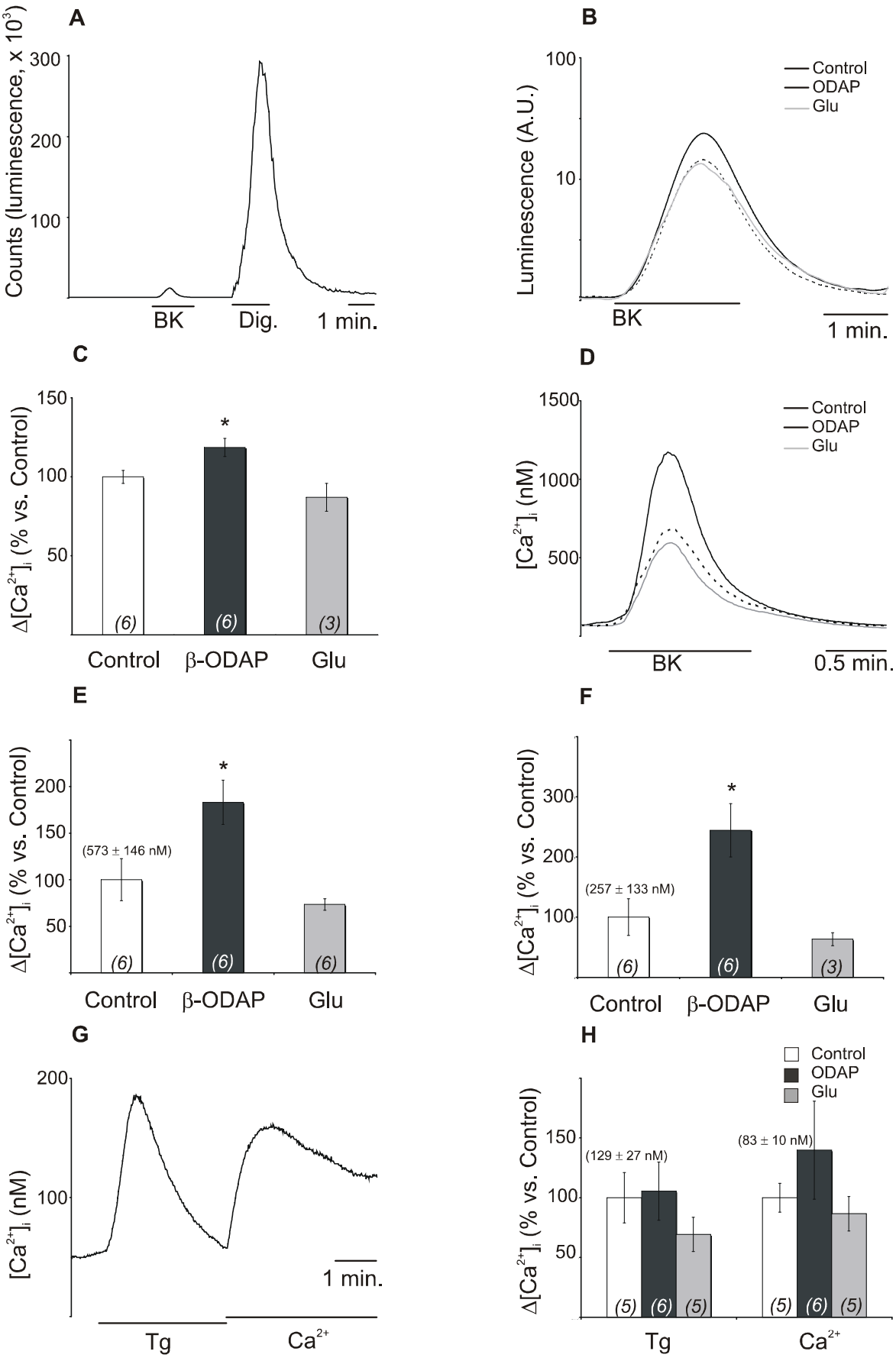
A
Counts (luminescence, x 10³)
300
200
100
BK
Dig.
1 min.
B
Luminescence (A.U.)
100
10
Control
ODAP
Glu
BK
1 min.
C
Δ[Ca²⁺]ᵢ (% vs. Control)
150
100
50
*
(6)
(6)
(3)
Control
β-ODAP
Glu
D
[Ca²⁺]ᵢ (nM)
1500
1000
500
Control
ODAP
Glu
BK
0.5 min.
E
Δ[Ca²⁺]ᵢ (% vs. Control)
200
150
100
50
(573 ± 146 nM)
*
(6)
(6)
(6)
Control
β-ODAP
Glu
F
Δ[Ca²⁺]ᵢ (% vs. Control)
300
200
100
(257 ± 133 nM)
*
(6)
(6)
(3)
Control
β-ODAP
Glu
G
[Ca²⁺]ᵢ (nM)
200
100
1 min.
Tg
Ca²⁺
H
Δ[Ca²⁺]ᵢ (% vs. Control)
150
100
50
Control
ODAP
Glu
(129 ± 27 nM)
(83 ± 10 nM)
(5)
(6)
(5)
(5)
(6)
(5)
Tg
Ca²⁺

Fig. 13: Effect of L-β-ODAP and L-glutamate on cytoplasmic Ca^{2+} changes. A. Example trace demonstrating an aequorin-based experiment. Exposure to bradykinin (BK) triggered a $[Ca^{2+}]_i$ transient after which digitonin (100 μM) was applied to determine the maximal signal. **B.** Representative aequorin experiment illustrating BK (300 nM) -triggered $[Ca^{2+}]_i$ transients (expressed as arbitrary units [A.U.]) in N2a cells under control conditions and after exposure to L-β-ODAP (2 mM, 24 h) or L-glutamate (2 mM, 24 h). **C.** Summary graph of aequorin experiments illustrating that L-β-ODAP significantly potentiated the responses while L-glutamate had no effect. Average data expressed as mean ± S.E.M. with (*n*) representing the number of experiments; the star sign indicates significantly above control with $p < 0.05$. **D.** Representative Fura-2 experiment illustrating BK (1 μM) -triggered $[Ca^{2+}]_i$ transients under various conditions. **E.** Summary graph representing average data from experiments illustrated in panel D, demonstrating significant potentiation of induced $[Ca^{2+}]_i$ transients by L-β-ODAP. The value above the control bar refers to the relative change in Ca^{2+} concentration expressed as a percentage. **F.** Similar experiment as in panel E but now under extracellular Ca^{2+}-free conditions (no added Ca^{2+} with 1 mM EGTA), demonstrating that L-β-ODAP still potentiates the $[Ca^{2+}]_i$ transients. **G.** Fura-2 experiment with store-emptying/Ca^{2+} re-introduction to investigate effects at the level of store-operated Ca^{2+} entry (SOCE). Cells were first exposed to extracellular Ca^{2+}-free conditions (solution as in panel F, applied 1 min) followed by store-emptying with thapsigargin (Tg - 2 μM, 3 min – again Ca^{2+}-free conditions) that resulted in a $[Ca^{2+}]_i$ transient. Re-introduction of extracellular Ca^{2+} (0.95 mM) triggered an additional $[Ca^{2+}]_i$ transient the amplitude of which is representative for SOCE. **H.** Summary graph of experiments as illustrated in panel G. 'Tg' represents the $[Ca^{2+}]_i$ transients triggered by Tg while 'Ca^{2+}' represents the transients associated with re-introduction of extracellular Ca^{2+}. The two types of $[Ca^{2+}]_i$ responses were not affected by L-β-ODAP or L-glutamate treatment.

The stronger ER Ca^{2+} uptake observed in cells treated with L-β-ODAP may result from an increased SERCA pump activity and therefore the expression of the SERCA protein was checked. Western Blot analysis suggested a small but non-significant increase in SERCA protein expression after 24 h L-β-ODAP treatment (Fig. 15). L-glutamate treatment had no discernable influence. Another possibility is that L-β-ODAP induces ER volumetric changes, for example decreasing the ER volume and thereby increasing $[Ca^{2+}]_{ER}$. However, visual inspection of electron microscopy images did not indicate any change in ER morphology with L-β-ODAP or L-glutamate (data not shown). Additional ER Ca^{2+} uptake experiments were performed in permeabilized cells, to exclude a possible contribution of the plasma membrane. Cell permeabilization was done with short digitonin exposure (100 μM, 1 min) and ER Ca^{2+} loading was then performed by switching from Ca^{2+}-free to 200 nM (cytoplasmic) free Ca^{2+}. Under those conditions, L-β-ODAP failed to potentiate $[Ca^{2+}]_{ER}$ increases (Fig. 14C-D).

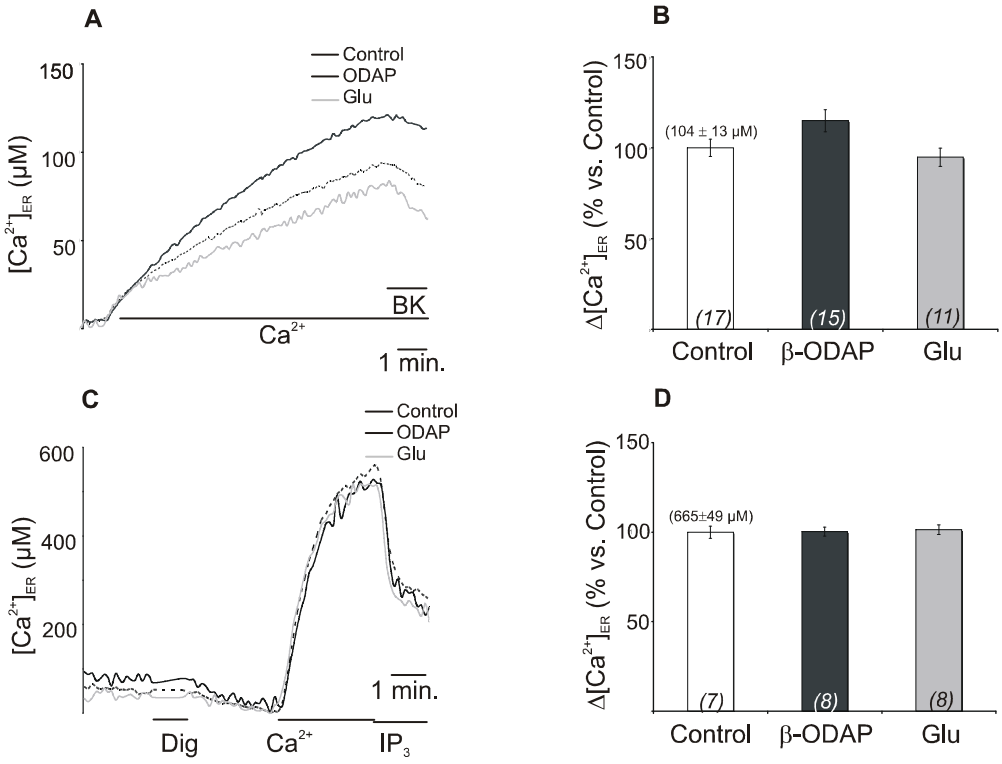

Fig. 14: L-β-ODAP and L-glutamate effects on ER Ca^{2+}. A. Representative experiment illustrating ER Ca^{2+} uptake in intact cells induced by switching from low Ca^{2+} (nominal Ca^{2+}-free KRB-Hepes with 1 mM EGTA) to a 1.8 mM $CaCl_2$ containing solution (horizontal bar marked 'Ca^{2+}'). ER Ca^{2+} uptake was potentiated by L-β-ODAP treatment (2 mM, 24 h; $p > 0.05$) and not influenced by L-glutamate (2 mM, 24 h; $p > 0.05$). Stimulation of the cells with BK (1 µM) caused a decrease of $[Ca^{2+}]_{ER}$ (recovery trace truncated shortly after BK). **B.** Summary graph representing average data from experiments illustrated in A. **C.** Representative experiment illustrating ER Ca^{2+} uptake in permeabilized cells. Permeabilization of the cells was obtained by a 1 min superfusion of the coverslips with a digitonin (Dig, 100 µM) containing Ca^{2+}-free intracellular solution. ER Ca^{2+} uptake was stimulated by switching to 200 nM free Ca^{2+} solution (bar marked 'Ca^{2+}'). ER Ca^{2+} uptake was not changed by L-β-ODAP or L-glutamate treatment (2 mM, 24 h; $p > 0.05$). Stimulation of the cells with IP_3 (10 µM), triggering store release, caused a decrease of $[Ca^{2+}]_{ER}$. **D.** Summary data from experiments illustrated in C.

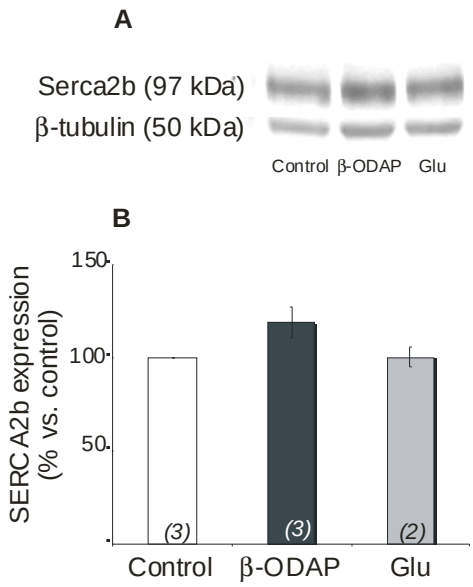

Fig. 15: Western blot analysis for SERCA2b. A. Representative western blot of SERCA2b showing a slightly increased expression of this protein in cells treated with L-β-ODAP (2 mM, 24 h), but not with L-glutamate (2 mM, 24 h) (β-tubulin serves as a loading control) . **B.** Average data summarizing the relative effect on SERCA2b expression.

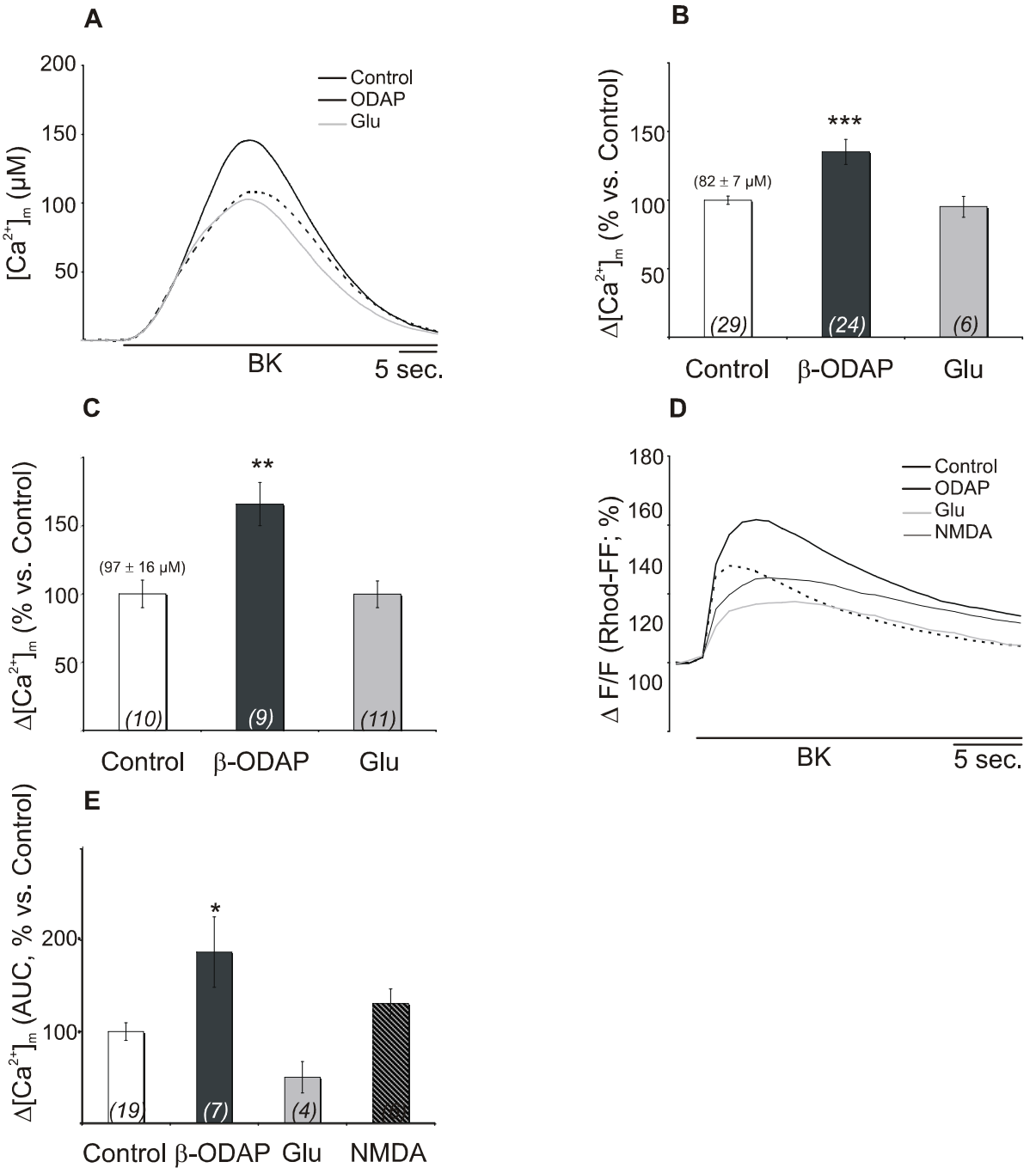

Fig. 16: L-β-ODAP and L-glutamate effects on mitochondrial Ca^{2+}. A. Representative experiment showing a BK (1 µM) -triggered $[Ca^{2+}]_m$ transient that was potentiated by L-β-ODAP treatment (2 mM, 24 h) while not being influenced by L-glutamate (2 mM, 24 h). **B** Summary data of experiments as described in A. *** significantly above control with $p < 0.001$. **C.** Summary data of $[Ca^{2+}]_m$ measurements as performed in A but now in the absence of extracellular Ca^{2+}. ** significantly above control with $p < 0.01$. **D.** Representative experiment of $[Ca^{2+}]_m$ measurements performed with Rhod-FF, demonstrating a potentiation of the transients by L-β-ODAP treatment but not L-glutamate or NMDA treatment. The Rhod-FF signal is expressed as relative fluorescence changes (ΔF/F). **E.** Summary graph of experiments as shown in D. The ordinate expresses the area under the curve (AUC) of the $[Ca^{2+}]_m$ trace that was set to 100 % for experiments under control conditions. * significantly above control with $p<0.05$.

L-β-ODAP treatment potentiates BK-triggered mitochondrial Ca^{2+} uptake

We subsequently studied whether L-β-ODAP affected mitochondrial Ca^{2+} transport, making use of N2a-combiAEQ cells that stably express aequorin in their mitochondria. In intact control cells, stimulation with BK triggered a transient increase in $[Ca^{2+}]_m$ (Fig. 16A-B). This BK-triggered change in $[Ca^{2+}]_m$ was significantly larger in cells treated with L-β-ODAP, a potentiating effect that was ~35 % above control responses ($p < 0.001$, Fig. 16A-B). These results were confirmed when Rhod-FF was used to record $[Ca^{2+}]_m$ changes (~87-% potentiation above control, $p < 0.05$, Fig. 16D-E). Cells treated with L-glutamate did not display a potentiation of BK-triggered $[Ca^{2+}]_m$ changes. The difference between L-β-ODAP and L-glutamate may result from the fact that L-glutamate can be metabolized whereas L-β-ODAP, entering the cell via glutamate/cystine exchange transport (x_c^- antiporter), is probably not metabolized and may therefore accumulate (Warren et al. 2004). NMDA, which like L-β-ODAP is transported into the cell by a carrier and is not further metabolized (Skerritt and Johnston 1981), had no effect (Fig. 16D-E), indicating that intracellular accumulation of a non-metabolized amino acid is not responsible for the altered mitochondrial Ca^{2+} uptake observed in L-β-ODAP treated cells. To investigate the contribution of Ca^{2+} entry, mitochondrial aequorin experiments were repeated under extracellular Ca^{2+}-free conditions (no added Ca^{2+} with 1 mM EGTA). Under those conditions, L-β-ODAP again potentiated the BK-triggered $[Ca^{2+}]_m$ elevation (~66 % potentiation above control; $p < 0.001$, Fig. 16C), suggesting that increased Ca^{2+} entry is not involved in the potentiation of mitochondrial Ca^{2+} uptake.

Mitochondrial membrane potential (Ψ_m)

Increased Ca^{2+} loading of mitochondria is a potential first step toward cell death with consequent loss of the negative mitochondrial membrane potential (Ψ_m) that is normally in the range of -180 mV (Duchen 2000). Conversely, increased Ca^{2+} loading can also be the consequence of a more negative Ψ_m since Ca^{2+} uptake in mitochondria depends exponentially on Ψ_m (Valero et al. 2008). The effect of L-β-ODAP on Ψ_m were further explored as measured with rhodamine-123 (Rh-123) in N2a cells. Control experiments demonstrated that Ψ_m was significantly attenuated by FCCP (10 µM, 15 min), which allows protons to flow back thereby dissipating Ψ_m (Fig. 17A-B). By contrast, plasma membrane depolarization with 50 mM extracellular potassium did not affect the Rh-123 signal, demonstrating that Rh-123 is effectively reporting Ψ_m and not the plasma membrane potential V_m (Fig. 17A). N2a cells treated with L-β-ODAP (2 mM, 24 h) showed a strongly hyperpolarized Ψ_m while L-glutamate treatment had no effect (Fig. 17B). Mitochondria thus hyperpolarize with L-β-ODAP and

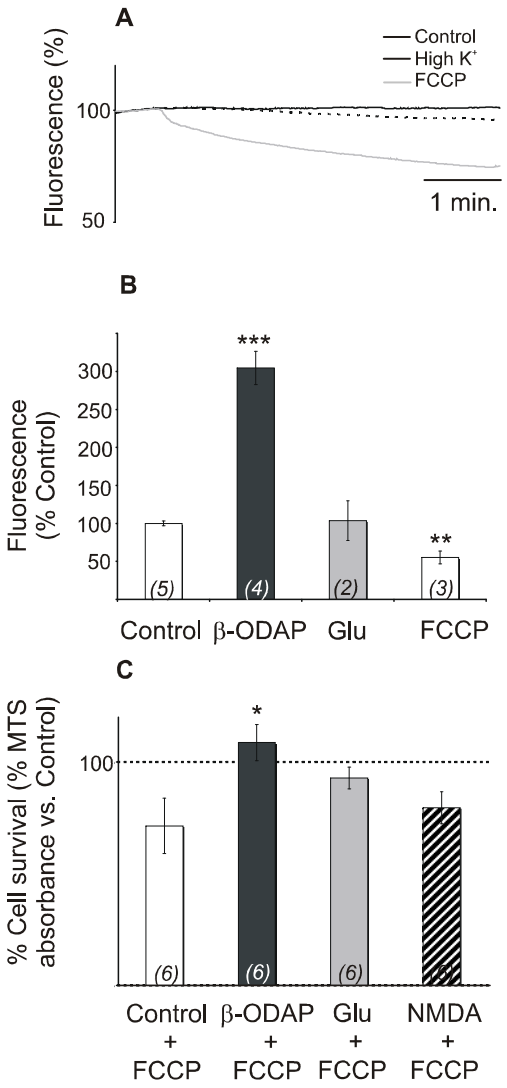

this is expected to exert an increased electrochemical driving force on Ca^{2+} to enter the mitochondria.

L-β-ODAP protects N2a cells from FCCP-induced cell death

Depolarization of the mitochondrial membrane is thought to be a crucial event in cell toxicity. Since L-β-ODAP hyperpolarizes mitochondria, it was investigated whether this substance influenced cell death induced by mitochondrial depolarization with FCCP. Cell survival decreased after FCCP treatment (100 nM, 6 h) and cells pretreated with L-β-ODAP, but not L-glutamate or NMDA (2 mM, 24 h), protected the cells from cell death induced in this way (Fig. 17C).

Fig. 17: L-β-ODAP and L-glutamate effects on Ψ_m. A. Control experiments performed on Rh-123 loaded cells. Plasma membrane depolarization with 50 mM extracellular K^+ did not affect the Rh-123 signal, demonstrating that Rh-123 effectively reports Ψ_m and not the plasma membrane potential V_m. In contrast, dissipating Ψ_m with FCCP (10 µM) decreased the Rh-123 signal, representing mitochondrial depolarization. **B.** Ψ_m was significantly hyperpolarized in cells treated with L-β-ODAP (2 mM, 24 h), while L-glutamate (2 mM, 24 h) had no effect. *** significantly above control with $p<0.001$. **C.** Exposure to FCCP (100 nM, 6 h) triggered cell death (quantified by MTS absorbance) that was prevented by L-β-ODAP (2 mM, 24 h; * $p < 0.05$) but not by L-glutamate or NMDA (2 mM, 24 h).

Mitochondrial ATP production

Ca^{2+} accumulation in the mitochondrial matrix can be a positive modulator of mitochondrial ATP synthesis (Denton et al. 1988) and it was further tested whether the rate of intracellular ATP synthesis was influenced by L-β-ODAP or L-glutamate. Measurements in N2a cells with a luciferin/luciferase based assay in combination with an ATP releasing reagent demonstrated that L-β-ODAP had no effect on the intracellular ATP concentration (averaging 1.67 ± 0.14 µM/mg protein

over all conditions, n=31). A probable reason for this result is that an increased mitochondrial ATP production is obscured by a decreased glycolytic ATP synthesis. To further sort out the consequences of an increased mitochondrial Ca^{2+} uptake, the cells were exposed to L-β-ODAP under low extracellular glucose conditions. Control cells cultured 6 h under low glucose (0.25 mM) showed a decreased cell survival amounting to 85.3 ± 3.6 %, significantly below the 100 % survival under normal glucose conditions (n = 6, $p < 0.05$). Treatment of the cells with L-β-ODAP (2 mM, 24 h) protected the cells from the low glucose-triggered cell death, restoring the survival rate to 104.3 ± 5.5 % (n = 6; not different from non-treated cells in normal glucose). This result indicates that L-β-ODAP treatment indeed stimulates mitochondrial ATP production, presumably via the increased $[Ca^{2+}]_m$.

3.3.5. Discussion

The present study was performed to investigate the effect of the neurotoxin L-β-ODAP, a major toxin involved in motor neuron degeneration in neurolathyrism, on the intracellular Ca^{2+} homeostasis. N2a neuroblastoma cells were chosen to specifically focus on the intrinsic effects of the toxin on cellular Ca^{2+} handling and separate these effects from the alterations associated with execution of the pathways leading to cell death.

L-β-ODAP is an established excitotoxin for motor neurons that exerts its effects via AMPA-receptor activation, resulting in Ca^{2+} overload and cell death (Cemerikic et al. 2001; Amba et al. 2002). No information is available on the concentrations of L-β-ODAP in the brain; the presently used 2 mM was based on concentrations used by other workers in the field (0.5 - 3 mM range (Staton and Bristow 1997; Saeed et al. 2008)). Such a concentration of L-β-ODAP appeared to influence the cellular Ca^{2+} homeostasis in N2a cells at various levels. First of all, $[Ca^{2+}]_i$ changes triggered with BK were potentiated by L-β-ODAP treatment. BK-triggered $[Ca^{2+}]_i$ changes involve Ca^{2+} release from ER stores (Yano et al. 1984) and L-β-ODAP potentiation of these changes is therefore likely to be the consequence of increased ER Ca^{2+} loading, brought about by enhanced SERCA pump activity. In the absence of extracellular Ca^{2+}, the potentiating effect of L-β-ODAP on $[Ca^{2+}]_i$ responses was still observed, suggesting that Ca^{2+} movements over the plasma membrane are not involved. This was confirmed by the store-emptying/Ca^{2+} re-introduction experiments (Fig. 13G-H) that demonstrate no significant influence of L-β-ODAP on SOCE (Venkatachalam et al. 2002). The absence of L-β-ODAP potentiation of ER Ca^{2+} uptake in permeabilized cells (Fig. 14C-D) was somewhat unexpected: this protocol shunts Ca^{2+} entry pathways (SOCE and others) that were not significantly influenced by L-β-ODAP, as already pointed out. However, it is possible that digitonin permeabilization also disrupts

membrane systems inside the cell thereby disturbing some of the intermediate transport/signaling steps on which L-β-ODAP acts.

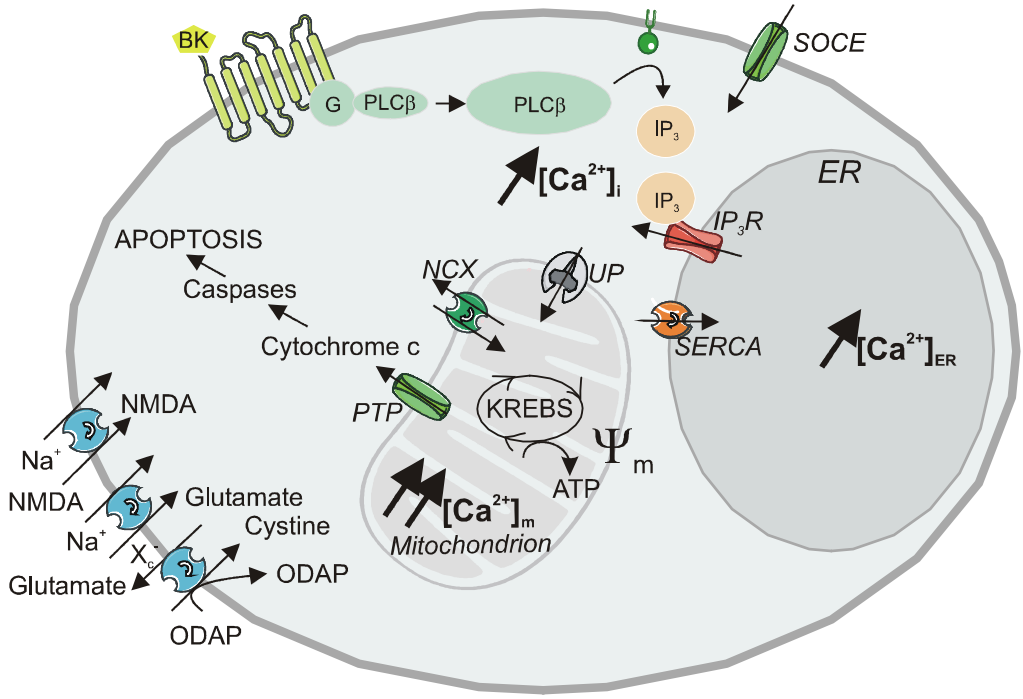

Fig. 18: **Summary diagram of L-β-ODAP effects on intracellular Ca^{2+} homeostasis.** BK activates PLC-β and generates IP_3 that opens IP_3 receptor channels (IP_3-R) in the ER, thereby releasing Ca^{2+} into the cytoplasm and increasing $[Ca^{2+}]_i$. The released Ca^{2+} is taken up by mitochondria via de uniporter (UP), attracted by a negative mitochondrial membrane potential (Ψ_m). Store-operated Ca^{2+} entry (SOCE) helps to refill the Ca^{2+} stores in concert with the SERCA pump and Ca^{2+} may leave the mitochondria via Na^+/Ca^{2+} exchange transport (NCX). 24 h exposure to L-β-ODAP potentiated the BK-triggered $[Ca^{2+}]_i$ transients (oblique arrow left of $[Ca^{2+}]_i$) and slightly (non-significantly) increased $[Ca^{2+}]_{ER}$ loading (oblique arrow left of $[Ca^{2+}]_{ER}$) and SERCA pump expression. The larger $[Ca^{2+}]_i$ transients and increased $[Ca^{2+}]_{ER}$ filling lead to increased mitochondrial Ca^{2+} uptake. This effect stimulates mitochondrial ATP generation that hyperpolarizes Ψ_m, thereby attracting more Ca^{2+} resulting in a strong potentiation of $[Ca^{2+}]_m$ changes (double arrows left of $[Ca^{2+}]_m$). The continuation of this cycle may lead to opening of the permeability transition pore (PTP), cytochrome C release and induction of apoptosis via caspase signaling. In N2a cells the cycle stops before induction of apoptosis, because these cells lack AMPA-receptors and have a stronger Ca^{2+} buffering capacity compared to the motor neurons that are the specific target of L-β-ODAP in neurolathyrism. L-β-ODAP can enter the cells via the x^- antiporter, thereby accumulating and exerting its effects on cellular Ca^{2+} handling. L-glutamate and NMDA make their way into the cells via Na^+-dependent transporters; in contrast to L-glutamate NMDA cannot further be metabolized and may, like L-β-ODAP accumulate. Importantly, NMDA had no effect on mitochondrial Ca^{2+} uptake pointing to a specific effect of L-β-ODAP on Ca^{2+} homeostasis.

Mitochondria form an important uptake pathway for Ca^{2+} released from the ER and are capable of sensing microdomains of high $[Ca^{2+}]_i$ generated in close proximity to the ER Ca^{2+} release channels (Rizzuto et al. 1994; Campanella et al. 2004; Csordas et al. 2006). The strong potentiation of mitochondrial Ca^{2+} uptake by L-β-ODAP after the BK challenge may, in part, result from an increased load coming from the cytoplasm and ER. However, L-β-ODAP also strongly hyperpolarized Ψ_m, which is a major driving force for Ca^{2+} entry via the uniporter into the mitochondrial matrix (Duchen 2000; Gunter et al. 2000) and therefore a likely cause of the enhanced mitochondrial Ca^{2+} uptake. Mitochondrial Ca^{2+} accumulation is a positive modulator of mitochondrial ATP synthesis, due to the presence of Ca^{2+}-sensitive dehydrogenases in the matrix and inner mitochondrial membrane that contribute to ATP synthesis (Denton et al. 1988). L-β-ODAP had no measurable effect on the cellular ATP concentration but it is possible that the cells decrease glycolytic flux in response to increased mitochondrial ATP concentration (feedback actions via hexokinase, phosphofructokinase and pyruvate kinase) (Leybaert 2005). Treatment with L-β-ODAP, however, rescued the cells from cell death induced by exposure to low extracellular glucose conditions, suggesting that L-β-ODAP did indeed increase the rate of mitochondrial ATP synthesis.

Extensive mitochondrial Ca^{2+} uptake is a major factor in cell death associated with neurodegenerative diseases, including Alzheimer's disease. Mitochondrial Ca^{2+} loading stimulates the production of free radicals and may lead to an increased mitochondrial permeability and dissipation of ψ_m, thereby impairing mitochondrial function and leading to cell death via ATP depletion or opening of the permeability transition pore (Duchen 2000; King et al. 2001; Du et al. 2008; Sanz-Blasco et al. 2008). In addition, ER-mitochondrial Ca^{2+} movements play a key role in setting the stage to apoptotic cell death (Pinton et al. 2008). In the presently used N2a neuroblastoma cells, the observed mitochondrial Ca^{2+} accumulation did not lead to cell death, presumably because the AMPA-receptors that ignite the excitotoxic cascade are absent and because tumor cells have a higher mitochondrial Ca^{2+} buffering capacity compared to non-tumor cells (Rodriguez-Nieto and Zhivotovsky 2006). Additionally, the hyperpolarization of the Ψ_m by L-β-ODAP was also shown to be protective against cell death induced by mitochondrial depolarization brought about by FCCP. These data therefore suggest that we are focusing on an early stage in the cascade that potentially leads to cell death upon further progression. Additional experiments are required to verify this concept, but the data support the following sequence of events (Fig. 18): L-β-ODAP, via its intrinsic effects on cellular Ca^{2+} handling, enhances ER Ca^{2+} loading, resulting in increased mitochondrial Ca^{2+} uptake. This activates mitochondrial ATP generation and makes ψ_m more negative, thereby attracting more Ca^{2+}. This cycle continues until the mitochondrial Ca^{2+} load triggers the release of cytochrome C, paving the pathway toward execution of apoptosis – a stage not reached in N2a cells. In line with this proposal, recent

work has demonstrated that depolarizing ψ_m prevents the neurotoxic (apoptosis inducing) effect of Aβ oligomers (Sanz-Blasco et al. 2008), supporting increased mitochondrial negativity as a *primum movens* of Ca^{2+} overload. The current results differ from the reported inhibitory effect of L-β-ODAP on complex-I of the electron transfer chain (Sriram *et al.* 1998), which would result in mitochondrial depolarization. The most obvious explanation for this is that hyperpolarization is an early event that is transformed into depolarization when mitochondrial Ca^{2+} loading becomes more extensive thereby disturbing mitochondrial function. Finally and importantly, the prototypic excitotoxic substances L-glutamate and NMDA appeared not to affect mitochondrial Ca^{2+} handling, indicating that the reported alterations are specific for L-β-ODAP and not the consequence of accumulation into the cells.

3.3.6. Conclusion

These findings shed new light on the complex effects of chronic exposure to L-β-ODAP, which in an early phase subtly alters cellular Ca^{2+} handling to prepare for its final excitotoxic attack leading to extensive neuronal cell losses. Experiments are under way to investigate this cascade in motor neurons, which are the only cell type affected in neurolathyrism and are known for their high vulnerability to mitochondrial Ca^{2+} overload, due to a smaller number of Ca^{2+}-binding proteins (Hugon et al. 1993), a lower mitochondrial density (Grosskreutz et al. 2007) and relatively more Ca^{2+}-conducting AMPA-receptors (Van Damme et al. 2002a).

3.4. L-β-ODAP neurotoxicity – primary motor neurons

To extrapolate the results obtained in N2a neuroblastoma cells to primary cells, similar experiments were performed in primary motor neurons of the rat.

This section corresponds to the following reference: Marijke Van Moorhem, Elke Decrock, Elke De Vuyst, Marijke De Bock, Nan Wang, Fernand Lambein, Ludo Van Den Bosch, Luc Leybaert, 2011. L-β-N-oxalyl-α,β-diaminopropionic acid (L-β-ODAP) toxicity in motor neurons. NeuroReport 22(3):131-5.

3.4.1. Abstract

The excitatory amino acid L-β-N-oxalyl-α,β-diaminopropionic acid (L-β-ODAP) in *Lathyrus sativus* L. is proposed as the causative agent of the neurodegenerative disease neurolathyrism. The effect of L-β-ODAP was investigated on $[Ca^{2+}]_i$ handling, redox homeostasis and cell death in rat spinal motor neurons. L-β-ODAP and L-Glutamate (L-Glu) triggered $[Ca^{2+}]_i$ transients, which were inhibited by the α-amino-3-hydroxy-5-methyl-4-isoxazole propionic acid receptor (AMPA-R) blockers 2,3-dioxo-6-nitro-1,2,3,4-tetrahydrobenzo[f]quinoxaline-7-sulfonamide (NBQX) and 1-naphtyl acetylspermine (NAS), the latter specifically blocking Ca^{2+}-permeable AMPA-R. Additionally, NBQX, and to a lesser extent NAS, protected the neurons against cell death induced by L-β-ODAP or L-Glu. Methionine (Met) and cysteine (Cys) were also protective against neuronal cell death. It can be concluded that deregulation of $[Ca^{2+}]_i$ homeostasis and oxidative stress contribute to motor neuron cell death in neurolathyrism.

3.4.2. Introduction

Prolonged consumption of *Lathyrus sativus* L. seeds (grass pea) in an unbalanced diet is associated with the development of neurolathyrism, a disease characterized by spastic paraparesis due to the selective loss of motor neurons. A large number of studies have been devoted to the neuro-excitatory amino acid L-β-N-oxalyl-α,β-diaminopropionic acid (L-β-ODAP) since its discovery (Rao et al. 1964). As in other motor neuron diseases, excitotoxicity is a major proposed pathway for its etiology, causing neuronal injury by excessive or prolonged activation of L-Glu-receptors (L-Glu-R) with a subsequent rise in $[Ca^{2+}]_i$. L-β-ODAP has been shown to activate α-amino-3-hydroxy-5-methyl-4-isoxazole propionic acid receptors (AMPA-R) *in vitro* (Bridges et al. 1988) and *in vivo* (Spencer et al. 1987; Kusama-Eguchi et al. 2009), Motor neurons express a substantial fraction of Ca^{2+}-permeable AMPA-R, which are characterized by the absence of the GluR2 subunit (Carriedo et al. 1996). This opens up the possibility that L-β-ODAP triggers excitotoxicity by increasing $[Ca^{2+}]_i$ via GluR2-lacking

AMPA-R activation. Several studies have documented L-β-ODAP induced excitatory effects, but very sparse information is available on its influence on $[Ca^{2+}]_i$ responses (Amba et al. 2002).

L-β-ODAP was reported to inhibit mitochondrial complex-I (Sriram et al. 1998; Kenchappa et al. 2002) and the activity of reducing enzymes (Diwakar and Ravindranath 2007). It also inhibits the x_c^- antiporter, limiting the uptake of cystine in the cell and thus increasing oxidative stress (Warren et al. 2004), which may be exacerbated by the deficiency of grass pea for the sulphur-containing amino acids (SAA) Met and Cys (Lisiewska et al. 2001), two precursors for intracellular GSH synthesis. Additionally, deprivation of Met and Cys appeared to exacerbate the toxicity of high concentrations of L-β-ODAP in primary cultured spinal cord embryonic motor neurons, cortical primary cultured neurons and an L-Glu-sensitive NSC-34 cell line (Kusama-Eguchi et al. 2010b).

The aim of the present study was to investigate the involvement of excitotoxic Ca^{2+} entry and oxidative stress in neuronal cell death induced by relatively low L-β-ODAP concentrations. The results of this study provide evidence that L-β-ODAP concentrations in the tens of micromolar range induce neurotoxicity in primary spinal cord motor neurons. In addition, NAS, a specific inhibitor of Ca^{2+}-permeable AMPA-R (Koike et al. 1997), prevented Ca^{2+} entry and slightly promoted motor neuron survival following L-β-ODAP and L-Glu exposure. Moreover, inclusion of Met and Cys in the culture medium protected motor neurons from L-β-ODAP- and L-Glu-induced toxicity.

3.4.3. Methodology

Cell cultures

Spinal motor neurons were cultured as previously described (Vandenberghe et al. 1998), following procedures approved by the local ethical committee. In brief, ventral spinal cords were dissected from 14-day-old Wistar rat embryos in Hanks' balanced salt solution (HBSS: 0.81 mM $MgSO_4.7H_2O$, 0.95 mM $CaCl_2.2H_2O$, 137 mM NaCl, 0.18 mM $Na_2HPO_4.2H_2O$, 5.36 mM KCl, 0.44 mM KH_2PO_4, 5.55 mM D-Glucose, 25 mM Hepes, pH 7.4), cut in pieces of about 1 mm and digested for 15 min in 0.05 % trypsin in HBSS at 37 °C. After treatment with DNase, the tissue was further dissociated by trituration. A motor neuron-enriched neuronal population was purified from the ventral spinal cord by centrifugation on a 6.5 % metrizamide cushion and was cultured on a glial feeder layer, which had been pre-established on a 16-mm round glass coverslip or Petri dish coated with poly-L-ornithine and laminin. The culture medium consisted of L15 supplemented with sodium bicarbonate (0.2 %), glucose (3.6 mg/mL), progesterone (20 mM), insulin (5 µg/mL), putrescine (0.1 mM), conalbumin (0.1

mg/mL), sodium selenite (30 nM), penicillin (100 IU/mM), streptomycin (100 µg/mL) and horse serum (2 %). Most of the cells in culture are motor neurons (Van Damme et al. 2002b). The endogenous L-glutamate concentration of this medium is estimated to be 6 µM (Ye and Sontheimer 1998), whereas the concentration of Cys and Met in L-15 medium is 992 µM and 503 µM, respectively. Cultures were kept in a 7 % (v/v) CO_2 / 93 % O_2 humidified incubator at 37°C and neurons were used for experiments after being cultured for 6 - 9 days.

Survival experiments

Cultures were exposed in L15 medium to L-Glu (Sigma-Aldrich) or L-β-ODAP (kindly provided by S. L. N. Rao, Hyderabad, India) for 24 h at 37°C in a 7 % (v/v) CO_2 / 93 % O_2 incubator. To investigate the effect of SAA therapy, Met (2 µM; Sigma-Aldrich) or Cys (2 µM; Sigma-Aldrich) were supplemented to the medium, together with L-Glu (100 µM) or L-β-ODAP (33 µM) for 24 h. Similarly, NBQX (10 µM; Tocris-Bioscience, Missouri, USA) or NAS (100 µM; Sigma-Aldrich) was included to determine the involvement of AMPA-R. Neuronal survival was quantified by an observer blinded to the treatment protocol, directly counting unfixed neurons under phase contrast optics (Nikon, Tokyo, Japan) at 10 X magnification, immediately before and after treatment within an identified region of 1 cm^2. All phase-bright cells of neuronal morphology, without vacuolar inclusions and with intact neurites longer than twice the cell body diameter, were taken into account. The percentage of neuronal survival was determined as the ratio of the number of surviving neurons after 24 h treatment versus the number of neurons before the treatment, normalized to the corresponding controls.

Ca^{2+} imaging experiments

Motor neurons were loaded with the cytoplasmic Ca^{2+} probe Fluo-3-AM (5 µM; 37°C; 30 min; Molecular Probes) in HBSS-Hepes with probenecid (1 mM; Sigma-Aldrich) and pluronic acid (0.01 %; w/v; Sigma-Aldrich), followed by a 15 min de-esterification at 37°C. Imaging was performed on an inverted epifluorescence microscope (ex/em 482/535 nm; 50 nm bandwidth; Nikon Eclipse TE 300, Analis, Ghent, Belgium) with a x40 oil immersion objective. Results are expressed as ΔF/F.

Statistics

Statistical significance was determined by one way ANOVA (post-hoc Bonferroni) or Kruskal-Wallis (post-hoc Dunn) using GraphPad Instat software (GraphPad Software; San Diego, CA). Averaged data are expressed as mean ± S.E.M. In Ca^{2+} imaging experiments, *n* corresponds to the number of motor

neurons obtained from at least three different animals. In motor neuron survival experiments, *n* denotes the number of motor neuron culture dishes, again obtained in at least three different animals. Statistical significance is indicated by one, two or three symbols (* or #) for $p<0.05$; $p<0.01$ or $p<0.001$, resp.

3.4.4. Results

L-ß-ODAP triggers AMPA-R mediated $[Ca^{2+}]_i$ responses

To verify the Ca^{2+} excitability of the motor neurons, the cultures were superfused with L-Glu while recording $[Ca^{2+}]_i$ changes with Fluo-3. Both L-Glu (300 µM) and L-β-ODAP (300 µM), applied during 1 min, induced comparable Ca^{2+} responses (inset to Fig. 19A). The type of ionotropic Glu-R contributing to this Ca^{2+} response was identified by administering specific blockers 1 min before and during the 1 min challenge with L-Glu or L-β-ODAP. The reversibility of the responses was tested by washing out the receptor blockers (2 min) and re-applying L-Glu or L-β-ODAP (1 min) (Fig. 19A). N-methyl-D-aspartate receptors (NMDA-R) were not involved in the recorded Ca^{2+} responses, since administration of the NMDA-R antagonist (+)-5-methyl-10,11-dihydro-S*H*-dibenzo[a,d]cyclohepten-5,10-imine maleate (MK-801; 10 µM) did not reduce L-Glu-induced Ca^{2+} transients (96 ± 9 % vs 100 %; $p>0.05$; data not shown). AMPA-R were, however, clearly involved as the AMPA-R antagonist NBQX (10 µM) significantly inhibited Ca^{2+} responses triggered by L-Glu (82 ± 6 % vs 100 %; $p<0.05$) and L-β-ODAP (56 ± 6 % vs; 100 %; $p<0.001$) (Fig. 19B). NAS (100 µM), which selectively blocks Ca^{2+}-permeable AMPA-R (Van Damme et al. 2002b), significantly decreased the Ca^{2+} responses induced by L-Glu (42 ± 8 % vs; 100 %; $p<0.001$) and L-β-ODAP (56 ± 14 % vs 100 %; $p<0.001$), pointing to the contribution of Ca^{2+} permeable AMPA-R to these responses.

L-ß-ODAP and L-Glu induce motor neuron death by excitotoxicity and oxidative stress

To investigate the mechanism of L-β-ODAP toxicity, the toxic concentration was verified first for primary rat spinal motor neurons by quantifying neuronal survival (see experimental procedures). Fig. 20A depicts the neuronal survival after treatment with L-β-ODAP or L-Glu in culture medium for 24 h. Neuronal survival was expressed relative to the survival under control conditions (dotted lines in Fig. 20) which corresponded to 81 ± 3 % cell survival (n = 18). L-β-ODAP was more toxic than L-Glu, as 33 µM L-β-ODAP and 100 µM L-Glu brought about a similar toxicity level (66 ± 5 % vs 56 ± 9 %, resp.).

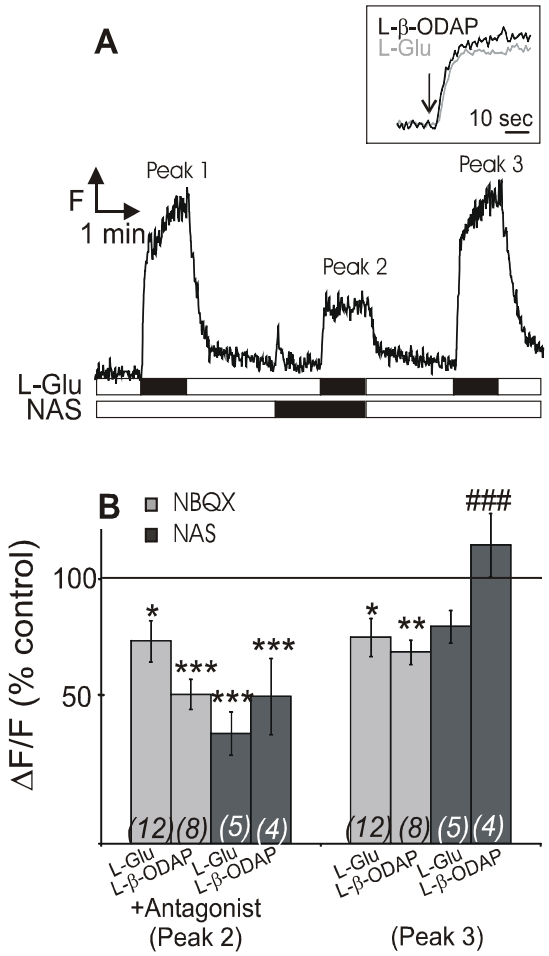

Fig. 19: L-β-ODAP and L-Glu-triggered cytoplasmic Ca^{2+} responses involve AMPA-R activation. A. Example trace of Ca^{2+} responses (measured with Fluo-3) upon exposure of motor neurons in culture to L-Glu (300 µM). The L-Glu-induced Ca^{2+} response was inhibited by NAS (100 µM, added 1 min before the L-Glu challenge). NAS inhibition disappeared after 2 min wash-out. **Inset:** Ca^{2+} responses to L-β-ODAP (300 µM) or L-Glu (300 µM) were similar in magnitude and kinetics. Inhibition experiments were also performed with MK-801 or NBQX (10 µM) instead of NAS, making use of both L-Glu and L-β-ODAP as a stimulus - the average results of these experiments are shown in the panels below. **B.** Summary graph of inhibition of L-Glu- or L-β-ODAP-induced Ca^{2+} responses by AMPA- and NMDA-R antagonists. Control responses corresponding to Peak 1 in panel A were measured as ΔF/F and normalized to 100% (dotted line). L-Glu-triggered Ca^{2+} responses were significantly inhibited by NBQX and NAS, with the latter displaying the strongest effect (Peak 2). For L-β-ODAP, NBQX and NAS inhibited the Ca^{2+} responses with the same potency. Inhibition by NAS was largely reversible upon wash-out while the NBQX effect displayed less recovery (Peak 3). (*) indicates significantly different from control (dotted line) (*p<0.05 - **p<0.01 - ***p<0.001), (#) indicates significantly different from the corresponding bar under 'Peak 2' (### p<0.001).

To determine which subtypes of ionotropic Glu-R contributed to the toxicity of L-β-ODAP, cultures were treated with NBQX or NAS. NMDA-R antagonists were not included, since MK-801 did not influence L-Glu-induced Ca^{2+} responses. Exposure to NBQX or NAS only did not reduce the number of surviving cells (76 ± 6 % and 86 ± 6 % survival resp., not different from 81 ± 3 % survival under control conditions). Inclusion of NAS (100 µM) during the excitotoxic challenge slightly prevented the loss of viability caused by L-β-ODAP or L-Glu, bringing cell survival back to control levels (Fig. 20B). For NBQX (10 µM) the effect was more pronounced (Fig. 20B). These results suggest that Ca^{2+} entry through AMPA-R contributes to L-β-ODAP- and L-Glu-induced neurotoxicity.

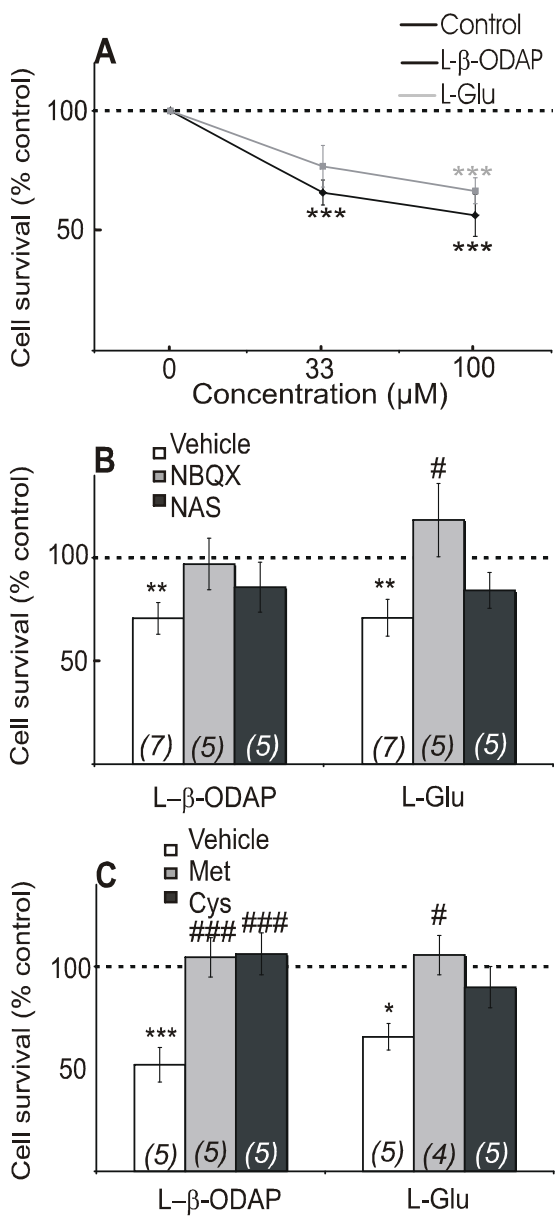

Fig. 20: Motor neuron survival after treatment with L-β-ODAP or L-Glu for 24 h. A. Concentration-response curve for L-β-ODAP and L-Glu (24 h). Motor neuron survival after exposure to vehicle was normalized to 100% (dotted line). The survival decreased after treatment with 33 µM L-β-ODAP and 100 µM L-Glu. (*) indicates significantly different from control. **B.** Summary graph of survival experiments with AMPA-R blockers. NBQX slightly improved neuronal survival after exposure to L-β-ODAP (97±12% vs 71±8%; p>0.05) and significantly improved survival after L-Glu exposure (118±18% vs 71±9%; p<0.05). The effect of NAS was less pronounced (both for L-β-ODAP (95±9% vs 71±8%; p>0.05) and L-Glu (84±9% vs 71±9%; p>0.05)) but apparently sufficient to bring neuronal survival within the normal control range. Significant differences are indicated by (*) compared to control (dotted line - ** p<0.01). (#) compares to the open bar for L-Glu (# p<0.05). **C.** Summary graph of survival experiments with SAA. Motor neuron survival increased after supplying the treatment medium with additional Met (104±10%) or Cys (106±10%), compared to neurons exposed to L-β-ODAP in normal medium (52±8%). Similar results were found for L-Glu-induced toxicity (106±10% for Met, 90±10% for Cys, vs 66±6% for L-Glu); the Cys effect was less pronounced here but still strong enough to restore survival to control levels. (*) indicates significantly different from control (dotted line -*p<0.05 -***p<0.001) – (#) is significantly different from the open bar of the L-β-ODAP or L-Glu exposure (# p<0.05- ### p<0.001).

Ca^{2+}-induced cell death is likely to be associated with a component of oxidative stress. Grass pea is deficient for Met and Cys, two precursors of endogenous reducing agent GSH. To evaluate the involvement of oxidative stress in L-β-ODAP- or L-Glu-induced neurotoxicity, motor neuron survival was studied after treatment with Met (2 µM) or Cys (2 µM) supplied in the treatment medium together with L-β-ODAP (33 µM) or L-Glu (100 µM) for 24 h. Exposure to Met or Cys only did not affect cell survival (72 ± 10 % and 80 ± 5 % survival resp., not different from 81 ± 3 % control survival). These data show that the inclusion of Met or Cys resulted in protection of motor neurons against L-β-ODAP- or Glu-induced toxicity (Fig. 20C).

3.4.5. Discussion

This research work focused on mechanisms involved in neurolathyrism, a pure motor neuron degenerative disease. For this purpose, the toxicity of the causative toxic agent, L-β-ODAP, was studied in rat primary co-cultured spinal cord motor neurons, one of the best *in vitro* models to study motor neuron diseases. The results of this study provide evidence that NAS (a specific inhibitor of Ca^{2+}-permeable AMPA-R (Koike et al. 1997)) prevented Ca^{2+} entry and slightly improved motor neuron survival following L-β-ODAP or L-Glu exposure. In addition, inclusion of Met and Cys in the culture medium protected motor neurons from L-β-ODAP- and L-Glu-induced toxicity.

Activation of AMPA-R is one of the suggested mechanisms for L-β-ODAP-induced excitotoxicity. So far, the involvement of Ca^{2+}-permeable AMPA-R has only been studied in *Xenopus* oocytes expressing cloned Glu-R (Kusama-Eguchi et al. 1996). The results of this study further confirm that motor neurons express Ca^{2+}-permeable AMPA-R (Van Damme et al. 2002a) and bring up novel data supporting a role of Ca^{2+}-permeable AMPA-R in Ca^{2+} transients triggered by L-β-ODAP in motor neurons. NMDA-R activation was not involved in the observed Ca^{2+} responses, as indicated by the experiments with MK-801, which is in line with a previous study (Van Den Bosch et al. 2006).

L-β-ODAP may also activate other pathways like Ca^{2+}-impermeable AMPA-R and voltage-gated Ca^{2+} channels. As a consequence, neuronal depolarization may lead to additional Ca^{2+} entry (Dayanithi et al. 2006). This might explain the residual Ca^{2+} peak after L-Glu stimulation in the presence of NAS (Fig. 19). In addition, this may explain why NAS was less efficient than NBQX in promoting motor neuron survival after L-β-ODAP or L-Glu exposure (Fig. 20B).

Motor neurons are specifically vulnerable to oxidative stress having particularly low levels of reduced GSH (Ratan et al. 1994). Supplying precursors of GSH (Met and Cys) appeared to be clearly protective for motor neurons exposed to L-β-ODAP or L-Glu, indicating the involvement of oxidative stress, possibly as a downstream event of AMPA-R activation as suggested by the experiments with NBQX or NAS. Increased free-radical generation and more pronounced loss of antioxidant capacity will result in a collapse of the mitochondrial membrane potential, ultimately leading to necrosis or apoptosis (Orrenius et al. 2003; Csordas and Hajnoczky 2009). The effect of supplying Met or Cys to motor neurons exposed to L-β-ODAP was also studied recently by Kusama-Eguchi *et al.*, after inducing a deficiency-state for these SAA (Kusama-Eguchi et al. 2010b). In the present study, no deficiency was induced. Instead, supplemental Met and Cys appeared to efficiently protect against L-β-ODAP-induced neuronal cell death. Moreover, by comparing the effectiveness of AMPA-R blockers and SAA

in preventing cell death upon exposure to L-β-ODAP, it appears that oxidative stress is probably more important for L-β-ODAP neurotoxicity than Ca^{2+}-related excitotoxicity. Comparison of the two major proposed mechanisms for L-β-ODAP-induced neurodegeneration in the very same experimental setup brings new valuable insights in the etiology of neurolathyrism.

Neurolathyrism has so far no treatment and the knowledge of involved mechanisms should help finding appropriate treatments. However, preventive measures are probably more appropriate, such as supplying a balanced diet or food supplements. Epidemiological data indeed suggest that cereals may compensate for the Met and Cys deficiency of grass pea (Getahun et al. 2003). This suggestion is further supported by the present *in vitro* data, where supplemental addition of Met or Cys in the treatment medium of motor neurons protected the cells against L-Glu or L-β-ODAP induced toxicity.

3.4.6. Conclusion

This study demonstrates that Ca^{2+}-permeable AMPA-R contribute to altered $[Ca^{2+}]_i$-handling caused by L-β-ODAP and that Met and Cys protect motor neurons against L-β-ODAP-induced toxicity. As a result, deregulation of $[Ca^{2+}]_i$ homeostasis and oxidative stress are proposed as leading instigators of motor neuron cell death in neurolathyrism, giving a cellular basis to develop novel preventive approaches toward this somewhat overlooked disease.

CHAPTER 4

General discussion, conclusions and future perspectives

CHAPTER 4: General discussion, conclusions and future perspectives

The overall aim of the study was to better understand the mechanisms that are responsible for the degeneration of motor neurons in neurolathyrism patients. In particular, the effects of L-β-ODAP on BBB endothelial cells, glial cells and neurons were investigated and amino acid metabolism was studied in urine of neurolathyrism patients and healthy control subjects.

4.1. Effect of L-β-ODAP on the BBB

Previous studies showed that L-β-ODAP was detected in blood after grass pea consumption (Pratap Rudra et al. 2004) and in the CNS of most species, though this conclusion relies on experimental models - with the restriction that so far no satisfying animal model has been identified for neurolathyrism. It was suggested that entry of L-β-ODAP into the CNS may be a time dependent phenomenon and may be favoured by an immature BBB or a disturbance of some physiological balance brought about by L-β-ODAP (Rao 1978).

In section 3.1 we demonstrated that 6 days exposure to relatively low concentrations of L-β-ODAP (but not to L-glutamate) increased the *in vitro*-measured BBB permeability, while acute exposure to higher concentration had no such effect. This result is in line with the epidemiological evidence that grass pea consumption for a long period leads to neurolathyrism, whereas a single dose of high L-β-ODAP concentrations does not lead to neurolathyrism. Higher L-β-ODAP concentrations had no effect on the *in vitro*-measured BBB permeability, suggesting that L-β-ODAP has a bimodal concentration-response curve for its effects on the BBB endothelium. Increased BBB permeability consequent to L-β-ODAP exposure may serve as an entry point of L-β-ODAP into the CNS (Fig. 23). The mechanism by which L-β-ODAP increases BBB permeability is currently not known, but oxidative stress may be a contributing factor. More specifically, ROS have been shown to activate the phosphatidylinositol 3 (PI_3)-kinase and protein kinase B (PKB, a.k.a. Akt) pathway in brain endothelial cells, which results in a redistribution and disappearance of the tight junction proteins occludin and claudin 5. As a consequence, the BBB permeability will increase, allowing neurotoxins and inflammatory cells to enter the brain (Halliwell 2006; Schreibelt et al. 2007). In glial and neuronal cells L-β-ODAP-induced cell death was shown to be related to oxidative stress, suggesting that oxidative stress may also play a role in endothelial cell death, though additional experiments are needed to support this hypothesis. Interestingly, L-glutamate generally had no effect on the BBB permeability, pointing to a specificity of the effect of L-β-ODAP, different from its so-called analogue excitotoxic amino acid.

4.2. L-β-ODAP gliotoxicity

Once L-β-ODAP has made its entry into the CNS, it can exert its toxic effects on neurons, more specifically on motor neurons. Although neurolathyrism research has largely focused on the direct action of L-β-ODAP at glutamate receptors, triggering neurotoxicity, non-neuronal cells may also be involved in this process. More specifically, astrocytes have been shown to play an important role in neurovascular and neurometabolic coupling, in defending neurons against oxidative injury, pH buffering, the glutamate–glutamine cycle and K^+ buffering (Allaman et al. 2011). Therefore, in section 3.2, gliotoxicity of L-β-ODAP, compared to L-glutamate, was investigated.

Our experiments on C6 glioma cells revealed that L-β-ODAP and L-glutamate induced cell death after 24 h, and the concentration needed to induce ± 50 % cell death was three times less for L-β-ODAP (5 mM) compared to L-glutamate (15 mM). In primary glial cells, the same concentration of L-β-ODAP (5 mM) induced cell death after 24 h, whereas L-glutamate was never toxic even at high millimolar concentrations. This difference is probably related to the metabolism of L-glutamate by the action of glutamine synthetase. It is known that C6 glioma cells are not able to convert L-glutamate to glutamine (Brennan et al. 2006), and glutamine synthetase does not convert L-β-ODAP, which points to intracellular accumulation of these amino acids, apparently becoming toxic at threshold levels of 5 mM (L-β-ODAP) or 15 mM (L-glutamate in C6 glioma cells).

Gliotoxicity studied in C6 glioma cells was prevented by adding antioxidative acids (Cys or Asc) to the medium, but these compounds did not have any effect on the L-β-ODAP–induced cell death in primary glial cells.

In the cultured primary glial cells, microglia appeared to be the most vulnerable type of glial cells for L-β-ODAP-induced cell death, which is a novel observation. In addition, astrocytes showed swollen mitochondria upon exposure to L-β-ODAP. Swollen mitochondria have been observed in many neurodegenerative diseases: Parkinson's disease, Alzheimer's disease, Huntington's disease, ischemia/stroke, ALS and epilepsy (Perkins et al. 2009), and may correspond to an early stage in mitochondrial dysfunction, which can ultimately lead to cell death.

Microglia and astrocytes are crucial for neuronal survival. In response to activation of glutamatergic neurons, released L-glutamate will be taken up from the extracellular space by surrounding astrocytes to be converted to glutamine. It is also known that following L-glutamate uptake, more lactate is released in the extracellular space. Lactate is then shuttled to neurons that, in turn, use it as

an energy substrate (Allaman et al. 2011). As a consequence, an imbalance of one of the steps in astrocytic L-glutamate uptake can contribute to extracellular accumulation of L-glutamate to pathological levels or may generally impair neuronal survival by depleting energy delivery from lactate. Additionally, in response to neuronal depolarization, K^+ will be released into the extracellular space. Excessive extracellular K^+ normally is buffered by astrocytes as it is spread across the astrocytic network via gap junctions (Allaman et al. 2011). Astrocytes are also involved in the protection of neurons against oxidative stress by providing Asc, which can not only be used directly in astrocytes but also released and taken up by neurons for ROS scavenging. Also astrocyte-derived GSH may be released in the extracellular space, where it is cleaved by the astrocytic ectoenzyme γ-glutamyl transpeptidase. The resulting dipeptide, CysGly, is cleaved by the neuronal ectopeptidase aminopeptidase N, forming Cys and glycine, which serve as precursors for neuronal GSH synthesis. Enhancing GSH production and release from astrocytes via overexpression of the cystine/glutamate exchanger (x_c^-) has been shown to be neuroprotective (Allaman et al. 2011). In summary, astrocytic dysfunction or death will impair neuronal survival by affecting L-glutamate metabolism and subseguent lactate supply, decreasing K^+ buffering and impairing the defense against oxidative stress.

Microglia are the resident, innate immune cells of the brain, and they are involved in neuroinflammation. Sustained microglial activation during chronic neuroinflammation, which has been proposed to contribute to neurodegeneration in several neurodegenerative diseases such as Parkinson's disease, Alzheimer's disease and ALS, was proposed to be responsible for the progression of the diseases (Frank-Cannon et al. 2009). In case of neurolathyrism, microglia appeared to be specifically vulnerable to L-β-ODAP, when exposed to 3 mM L-β-ODAP for 24 h. More evidence is needed to support this hypothesis, but the toxicity of L-β-ODAP for microglia, which prevents sustained activation of microglial cells, might be in line with the non-progressive nature of neurolathyrism. On the contrary, a provocative recent report has suggested that the loss of the neuron-supporting and neuroprotective effects of microglia rather than microglial activation may contribute to the onset of sporadic Alzheimer's disease (Streit et al. 2009), suggesting that microglial death observed upon exposure to L-β-ODAP may contribute to the onset of neurolathyrism.

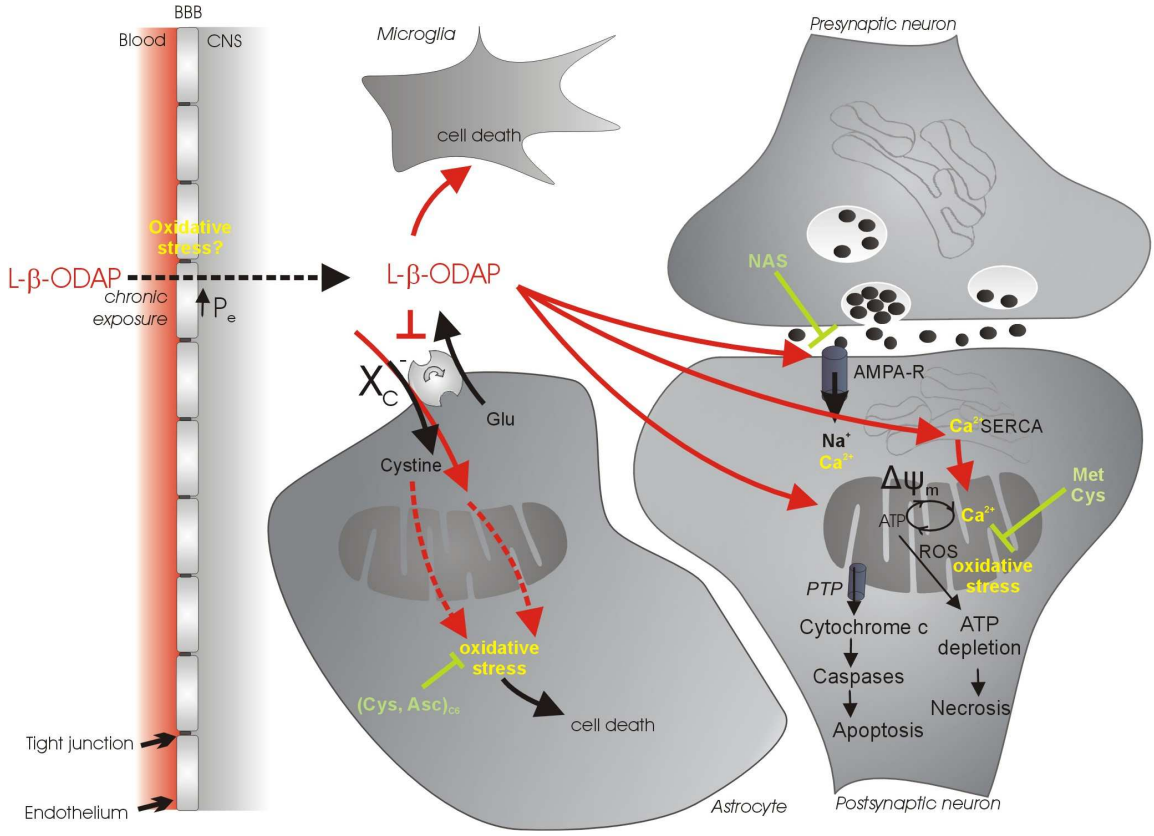

Fig. 23: Scheme summarizing the effect of L-β-ODAP on the neurovascular unit, including BBB endothelial cells, glial cells and neuronal cells. Chronic exposure of BBB endothelial cells results in increased permeability, which may allow passage of L-β-ODAP from the blood into the neural tissue. In neurons, L-β-ODAP activates AMPA-Rs, including Ca^{2+}-permeable ones, increasing $[Ca^{2+}]_i$. L-β-ODAP promotes ER Ca^{2+} loading and induces hyperpolarization of the ψ_m, which will result in Ca^{2+}-accumulation in mitochondria and increased oxidative stress. This will lead to cell death via necrotic or apoptotic pathways. Glial cells are also affected by L-β-ODAP: microglia are specifically vulnerable to L-β-ODAP-induced toxicity, and in astrocytes L-β-ODAP affects the function of mitochondria, which may contribute to increased oxidative stress and cell death. Both cell types are crucial for neuronal survival: astrocytes have a well documented role as a glutamate re-uptake pathway, as suppliers of energy substrates and as buffer/suppliers for ions and various metabolites.

The concentrations of L-β-ODAP used in the gliotoxicity studies, are relatively high when compared to the L-β-ODAP concentrations that have been reported in the CNS. There are three independent studies available describing L-β-ODAP concentrations in the brain, in blood or in blood plasm following L-β-ODAP application or consumption of grass pea. The reported 32.38 µM CSF concentration of L-β-ODAP, following administration of 200 mg radioactively-labeled L-β-ODAP and subsequent measurement of the radioactivity in CSF samples obtained after lumbar punction of two monkeys (Rao 1978), is much lower than the concentrations inducing gliotoxicity, but corresponds well to the concentrations necessary to obtain neurotoxicity (33 µM). The same paper reported 0.17 % radioactivity in the CNS (relative to the injected dose) and we made an approximate calculation of concentrations to be expected in the brain tissue. Assuming that the average brain volume of male

Rhesus monkeys is 89 mL (Franklin et al. 2000), 1.898 µmol L-β-ODAP (0.17 % of 200 mg L-β-ODAP) corresponds to ~21 µM if L-β-ODAP would be distributed over the intra- and extracellular space. If distributed over the extracellular compartment only, a concentration of ~107 µM is expected, since the extracellular volume is known to represent 20 % of the brain volume (Sykova and Nicholson 2008) (17.8 mL). These first order estimates suggest a brain concentration range of ~20-100 µM that is well in accordance with the CSF data reported by Rao (1978). In a second study, a maximal concentration of 177 µM L-β-ODAP was detected in blood 4 h after grass pea (100 g) consumption (Pratap Rudra et al. 2004). This concentration is in the range of the 200 µM L-β-ODAP that was found to result in increased permeability of the BBB. The third study reporting L-β-ODAP concentrations in plasma of a healthy volunteer, detected 5.25 µM L-β-ODAP 5 h after consumption of 200 g boiled grass pea, which is much lower than the concentration observed in the second study. These three studies report relatively low L-β-ODAP concentrations (5 to 200 µM range), but these were registered after one single intake event of grass pea or L-β-ODAP. Several studies have already suggested that the onset of neurolathyrism is a result of more a time than a concentration dependent exposure to L-β-ODAP, raising the possibility that higher L-β-ODAP levels would be found in neurolathyrism patients, as a result of accumulation of L-β-ODAP in blood and/or CNS upon prolonged exposure.

4.3. L-β-ODAP neurotoxicity

The two main mechanisms proposed to induce neurodegeneration are excitotoxicity and oxidative stress. A key factor in excitotoxic damage is intracellular Ca^{2+} overload, consequent to excessive stimulation of glutamatergic neurons. Since neurolathyrism occurs after chronic consumption of grass pea, containing L-β-ODAP, the effect of chronic exposure (24 h) of neuronal cells to L-β-ODAP on intracellular Ca^{2+} homeostasis was studied, as is described in section 3.3. In N2a neuroblastoma cells it was possible to study Ca^{2+} in subcellular compartments and because of the absence of AMPA- and NMDA-R, that generally contribute to the excitotoxic cascade, the intrinsic effects of L-β-ODAP could be studied, separate from the major disturbance of Ca^{2+} homeostasis as a consequence of cell death. In addition, the higher mitochondrial Ca^{2+} buffering capacity of tumor cells (Rodriguez-Nieto and Zhivotovsky 2006) probably protects N2a neuroblastoma cells against excitotoxic cell death, allowing us to study an early stage in the excitotoxic cascade that may act to prepare the pathological cascade leading to neuronal cell death. The results showed that $[Ca^{2+}]_i$ changes triggered with BK were potentiated by L-β-ODAP treatment, as a consequence of increased ER Ca^{2+} loading, brought about by enhanced SERCA pump activity, whereas Ca^{2+} movements over the plasma membrane appeared not to be involved. In addition, a strong potentiation of mitochondrial Ca^{2+} uptake by L-β-ODAP after the BK challenge was suggested to result from an increased cytoplasmic and endoplasmic

Ca^{2+} load and from a hyperpolarized Ψ_m with concomitant increased mitochondrial ATP synthesis. In line with these results described for entry of L-β-ODAP in the CNS, we found that the prototypic excitotoxic substances L-glutamate and NMDA did not affect mitochondrial Ca^{2+} handling, indicating that the reported alterations are again specific for L-β-ODAP and not the consequence of accumulation of L-β-ODAP into the cells.

Additional experiments are required to verify this hypothesis, but based on the data presented in section 3.3 and based on published data (Duchen 2000; King et al. 2001; Du et al. 2008; Sanz-Blasco et al. 2008), the following sequence of events was proposed (Fig. 23): L-β-ODAP enhances ER Ca^{2+} loading, resulting in increased mitochondrial Ca^{2+} uptake. This activates mitochondrial ATP generation and hyperpolarizes the ψ_m, which attracts more Ca^{2+}. This cycle of mitochondrial Ca^{2+} loading produces free radicals and increases the mitochondrial permeability, dissipating the Ψ_m. This results in opening of the PTP, ATP depletion or the release of cytochrome C, triggering the apoptotic or necrotic pathway – a stage not reached in N2a cells.

In section 3.4, the toxicity of L-β-ODAP was studied in primary co-cultured spinal cord motor neurons, an appropriate *in vitro* model to study motor neuron diseases. In contrast with N2a neuroblastoma cells, these primary motor neurons do express functional AMPA-R, though no NMDA-R, and have particularly low Ca^{2+} buffering capacity (Hugon et al. 1993). Therefore, both acute (minutes) and chronic (24 h) effects of L-β-ODAP were studied in this experimental model. The current results provide evidence that NBQX (an AMPA-R antagonist) and NAS (a specific inhibitor of Ca^{2+}-permeable AMPA-R (Koike et al. 1997)) prevented Ca^{2+} entry and improved motor neuron survival following L-β-ODAP or L-Glu exposure. In addition, inclusion of Met and Cys in the culture medium protected motor neurons from L-β-ODAP- and L-Glu-induced toxicity.

As discussed in section 3.3, mitochondrial Ca^{2+} overload may increase free radical generation, which, on its turn, can cause a collapse of the ψ_m, ultimately leading to necrosis or apoptosis (Orrenius et al. 2003; Csordas and Hajnoczky 2009). Assuming that the hyperpolarization of the ψ_m observed in N2a neuroblastoma cells also occurs in motor neurons, Ca^{2+} entering the cytoplasm of motor neurons through Ca^{2+}-permeable AMPA-R upon exposure to L-β-ODAP might accumulate in mitochondria. Mitochondrial Ca^{2+} loading may then increase the production of free radicals, paving the way towards cell death. This hypothesis is partially confirmed by the protective effects of NBQX and NAS against L-β-ODAP- or L-glutamate-induced cell death, which prevents intracellular Ca^{2+} entry. In addition, and in accordance to gliotoxicity studied in C6 glioma cells, the protective effect of Met and Cys, two precursors of GSH, confirms the involvement of oxidative stress, probably preceeding mitochondrial dysfunction and cell death.

4.4. Future perspectives

Several interesting future perspectives arise from the currently presented data.

In vitro, the hypothesis of L-β-ODAP-induced mitochondrial Ca^{2+} overload in motor neurons, preceding neurodegeneration, can be investigated in the existing neuro-glia co-cultures. Therefore, longer exposure times (> 24 h) combined with lower L-β-ODAP concentrations (< 33 µM) should be tested to evaluate the effect of chronic grass pea intake on neuronal functioning, in line with our findings in N2a neuroblastoma cells.

Our novel finding of microglial death upon exposure to L-β-ODAP should also be explored by investigating the amount of microglial cell death and whether microglial activation preceeds microglial cell death. For this purpose, microglial cells such as murine microglial BV2 cells or primary microglia-neuron co-cultures can be exposed to lower L-β-ODAP concentrations (< 3 mM) and/or shorter exposure times (< 24 h), and microglial cell activation can be detected by measuring NO_2^- production or the release of pro-inflammatory cytokines such as TNF-α and interleukin-6 (IL-6) (McArthur et al. 2010). If so, an interesting link with other neurodegenerative diseases such as Alzheimer's disease is found, opening up the possibility that immune responses are also involved in the onset of neurolathyrism.

Another novel finding, the mitochondrial swelling in astrocytes upon exposure to L-β-ODAP, should also be explored by ultrastructural analysis at different time points, to elucidate different stages in mitochondrial swelling. In addition, determining pro-apoptotic factors such as cytochrome c, that is probably released subsequent to mitochondrial swelling (Perkins et al. 2009) may elucidate the relevance of swollen mitochondria in neurodegeneration.

In vitro experiments are interesting to study isolated mechanisms in rather reduced model systems consisting of neurons only or neurons in co-culture with astrocytes. However, L-β-ODAP concentrations needed to study some *in vitro* effect will always be difficult to compare to *in vivo* situations, as neurons are actually part of a complex network, the 'neurovascular unit', encompassing nerve cells, glial cells, vascular cells, blood cells, the basal lamina and extracellular matrix components. Communication between these diverse cell types is essential to understand the full picture of neurotoxicity and should include the important communication link towards the vascular cells and the BBB that is the first passage point for L-β-ODAP to enter the CNS. Therefore, the toxicity of L-β-ODAP should also be studied *in vitro* in organotypic slices and co-cultures, to elucidate the contribution of different cell types to neurotoxicity, but also *in vivo* after a monotonous diet of grass pea, or injection of L-β-ODAP. An important restriction for *in vivo* experiments is, however, the lack of an appropriate animal model. *In vivo* experiments might also answer the question whether L-β-ODAP accumulates in the CNS of neurolathyrism patients, as was suggested by our BBB experiments,

reaching high concentrations comparable to our *in vitro* experiments. Therefore, blood and CSF levels of L-β-ODAP can be determined in animals with neurolathyrism symptoms that rely on a monotoneous grass pea diet at different time points, to evaluate the time-dependent effect of grass pea consumption. In addition to detecting CSF concentrations of L-β-ODAP, the BBB permeability can also be studied by the application of Evan's Blue tracer, upon grass pea consumption or exposure of the animals to L-β-ODAP. As previously suggested, L-β-ODAP and/or malnutrition may also be involved in increasing the permeability of the BBB by inducing an immune response or an impaired body's response to infection (Kurpad 2006), which may alter the BBB function and initiate a pathological cascade. Therefore, not only the BBB integrity, but also the inflammatory response should be studied *in vivo*, by determining the presence of inflammatory mediators including cytokines , TNF-α, interferon-γ and chemokines, matrix metalloproteinases, free radicals such as O_2^-, H_2O_2, OH^-NOO^- and lipid mediators including prostaglandin E2 and F2a (Stamatovic et al. 2008) with special attention to a time-dependent instead of a concentration-dependent effect of L-β-ODAP. If an inflammatory component is indeed involved, then anti-inflammatory (such as non-steroidal anti-inflammatory drugs) or immune-suppressive (such as glucocorticoids) treatment schedules may be considered for neurolathyrism. Additionally, adding antioxidants to the diet must be considered as a preventive measure.

The recent findings of a decreased VEGF level in neurolathyric rats (Kusama-Eguchi et al. 2010a), presents a link with other neurodegenerative diseases such as ALS (Poesen et al. 2008) and Parkinson's disease (Falk et al. 2009). VEGF may also be involved in brain tissue repair (Krum and Khaibullina 2003). These 'multitasking' effects make VEGF a suitable candidate for therapeutic studies (Ruiz de Almodovar et al. 2009) by either adding exogenous VEGF-B (a structural homolog of VEGF, which exerts neuroprotective effects rather than acting as an angiogenic factor in the nervous system) or up-regulating the endogenous VEGF-B levels. Therefore, working with VEGF in a neurolathyrism model could provide valuable insights regarding the process of neurodegeneration in a multicellular model.

Appendix

Neurolathyrism research in Ethiopia

APPENDIX: Neurolathyrism research in Ethiopia

1. Abstract

To study the effect of changing a grass pea rich diet in a diet without grass pea on the free amino acid profile in urine and plasma, samples were collected from 50 randomly selected participants, before and after 7 and 14 days of a grass pea free diet (21 neurolathyrism patients and 29 controls), living in North Gonder, Ethiopia. The participants were interviewed using questionnaires. In general, the questionnaires indicated that all participants were aware of neurolathyrism as a consequence of grass pea, and as a disease without cure. The mean age of onset of neurolathyrism for the patients included in this survey was 23 years, most of them resided in stage 2, and the main problem they reported was back pain. Grass pea food was prepared in various ways but the most popular were baked preparations or using it as a sauce. The most commonly used additives to grass pea were shallot onions and ginger. Compared to controls, neurolathyrism patients consumed the green unripe seeds more frequently, they used to eat grass pea without any additional ingredients for a longer period and they added chick pea, sorghum and wheat less frequently to grass pea. High performance liquid chromatography (HPLC) analysis of a selection of 6 patients and 5 controls with similar age and living in the same village showed higher values of homoarginine in patients compared to controls.

2. Aim of the study

In a previous study, some urinary amino acids were found to be different in neurolathyrism patients compared to control subjects, suggesting that the amino acid metabolism of neurolathyrism patients may be altered. However, no data were available on the food habits of these subjects, and no corresponding blood samples or samples from the grass pea seeds they consumed were available. We therefore wanted to study the free amino acids in urine and plasma samples from patients and healthy subjects living in the same area, more specifically when a grass pea rich diet was replaced by a grass pea free diet during two weeks. Using a questionnaire, the representability of our participants was verified and additional information was included such as their age, living area and food habits, which may be linked to the results of their urine or blood samples that were collected.

3. Introduction

Neurolathyrism is a neurodegenerative disease with a nutritional cause. We therefore studied the effects of nutrition on the metabolism of neurolathyrism patients, to possibly correlate metabolic alterations to neurological deficits. The location where neurolathyrism patients were recruited for

this study, was selected based on data from previous epidemiological reports. In the mid seventies an epidemic of neurolathyrism was reported in the northwest region of Ethiopia, and peak occurrences were observed during the 1984/85 major famine and in 1994 (Getahun et al. 1999; Getahun et al. 2002b). We therefore selected participants for this survey in North Gonder.

Since previous studies indicated some factors associated with a certain susceptibility for neurolathyrism, such as young age and male sex (Haimanot et al. 1990; Haque et al. 1996), exclusive use of clay utensils (Getahun et al. 2005), low socio-economic status (Spencer 1999) and the manner of grass pea food preparation, these factors were included in the questionnaire. Similarly, roasted, boiled and raw unripe seeds have been associated with an increased risk for neurolathyrism, whereas no raised risk has been noted for the fermented pancake, unleavened bread or gravy preparations. It has been suggested that the use of more than one third cereals in a *L. sativus* flour mixture or mixing the food with gravy that contains condiments with antioxidant activity reduces the risk for paralysis (Getahun et al. 1999; Getahun et al. 2002a; Getahun et al. 2003; Getahun et al. 2005). Cooking grass pea in clay utensils has been described to more than quadruple the risk to develop neurolathyrism (Getahun et al. 2005).

The degree of neurological impairment has been classified according to the extent of walking difficulty and the need for physical support: stage 1 corresponds to mildly affected subjects having difficulty with running but being able to walk without aid ("no-stick stage"). Stages 2 and 3 represent more severely affected patients who require the support of one ("1-stick stage") or two crutches ("2-stick stage"). The most serious cases cannot stand and are forced to crawl or to use a wheelchair ("crawler stage"; stage 4), which is most uncommon in the affected areas of Ethiopia or Bangladesh (Hugon et al. 1988). Previous studies indicated that most neurolathyrism patients resided in one of the first two stages (Haimanot et al. 1990). The awareness of neurolathyrism as an incurable disease following grass pea consumption has also been evaluated before, indicating that most health workers and neurolathyrism patients know that neurolathyrism is incurable but preventable. However, some Ethiopian patients seek, in addition to consulting a health institution, also relief from holy water, massage with different oils and lubricants, an Islamic service or a traditional healer (Haimanot et al. 1990; Getahun et al. 2002b).

Differences in metabolism between neurolathyrism patients and controls have been tested in a study where the urinary amino acids from 5 neurolathyrism patients and 9 healthy subjects in Ethiopia were analyzed by HPLC after phenyl isothiocyanate (PITC) derivatization and the trace elements Cu^{2+}, Zn^{2+} and Mn^{2+} of urine and seeds were determined by atomic absorption spectroscopy. The results indicated that the free amino acids aspartic acid, glycine, β-aminoisobutyric acid, arginine, α-aminoadipic acid and phenylalanine were statistically higher ($p < 0.05$) in urine from patients than in urine from control subjects and the trace element copper was also statistically higher ($p < 0.05$) in

urine from patients. It was therefore concluded that the amino acid metabolism of neurolathyrism patients may be disturbed and that trace elements such as copper may also be involved in the etiology of neurolathyrism since high copper is related to oxidative stress and mitochondrial dysfunction (Rossi et al. 2004).

In the present study urine and plasma samples were collected from patients who developed neurolathyrism generally during the epidemic of the nineties and compared the free amino acid profile to that of healthy human subjects living in the same area as the patients. More specifically, the possible change in amino acid profile when a grass pea rich diet is replaced by a grass pea deficient diet was studied over a two week period. Using a questionnaire, additional information about the participants was collected including their age, living area and food habits, which made it possible to select 6 patients and 5 controls of comparable age and living in the same village for prelevation of urine sample and subsequent analysis. Grass pea seeds consumed by the participants were also collected to determine the content of L-β-ODAP. The aim was to gather new information on the amino acid metabolism of neurolathyrism patients, thereby contributing to a better understanding of the etiology of neurolathyrism, which may ultimately result in the amelioration of the quality of life of the poorest of the poor in developing countries, with special attention towards a safe nutrition.

This study generally confirms previously reported epidemiological data. Consumption of green unripe seeds, monotonous grass pea consumption for a long period and less addition of antioxidant containing additives were suggested to be risk factors to develop neurolathyrism. Additionally, higher values of homoarginine were found in urine from neurolathyrism patients compared to controls.

4. Methodology

Study design

For this study, performed in 2007, 50 Ethiopian people (male; > 18 years old) were selected in a neurolathyrism-prone area: the villages Achara (n = 4), Jarjar (n = 23), Arebia-Abalibanos (n = 11), Adisgedinge/Debre Zuria (n = 11) and Weyina Tana (n = 1) (Amhara region, North Gonder zone, Dembia woreda) (Fig. 21A). Ethical approval was obtained from Ghent University and all people included in this survey agreed to participate in the study by an oral informed consent. Of those 50 people, 21 were neurolathyrism patients and 29 were controls. The following criteria were used by the researcher and her Ethiopian colleagues to define neurolathyrism cases: a history of grass pea consumption and an obvious symmetrical spastic leg weakness without sensory deficit. Both patients and controls originally declared to consume grass pea at the start of the study (= week 0), though

some of them actually stopped eating grass pea before, as they informed us after being included in this study. At week 0 the participants answered a questionnaire and a blood and urine sample were taken (= sample I). From that day, a grass pea-free diet was supplied to all participants during two weeks. This diet consists of one '*injera*' (a pancake made of teff and/or sorghum) per person per meal, with sauce made of chick pea (95 %) and spices such as garlic and 'berbere' (a mixture of spices such as chili peppers, ginger, cloves (*Syzygium aromaticum)*, coriander, allspice (the dried unripe fruits of *Pimenta dioica)*, rue berries (*Ruta*), and ajwain (*Trachyspermum copticum)*) (5 %). After 1 and 2 weeks, a second and third blood and urine sample was taken (= sample II and III, resp.) (Fig. 21B). The analyzed urine samples discussed in this section come from 6 patients and 5 controls, living in the same area (Jarjar), and being of the same age (patients: 43 ± 15 years old; controls: 43 ± 3 years old). Other urine samples and all blood samples were collected, but still need to be analyzed.

Sample collection

Blood samples were collected by a nurse and directly stored in heparin-tubes (kindly provided by Prof. Dr. J. Philippé) in ice boxes for 4 - 6 hours. After centrifugation, the plasma was isolated and stored in cryo-vials at -20°C.
Urine samples were collected in 15 mL tubes (VWR International, Leuven, Belgium) and were kept in ice boxes (4 – 6 h) before storage at -20°C.

Questionnaires

At the start of the study, people were registered by a questionnaire (see annex), including population data, patient history, knowledge about neurolathyrism and habits of eating grass pea. As most people were analphabetic, the questionnaires were filled out by Ethiopian scientists, translating all questions and answers simultaneously from English to Amharic and *vice versa*.
For every answer, presented in the section 'results', the percentage is calculated corresponding to the number of participants that actually answered that specific question.
HPLC analysis of urine samples

A selection of urine samples from subjects with the same age and living in the same village was analyzed by HPLC to study the effect of a balanced diet on the amino acid content of urine samples from neurolathyrism patients compared to controls, over a two week period. Samples from participants not eating grass pea anymore at the start of the study were excluded from the analysis.

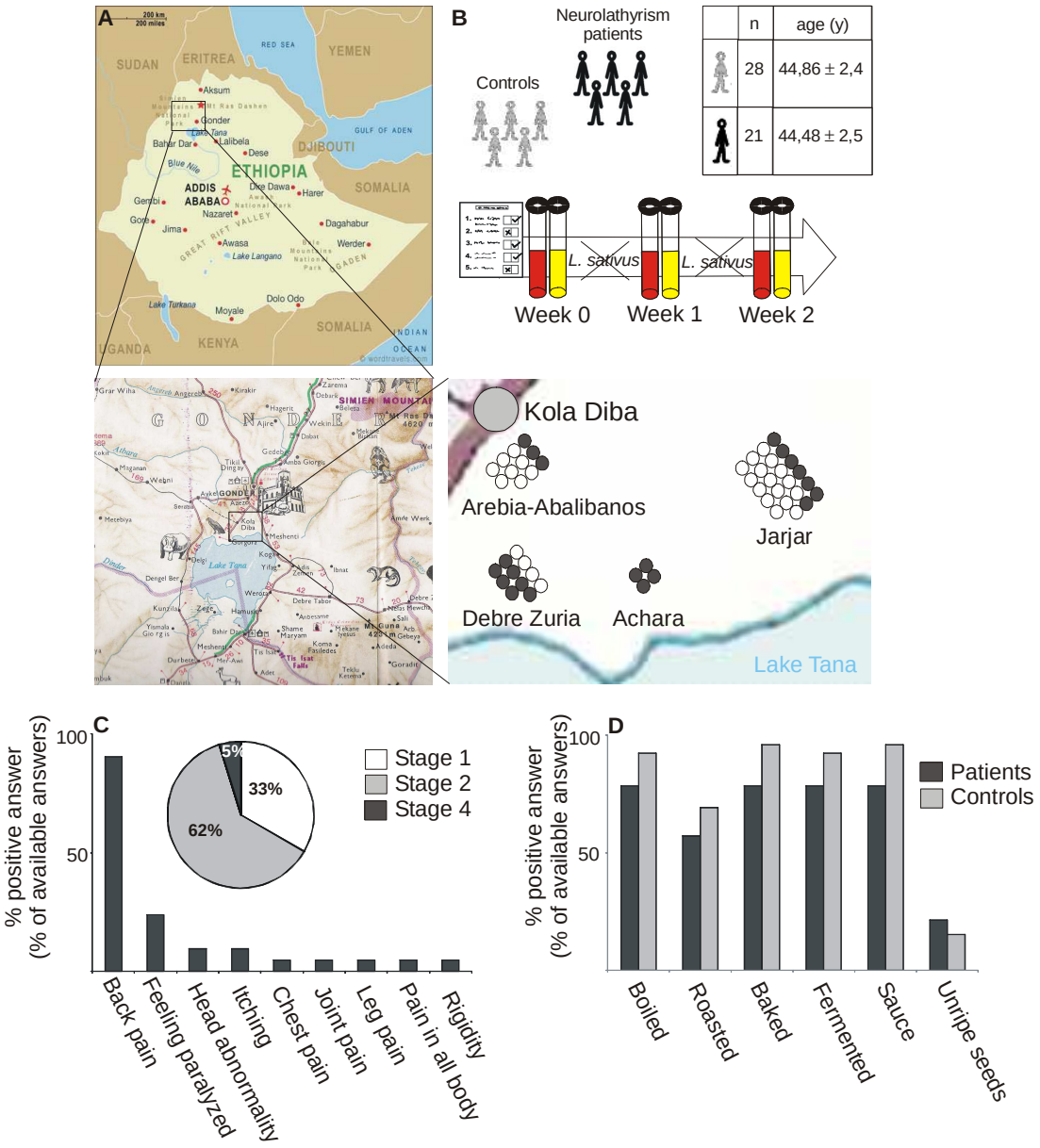

Fig. 21: Localization of the study and study design. A. Localization of the study area. All participants were selected in villages nearby Lake Tana: Achara (n = 4), Jarjar (n = 23), Arebia-Abalibanos (n = 11), Adisgedinge/Debre Zuria (n = 11) and Weyina Tana (n = 1) (Dembia woreda, North Gonder zone, Amhara region, Ethiopia). **B.** Study design. 50 people (21 neurolathyrism patients and 28 controls) from comparable age (patients: 44,48 ± 2,5 years old; controls: 44,86 ± 2,4 years old) and living areas (see A), stating that they frequently consumed grass pea, were asked to answer a questionnaire at the start of the study (= week 0), and a blood and urine sample was taken (= sample I). From that day, all participants were offered a grass pea-free diet during two weeks. After 1 and 2 weeks, a second and third blood and urine sample was taken (= sample II and III, resp.). **C.** Neurolathyrism patients included in the study: 33 % (7 patients) needed no help for walking (stage 1), 62 % (12 patients) needed one stick (stage 2) and 5 % (1 patient) could not walk anymore (stage 4). Besides 'being crippled', the patients complained of other symptoms, of which back pain was the problem most frequently mentioned (by 90 %). **D.** Grass pea preparation. The most popular ways to prepare grass pea is as bread (baked) and as sauce. Generally, patients use less different preparation methods than controls. And the unripe seeds are consumed more frequently by patients compared to controls.

The HPLC analysis was performed as previously described (Kuo et al. 2007): 200 µL of each urine sample was mixed with 3 volumes of 95 % ethanol and 5 µL of internal standard (0.1 M DL-allylglycine; Sigma-Aldrich, Bornem, Belgium) and kept at 4 °C overnight. After centrifugation, the supernatant was dried under vacuum in an Eppendorf Concentrator 5301 at 45 °C and further derivatized with PITC (99 %, Sigma-Aldrich, Bornem, Belgium) and dissolved in 250 µL of buffer A (0.1 M ammonium acetate, pH 6.5) as previously reported (Kuo et al. 2003). An aliquot of 20 µL was injected in HPLC (Waters 625 equipped with Waters 991 Photo Diode Array detector) and analyzed by a reversed-phase C18 column (Alltima C18, 5 µ, 250 mm × 4.6 mm, Alltech) at 43°C. Buffer A and buffer B (0.1 M ammonium acetate/acetonitrile/methanol; 44/46/10 by volume; pH 6.5) were used in a 50 min gradient program to separate the amino acids. The results were compared with that of standard amino acids (AA-S-18, Sigma) and integrated by Waters Millennium software version 1.10. Each urine extract was analyzed twice and the overall mean value was calculated.

Statistics

Descriptive statistics were used for socio-demographic variables. Fisher's exact test was used to compare proportions, to obtain the odds ratio (OR), associated 95 % confidence interval (CI) and the p-value. Means were compared by student t-test (parametric test for two variables), Mann-Whitney test (non-parametric test for two variables), one-way ANOVA (parametric test for more than two variables) or Kruskal-Wallis test (non-parametric test for more than two variables) using GraphPad Instat software (GraphPad Software; San Diego, CA). Values represent mean ± S.E.M., *n* is the number of patients or samples. Statistical significance is indicated in the graphs by one, two or three symbols for $p < 0.05$, $p < 0.01$ or $p < 0.001$ respectively.

5. Results

Questionnaires

All (except one) participants confirmed to know neurolathyrism, with grass pea being somehow involved in this crippling disorder. Only two people proposed a treatment for neurolathyrism: drinking 'holy water' and drinking fresh butter and honey, the other people stated there is no cure available.

When asked for the consequences of neurolathyrism in life (from 43 participants; 7 answers were missing), economical consequences (poverty, low productivity and inability to work) were mentioned

most frequently (by 28 people), followed by social problems (social outcast; n = 25) and problems with health (pain, inability to walk; n = 19).

The patients in this study were affected by neurolathyrism for 2 – 32 years (21 ± 9 years). The mean age at onset was 23 ± 3 years, varying between 3 and 50. Most patients resided in stage 2 (n = 13; 62 %), followed by 7 patients in stage 1 (33 %), 1 in stage 4 (5 %) and none in stage 3.

Only one patient declared having no other problems than being crippled, but the other 20 mentioned additional problems such as back pain (n = 19; 90 %) and having the subjective feeling of being paralyzed (n = 5; 24 %). Itching, head abnormality, joint pain, leg pain, chest pain, pain all over the body and rigidity were also mentioned by only one or two participants.

Of all participants, 40 were still eating grass pea at the start of the study; 3 controls and 7 patients stopped eating grass pea 2 – 32 years ago, of whom only 3 patients stopped eating grass pea right after they were affected by neurolathyrism, the others discontinued its consumption a few years later. Most participants (patients as well as controls) consumed grass pea 2 (38 %) or 3 (35 %) times per day in their meals. When asked for the quantity of grass pea used daily, more patients (71 %) stated to consume more than 200 g grass pea per day than did the controls (46 %) (OR (95 % CI) = 0.34 (0.09 – 1.38); $p > 0.05$).

Generally (for both patients and controls), the most popular way to consume grass pea was as baked bread ('*kita*'; 92.3 %) and used as sauce ('*shiro wot*'; 92.3 %), followed by the fermented ('*elbet*'; 89.7 %) and boiled ('*nifro*'; 89.7 %) preparations. Fewer participants used the seeds in their roasted ('*kolo'*; 66.7 %) or unripe ('*eshet*'; 17.9 %) form. Interestingly, more patients (21.4 %) used to eat the green unripe seeds compared to controls (16 %) (OR (95 % CI) = 1.5 (0.28 – 7.91); $p > 0.05$).

All participants used clay utensils, some of them - less patients (50 %) than controls (84 %) - additionally used metal utensils to prepare grass pea meals (OR (95 % CI) = 1.68 (0.57 – 4.93); $p > 0.05$).

Almost all participants (95 %) used local grass pea, except for two buying their grass pea in a nearby village (Robit).

Except for 2 patients and 1 control, most people add other ingredients to grass pea, with the most popular ingredients being shallot onions (46 %), ginger (41 %) and 'spices' (38 %; not further specified). Some ingredients were less frequently added to grass pea by patients compared to non-patients such as chick pea (17 % vs. 44 %; OR (95 % CI) = 0.25 (0.05 – 1.41); $p > 0.05$), sorghum (17 % vs. 32 %; OR (95 % CI) = 0.43 (0.07 – 2.41); $p > 0.05$) and wheat (8 % vs. 32 %; OR (95 % CI) = 0.19 (0.021 – 1.77); $p > 0.05$) (table 10). Only 4 participants mentioned the use of vegetable oil, all of them controls.

The majority of the participants (74 %), both patients and controls, declared that they had ever eaten only grass pea, without the addition of other ingredients. The average period of monotonous

consumption of grass pea was longer for patients (13 ± 5 months) than for non-patients (4 ± 1 months; $p > 0.05$ vs. patients). The reasons for adopting a grass pea diet without any additional food supplements were poverty and food shortage, especially when other crops failed after drought or flood.

	All participants (n=37)		Patients (n=12)		Controls (n=25)	
	n	%	N	%	n	%
Shallot onions	17	46	6	50	11	44
ginger	15	41	6	50	9	36
spices	14	38	5	42	9	36
chickpea	13	35	2	17	11	44
salt	11	30	4	33	7	28
sorghum	10	27	2	17	8	32
garlic	9	24	4	33	5	20
wheat	9	24	1	8	8	32
pepper	6	16	4	33	2	8
faba bean	6	16	0	0	6	24
fenugreek	6	16	3	25	3	12
oil	4	11	0	0	4	16
lentil	2	5	1	8	1	4
tena adam	2	5	0	0	2	8
onion	1	3	0	0	1	4
safflower	1	3	0	0	1	4
maize	1	3	0	0	1	4
basil	1	3	0	0	1	4

Table 10: Ingredients added to grass pea. The most popular ingredients added to grass pea were shallot onions (46 %), ginger (41 %) and 'spices' (38 %; not further specified). Some ingredients were less frequently added to grass pea by patients compared to non-patients such as chick pea (17 % vs. 44 %), sorghum (17 % vs. 32 %) and wheat (8 % vs. 32 %). n = all people still consuming grass pea at the start of the study, who answered this question.

Free amino acids in urine

A previous study of urine sample analysis by reversed phase HPLC already suggested some differences between neurolathyrism patients compared to healthy controls (Kuo et al. 2007). Our study is the first report of the evolution of amino acid content in urine, when patients and controls replaced their grass pea-rich diet by a grass pea free one for a period of two weeks.

The mean amino acid content in urine samples from patients and controls are shown in figure 22A. The most prominent peaks in the urine sample analysis of neurolathyrism patients corresponded to homoarginine and β-aminoisobutyric acid. For homoarginine we noticed generally higher concentrations (70 ± 17 % vs. 19 ± 4 %; $p < 0.05$) and higher concentrations at the start of the study (132 ± 32 % vs. 22 ± 6 %; $p < 0.01$) that recovered to control levels during the following two weeks of 'balanced' diet (39 ± 15 % vs. 28 ± 6 %; $p > 0.05$ after 1 week; 32 ± 17 % vs. 9 ± 2 %; $p > 0.05$ after 2 weeks) (Fig. 22B).

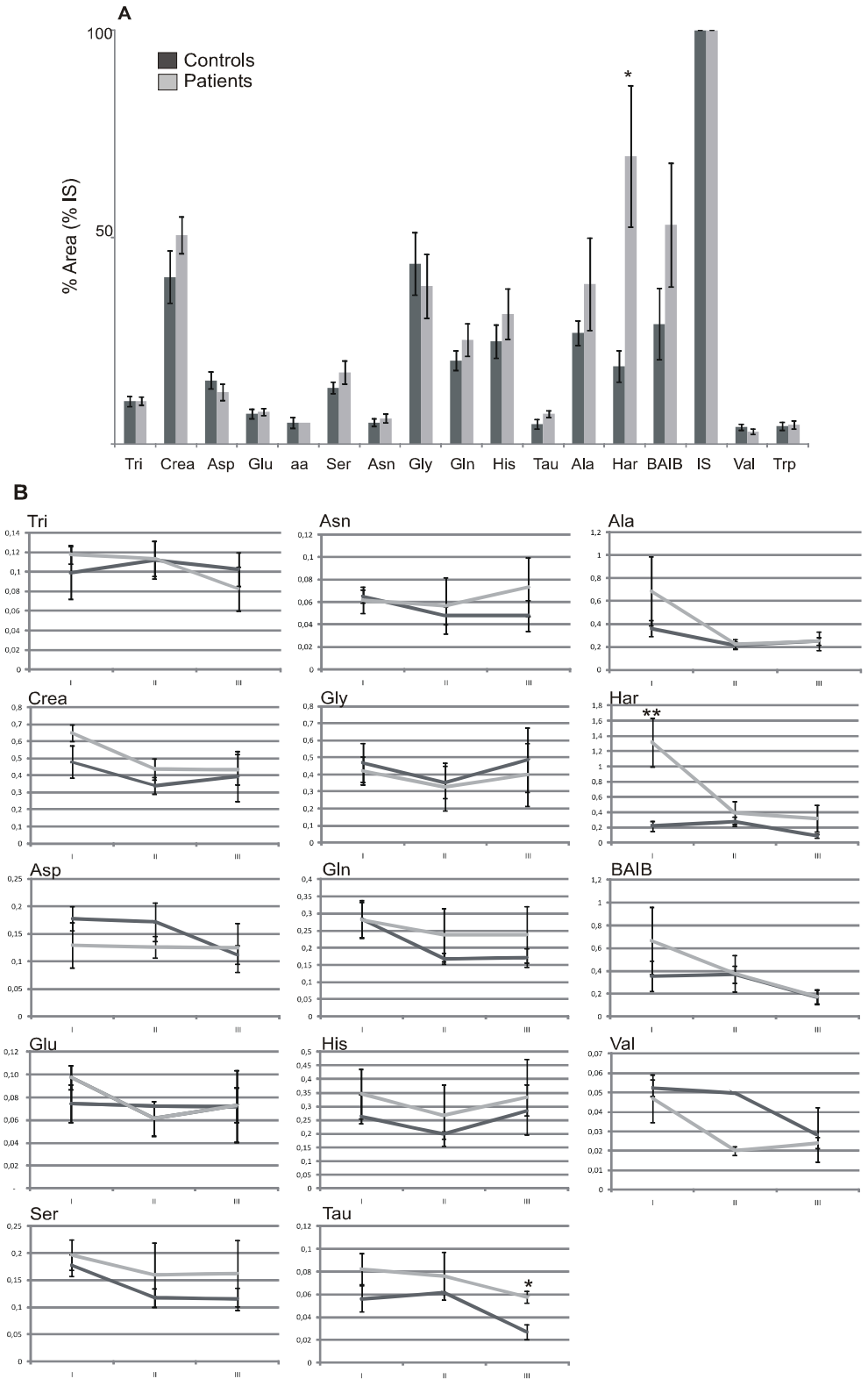

Fig. 22: HPLC analysis of urine samples. A. Summary graph of the average % Area (relative to the internal standard (IS)) of different amino acids, calculated as the average of samples I-II-III (from week 0-1-2). Higher homoarginine (Har) levels were found in urine from neurolathyrism patients (n = 6) compared to controls (n = 5). **B.** Evolution of amino acids in urine over time (samples I-II-III, corresponding to week 0-1-2). At week 0, higher levels were found for Har in urine of patients compared to controls at the start of the study and for Tau the difference became significant after 2 weeks. For aa and Trp not enough values were available to calculate the evolution over time.

6. Discussion

In line with previous publications, our results confirm the general awareness of people that neurolathyrism is a consequence of grass pea consumption, and it is generally known that no cure is available. As in other studies, we found that most patients resided in one of the first two stages (Haimanot et al. 1990). Besides spasticity of the legs, the main problem mentioned by neurolathyrism patients was back pain. In addition, head abnormality was also mentioned by two participants, which may refer to what was previously reported as cognitive deficits, mood disturbances and vivid dreams (Kunig et al. 1994), though the cognitive state of neurolathyrism patients normally does not show a decline (Spencer 1995; Paleacu et al. 1999).

The mean age of onset was 23 years, which corresponds to previous epidemiological data that young males between 15 and 25 years old are preferentially affected by neurolathyrism (Haque et al. 1996; Getahun et al. 1999).

The most popular way to prepare grass pea food was to bake it (*'kita'*) and use it as a sauce (*'shiro wot'*), which has previously been determined not to raise the risk to develop neurolathyrism. Some differences between patients and controls were raised, but appeared not to be statistically significant, such as the consumption of green unripe seeds, which has been associated with an increased risk for neurolathyrism (Getahun et al. 1999; Getahun et al. 2002a; Getahun et al. 2003; Getahun et al. 2005) and the period of monotonous grass pea consumption.

The most commonly used additives to grass pea were shallot onions and ginger. The addition of chick pea, sorghum and wheat to grass pea may serve as a protective measure, though no statistical significance was obtained for a more frequent addition of these ingredients by controls compared to patients. It has been suggested before, however, that more than one third cereals (sorghum, wheat, maize, teff) in a *L. sativus* flour mixture or mixing the food with gravy that contains condiments with antioxidant activity reduces the risk for paralysis (Getahun et al. 1999; Getahun et al. 2002a; Getahun et al. 2003; Getahun et al. 2005). Some condiments were used by some of the controls and by none of the patients: Faba bean, oil, tena adam, onion, safflower, maize and basil. The vegetable oil used by four controls and by none of the participants is probably safflower oil, the most popular oil in this part of Ethiopia. Safflower oil is rich in polyunsaturated fatty acids. Several of these condiments have never before been implicated in studies on neurolathyrism. The consumption of these condiments may be linked to the better economic status of the controls than the neurolathyrism patients, but they also may contribute to the better defense against oxidative stress.

Since cooking grass pea in clay utensils has been reported to more than quadruple the risk to develop neurolathyrism (Getahun et al. 2005), the exclusive use of clay utensils was investigated in this study.

A tendency was observed that less patients used metal utensils instead of traditional clay pots to prepare their grass pea food, but no statistical significance was obtained.

HPLC analysis of urine samples from a selection of 6 patients and 5 controls (with similar age and living in the same village) indicated elevated levels of homoarginine in urine of neurolathyrism patients. Interestingly, the increased homoarginine excretion normalized to control levels after two weeks of a grass pea deficient diet. The current study is of a preliminary nature with a larger sample analysis needed to provide higher statistical significance of these results.

Compared to this report, the present study indicates a more prominent presence of homoarginine. In the present study, the participants were still consuming grass pea, which is rich in homoarginine (up to 1% of seed weight), while in the study of Kuo et al., the patients were supposed to have abandoned grass pea from their diet. This might explain why homoarginine is found in our results and not in the previously reported analysis. Additionally, homoarginine has been found to inhibit the activity of some intestinal alkaline phosphatases. Decreased alkaline phosphatase activity has been associated with a number of different conditions including Zn^{2+} and Mg^{2+} deficiency, hypothyroidism, anemia/vitamin B12 deficiency and malnutrition/protein deficiency. Therefore, increased homoarginine excretion may indirectly indicate malnutrition as a predisposing factor or a consequence of the development of neurolathyrism or Mg^{2+}/Zn^{2+} deficiency.

Finally, no L-β-ODAP was found in the urine samples, in line with the previous suggestion that dietary L-β-ODAP is largely metabolized or detoxified by humans (Pratap Rudra et al. 2004).

7. Conclusion

Our results generally confirm previously reported epidemiological data, as well as results obtained from urine sample analysis. While this study can be considered a pilot study, the results point to the involvement of oxidative stress in the etiology of neurolathyrism. Therefore, the remaining urine samples and blood samples collected for this study should be analyzed to investigate whether the consumption of several condiments with antioxidant properties should be further evaluated as potential protective factors.

Acknowledgements

Our work is supported by a Ph.D. grant of the Flemish Interuniversity Council (VLIR-UOS), the Fund for Scientific Research Flanders, Belgium (FWO, grant nos. G.0354.07, G0140.08 and 3G.0134.09 to L.L. and G.0608.09 to L.V.D.B.) and the Interuniversity Attraction Poles Program (Belgian Science Policy, project P6/31 to L.L and P6/43 to L.V.D.B.).

Dankjewel!

Ik zeg al twee jaar “ik moet mijn doctoraat nog afwerken”.. en nu is het zover! Dit was onmogelijk geweest zonder ‘omkadering’. En nu kan ik jullie hier eindelijk eens deftig voor bedanken.

Bedankt Prof. Dr. Luc Leybaert, voor de mogelijkheid om bij u te doctoreren met een eerder apart onderzoeksproject. Deze ‘adoptie’ zorgde voor de ideale combinatie: een project waar ik met hart en ziel achter sta, en de fundamentele benadering ervan die ik eerder al leerde kennen door mijn licentiaatsthesis.

Dit project was er helemaal niet geweest zonder mijn co-promotor Hon. Prof. Dr. Fernand Lambein, het kloppend hart van het neurolathyrisme-onderzoek. Het was echt een hele eer om zo veel van u te kunnen leren. Bovendien zorgde uw zeer menselijke aanpak en interesse in het leven naast het onderzoek voor een extra motivatie. Hartelijk dank hiervoor.

Prof. Dr. G. Callewaert, niet alleen bedankt voor de efficiënte samenwerking, maar ook bedankt voor uw recht-door-zee aanpak. Beide leidden tot een aanzienlijk onderdeel van deze thesis, maar ook tot de ‘goesting’ om altijd te blijven zoeken naar het waarom van de resultaten.

Prof. Dr. Peter Nunn, thank you very much for your detailed revison of the thesis and papers. Your comments and suggestions attributed a lot to the quality of this research project.

Ik wil ook graag de andere juryleden bedanken voor hun interesse en tijd die ze aan deze thesis besteedden: Prof. Dr. Claude Cuvelier, Prof. Dr. Jan Phillippé, Prof. Dr. Koen Paemeleire en Prof. Dr. Hubert Thierens en Dr. Joëlle Nsimire Chabwine.

Prof. Dr. Ludo Van Den Bosch, hartelijk dank voor de zeer interessante samenwerking. De Leuvense experimenten maakten dit onderzoek minder geïsoleerd door de vergelijking met ALS.

Uiteraard ook een dikke dankjewel voor mijn labo-genootjes: Nan, Marijke, Katleen, Elke DV , Mélissa, en in het bijzonder mijn bureaugenootje Elke DC. Jouw perfectionisme werkte aanstekelijk en daarnaast deed het altijd deugd om bij jou even ‘labo-(en andere)-stoom’ af te laten. Dankjewel! Ook dank aan de thesisstudenten, in het bijzonder aan Barbara, Laura en Julie, stuk voor stuk toffe madammen! Het labo was ook lang niet zo plezant geweest zonder de hulp van Eric, André, Julien, Dirk, Tom, Cyriel en Bart en op het einde de immer praktische Kirsten. Ik had in de Ledeganck geen HPLC-analyses kunnen doen zonder de zorgzame hulp van Diana (Dr. Yu-Haey Kuo). Daarnaast was de samenwerking met Sylvia, Katerine, Véronique en Ine heel plezant en vruchtbaar, vooral tijdens de voorbereiding van de workshop. In Kortrijk kon ik altijd rekenen op de hulp van Evelyne, Eline, en Liesbeth, van Els en Donald en van Prof. Dr. P. De Smet. En in Leuven was ik nergens geweest zonder de sympathieke hulp van Wendy, Dora en Elke. Dankjewel!

Maxime, thanks for the very nice and interesting cooperation. I know we did not complete all experiments we planned, but thanks to you a very interesting chapter is included in this thesis.

Special thanks to Dr. Asnake Fikre, Dr. Alemayehu Mekonnen and Lijalem Korbu. They added an interesting dimension to this project and helped me a lot with the field study in Ethiopia. Thanks!

Voor de administratie van mijn beurs kon ik steeds terecht bij Nancy Terryn, Helke Baeyens, Stefan Wellens en Sam Geerts. Heel erg bedankt voor de sympathieke manier waarop ik telkens verder geholpen werd met administratieve beslommeringen.

Een ferme dankjewel gaat naar vrienden, die geduldig bleven knikken als mijn thesis een reden was om te klagen of planningen in de war te sturen.. en die in me bleven geloven. In het bijzonder dankjewel Leen, Lisa, Valerie, Mieke en Kaat voor de ontspanning tijdens een 'deetje' of via postpakketjes e.d. Mouna en Servaas, niet alleen de toffe reizen samen zorgden voor de nodige ontspanning, maar ook de etentjes, babbels, en de onvoorwaardelijke steun de afgelopen jaren.. dat is van onschatbare waarde, merci! Stonden ook altijd klaar voor een portie gezelligheid en waren geïnteresseerd in de thesis-vorderingen: Marjan en Johan, Nathalie, Kin-Chun en Ellen, Pieter en Nele, Robby en Katrijn, Tom en Katlijn, Steven en Marieke, Pauline, Tessa en Jens, Fien en Joachim.

Niet in het minst wil ik mijn familie bedanken. Tantes en nonkels, neven en nichten, ze wilden allemaal graag weten waar ik mee bezig was en hoe ver ik ermee stond. Mijn schoonfamilie (Fredy, Christine, Bart, Merel en Lise), dankjewel voor de massale praktische hulp waardoor ik meer ademruimte kreeg voor de thesis. Dank voor de enthousiaste en (soms kritische) motiverende steun van Els en Roel en de charmerende vreugde van Thomas en Kasper.

En, zo onmisbaar, mama en papa. Jullie 'dankwoordje' klinkt sowieso te klein voor wat jullie voor me betekenen. Jullie geloven in mij, en het is dankzij jullie dat ik ben wie ik ben en sta waar ik sta. Ik weet dat ik jullie nu apetrots maak, en dat vind ik superleuk. Want dit is het resultaat van alle kansen die jullie me geven en gegeven hebben. Zoals je als ouder wil dat je kinderen gelukkig zijn, zo wil je als kind dat je ouders trots op je zijn.

En.. last but not least.. mijn Timmie. De laatste twee jaren liep niets echt volgens plan, als ik het zo mag uitdrukken. Maar nu zijn we aan een nieuw hoofdstuk begonnen . Jij hebt me op alle gebieden gesteund: moreel, praktisch, inhoudelijk,.. en bent er altijd in blijven geloven, en je hebt me alle vrijheid gegeven die ik me kon wensen, terwijl je nu ook niet altijd veel reserve had. Dankjewel! En een dikke knuffel voor onze kleine Robbe, je begrijpt niets van de inhoud, maar je slaagt er wel in om me met je lachjes en geluidjes alles te doen relativeren!

References

Abbott, N. J., A. A. K. Patabendige, D. E. M. Dolman, S. R. Yusof and D. J. Begley (2010). "Structure and function of the blood–brain barrier." Neurobiol Dis **37**(1): 13-25.

Addis, G. and R. K. J. Narayan (1994). "Developmental Variation of the Neurotoxin, β-N-Oxalyl-L-α,β-Diamino Propionic-Acid (Odap), in *Lathyrus sativus*." Annals of Botany **74**(3): 209-215.

Albasanz, J. L., M. Ros and M. Martin (1997). "Characterization of metabotropic glutamate receptors in rat C6 glioma cells." Eur J Pharmacol **326**(1): 85-91.

Allaman, I., M. Belanger and P. J. Magistretti (2011). "Astrocyte-neuron metabolic relationships: for better and for worse." Trends Neurosci **34**(2): 76-87.

Amara, A., M. Coussemacq and M. Geffard (1995). "Molecular detection of methionine in rat brain using specific antibodies." Neurosci Lett **185**(3): 147-50.

Amba, A., K. Seth, M. Ali, M. Das, A. K. Agarwal, S. K. Khanna and P. K. Seth (2002). "Comparative effect of dietary administration of *Lathyrus sativus* pulse on behaviour, neurotransmitter receptors and membrane permeability in rats and guinea pigs." J Appl Toxicol **22**(6): 415-21.

Appel, S. H., D. R. Beers and J. S. Henkel (2009). "T cell-microglial dialogue in Parkinson's disease and amyotrophic lateral sclerosis: are we listening?" Trends Immunol **31**(1): 7-17.

Arundine, M. and M. Tymianski (2003). "Molecular mechanisms of calcium-dependent neurodegeneration in excitotoxicity." Cell Calcium **34**(4-5): 325-37.

Behl, C., T. Skutella, F. Lezoualc'h, A. Post, M. Widmann, C. J. Newton and F. Holsboer (1997). "Neuroprotection against oxidative stress by estrogens: structure-activity relationship." Mol Pharmacol **51**(4): 535-41.

Bell, E. A. (2003). "Nonprotein amino acids of plants: significance in medicine, nutrition, and agriculture." J Agric Food Chem **51**(10): 2854-65.

Berridge, M. J., P. Lipp and M. D. Bootman (2000). "The versatility and universality of calcium signalling." Nat Rev Mol Cell Biol **1**(1): 11-21.

Booher, J. and M. Sensenbrenner (1972). "Growth and cultivation of dissociated neurons and glial cells from embryonic chick, rat and human brain in flask cultures." Neurobiology **2**(3): 97-105.

Boston-Howes, W., S. L. Gibb, E. O. Williams, P. Pasinelli, R. H. Brown and D. Trotti (2006). "Caspase-3 cleaves and inactivates the glutamate transporter EAAT2." J Biol Chem **281**: 14076-14084.

Brennan, L., P. M. Alves, C. Hewage, J. P. Malthouse and G. J. McBean (2006). "Impact of the gliotoxin L-serine-O-sulphate on cellular metabolism in cultured rat astrocytes." Neurochem Int **48**(8): 739-45.

Bridges, R. J., C. Hatalski, S. N. Shim and P. B. Nunn (1991). "Gliotoxic properties of the Lathyrus excitotoxin β-N-oxalyl-L-α,β-diaminopropionic acid (β-L-ODAP)." Brain Res **561**(2): 262-8.

Bridges, R. J., M. M. Kadri, D. T. Monaghan, P. B. Nunn, J. C. Watkins and C. W. Cotman (1988). "Inhibition of [^{3}H]α-amino-3-hydroxy-5-methyl-4-isoxazolepropionic acid binding by the excitotoxin β-N-oxalyl-L-α,β-diaminopropionic acid." Eur J Pharmacol **145**(3): 357-9.

Bridges, R. J., D. R. Stevens, J. S. Kahle, P. B. Nunn, M. Kadri and C. W. Cotman (1989). "Structure-function studies on N-oxalyl-diamino-dicarboxylic acids and excitatory amino acid receptors: evidence that β-L-ODAP is a selective non-NMDA agonist." J Neurosci **9**(6): 2073-9.

Brini, M., R. Marsault, C. Bastianutto, J. Alvarez, T. Pozzan and R. Rizzuto (1995). "Transfected aequorin in the measurement of cytosolic Ca^{2+} concentration ($[Ca^{2+}]_c$). A critical evaluation." J Biol Chem **270**(17): 9896-903.

Brown, G. C. (2010). "Nitric oxide and neuronal death." Nitric Oxide **23**(3): 153-65.

Campanella, M., P. Pinton and R. Rizzuto (2004). "Mitochondrial Ca^{2+} homeostasis in health and disease." Biol Res **37**(4): 653-60.

Carpenter, R. H. S. (2003). Neurophysiology. London, Arnold.

Carriedo, S. G., H. Z. Yin and J. H. Weiss (1996). "Motor neurons are selectively vulnerable to AMPA/kainate receptor-mediated injury in vitro." J Neurosci **16**(13): 4069-79.

Cassina, P., A. Cassina, M. Pehar, R. Castellanos, M. Gandelman, A. de Leon, K. M. Robinson, R. P. Mason, J. S. Beckman, L. Barbeito and R. Radi (2008). "Mitochondrial dysfunction in SOD1G93A-bearing astrocytes promotes motor neuron degeneration: prevention by mitochondrial-targeted antioxidants." J Neurosci **28**(16): 4115-22.

Cecchelli, R., B. Dehouck, L. Descamps, L. Fenart, V. V. Buee-Scherrer, C. Duhem, S. Lundquist, M. Rentfel, G. Torpier and M. P. Dehouck (1999). "In vitro model for evaluating drug transport across the blood-brain barrier." Adv Drug Deliv Rev **36**(2-3): 165-178.

Cemerikic, D., V. Nedeljkov, S. Lopicic, S. Dragovic and B. Beleslin (2001). "Excitotoxicity of *Lathyrus sativus* neurotoxin in leech retzius neurons." Physiol Res **50**(2): 205-14.

Chase, L. A., N. L. Peterson and J. F. Koerner (2007). "The lathyrus toxin, β-N-oxalyl-L-α,β-diaminopropionic acid (ODAP), and homocysteic acid sensitize CA1 pyramidal neurons to cystine and L-2-amino-6-phosphonohexanoic acid." Toxicol Appl Pharmacol **219**(1): 1-9.

Cheema, P. S., K. Malathi, Padmanab.G and P. S. Sarma (1969). "Neurotoxicity of β-N-Oxalyl-L-α,β-Diaminopropionic Acid Neurotoxin from Pulse *Lathyrus Sativus*." Biochem J **112**(1): 29-&.

Choi, Y. K. and K. W. Kim (2008). "Blood-neural barrier: its diversity and coordinated cell-to-cell communication." BMB Rep **41**(5): 345-52.

Clapham, D. E. (2007). "Calcium signaling." Cell **131**(6): 1047-58.

Cohn, D. and M. Streifler (1981). "Human neurolathyrism, a follow-up study of 200 patients. Part I: Clinical investigation." Schweiz Arch Neurol Neurochir Psychiatr **128**(1): 151-6.

Conn, H. O., M. Rossle, L. Levy and F. X. Glocker (2006). "Portosystemic myelopathy: Spastic paraparesis after portosystemic shunting." Scand J Gastroenterol **41**(5): 619-625.

Corona, J. C. and R. Tapia (2007). "Ca^{2+}-permeable AMPA receptors and intracellular Ca^{2+} determine motoneuron vulnerability in rat spinal cord in vivo." Neuropharmacology **52**(5): 1219-28.

Csordas, G. and G. Hajnoczky (2009). "SR/ER-mitochondrial local communication: calcium and ROS." Biochim Biophys Acta **1787**(11): 1352-62.

Csordas, G., C. Renken, P. Varnai, L. Walter, D. Weaver, K. F. Buttle, T. Balla, C. A. Mannella and G. Hajnoczky (2006). "Structural and functional features and significance of the physical linkage between ER and mitochondria." J Cell Biol **174**(7): 915-21.

Danbolt, N. C. (2001). "Glutamate uptake." Prog Neurobiol **65**(1): 1-105.

David, Y., L. P. Cacheaux, S. Ivens, E. Lapilover, U. Heinemann, D. Kaufer and A. Friedman (2009). "Astrocytic dysfunction in epileptogenesis: consequence of altered potassium and glutamate homeostasis?" J Neurosci **29**(34): 10588-99.

Davis, A. J., P. B. Nunn, P. O'Brien, L. D. Pettit and G. F. Wang (1990). "Facile Isolation, from *L sativus* Seed, of the Neurotoxin β-N-Oxalyl-L-α,β-Diaminopropionic Acid as the Copper Complex and Studies of the Coordination Chemistry of Copper and Zinc with the Amino Acid in Aqueous Solution." J Inorg Biochem. **39**(3): 209-216.

Dayanithi, G., I. Mechaly, C. Viero, H. Aptel, S. Alphandery, S. Puech, F. Bancel and J. Valmier (2006). "Intracellular Ca^{2+} regulation in rat motoneurons during development." Cell Calcium **39**(3): 237-46.

De Falco, E. and A. Pardo (2000). "Agronomic evaluation of Italian ecotypes of *Lathyrus sativus* L. in a hilly area of southern Italy." Lathyrus Lathyrism Newsletter **1**: 27.

Denton, R. M., G. A. Rutter, P. J. Midgley and J. G. McCormack (1988). "Effects of Ca^{2+} on the activities of the calcium-sensitive dehydrogenases within the mitochondria of mammalian tissues." J Cardiovasc Pharmacol **12 Suppl 5**: S69-72.

Devi, L., V. Raghavendran, B. M. Prabhu, N. G. Avadhani and H. K. Anandatheerthavarada (2008). "Mitochondrial import and accumulation of α-synuclein impair complex I in human dopaminergic neuronal cultures and Parkinson disease brain." J Biol Chem **283**(14): 9089-100.

Diwakar, L., R. S. Kenchappa, J. Annepu, U. Saeed, R. Sujanitha and V. Ravindranath (2006). "Down-regulation of glutaredoxin by estrogen receptor antagonist renders female mice susceptible to excitatory amino acid mediated complex I inhibition in CNS." Brain Res **1125**(1): 176-84.

Diwakar, L. and V. Ravindranath (2007). "Inhibition of cystathionine-γ-lyase leads to loss of glutathione and aggravation of mitochondrial dysfunction mediated by excitatory amino acid in the CNS." Neurochem Int **50**(2): 418-26.

Doble, A. (1999). "The role of excitotoxicity in neurodegenerative disease: implications for therapy." Pharmacol Ther **81**(3): 163-221.

Donaghy, M. (1999). "Classification and clinical features of motor neurone diseases and motor neuropathies in adults." J Neurol **246**(5): 331-3.

Drory, V. E., M. J. Rabey and D. F. Cohn (1992). "Electrophysiologic features in patients with chronic neurolathyrism." Acta Neurol Scand **85**: 401-403.

Du, H., L. Guo, F. Fang, D. Chen, A. A. Sosunov, G. M. McKhann, Y. Yan, C. Wang, H. Zhang, J. D. Molkentin, F. J. Gunn-Moore, J. P. Vonsattel, O. Arancio, J. X. Chen and S. D. Yan (2008). "Cyclophilin D deficiency attenuates mitochondrial and neuronal perturbation and ameliorates learning and memory in Alzheimer's disease." Nat Med **14**(10): 1097-105.

Duchen, M. R. (2000). "Mitochondria and calcium: from cell signalling to cell death." J Physiol **529 Pt 1**: 57-68.

El Rouby, D. H., M. H. Bashir and N. S. Korany (2008). "Ultrastructural and histomorphometric alterations of rat jaw bones after experimental induction of lathyrism." Arch Oral Biol **53**(10): 916-923.

Elliott, J. L. and W. D. Snider (1995). "Parvalbumin Is a Marker of Als-Resistant Motor-Neurons." Neuroreport **6**(3): 449-452.

Emerit, J., M. Edeas and F. Bricaire (2004). "Neurodegenerative diseases and oxidative stress." Biomed Pharmacother **58**(1): 39-46.

Estevez, A. G., J. P. Crow, J. B. Sampson, C. Reiter, Y. Zhuang, G. J. Richardson, M. M. Tarpey, L. Barbeito and J. S. Beckman (1999). "Induction of nitric oxide-dependent apoptosis in motor neurons by zinc-deficient superoxide dismutase." Science **286**(5449): 2498-500.

Falk, T., S. Zhang and S. J. Sherman (2009). "Vascular endothelial growth factor B (VEGF-B) is up-regulated and exogenous VEGF-B is neuroprotective in a culture model of Parkinson's disease." Mol Neurodegener **4**: 49.

Farooqui, A. A., W. Y. Ong and L. A. Horrocks (2004). "Biochemical aspects of neurodegeneration in human brain: involvement of neural membrane phospholipids and phospholipases A2." Neurochem Res **29**(11): 1961-77.

Ferro-Luzzi, G. (1947). "Malti da sebere e lathyrismo in Eritrea." Bull Soc Ital Med Igien Trop **l7**: 483-493.

Foskett, J. K., C. White, K. H. Cheung and D. O. Mak (2007). "Inositol trisphosphate receptor Ca^{2+} release channels." Physiol Rev **87**(2): 593-658.

Frank-Cannon, T. C., L. T. Alto, F. E. McAlpine and M. G. Tansey (2009). "Does neuroinflammation fan the flame in neurodegenerative diseases?" Mol Neurodegener **4**: 47.

Franklin, M. S., G. W. Kraemer, S. E. Shelton, E. Baker, N. H. Kalin and H. Uno (2000). "Gender differences in brain volume and size of corpus callosum and amygdala of rhesus monkey measured from MRI images." Brain Res **852**(2): 263-7.

Fulda, S., A. M. Gorman, O. Hori and A. Samali (2010). "Cellular stress responses: cell survival and cell death." Int J Cell Biol **2010**: 23.

Gannon, R. L. and D. M. Terrian (1989). "BOAA selectively enhances L-glutamate release from guinea pig hippocampal mossy fiber synaptosomes." Neurosci Lett **107**(1-3): 289-94.

Genoud, C., C. Quairiaux, P. Steiner, H. Hirling, E. Welker and G. W. Knott (2006). "Plasticity of astrocytic coverage and glutamate transporter expression in adult mouse cortex." PLoS Biol **4**(11): e343.

Getahun, H., F. Lambein and P. Van der Stuyft (2002a). "ABO blood groups, grass pea preparation, and neurolathyrism in Ethiopia." Trans R Soc Trop Med Hyg **96**(6): 700-3.

Getahun, H., F. Lambein and M. Vanhoorne (2002b). "Neurolathyrism in Ethiopia: assessment and comparison of knowledge and attitude of health workers and rural inhabitants." Soc Sci Med **54**(10): 1513-24.

Getahun, H., F. Lambein, M. Vanhoorne and P. Van der Stuyft (2003). "Food-aid cereals to reduce neurolathyrism related to grass-pea preparations during famine." Lancet **362**(9398): 1808-10.

Getahun, H., F. Lambein, M. Vanhoorne and P. Van der Stuyft (2005). "Neurolathyrism risk depends on type of grass pea preparation and on mixing with cereals and antioxidants." Trop Med Int Health **10**(2): 169-78.

Getahun, H., A. Mekonnen, R. TekleHaimanot and F. Lambein (1999). "Epidemic of neurolathyrism in Ethiopia." Lancet **354**(9175): 306-7.

Giacomello, M., I. Drago, P. Pizzo and T. Pozzan (2007). "Mitochondrial Ca^{2+} as a key regulator of cell life and death." Cell Death Differ **14**(7): 1267-74.

Gongke, Z., K. Yingzhen, C. Kairong, L. Zhixiao and W. Yafu (2001). "Hydroxyl radical scavenging activity of β-N-oxalyl-L-α, β-diaminoproionic acid." Phytochemistry **58**: 759-762.

Gonzalez-Forero, D., F. Portillo, L. Gomez, F. Montero, S. Kasparov and B. Moreno-Lopez (2007). "Inhibition of resting potassium conductances by long-term activation of the NO/cGMP/protein kinase G pathway: a new mechanism regulating neuronal excitability." J Neurosci **27**(23): 6302-12.

Gopalan, C. (1999). "The changing epidemiology of malnutrition in a developing society - The effect of unforeseen factors." Bull Nutr Found India **20**: 1-5.

Grosskreutz, J., K. Haastert, M. Dewil, P. Van Damme, G. Callewaert, W. Robberecht, R. Dengler and L. Van Den Bosch (2007). "Role of mitochondria in kainate-induced fast Ca^{2+} transients in cultured spinal motor neurons." Cell Calcium **42**(1): 59-69.

Gunter, T. E., L. Buntinas, G. Sparagna, R. Eliseev and K. Gunter (2000). "Mitochondrial calcium transport: mechanisms and functions." Cell Calcium **28**(5-6): 285-96.

Haimanot, R. T., Y. Kidane, E. Wuhib, A. Kalissa, T. Alemu, Z. A. Zein and P. S. Spencer (1990). "Lathyrism in rural northwestern Ethiopia: a highly prevalent neurotoxic disorder." Int J Epidemiol **19**(3): 664-72.

Halliwell, B. (2006). "Oxidative stress and neurodegeneration: where are we now?" J Neurochem **97**(6): 1634-58.

Haque, A., M. Hossain, J. K. Khan, Y. H. Kuo, F. Lambein and J. De Reuck (1994). "New findings and symptomatic treatment for neurolathyrism, a motor neuron disease occurring in north west Bangladesh." Paraplegia **32**(3): 193-5.

Haque, A., M. Hossain, F. Lambein and E. A. Bell (1997). "Evidence of osteolathyrism among patients suffering from neurolathyrism in Bangladesh." Natural Toxins **5**: 43-46.

Haque, A., M. Hossain, G. Wouters and F. Lambein (1996). "Epidemiological study of lathyrism in northwestern districts of Bangladesh." Neuroepidemiology **15**(2): 83-91.

Haque, A., J. K. Khan, G. Wouters, M. Hossain and F. Lambein (1995). "Study of HTLV-I antibodies in CSF and serum of neurolathyrism patients in Bangladesh." Ann Soc Belg Med Trop **75**(2): 131-4.

Hatashita, S. and J. T. Hoff (1990). "Brain edema and cerebrovascular permeability during cerebral ischemia in rats." Stroke **21**(4): 582-8.

Heine, V. M., J. Zareno, S. Maslam, M. Joels and P. J. Lucassen (2005). "Chronic stress in the adult dentate gyrus reduces cell proliferation near the vasculature and VEGF and Flk-1 protein expression." Eur J Neurosci **21**(5): 1304-14.

Henkel, J. S., J. I. Engelhardt, L. Siklos, E. P. Simpson, S. H. Kim, T. Pan, J. C. Goodman, T. Siddique, D. R. Beers and S. H. Appel (2004). "Presence of dendritic cells, MCP-1, and activated microglia/macrophages in amyotrophic lateral sclerosis spinal cord tissue." Ann Neurol **55**(2): 221-35.

Herr, I. and K. M. Debatin (2001). "Cellular stress response and apoptosis in cancer therapy." Blood **98**(9): 2603-14.

Hertz, L. (2006). "Glutamate, a neurotransmitter--and so much more. A synopsis of Wierzba III." Neurochem Int **48**(6-7): 416-25.

Higgins, C. M., C. Jung and Z. Xu (2003). "ALS-associated mutant SOD1G93A causes mitochondrial vacuolation by expansion of the intermembrane space and by involvement of SOD1 aggregation and peroxisomes." BMC Neurosci **4**: 16.

Himi, T., M. Ikeda, T. Yasuhara, M. Nishida and I. Morita (2003). "Role of neuronal glutamate transporter in the cysteine uptake and intracellular glutathione levels in cultured cortical neurons." J Neural Transm **110**(12): 1337-48.

Hirsch, E. C., S. Hunot, B. Faucheux, Y. Agid, Y. Mizuno, H. Mochizuki, W. G. Tatton, N. Tatton and W. C. Olanow (1999). "Dopaminergic neurons degenerate by apoptosis in Parkinson's disease." Mov Disord **14**(2): 383-5.

Hugon, J., F. Hugon, F. Esclaire, M. Lesort and A. G. Diop (1996). "The presence of calbindin in rat cortical neurons protects in vitro from oxidative stress." Brain Res **707**(2): 288-92.

Hugon, J., A. Ludolph, D. N. Roy, H. H. Schaumburg and P. S. Spencer (1988). "Studies on the etiology and pathogenesis of motor neuron diseases. II. Clinical and electrophysiologic features of pyramidal dysfunction in macaques fed Lathyrus sativus and IDPN." Neurology **38**(3): 435-42.

Hugon, J., A. C. Ludolph, P. S. Spencer, S. Gimenez Roldan and J. L. Dumas (1993). "Studies of the etiology and pathogenesis of motor neuron diseases. III. Magnetic cortical stimulation in patients with lathyrism." Acta Neurol Scand **88**(6): 412-6.

Ikegami, F., K. Kusama-Eguchi, E. Sugiyama, K. Watanabe, F. Lambein and I. Murakoshi (1995). "Interaction of some plant heterocyclic β-substituted alanines with rat brain N-methyl-D-aspartate (NMDA) receptors." Biol Pharm Bull **18**(2): 360-2.

Ilieva, H., M. Polymenidou and D. W. Cleveland (2009). "Non-cell autonomous toxicity in neurodegenerative disorders: ALS and beyond." J Cell Biol **187**(6): 761-72.

Imura, T., S. Shimohama, T. Kageyama and J. Kimura (1999). "Selective induction of glial glutamate transporter GLT-1 by hypertonic stress in C6 glioma cells." Biochim Biophys Res Commun **265**(1): 240-5.

Ince, P., N. Stout, P. Shaw, J. Slade, W. Hunziker, C. W. Heizmann and K. G. Baimbridge (1993). "Parvalbumin and calbindin D-28k in the human motor system and in motor neuron disease." Neuropathol Appl Neurobiol **19**(4): 291-9.

Jackson, M., G. Steers, P. N. Leigh and K. E. Morrison (1999). "Polymorphisms in the glutamate transporter gene EAAT2 in European ALS patients." J Neurol **246**: 1140-1144.

Jahan, K. and K. Ahmad (1993). "Studies on neurolathyrism." Environ Res **60**(2): 259-66.

Jain, R. K., M. A. Junaid and S. L. Rao (1998). "Receptor interactions of β-N-oxalyl-L-α,β diaminopropionic acid, the *Lathyrus sativus* putative excitotoxin, with synaptic membranes." Neurochem Res **23**(9): 1191-6.

Jope, R. S., X. H. Li, G. C. Ormandy, L. Song and M. B. Williams (1990). "Reduction of Na^+ enhances phosphoinositide hydrolysis and differentiates the stimulatory and inhibitory responses to quisqualate in rat brain slices." Brain Res **536**(1-2): 251-6.

Kato, S., K. Negishi, K. Mawatari and C. H. Kuo (1992). "A mechanism for glutamate toxicity in the C6 glioma cells involving inhibition of cystine uptake leading to glutathione depletion." Neuroscience **48**(4): 903-14.

Kawamoto, S., S. Uchino, K. Q. Xin, S. Hattori, K. Hamajima, J. Fukushima, M. Mishina and K. Okuda (1997). "Arginine-481 mutation abolishes ligand-binding of the AMPA-selective glutamate receptor channel α1-subunit." Brain Res Mol Brain Res **47**(1-2): 339-44.

Kenchappa, R. S., L. Diwakar, J. Annepu and V. Ravindranath (2004). "Estrogen and neuroprotection: higher constitutive expression of glutaredoxin in female mice offers protection against MPTP-mediated neurodegeneration." FASEB J **18**(10): 1102-4.

Kenchappa, R. S., L. Diwakar, M. R. Boyd and V. Ravindranath (2002). "Thioltransferase (glutaredoxin) mediates recovery of motor neurons from excitotoxic mitochondrial injury." J Neurosci **22**(19): 8402-10.

Kenchappa, R. S. and V. Ravindranath (2003). "Glutaredoxin is essential for maintenance of brain mitochondrial complex I: studies with MPTP." FASEB J **17**(6): 717-9.

Kessler, A. (1947). "Lathyrismus." Monatsschrift Psychiatrie und Neurologie **113**: 76-92.

Khan, J. K., N. Kebede, Y. H. Kuo, F. Lambein and A. De Bruyn (1993). "Analysis of the neurotoxin β-ODAP and its α-isomer by precolumn derivatization with phenylisothiocyanate." Anal Biochem **208**(2): 237-40.

Khan, J. K., Y. H. Kuo, A. Haque and F. Lambein (1995). "Inhibitory and excitatory amino acids in cerebrospinal fluid of neurolathyrism patients, a highly prevalent motorneurone disease." Acta Neurol Scand **91**(6): 506-10.

Khan, J. K., Y. H. Kuo, N. Kebede and F. Lambein (1994). "Determination of Nonprotein Amino-Acids and Toxins in *Lathyrus* by High-Performance Liquid-Chromatography with Precolumn Phenyl Isothiocyanate Derivatization." J Chromatog **687**(1): 113-119.

King, T. D., G. N. Bijur and R. S. Jope (2001). "Caspase-3 activation induced by inhibition of mitochondrial complex I is facilitated by glycogen synthase kinase-3β and attenuated by lithium." Brain Res **919**(1): 106-14.

Kocsis, P., S. Farkas, L. Fodor, N. Bielik, M. Than, S. Kolok, A. Gere, M. Csejtei and I. Tarnawa (2005). "Tolperisone-type drugs inhibit spinal reflexes via blockade of voltage-gated sodium and calcium channels." J Pharmacol Exp Ther **315**(3): 1237-46.

Koike, M., M. Iino and S. Ozawa (1997). "Blocking effect of 1-naphthyl acetyl spermine on Ca^{2+}-permeable AMPA receptors in cultured rat hippocampal neurons." Neurosci Res **29**(1): 27-36.

Korus, A., Z. Lisiewska and W. Kmiecik (2003). "Content of amino acids in fresh and preserved physiologically immature grass pea (*Lathyrus sativus* L.) seeds." Eur Food Res Technol **217**(2): 148-153.

Kreutzberg, G. W. (1996). "Microglia: a sensor for pathological events in the CNS." Trends Neurosci **19**(8): 312-8.

Krum, J. M. and A. Khaibullina (2003). "Inhibition of endogenous VEGF impedes revascularization and astroglial proliferation: roles for VEGF in brain repair." Exp Neurol **181**(2): 241-57.

Kruman, II, W. A. Pedersen, J. E. Springer and M. P. Mattson (1999). "ALS-linked Cu/Zn-SOD mutation increases vulnerability of motor neurons to excitotoxicity by a mechanism involving increased oxidative stress and perturbed calcium homeostasis." Exp Neurol **160**(1): 28-39.

Kunig, G., J. Hartmann, B. Niedermeyer, J. Deckert, G. Ransmayr, H. Heinsen, H. Beckmann and P. Riederer (1994). "Excitotoxins L-β-oxalyl-amino-alanine (L-BOAA) and 3,4,6-trihydroxyphenylalanine (6-OH-DOPA) inhibit [^{3}H] α-amino-3-hydroxy-5-methyl-4-isoxazole-propionic acid (AMPA) binding in human hippocampus." Neurosci Lett **169**(1-2): 219-22.

Kuo, Y. H., H. M. Bau, P. Rozan, B. Chowdhury and F. Lambein (2000). "Reduction efficiency of the neurotoxin β-ODAP in low-toxin varieties of *Lathyrus sativus* seeds by solid state fermentation with Aspergillus oryzae and Rhizopus microsporus var chinensis." J Sci Food Agric **80**(15): 2209-2215.

Kuo, Y. H., B. Defoort, H. Getahun, R. Tekle Haimanot and F. Lambein (2007). "Comparison of urinary amino acids and trace elements (copper, zinc and manganese) of recent neurolathyrism patients and healthy controls from Ethiopia." Clin Biochem **40**(5-6): 397-402.

Kuo, Y. H., F. Ikegami and F. Lambein (2003). "Neuroactive and other free amino acids in seed and young plants of Panax ginseng." Phytochemistry **62**(7): 1087-91.

Kurpad, A. V. (2006). "The requirements of protein amino acid during acute chronic infections." Indian J Med Res **124**(2): 129-48.

Kusama-Eguchi, K., F. Ikegami, T. Kusama, F. Lambein and K. Watanabe (1996). "Effects of β-ODAP and its biosynthetic precursor on the electrophysiological activity of cloned glutamate receptors." Environ Toxicol Pharmacol **2**(4): 339-342.

Kusama-Eguchi, K., F. Ikegami, T. Kusama, A. Suda, Y. Ogawa, K. Igarashi and K. Watanabe (2005). "A rat model of neurolathyrism: repeated injection of L-β-ODAP induces the paraparesis of the hind legs." Amino Acids **28**(2): 139-43.

Kusama-Eguchi, K., T. Kusama, F. Ikegami, F. Lambein and K. Watanabe (1997). "Inhibitory activity of a naturally occurring heterocyclic β-substituted alanine, β-(isoxazolin-5-on-4-yl)-L-alanine, on the L-glutamate/L-aspartate transporter (GLAST) expressed in *Xenopus* oocytes." Brain Res Mol Brain Res **52**(1): 166-9.

Kusama-Eguchi, K., T. Kusama, A. Suda, T. Masuko, M. Yamamoto, F. Ikegami, K. Igarashi, Y. H. Kuo, F. Lambein and K. Watanabe (2004). "Partial involvement of group I metabotropic glutamate receptors in the neurotoxicity of 3-N-oxalyl-L-2,3-diaminopropanoic acid (L-β-ODAP)." Biol Pharm Bull **27**(7): 1052-8.

Kusama-Eguchi, K., Y. Yamazaki, T. Ueda, A. Suda, Y. Hirayama, F. Ikegami, K. Watanabe, M. May, F. Lambein and T. Kusama (2009). "Hind-limb paraparesis in a rat model for neurolathyrism associated with apoptosis and an impaired vascular endothelial growth factor system in the spinal cord." **DOI 10.1002/cne.22257**

Kusama-Eguchi, K., Y. Yamazaki, T. Ueda, A. Suda, Y. Hirayama, F. Ikegami, K. Watanabe, M. May, F. Lambein and T. Kusama (2010a). "Hind-limb paraparesis in a rat model for neurolathyrism associated with apoptosis and an impaired vascular endothelial growth factor system in the spinal cord." J Comp Neurol **518** (6): 928-942.

Kusama-Eguchi, K., N. Yoshino, A. Minoura, K. Watanabe, T. Kusama, F. Lambein and F. Ikegami (2010b). "Sulfur amino acids deficiency caused by grass pea diet plays an important role in the toxicity of L-β-ODAP by increasing the oxidative stress: Studies on a motor neuron cell line." Food Chem Toxicol.

La Bella, V., M. E. Alexianu, L. V. Colom, A. Ionescu, A. H. Mohamed and S. H. Appel (1996). "Apoptosis induced by β-N-oxalylamino-L-alanine on a motoneuron hybrid cell line." Neuroscience **70**(4): 1039-52.

La Bella, V., F. Brighina, F. Piccoli and R. Guarneri (1993). "Effect of β-N-oxalylamino-L-alanine on cerebellar cGMP level in vivo." Neurochem Res **18**(2): 171-5.

La Bella, V. and F. Piccoli (2000). "Differential effect of β-N-oxalylamino-L-alanine, the *Lathyrus sativus* neurotoxin, and (+/-)-α-amino-3-hydroxy-5-methylisoxazole-4-propionate on the excitatory amino acid and taurine levels in the brain of freely moving rats." Neurochem Int **36**(6): 523-30.

Lai, E., T. Teodoro and A. Volchuk (2007). "Endoplasmic reticulum stress: signaling the unfolded protein response." Physiology (Bethesda) **22**: 193-201.

Lambein, F., D. Diasolua Ngudi and Y. H. Kuo (2001). "Vapniarca revisited: Lessons from an inhuman human experience." Lathyrus Lathyrism Newsletter **2**: 5-7.

Lambein, F., R. Haque, J. K. Khan, N. Kebede and Y. H. Kuo (1994). "From soil to brain: zinc deficiency increases the neurotoxicity of *Lathyrus sativus* and may affect the susceptibility for the motorneurone disease neurolathyrism." Toxicon **32**(4): 461-6.

Lambein, F., Y. H. Kuo, K. Kusama-Eguchi and F. Ikegami (2007). "3-N-oxalyl-L-2,3-diaminopropanoic acid, a multifunctional plant metabolite of toxic reputation." Arkivoc: 45-52.

Lewerenz, J., M. Klein and A. Methner (2006). "Cooperative action of glutamate transporters and cystine/glutamate antiporter system X_c^- protects from oxidative glutamate toxicity." J Neurochem **98**(3): 916-25.

Leybaert, L. (2005). "Neurobarrier coupling in the brain: a partner of neurovascular and neurometabolic coupling?" J Cereb Blood Flow Metab **25**(1): 2-16.

Lindholm, D., H. Wootz and L. Korhonen (2006). "ER stress and neurodegenerative diseases." Cell Death Differ **13**(3): 385-92.

Lindstrom, H., J. Luthman, P. Mouton, P. Spencer and L. Olson (1990). "Plant-derived neurotoxic amino acids (β-N-oxalylamino-L-alanine and β-N-methylamino-L-alanine): effects on central monoamine neurons." J Neurochem **55**(3): 941-9.

Lisiewska, Z., W. Kmiecik and A. Korus (2001). "Content of nitrogen compounds in raw and preserved seeds of grass pea (*Lathyrus sativus* L.)." Eur Food Res Technol **213**(4-5): 343-348.

Liu, X., T. Rush, J. Zapata and D. Lobner (2009). "β-N-methylamino-l-alanine induces oxidative stress and glutamate release through action on system X_c^-." Exp Neurol **217**(2): 429-33.

Ludolph, A. C., J. Hugon, M. P. Dwivedi, H. H. Schaumburg and P. S. Spencer (1987). "Studies on the aetiology and pathogenesis of motor neuron diseases. 1. Lathyrism: clinical findings in established cases." Brain **110 (Pt 1)**: 149-65.

Ludolph, A. C. and P. S. Spencer (1996). "Toxic models of upper motor neuron disease." J Neurol Sci **139 Suppl**: 53-9.
Lynch, D., C. Wanglund, R. Spathis, C. W. Chan, D. M. Reiff, J. K. Lum and R. M. Garruto (2008). "The contribution of mitochondrial dysfunction to a gene-environment model of Guamanian ALS and PD." Mitochondrion **8**(2): 109-16.
MacDonald, J. F. and M. E. Morris (1984). "*Lathyrus* excitotoxin: mechanism of neuronal excitation by L-2-oxalylamino-3-amino- and L-3-oxalylamino-2-amino-propionic acid." Exp Brain Res **57**(1): 158-66.
Mackenzie, G. G., M. P. Zago, L. Aimo and P. I. Oteiza (2007). "Zinc deficiency in neuronal biology." IUBMB Life **59**(4-5): 299-307.
Malisza, K. L., C. J. Briggs and B. B. Hasinoff (1997). "Electron paramagnetic spin trapping studies of the system containing the copper(II) complex of the neurotoxin β-ODAP (3-N-oxalyl-L-2,3-diaminopropanoic acid) and hydrogen peroxide." J Inorg Biochem **65**(4): 251-255.
Manthey, D. and C. Behl (2006). "From structural biochemistry to expression profiling: neuroprotective activities of estrogen." Neuroscience **138**(3): 845-50.
Maragakis, N. J. and J. D. Rothstein (2004). "Glutamate transporters: animal models to neurologic disease." Neurobiol Dis **15**(3): 461-73.
Marambaud, P., U. Dreses-Werringloer and V. Vingtdeux (2009). "Calcium signaling in neurodegeneration." Mol Neurodegener **4**: 20.
Martin, L. J. (1999). "Neuronal death in amyotrophic lateral sclerosis is apoptosis: possible contribution of a programmed cell death mechanism." J Neuropathol Exp Neurol **58**(5): 459-71.
Martınez-Chantar, M. L., M. U. Latasa, M. Varela-Rey, S. C. Lu, E. R. Garcı´a-Trevijano, J. M. Mato and M. A. Avila (2003). "L-Methionine availability regulates expression of the methionine adenosyltransferase 2A gene in human hepatocarcinoma cells." J Biol Chem **278**(22): 19885–1989.
Mathie, A., G. L. Sutton, C. E. Clarke and E. L. Veale (2006). "Zinc and copper: Pharmacological probes and endogenous modulators of neuronal excitability." Pharmacol Ther **111**(3): 567-583.
Mattiazzi, M., M. D'Aurelio, C. D. Gajewski, K. Martushova, M. Kiaei, M. F. Beal and G. Manfredi (2002). "Mutated human SOD1 causes dysfunction of oxidative phosphorylation in mitochondria of transgenic mice." J Biol Chem **277**(33): 29626-33.
McArthur, S., E. Cristante, M. Paterno, H. Christian, F. Roncaroli, G. E. Gillies and E. Solito (2010). "Annexin A1: a central player in the anti-inflammatory and neuroprotective role of microglia." J Immunol **185**(10): 6317-28.
McBean, G. J. (2002). "Cerebral cystine uptake: a tale of two transporters." Trends Pharmacol Sci **23**(7): 299-302.
McCombe, P. A. and R. D. Henderson (2010). "Effects of gender in amyotrophic lateral sclerosis." Gend Med **7**(6): 557-70.
Mehta, T., A. J. Parker, P. K. Cusick, N. S. Zarghami and B. E. Haskell (1980). "*Lathyrus sativus* Neurotoxin - Evidence of Selective Retention in Monkey Tissue." Toxicol App Pharmacol **52**(1): 54-61.
Meldrum, B. S. (2000). "Glutamate as a neurotransmitter in the brain: review of physiology and pathology." J Nutr **130**(4S Suppl): 1007S-15S.
Melka, A., R. Tekle Haimanot and F. Lambein (1997). "Symptomatic treatment of neurolathyrism with Tolperizone HCL (Mydocalm): A randomized double blind and placebo controlled drug trial." Ethiop Med J **35**(2): 77-91.
Mera, M., A. Montenegro, N. Espinoza and N. Guete (2000). "Research backs grass pea exports by small Chilean farmers." Lathyrus Lathyrism Newsletter **1**: 31.
Mikic, A., V. Mihailovic, B. Cupina, B. Duric, D. Krstic, M. Vasic, S. Vasiljevic, D. Karagic and V. Dordevic (2010). "Towards the re-introduction of grass pea (*Lathyrus sativus*) in the West Balkan Countries: The case of Serbia and Srpska (Bosnia and Herzegovina)." Food Chem Toxicol.
Milczak, M., M. Pedzinski, H. Mnichowska, K. Szwed-Urbas and W. Rybinski (2001). "Creative breeding of grass pea (*Lathyrus sativus* L.) in Poland." Lathyrus Lathyrism Newsletter **2**: 85-88.
Miller, S., P. B. Nunn and R. J. Bridges (1993). "Induction of astrocyte glutamine synthetase activity by the *Lathyrus* toxin β-N-oxalyl-L-α,β-diaminopropionic acid (β-L-ODAP)." Glia **7**(4): 329-36.
Murphy, T. H., R. L. Schnaar and J. T. Coyle (1990). "Immature cortical neurons are uniquely sensitive to glutamate toxicity by inhibition of cystine uptake." FASEB J **4**(6): 1624-33.
Murti, V. V. S., T. R. Seshadri and T. A. Venkitasubramanian (1964). "Neurotoxic Compounds of the Seeds of *Lathyrus sativus*." Phytochemistry **3**(1): 73-78.
Muyderman, H., P. G. Hutson, D. Matusica, M. L. Rogers and R. A. Rush (2009). "The human G93A-superoxide dismutase-1 mutation, mitochondrial glutathione and apoptotic cell death." Neurochem Res **34**(10): 1847-56.
Nakagawa, T., H. Zhu, N. Morishima, E. Li, J. Xu, B. A. Yankner and J. Yuan (2000). "Caspase-12 mediates endoplasmic-reticulum-specific apoptosis and cytotoxicity by amyloid-β." Nature **403**(6765): 98-103.
Niswender, C. M. and P. J. Conn (2010). "Metabotropic glutamate receptors: physiology, pharmacology, and disease." Annu Rev Pharmacol Toxicol **50**: 295-322.
Nunn, P. B., E. A. Bell, A. A. Watson and R. J. Nash (2010). "Toxicity of non-protein amino acids to humans and domestic animals." Nat Prod Commun **5**(3): 485-504.
Ochu, E. E., N. J. Rothwell and C. M. Waters (1998). "Caspases mediate 6-hydroxydopamine-induced apoptosis but not necrosis in PC12 cells." J Neurochem **70**(6): 2637-40.
Oldendorf, W. H. and J. Szabo (1976). "Amino acid assignment to one of three blood-brain barrier amino acid carriers." Am J Physiol **230**(1): 94-8.
Olney, J. (1969). "Brain lesions, obesity, and other disturbances in mice treated with monosodium glutamate." Science **164**: 719-721.

Olney, J. W., C. H. Misra and V. Rhee (1976). "Brain and retinal damage from lathyrus excitotoxin, β-N-oxalyl-L-α,β-diaminopropionic acid." Nature **264**(5587): 659-61.

Ormandy, G. C. and R. S. Jope (1990). "Inhibition of phosphoinositide hydrolysis by the novel neurotoxin β-N-oxalyl-L-α,β-diaminopropionic acid (L-BOAA)." Brain Res **510**(1): 53-7.

Orrenius, S., B. Zhivotovsky and P. Nicotera (2003). "Regulation of cell death: the calcium-apoptosis link." Nat Rev Mol Cell Biol **4**(7): 552-65.

Padmajaprasad, V., M. Kaladhar and R. V. Bhat (1997). "Thermal isomerisation of β-N-oxalyl-L-α,β-diaminopropionic acid, the neurotoxin in *Lathyrus sativus*, during cooking." Food Chemistry **59**(1): 77-80.

Pai, K. S. and V. Ravindranath (1993). "L-BOAA induces selective inhibition of brain mitochondrial enzyme, NADH-dehydrogenase." Brain Res **621**(2): 215-21.

Paleacu, D., D. F. Cohn and J. M. Rabey (1999). "Cognitive evaluation of patients with chronic neurolathyrism." Parkinsonism Relat Disord **5**(1-2): 55-8.

Palecek, J., M. B. Lips and B. U. Keller (1999). "Calcium dynamics and buffering in motoneurones of the mouse spinal cord." J Physiol **520 Pt 2**: 485-502.

Pan, W., W. A. Banks and A. J. Kastin (1997). "Permeability of the blood-brain and blood-spinal cord barriers to interferons." J Neuroimmunol **76**(1-2): 105-11.

Parker, A. J., T. Mehta, N. S. Zarghami, P. K. Cusick and B. E. Haskell (1979). "Acute Neurotoxicity of the *Lathyrus sativus* Neurotoxin, L-3-Oxalylamino-2-Aminopropionic Acid, in the Squirrel-Monkey." Toxicol App Pharmacol **47**(1): 135-143.

Pearson, S. and P. B. Nunn (1981). "The neurolathyrogen, β-N-oxalyl-L-α,β-diaminopropionic acid, is a potent agonist at 'glutamate preferring' receptors in the frog spinal cord." Brain Res **206**(1): 178-82.

Pena-Chocarro, L. and L. Z. Pena (1999). "History and traditional cultivation of *Lathyrus sativus* L. and *Lathyrus cicera* L. in the Iberian peninsula." Vegetation History and Archaeobotany **8**(1-2): 49-52.

Perez-Gracia, E., B. Torrejon-Escribano and I. Ferrer (2008). "Dystrophic neurites of senile plaques in Alzheimer's disease are deficient in cytochrome c oxidase." Acta Neuropathol **116**(3): 261-8.

Perkins, G., E. Bossy-Wetzel and M. H. Ellisman (2009). "New insights into mitochondrial structure during cell death." Exp Neurol **218**(2): 183-92.

Pinton, P., C. Giorgi, R. Siviero, E. Zecchini and R. Rizzuto (2008). "Calcium and apoptosis: ER-mitochondria Ca^{2+} transfer in the control of apoptosis." Oncogene **27**(50): 6407-18.

Poesen, K., D. Lambrechts, P. Van Damme, J. Dhondt, F. Bender, N. Frank, E. Bogaert, B. Claes, L. Heylen, A. Verheyen, K. Raes, M. Tjwa, U. Eriksson, M. Shibuya, R. Nuydens, L. Van Den Bosch, T. Meert, R. D'Hooge, M. Sendtner, W. Robberecht and P. Carmeliet (2008). "Novel role for vascular endothelial growth factor (VEGF) receptor-1 and its ligand VEGF-B in motor neuron degeneration." J Neurosci **28**(42): 10451-9.

Ponseti, I. V. and R. A. Brand (2008). "50 years ago in CORR - Skeletal lesions produced by aminonitriles." Clin Orthop Rel Res **466**(1): 255-256.

Pratap Rudra, M. P., M. R. Singh, M. A. Junaid, P. Jyothi and S. L. Rao (2004). "Metabolism of dietary ODAP in humans may be responsible for the low incidence of neurolathyrism." Clin Biochem **37**(4): 318-22.

Ramachandran, S., A. Bairagi and A. K. Ray (2005). "Improvement of nutritive value of grass pea (*Lathyrus sativus*) seed meal in the formulated diets for rohu, Labeo rohita (Hamilton) fingerlings after fermentation with a fish gut bacterium." Bioresour Technol **96**(13): 1465-72.

Rao, S. D., S. A. Banack, P. A. Cox and J. H. Weiss (2006). "BMAA selectively injures motor neurons via AMPA/kainate receptor activation." Exp Neurol **201**(1): 244-52.

Rao, S. L. (1978). "Entry of β-N-oxalyl-L-α,β-diaminopropionic acid, the *Lathyrus sativus* neurotoxin into the central nervous system of the adult rat, chick and the rhesus monkey." J Neurochem **30**(6): 1467-70.

Rao, S. L. N., P. S. Sarma and P. R. Adiga (1964). "The isolation and Characterization of β-N-Oxalyl-L-α,β-Diaminopropionic Acid: a Neurotoxin from the Seeds of *Lathyrus sativus*." Biochemistry **3**(3): 432-436.

Rao, S. L. N., P. S. Sarma, K. S. Mani, T. R. R. Rao and Sriramac.S (1967). "Experimental Neurolathyrism in Monkeys." Nature **214**(5088): 610-&.

Ratan, R. R., T. H. Murphy and J. M. Baraban (1994). "Macromolecular synthesis inhibitors prevent oxidative stress-induced apoptosis in embryonic cortical neurons by shunting cysteine from protein synthesis to glutathione." J Neurosci **14**(7): 4385-92.

Ravindranath, V. (2002). "Neurolathyrism: mitochondrial dysfunction in excitotoxicity mediated by L-β-oxalyl aminoalanine." Neurochem Int **40**(6): 505-9.

Reiner, A., L. Medina, G. Figueredo-Cardenas and S. Anfinson (1995). "Brainstem motoneuron pools that are selectively resistant in amyotrophic lateral sclerosis are preferentially enriched in parvalbumin: evidence from monkey brainstem for a calcium-mediated mechanism in sporadic ALS." Exp Neurol **131**(2): 239-50.

Ressler, C. (1962). "Isolation and identification from common vetch of the neurotoxin β-cyano-L-alanine, a possible factor in neurolathyrism." J Biol Chem **237**: 733-5.

Rizzuto, R., C. Bastianutto, M. Brini, M. Murgia and T. Pozzan (1994). "Mitochondrial Ca^{2+} homeostasis in intact cells." J Cell Biol **126**(5): 1183-94.

Rizzuto, R., M. Brini, C. Bastianutto, R. Marsault and T. Pozzan (1995). "Photoprotein-mediated measurement of calcium ion concentration in mitochondria of living cells." Methods Enzymol **260**: 417-28.

Rizzuto, R., P. Pinton, W. Carrington, F. S. Fay, K. E. Fogarty, L. M. Lifshitz, R. A. Tuft and T. Pozzan (1998). "Close contacts with the endoplasmic reticulum as determinants of mitochondrial Ca^{2+} responses." Science **280**(5370): 1763-6.

Rodriguez-Nieto, S. and B. Zhivotovsky (2006). "Role of alterations in the apoptotic machinery in sensitivity of cancer cells to treatment." Curr Pharm Des **12**(34): 4411-25.

Rosen, D. R., T. Siddique, D. Patterson, D. A. Figlewicz, P. Sapp, A. Hentati, D. Donaldson, J. Goto, J. P. O'Regan, H. X. Deng and et al. (1993). "Mutations in Cu/Zn superoxide dismutase gene are associated with familial amyotrophic lateral sclerosis." Nature **362**(6415): 59-62.

Ross, S. M., D. N. Roy and P. S. Spencer (1985). "β-N-Oxalylamino-L-alanine: action on high-affinity transport of neurotransmitters in rat brain and spinal cord synaptosomes." J Neurochem **44**(3): 886-92.

Ross, S. M., D. N. Roy and P. S. Spencer (1989). "β-N-oxalylamino-L-alanine action on glutamate receptors." J Neurochem **53**(3): 710-5.

Ross, S. M. and P. S. Spencer (1987). "Specific Antagonism of Behavioral Action of Uncommon Amino-Acids Linked to Motor-System Diseases." Synapse **1**(3): 248-253.

Rossi, L., M. F. Lombardo, M. R. Ciriolo and G. Rotilio (2004). "Mitochondrial dysfunction in neurodegenerative diseases associated with copper imbalance." Neurochem Res **29**(3): 493–504.

Roy, D. N., Nagaraja.V and C. Gopalan (1963). "Production of Neurolathyrism in Chicks by Injection of *Lathyrus sativus* Concentrates." Current Science **32**(3): 116-&.

Rudra, M. N. and L. M. Chaudhury (1952). "Preliminary note on methionine excretion in lathyrism." Current Science **4**: 99-100.

Ruiz de Almodovar, C., D. Lambrechts, M. Mazzone and P. Carmeliet (2009). "Role and therapeutic potential of VEGF in the nervous system." Physiol Rev **89**(2): 607-48.

Sabri, M. I., B. Lystrup, D. N. Roy and P. S. Spencer (1995). "Action of β-N-oxalylamino-L-alanine on mouse brain NADH-dehydrogenase activity." J Neurochem **65**(4): 1842-8.

Saeed, U., L. Durgadoss, R. K. Valli, D. C. Joshi, P. G. Joshi and V. Ravindranath (2008). "Knockdown of cytosolic glutaredoxin 1 leads to loss of mitochondrial membrane potential: implication in neurodegenerative diseases." PLoS ONE **3**(6): e2459.

Saggioro, D., M. Silic-Benussi, R. Biasiotto, D. M. D'Agostino and V. Ciminale (2009). "Control of cell death pathways by HTLV-1 proteins." Front Biosci **14**: 3338-51.

Samantaray, S., V. H. Knaryan, M. K. Guyton, D. D. Matzelle, S. K. Ray and N. L. Banik (2007). "The parkinsonian neurotoxin rotenone activates calpain and caspase-3 leading to motoneuron degeneration in spinal cord of Lewis rats." Neuroscience **146**(2): 741-55.

Sanz-Blasco, S., R. A. Valero, I. Rodriguez-Crespo, C. Villalobos and L. Nunez (2008). "Mitochondrial Ca^{2+} overload underlies Aβ oligomers neurotoxicity providing an unexpected mechanism of neuroprotection by NSAIDs." PLoS ONE **3**(7): e2718.

Schiess, M. C., J. L. Barnes, T. M. Ellmore, B. J. Poindexter, K. Dinh and R. J. Bick (2010). "CSF from Parkinson disease Patients Differentially Affects Cultured Microglia and Astrocytes." BMC Neurosci **11**(1): 151.

Schreibelt, G., G. Kooij, A. Reijerkerk, R. van Doorn, S. I. Gringhuis, S. van der Pol, B. B. Weksler, I. A. Romero, P. O. Couraud, J. Piontek, I. E. Blasig, C. D. Dijkstra, E. Ronken and H. E. de Vries (2007). "Reactive oxygen species alter brain endothelial tight junction dynamics via RhoA, PI3 kinase, and PKB signaling." FASEB J **21**(13): 3666-76.

Schubert, D. and D. Piasecki (2001). "Oxidative glutamate toxicity can be a component of the excitotoxicity cascade." J Neurosci **21**(19): 7455-7462.

Shahi, K. and M. Baudry (1992). "Increasing binding affinity of agonists to glutamate receptors increases synaptic responses at glutamatergic synapses." Proc Natl Acad Sci U S A **89**(15): 6881-5.

Shasi Vardhan, K., M. P. Pratap Rudra and S. L. Rao (1997). "Inhibition of tyrosine aminotransferase by β-N-oxalyl-L-α,β-diaminopropionic acid, the *Lathyrus sativus* neurotoxin." J Neurochem **68**(6): 2477-84.

Shaw, P. J. (2005). "Molecular and cellular pathways of neurodegeneration in motor neurone disease." J Neurol Neurosurg Psychiatry **76**(8): 1046-57.

Shi, P., J. Gal, D. M. Kwinter, X. Liu and H. Zhu (2010). "Mitochondrial dysfunction in amyotrophic lateral sclerosis." Biochim Biophys Acta **1802**(1): 45-51.

Shimizu, S., M. Narita and Y. Tsujimoto (1999). "Bcl-2 family proteins regulate the release of apoptogenic cytochrome c by the mitochondrial channel VDAC." Nature **399**(6735): 483-7.

Shinomol, G. K. and Muralidhara (2007). "Differential induction of oxidative impairments in brain regions of male mice following subchronic consumption of Khesari dhal (*Lathyrus sativus*) and detoxified Khesari dhal." Neurotoxicology.

Silic-Benussi, M., R. Biasiotto, V. Andresen, G. Franchini, D. M. D'Agostino and V. Ciminale (2010). "HTLV-1 p13, a small protein with a busy agenda." Mol Aspects Med.

Simpson, P. B. and J. T. Russell (1998). "Role of mitochondrial Ca^{2+} regulation in neuronal and glial cell signalling." Brain Res Brain Res Rev **26**(1): 72-81.

Singh, M. R., M. P. Pratap Rudra, S. L. Rao and S. S. Singh (2004). "*In vitro* activation of protein kinase C by β-N-oxalyl-L-α,β-diaminopropionic acid, the *Lathyrus sativus* neurotoxin." Neurochem Res **29**(7): 1343-8.

Skerritt, J. H. and G. A. Johnston (1981). "Uptake and release of N-methyl-D-aspartate by rat brain slices." J Neurochem **36**(3): 881-5.

Smaili, S., H. Hirata, R. Ureshino, P. T. Monteforte, A. P. Morales, M. L. Muler, J. Terashima, K. Oseki, T. R. Rosenstock, G. S. Lopes and C. Bincoletto (2009). "Calcium and cell death signaling in neurodegeneration and aging." An Acad Bras Cienc **81**(3): 467-75.

Smith, Q. R. (2000). "Transport of glutamate and other amino acids at the blood-brain barrier." J Nutr **130**(4S Suppl): 1016S-22S.

Spencer, P. S. (1995). "Lathyrism." Handbook of Clinical Neurology **21**: 1-20.

Spencer, P. S. (1999). "Food toxins, ampa receptors, and motor neuron diseases." Drug Metab Rev **31**(3): 561-87.

Spencer, P. S., J. Hugon, A. Ludolph, P. B. Nunn, S. M. Ross, D. N. Roy and H. H. Schaumburg (1987). "Discovery and partial characterization of primate motor-system toxins." Ciba Found Symp **126**: 221-38.

Spencer, P. S., D. N. Roy, A. Ludolph, J. Hugon, M. P. Dwivedi and H. H. Schaumburg (1986). "Lathyrism: evidence for role of the neuroexcitatory aminoacid BOAA." Lancet **2**(8515): 1066-7.

Sreeja, V. G., N. Nagahara, Q. Li and M. Minami (2003). "New aspects in pathogenesis of konzo: neural cell damage directly caused by linamarin contained in cassava (Manihot esculenta Crantz)." Br J Nutr **90**(2): 467-72.

Sriram, K., S. K. Shankar, M. R. Boyd and V. Ravindranath (1998). "Thiol oxidation and loss of mitochondrial complex I precede excitatory amino acid-mediated neurodegeneration." J Neurosci **18**(24): 10287-96.

Stamatovic, S. M., R. F. Keep and A. V. Andjelkovic (2008). "Brain endothelial cell-cell junctions: how to "open" the blood brain barrier." Curr Neuropharmacol **6**(3): 179-92.

Staton, P. C. and D. R. Bristow (1997). "The dietary excitotoxins β-N-methylamino-L-alanine and β-N-oxalylamino-L-alanine induce necrotic- and apoptotic-like death of rat cerebellar granule cells." J Neurochem **69**(4): 1508-18.

Steele, J. C. and P. L. McGeer (2008). "The ALS/PDC syndrome of Guam and the cycad hypothesis." Neurology **70**(21): 1984-90.

Streit, W. J., H. Braak, Q. S. Xue and I. Bechmann (2009). "Dystrophic (senescent) rather than activated microglial cells are associated with tau pathology and likely precede neurodegeneration in Alzheimer's disease." Acta Neuropathol **118**(4): 475-85.

Striefler, M., D. F. Cohn, A. Hirano and E. Schujman (1977). "The central nervous system in a case of neurolathyrism." Neurology **27**(12): 1176-8.

Sykova, E. and C. Nicholson (2008). "Diffusion in brain extracellular space." Physiol Rev **88**(4): 1277-340.

Szabadkai, G., A. M. Simoni, M. Chami, M. R. Wieckowski, R. J. Youle and R. Rizzuto (2004). "Drp-1-dependent division of the mitochondrial network blocks intraorganellar Ca^{2+} waves and protects against Ca^{2+}-mediated apoptosis." Mol Cell **16**(1): 59-68.

Szydlowska, K. and M. Tymianski "Calcium, ischemia and excitotoxicity." Cell Calcium **47**(2): 122-9.

Targos, B., J. Baran0ska and P. Pomorski (2005). "Store-operated calcium entry in physiology and pathology of mammalian cells." Acta Biochim Pol **52**(2): 379-409.

Tekle Haimanot, R., F. Lambein and A. Feleke (2005). "Is lathyrism still endemic in northern Ethiopia? - The case of Legambo Woreda (district) in the South Wollo Zone, Amhara National Regional State." Ethiopian Journal of Health Development **19**(3): 230-236.

Thastrup, O., A. P. Dawson, O. Scharff, B. Foder, P. J. Cullen, B. K. Drobak, P. J. Bjerrum, S. B. Christensen and M. R. Hanley (1989). "Thapsigargin, a novel molecular probe for studying intracellular calcium release and storage." Agents Actions **27**(1-2): 17-23.

Tor-Agbidye, J., V. S. Palmer, M. R. Lasarev, A. M. Craig, L. L. Blythe, M. I. Sabri and P. S. Spencer (1999a). "Bioactivation of cyanide to cyanate in sulfur amino acid deficiency: relevance to neurological disease in humans subsisting on cassava." Toxicol Sci **50**(2): 228-35.

Tor-Agbidye, J., V. S. Palmer, P. S. Spencer, A. M. Craig, L. L. Blythe and M. I. Sabri (1999b). "Sodium cyanate alters glutathione homeostasis in rodent brain: relationship to neurodegenerative diseases in protein-deficient malnourished populations in Africa." Brain Res **820**(1-2): 12-9.

Traynelis, S. F., L. P. Wollmuth, C. J. McBain, F. S. Menniti, K. M. Vance, K. K. Ogden, K. B. Hansen, H. Yuan, S. J. Myers and R. Dingledine (2010). "Glutamate receptor ion channels: structure, regulation, and function." Pharmacol Rev **62**(3): 405-96.

Tshala-Katumbay, D., K. E. Eeg-Olofsson, T. Kazadi-Kayembe, T. Tylleskar and P. Fallmar (2002). "Analysis of motor pathway involvement in konzo using transcranial electrical and magnetic stimulation." Muscle Nerve **25**(2): 230-5.

Turner, M. R., A. Cagnin, F. E. Turkheimer, C. C. Miller, C. E. Shaw, D. J. Brooks, P. N. Leigh and R. B. Banati (2004). "Evidence of widespread cerebral microglial activation in amyotrophic lateral sclerosis: an [11C](R)-PK11195 positron emission tomography study." Neurobiol Dis **15**(3): 601-9.

Valero, R. A., L. Senovilla, L. Nunez and C. Villalobos (2008). "The role of mitochondrial potential in control of calcium signals involved in cell proliferation." Cell Calcium **44**(3): 259-69.

Van Damme, P., L. Van Den Bosch, E. Van Houtte, G. Callewaert and W. Robberecht (2002a). "GluR2-dependent properties of AMPA receptors determine the selective vulnerability of motor neurons to excitotoxicity." J Neurophysiol **88**(3): 1279-87.

Van Damme, P., L. Van Den Bosch, E. Van Houtte, J. Eggermont, G. Callewaert and W. Robberecht (2002b). "Na^+ entry through AMPA receptors results in voltage-gated K^+ channel blockade in cultured rat spinal cord motoneurons." J Neurophysiol **88**(2): 965-72.

Van Den Bosch, L. and W. Robberecht (2000). "Different receptors mediate motor neuron death induced by short and long exposures to excitotoxicity." Brain Res Bull **53**(4): 383-8.

Van Den Bosch, L., B. Schwaller, V. Vleminckx, B. Meijers, S. Stork, T. Ruehlicke, E. Van Houtte, H. Klaassen, M. R. Celio, L. Missiaen, W. Robberecht and M. W. Berchtold (2002a). "Protective effect of parvalbumin on excitotoxic motor neuron death." Exp Neurol **174**(2): 150-61.

Van den Bosch, L., B. Schwaller, V. Vleminckx, B. Meijers, S. Stork, T. Ruehlicke, E. Van Houtte, H. Klaassen, M. R. Celio, L. Missiaen, W. Robberecht and M. W. Berchtold (2002b). "Protective effect of parvalbumin on excitotoxic motor neuron death." Experimental Neurology **174**(2): 150-161.

Van Den Bosch, L., P. Van Damme, E. Bogaert and W. Robberecht (2006). "The role of excitotoxicity in the pathogenesis of amyotrophic lateral sclerosis." Biochim Biophys Acta **1762**(11-12): 1068-82.

Vandenberghe, W., L. Van Den Bosch and W. Robberecht (1998). "Glial cells potentiate kainate-induced neuronal death in a motoneuron-enriched spinal coculture system." Brain Res **807**(1-2): 1-10.

Venkatachalam, K., D. B. van Rossum, R. L. Patterson, H. T. Ma and D. L. Gill (2002). "The cellular and molecular basis of store-operated calcium entry." Nat Cell Biol **4**(11): E263-72.

Verkhratsky, A. (2004). "Endoplasmic reticulum calcium signaling in nerve cells." Biol Res **37**(4): 693-9.

Vyas, K. J. and J. H. Weiss (2009). "BMAA--an unusual cyanobacterial neurotoxin." Amyotroph Lateral Scler **10 Suppl 2**: 50-5.

Warren, B. A., S. A. Patel, P. B. Nunn and R. J. Bridges (2004). "The *Lathyrus* excitotoxin β-N-oxalyl-L-α,β-diaminopropionic acid is a substrate of the L-cystine/L-glutamate exchanger system x_c^-." Toxicol Appl Pharmacol **200**(2): 83-92.

Watkins, J. C., D. R. Curtis and T. J. Biscoe (1966). "Central effects of β-N-oxalyl-α,β-diaminopropionic acid and other *lathyrus* factors." Nature **211**(5049): 637.

Wedler, F. C., M. C. Vichnin, B. W. Ley, G. Tholey, M. Ledig and J. C. Copin (1994). "Effects of Ca^{2+} ions on Mn^{2+} dynamics in chick glia and rat astrocytes: potential regulation of glutamine synthetase." Neurochem Res **19**(2): 145-51.

Weintroub, S., D. F. Cohen, R. Salama, M. Streifler and S. L. Weissman (1980). "Skeletal findings in human neutrolathyrism. Is there a human osteolathyrism?" Eur Neurol **19**(2): 121-7.

Weiss, J. H., J. Y. Koh and D. W. Choi (1989). "Neurotoxicity of β-N-methylamino-L-alanine (BMAA) and β-N-oxalylamino-L-alanine (BOAA) on cultured cortical neurons." Brain Res **497**(1): 64-71.

Willis, C. L., B. S. Meldrum, P. B. Nunn, B. H. Anderton and P. N. Leigh (1993). "Neuronal damage induced by β-N-oxalylamino-L-alanine, in the rat hippocampus, can be prevented by a non-NMDA antagonist, 2,3-dihydroxy-6-nitro-7-sulfamoyl-benzo(F)quinoxaline." Brain Res **627**(1): 55-62.

Willis, C. L., B. S. Meldrum, P. B. Nunn, B. H. Anderton and P. N. Leigh (1994). "Neuroprotective effect of free radical scavengers on β-N-oxalylamino-L-alanine (BOAA)-induced neuronal damage in rat hippocampus." Neurosci Lett **182**(2): 159-62.

Wuytack, F., J. A. Eggermont, L. Raeymaekers, L. Plessers and R. Casteels (1989). "Antibodies against the non-muscle isoform of the endoplasmic reticulum Ca^{2+}-transport ATPase." Biochem J **264**(3): 765-9.

Yang, W. and M. S. Kilberg (2002). "Biosynthesis, intracellular targeting, and degradation of the EAAC1 glutamate/aspartate transporter in C6 glioma cells." J Biol Chem **277**(41): 38350-7.

Yano, K., H. Higashida, R. Inoue and Y. Nozawa (1984). "Bradykinin-induced rapid breakdown of phosphatidylinositol 4,5-bisphosphate in neuroblastoma X glioma hybrid NG108-15 cells." J Biol Chem **259**(16): 10201-7.

Yao, H. H., J. H. Ding, F. Zhou, F. Wang, L. F. Hu, T. Sun and G. Hu (2005). "Enhancement of glutamate uptake mediates the neuroprotection exerted by activating group II or III metabotropic glutamate receptors on astrocytes." J Neurochem **92**(4): 948-61.

Ye, Z. and H. Sontheimer (1998). "Astrocytes protect neurons from neurotoxic injury by serum glutamate." Glia **22**(3): 237-248.

Zaninovic, V. (2004). "Possible etiologies for tropical spastic paraparesis and human T lymphotropic virus I-associated myelopathy." Braz J Med Biol Res **37**(1): 1-12.

Curriculum vitae

PERSONAL DETAILS

Name	Van Moorhem Marijke
Date of birth	May 15, 1981
E-mail	marijkevanmoorhem@hotmail.be

WORKING EXPERIENCE

July 2010 – today
Part-time: Sceintific cooperator (Minerva n.v.), Ghent, Belgium
Part-time: Teacher (sciences, anatomy and physiology), KaHo Sint-Lieven, Sint-Niklaas and Ghent– Belgium

January 2010 – June 2010
Part-time: Sceintific cooperator (Department of General practice and primary health care), Ghent university, Ghent - Belgium
Part-time: Administrative assistant, KaHo Sint-Lieven, Sint-Niklaas – Belgium

October 2005 – january 2010, Ghent University, Ghent - Belgium
PhD student Biomedical Sciences "Etiology of neurolathyrism, a neurodegenerative disease with nutritional causes." (Prof. Dr. L. Leybaert, Em. Prof. Dr. F. Lambein)

July 2004-September 2005, Bio Minerals n.v., Destelbergen - Belgium
R&D Associate

April 2004-july 2004, KaHo Sint-Lieven, Sint-Niklaas - Belgium
Administrative assistant

TRAINING

2003-january 2004, Ghent University, Ghent - Belgium
Scientific cooperator "Etiology of neurolathyrism, a neurodegenerative disease with nutritional causes" (Prof. Dr. L. Leybaert, Prof. Dr. G. Callewaert)

1999–2003, Catholic University of Leuven, Leuven - Belgium
Master in Biomedical Sciences
Master thesis "Consequenties of SERCA3b overexpression in COS-cells."
Laboratory: Physiology (Prof. Dr. G. Callewaert)

1993–1999, Instituut Heilige Familie, Sint-Niklaas - Belgium
Latin-Sciences

PUBLICATIONS

Maria Carlota Vaz Patto, Colin David Hanbury, Marijke Van Moorhem, Fernand Lambein, Sergio Ochatt, Diego Rubiales. Genetics, Genomics and Breeding of Cool Season Grain Legumes, Chapter 4: Grass pea, p.151-204.

Van Moorhem M., Decrock E., De Vuyst E., De Bock M., Wang N., Lambein F., Van Den Bosch L., Leybaert L. Involvement of Ca^{2+} and oxidative stress in L-β-N-oxalyl-α,β-diaminopropionic acid and L-glutamate induced toxicity in motor neurons. Neuroreport. 2011 22(3):131-5.

Fikre A., Van Moorhem M., Ahmed S., Lambein F., Gheysen G. Studies on neurolathyrism in Ethiopia: dietary habits, perception of risks and prevention. Food Chem Toxicol. 2011 49(3):678-84.

Van Moorhem M., Lambein F., Leybaert L. Unraveling the mechanism of β-N-oxalyl-α,β-diaminopropionic acid (β-ODAP) induced excitotoxicity and oxidative stress, relevance for neurolathyrism prevention. Food and Chemical Toxicology. 2011 49(3):550-5.

Van Moorhem M., Decrock E., Coussee E., Faes L., De Vuyst E., Vranckx K., De Bock M., Wang N., Lambein F., Callewaert G., Leybaert L. β-ODAP alters mitochondrial Ca^{2+} handling as an early event in excitotoxicity. Cell Calcium. 2010 47(3):287-96.

De Vuyst E., Wang N., Decrock E., De Bock M., Vinken M., Van Moorhem M., Lai C., Culot M., Rogiers V., Cecchelli R., Naus C.C., Evans W.H., Leybaert L. Ca^{2+} regulation of connexin 43 hemichannels in C6 glioma and glial cells. Cell Calcium. 2009 46(3):176-87.

Decrock E., De Vuyst E., Vinken M., Van Moorhem M., Vranckx K., Wang N., Van Laeken L., De Bock M., D'Herde K., Lai C.P., Rogiers V., Evans W.H., Naus C.C., Leybaert L. Connexin 43 hemichannels contribute to the propagation of apoptotic cell death in a rat C6 glioma cell model. Cell Death Differ. 2009 16(1):151-63.

De Vuyst E., De Bock M., Decrock E., Van Moorhem M., Naus C., Mabilde C., Leybaert L. In situ bipolar electroporation for localized cell loading with reporter dyes and investigating gap junctional coupling. Biophys J. 2008 15;94(2):469-79.

Leybaert L., De Bock M., Van Moorhem M., Decrock E., De Vuyst E. Neurobarrier coupling in the brain: adjusting glucose entry with demand. J Neurosci Res. 2007 85(15):3213-20.

ORAL PRESENTATIONS

"Unraveling the mechanism of β-ODAP induced excitotoxicity and oxidative stress, relevance for neurolathyrism prevention." International workshop on the toxico-nutritional neurodegenerations konzo and lathyrism. Ghent, Belgium; September 22, 2009.

"Neurolathyrism, the crippling disease of the poor, can possibly be prevented." Dag van de Jonge Onderzoekers in de Afrikanistiek. Antwerp, Belgium; December 12, 2008.

"Neurolathyrism: 44 years of striving" Seminar with Prof. Dr P. Nunn (University of Portsmouth). Ghent, Belgium; November 21, 2008.

ABSTRACTS AND POSTER PRESENTATIONS

Van Moorhem M., Lambein F., Leybaert L. (2009) Unraveling the mechanism of β-ODAP induced excitotoxicity and oxidative stress, relevance for neurolathyrism prevention. International workshop on the toxico-nutritional neurodegenerations konzo and lathyrism. Ghent, Belgium; September 21-22, 2009.

Van Moorhem M., Decrock E., De Bock M., Wang N., De Vuyst E., Callewaert G., Van Den Bosch L., Lambein F., Leybaert L. (2009) Neuro- and gliotoxicity of the excitatory amino acid β-ODAP involves impaired free radical defense. European meeting on glial cells in health and disease. Paris, France; September 8-12, 2009.

Van Moorhem M., Decrock E., Coussee E., Faes L., De Vuyst E., Vranckx K., De Bock M., Wang N., Lambein F., Callewaert G., Leybaert L. (2009) β-ODAP-triggered mitochondrial calcium overload as an early event in excitotoxicity. 2nd Annual Meeting of IAP network. Molecular and cellular mechanisms of electrical excitability. Leuven, Belgium; January 7, 2009.

Van Moorhem M., Lambein F, Leybaert L. (2008) Neurolathyrism, the crippling disease of the poor, can possibly be prevented. GAPSYM2 Mobilities in Africa – Africa in mobility. Ghent, Belgium; December 16, 2008.

Van Moorhem M., Lambein F, Leybaert L. (2008) Neurolathyrism, the crippling disease of the poor, can possibly be prevented. Dag van de Jonge Onderzoekers in de Afrikanistiek. Antwerp, Belgium; December 12, 2008.

Van Moorhem M., Decrock E., Coussee E., Faes L., De Vuyst E., Vranckx K., De Bock M., Wang N., Lambein F., Callewaert G., Leybaert L. (2008) β-ODAP-triggered mitochondrial calcium overload as an early event in excitotoxicity. Belgian society of fundamental and clinical physiology and pharmacology; Autumn Meeting; Brussels, Belgium; November 8, 2008.

Van Moorhem M., Decrock E., Coussee E., Faes L., De Vuyst E., Vranckx K., De Bock M., Wang N., Lambein F., Callewaert G., Leybaert L. (2008) β-ODAP-triggered mitochondrial calcium overload as an early event in excitotoxicity. The Belgian brain congress. Oostend, Belgium; October 24-25, 2008.

Van Moorhem M., Fikre A., Lambein F, Leybaert L. (2008) *Lathyrus sativus* (grass pea), from toxic plant to wonder crop? Science with Africa; Addis Abeba, Ethiopia; March 3-7, 2008.

Van Moorhem M., Decrock E., Coussee E., Pille E., Lambein F., Vangheluwe P., Wuytack F., De Smet P., Callewaert G., Leybaert L. (2008) β-ODAP toxicity may be related to a disturbance of the cellular Ca^{2+} handling. Apoptosis world 2008; Kirchberg, Luxemburg; January 23-26, 2008 (Apoptosis world 2008, From mechanisms to applications, P125)

Van Moorhem M., Decrock E., De Bock M., De Vuyst E., Vangheluwe P., Wuytack F., De Smet P., Callewaert G., Lambein F., Leybaert L. (2007) Potential involvement of Ca^{2+} transport in β-ODAP toxicity. GAPSYM1 Heritage and/as reproduction in Africa; Ghent, Belgium; December 18, 2007.

Van Moorhem M., Decrock E., Coussee E., Pille E., Lambein F., Vangheluwe P., Wuytack F., De Smet P., Callewaert G., Leybaert L. (2007) β-ODAP toxicity may be related to a disturbance of the cellular Ca^{2+} handling. Belgian society of fundamental and clinical physiology and pharmacology; Leuven, Belgium; November 17, 2007.

Van Moorhem M., Decrock E., De Bock M., De Vuyst E., Van Den Bosch L., Callewaert G., Lambein F. and Leybaert L. (2006). Neurolathyrism: β-ODAP and the excitotoxicity hypothesis. Neurobelgium 2006; Genval, Belgium; November 10-11, 2006 (Acta Neurologica Belgica, supp 2006, 106, 1-2: P25).

Annex: Questionnaire for the participants

Date:

Researcher:

Patient information:
First name:
Family name:
Age:
Sex: M / F
Address:

Do you know neurolathyrism? Yes/No

What is the cause of neurolathyrism? .....

What is the consequence in life /economical, social/? .....

Can you treat neurolathyrism? Yes / No , if yes: How? .....

Respondent

- □ Patient

  How long? .....

  Which stage? 1st 2nd 3rd 4th

  Do you treat neurolathyrism? Yes / No , if yes: How? .....

  Along with the crippling, you have any other health problems/feelings? Yes/No

  What? .....

- □ Non-patient

Do you still eat guaya (*L. sativus*)?

- □ No
  - o How long did you stop eating guaya? .....
- □ Yes

How frequently do you eat guaya?

- □ < 1 times per day
- □ 1x per day
- □ 2x per day
- □ 3x per day
- □ > 3x per day

How much guaya do you eat per day?

- □ < 50 g
- □ 50 – 100 g
- □ 100 – 200 g
- □ > 200 g

How do you usually prepare guaya?

- □ Boil/nifro
- □ Roast/kolo
- □ Bake
- □ Fermented/elbet/
- □ Shiro wot/sauce
- □ Unripe seed
- □ Other: .....

What kind of utensil do you use to prepare guaya food?

- □ Clay
- □ Metal
- □ Others

Are you using the local guaya?

- □ Yes
- □ No

If no, where does it come from?.....

Do you add other ingredients to the guaya food?

- □ no
- □ yes

If yes, which ingredients and how much? .....

Have you ever eaten only guaya for a certain period (without addition of any other ingredients)?

- □ No
- □ yes

If yes, for how long? And why did you do so?

.....